https://theses.gla.ac.uk/

Theses Digitisation:

https://www.gla.ac.uk/myglasgow/research/enlighten/theses/digitisation/

This is a digitised version of the original print thesis.

Copyright and moral rights for this work are retained by the author

A copy can be downloaded for personal non-commercial research or study, without prior permission or charge

This work cannot be reproduced or quoted extensively from without first obtaining permission in writing from the author

The content must not be changed in any way or sold commercially in any format or medium without the formal permission of the author

When referring to this work, full bibliographic details including the author, title, awarding institution and date of the thesis must be given

Enlighten: Theses
https://theses.gla.ac.uk/
research-enlighten@glasgow.ac.uk

MASS TRANSFER STUDIES ON GAS ABSORPTION COLUMNS

A Thesis submitted to the University of Glasgow
in fulfilment of the requirements of the Degree
of Doctor of Philosophy.

by

DONALD MACKAY

Department of Chemical Technology
Royal College of Science and Technology
Glasgow.

August 1961.

ProQuest Number: 10656345

All rights reserved

INFORMATION TO ALL USERS
The quality of this reproduction is dependent upon the quality of the copy submitted.

In the unlikely event that the author did not send a complete manuscript
and there are missing pages, these will be noted. Also, if material had to be removed,
a note will indicate the deletion.

ProQuest 10656345

Published by ProQuest LLC (2017). Copyright of the Dissertation is held by the Author.

All rights reserved.
This work is protected against unauthorized copying under Title 17, United States Code
Microform Edition © ProQuest LLC.

ProQuest LLC.
789 East Eisenhower Parkway
P.O. Box 1346
Ann Arbor, MI 48106 – 1346

ACKNOWLEDGEMENTS

Thanks are due to Professor P.D.Ritchie B.Sc., Ph.D., F.R.I.C., F.P.I., M.I.Chem.E., F.R.S.E. for providing facilities for this work. The author is indebted to Dr.R.G.Gardner B.Sc., Ph.D., A.R.I.C., A.M.I.Chem.E. for his supervision and encouragement throughout the research. Acknowledgement is made to Mr.D.Smith A.R.C.S.T. for his help with the mathematical parts of this thesis, and to Messrs.Blairs Ltd. and the British Dyewood Coy.Ltd. for providing part of the equipment.

SUMMARY

The mass transfer and hydraulic characteristics of the Kuhni Distillation Plate have been studied using aqueous systems. The Kuhni Plate which is of Swiss origin, patented in 1937, has annular tunnel bubble caps with radial liquid flow from the periphery inwards to a central outlet well, from which the liquid is distributed to the periphery of the plate below by radial distribution tubes, giving co-ordinated reflux. Two sizes of plate were studied, 30 and 12 inches in diameter.

Mass transfer characteristics were studied using two gas absorption systems, the humidification of air as a gas phase resistant system and the desorption of oxygen from water by air as a liquid phase resistant system. Air rates ranged from 100 to 500 pounds per square foot of column area per hour and water rates from 100 to 1,000 pounds per square foot of column area per hour.

The plate efficiency was found to be relatively high and the relationship between the gas phase mass transfer coefficient and the gas contact time was of the form predicted by the Penetration Theory rather than the Two Film Theory of Mass Transfer. The Penetration Theory was further substantiated by consideration of the ratios of gas and liquid phase mass transfer coefficients and molecular diffusivities.

In general the efficiency of the 12 inch plate was lower than that of the 30 inch plate owing to the lower weir height and the shorter liquid residence time on the plate. The throughput of the Kuhni Plate was found to be low in comparison with other plates.

The hydraulic characteristics studied included plate pressure drop, clear liquid height, froth height, liquid hold-up, liquid residence time and the degree of liquid mixing. Plate pressure drops were found to be relatively high owing to the high "dry plate" pressure drop. It was found that the pressure drop characteristics could be improved by increasing the slot area although there was a corresponding reduction in efficiency. The effect of increasing the weir height was also studied and it is suggested that the performance of the plate can be improved by increasing both the slot area and the weir height. Froth heights were found to be low in comparison with other plates and it is probable that relatively little discrete bubbling takes place owing to the low weir height.

Liquid hold-up, residence time and mixing were studied by a tracer injection technique, and a steady state dye injection technique was used to give a qualitative indication of the degree of lateral mixing. A discrepancy was observed between the liquid hold-up calculated from the tracer injection method and from the clear liquid height measurements. The degree of liquid mixing was characterised by the Peclet Number and the "eddy diffusivity". The relationship between the liquid residence time distribution function and the Peclet Number was derived for radial flow plates and the Peclet Number used in the deduction of the liquid phase mass transfer data.

The effects of increasing the liquid viscosity on the gas and liquid phase mass transfer rates and on the liquid residence time, hold-up and degree of mixing were studied. The viscosities ranged from one to sixteen centiPoise and it was observed that the effect of increasing viscosity was complex, giving rise to maximum efficiencies in the four to eight centiPoise range.

The density, viscosity, vapour pressure, oxygen solubility and oxygen diffusivity of aqueous solutions of the viscosity increasing agent ("Cellofas B") were studied to enable a more complete evaluation to be made of the effects of liquid viscosity on mass transfer rates.

CONTENTS

1 INTRODUCTION

1:1 General 1
1:2 Introduction to Plate Efficiency 2
1:3 Efficiency Correlations 5
1:4 The Effect of Column Variables on Plate Efficiency 12
1:5 Comparison of Bubble Plates 16
1:6 Mass Transfer Theory 22
1:7 Liquid Mixing on Bubble Plates 27
1:8 Bubble Dynamics 35
1:9 Approach to the Problem 38

2 DESCRIPTION AND DESIGN OF THE EXPERIMENTS

2:1 The Humidification System 41
2:2 The Oxygen Desorption System 45
2:3 Selection of Viscosity-Increasing Agents 47
2:4 Selection of Liquid Residence Time Method 48
2:5 Alterations in Plate Design 51
2:6 Properties of "Collofas B" Solutions 52

3 DESCRIPTION OF THE APPARATUS

3:1 Design of the 30 inch Diameter Kuhni Plate 54
3:2 General Design of the 30 inch Kuhni Plate Plant 55
3:3 Modifications for Humidification Tests (30 inch Plate) 56
3:4 Modifications for Oxygen Desorption Tests (30 inch Plate) 57
3:5 Modifications for Residence Time Tests (30 inch Plate) 58
3:6 Design of the 12 inch Diameter Kuhni Plate 60
3:7 General Design of the 12 inch Kuhni Plate Plant 61
3:8 Modifications for Humidification Tests (12 inch Plate) 62
3:9 Modifications for Oxygen Desorption Tests (12 inch Plate) 62
3:10 Alterations in Plate Design (30 inch Plate) 63

4 EXPERIMENTAL PROCEDURE

4:1 Humidification Tests on both Kuhni Plates 64
4:2 Humidification Tests using Viscous Solutions 66
4:3 Oxygen Desorption Tests on both Kuhni Plates 67
4:4 Oxygen Desorption Tests using Viscous Solutions 68
4:5 Liquid Residence Time Tests on the 30 inch Kuhni Plate 69

5 DISCUSSION OF THE RESULTS

5:1 Residence Time and Liquid Hold-up Tests with Water 72
5:2 Residence Time and Liquid Hold-up Tests with Viscous Solutions 75
5:3 Pressure Drop and Froth Height Tests 79
5:4 Liquid Mixing Tests with Water 82
5:5 Dye Injection Tests with Water 85
5:6 Liquid Mixing Tests with Viscous Solutions 87
5:7 Gas Phase Efficiency Tests with Water 89
5:8 Gas Phase Efficiency Tests with Viscous Solutions 94
5:9 Liquid Phase Efficiency Tests with Water 99
5:10 Liquid Phase Efficiency Tests with Viscous Solutions 107
5:11 Tests with Varying Weir Height and Slot Area 111
5:12 Tests on the 12 inch Diameter Kuhni Plate 118
5:13 Comparative Performance of the Kuhni Plate and Other Plates 123

6 APPENDIX

A Specimen Calculations 125
B Derivation of Liquid Residence Time and Mixing Equations 134
C Oxygen Determination by the Winkler Method 140
D Properties of "Cellofas B" Solutions 143
E Properties of Sugar Solutions 151
F Conductivity Calibrations 151
G Maximum Probable Errors 152
TABULATED RESULTS 156
NOMENCLATURE 166
REFERENCES 170

SECTION 1

INTRODUCTION

1 : 1 General

Demands from design engineers for more reliable predictions of plate efficiency have resulted in a considerable volume of research, both industrial and academic, on mass transfer rates on bubble trays. Design calculations on gas absorption or distillation columns based on vapour-liquid equilibrium data give the number of theoretical plates required to achieve a given absorption, desorption or separation. Since no actual plate brings the vapour and liquid streams to equilibrium, it is necessary to know the plate efficiency, that is, the degree to which equilibrium is approached, to deduce the number of plates required.

At present, complete derivation of these efficiencies from a knowledge of mass transfer gained in wetted wall columns is impossible, owing to the complexity of the physical forces, and ignorance of the properties of the froth which exists on a bubbling plate. For progress to be made beyond purely empirical correlations of plate efficiency, attempts must be made to relate mass transfer theory to plate performance.

In this work an attempt is made to relate the performance of a bubble plate to modern theories of mass transfer and gas liquid dynamics. The bubble plate used in this investigation is the radial flow Kuhni Plate.

1 : 2 Introduction to Plate Efficiency

The effectiveness of a gas absorption plate as a mass transfer stage is most commonly expressed by its plate efficiency, which can be defined in three main ways as follows:

(i) Overall plate or column efficiency = E^O

This is the ratio of the number of theoretical plates to the actual number of plates in a column, and although widely used is of little theoretical importance.

(ii) Murphree point efficiency = E^*_{MV}

The approach to equilibrium in a small element of plate area is expressed by the "point efficiency". This is the ratio of the change in composition of the vapour passing through the element to the change that would have occurred had the outlet vapour reached equilibrium with the liquid in the element.

(iii) Murphree plate efficiency = E_{MV}

Integration of point efficiencies over the whole plate area gives the Murphree "Plate efficiency". This is defined as the ratio of the average change in vapour composition to the change that would have occurred had the outlet vapour reached equilibrium with the outlet liquid.

The Murphree efficiencies have been expressed above in terms of vapour composition but they can also be expressed in terms of changes in liquid composition.

Although the Murphree "point" efficiency can never exceed 100% the vapour "plate" efficiency may do so. This anomaly arises from the use of the outlet liquid as a source of the equilibrium vapour composition. If the liquid composition changes markedly across the plate, as may occur if there is little mixing, the outlet vapour may be enriched to a greater extent than the equilibrium value corresponding to the composition of the outlet liquid. In predictions of plate efficiency some knowledge of the degree of mixing is thus necessary.

Many workers have reported bubble plate efficiencies of distillation and gas absorption systems and many correlations of efficiency with column and system variables have been developed. It has been recognised that the plate efficiency depends on three groups of variables.

(i) The plate design, e.g. weir height, liquid path length, the size, number and spacing of the bubble caps or hole size and pitch for sieve plates.

(ii) The operating conditions, e.g. vapour and liquid rates, column temperature and pressure.

(iii) The physical properties of the system, e.g. liquid and vapour densities, viscosities, diffusivities and surface tensions.

In predicting and elucidating the effect of these variables it is necessary to appreciate that the plate efficiency depends ultimately on the rate of mass transfer through the bubble walls, and that this rate is controlled by the resistances existing in the interfacial boundary layers of both phases. The overall resistance is thus the sum of the resistances of both phases and possibly of the interface itself. The effect of operating variables on a system in which the resistance is predominantly in the gas phase differs from their effect on a predominantly liquid phase resistant system. Thus most workers have studied the effect of these variables on plate efficiency by using two systems, one in which the gas phase provides the entire resistance to mass transfer and one in which the resistance is provided by the liquid phase. Using such systems attempts have been made to explain and predict the efficiency characteristics of systems containing resistances in both phases. For gas phase resistant systems most workers have used ammonia absorption in water and humidification of air; for liquid phase resistant systems, absorption of carbon dioxide in water or desorption of oxygen from water.

1 : 3 Efficiency Correlations

A formidable amount of data has been reported on distillation and gas absorption plate efficiencies. Many correlations of these efficiencies with system physical properties, operating conditions, and plate design have been produced. These correlations are fairly satisfactory when applied to systems and conditions similar to those used in their development, but they may give conflicting and erroneous results when applied to differing systems. These discordant results may often be traced to a lack of appreciation of the factors involved, and to an insufficient understanding of the mass transfer mechanism involved. Considerable progress has been made, and modern correlations making use of current theories of mass transfer and liquid mixing appear to be very dependable.

In 1925 Murphree[1] suggested that efficiency correlation with system variables could be made by using a relationship of the form

$$E^*_{MV} = 1 - \exp(-A\, K_G\, t_C\, a'), \qquad (1;1)$$

where A = a constant,

a' = the interfacial area per mol of vapour, (ft^2/mol)

t_C = the contact time (sec.)

K_G = the mass transfer coefficient in gas terms (ft/hr)

This exponent bears a close resemblance to the "Transfer Unit" of Chilton and Colburn[2].

Walter and Sherwood[3] derived an empirical correlation based on Murphree's equation by considering efficiencies obtained with a bubble cap segment in a 2 inch diameter column. Both distillation and gas absorption systems of widely varying properties were used. The correlation is:

$$E^{*}_{MV} = 1 - \exp \left\{ \frac{-h}{\left[(2.50 + 0.37/H'P)\mu^{0.68} . \omega^{0.33}\right]} \right\} \quad (1;2)$$

where h = the submergence i.e. the vertical distance from the middle of the slot to the weir, (in.)

H' = Henry's Law constant (lb.mol/ft.^{3} atm)

P = total pressure, (atm)

μ = liquid viscosity (cP)

ω = slot width (in.)

The term $\omega^{0.33}$ was obtained from data of Carey, Griswold, Lewis and McAdams[4] who had determined the effect of slot width on efficiency using an ethanol - water rectification system. The term $0.37/HP$, suitable for gas absorption calculations, can be replaced by a term using relative volatility more suitable for distillation. Robinson and and Gilliland[5] suggested that the term "h" should be replaced by $(h')^{0.5}$ where h' is the vertical distance from the middle of the slots to the top of the liquid crest over the weir.

Drickamer and Bradford[6] produced a graphical correlation of plate efficiency against molal average liquid viscosity for the rectification of hydrocarbons.

O'Connell[7] extended and modified this correlation by introducing a gas solubility or relative volatility term which is combined with the liquid viscosity. This correlation is based on systems of widely varying properties and like that of Drickamer and Bradford contains no terms in plate design. It is thus an indication of the efficiency obtained on bubble plates of conventional design operating under optimum conditions. There is no theoretical justification for the use of the gas solubility - liquid viscosity product for correlating purposes but the correlation is widely used as a first approximation. Slanislaus & Smith[100] suggested that the ratio of solubility to viscosity would give a better correlation than the product.

Geddes[8] tried a more fundamental approach based on mass transfer to a stream of rising bubbles. It was assumed that bubble diameter is determined by buoyancy and surface tension as elucidated by Sugden[9] and that the rising velocity is that predicted by the correlation of O'Brien and Gosline[10]. From the bubble size, rising velocity and submergence, the contact time and interfacial area can be calculated. Mass transfer coefficients for both phases are derived using Higbie's[11] equation for the liquid phase, and a solution by Barrar[12] of Fick's second law of unsteady state diffusion for the gas phase. The mass transfer coefficients are combined to give an overall resistance and the Murphree vapour point efficiency deduced.

The assumption, in this derivation, of bubble diameter being that which occurs under near-static conditions has been shown to be erroneous, as Sugden's equation does not apply at the high slot velocities occuring in bubble caps. (This is discussed at greater length in the section on Bubble Dynamics). Although this correlation is good, it is complicated to use.

Chu, Donovan, Bosewell and Furmeister[13] in the light of a greater knowledge of bubble dynamics, proposed a correlation for Murphree vapour efficiency by revising that of Geddes and including a term in bubble diameter. This diameter can be estimated from one of two equations depending on the bubbling regime operating under the required conditions.

In the same work a correlation of overall efficiency based on O'Connell's graphical correlation is given and claimed to be more accurate. It is expressed as:

$$E^{o} = 45.6 \left(10^{-0.06 + 0.092h} \right) \left(\frac{L'}{G'} \right)^{0.245} \left(\frac{HP}{\mu_L} \right)^{0.380}_{\text{Feed}} \qquad (1;3)$$

where h = the submergence (in.)

L' = the liquid rate (lb mol/hr)

G' = the vapour rate - (lb mol/hr)

Bakowski[14], in a sequel to work by himself and Spells[15,16] on high speed filming of bubbling at vertical slots, derived a correlation based on the supposition that mass transfer to chains of bubbles is akin to mass transfer to a channel of vapour. The correlation agrees well with published data and is given below.

$$E_{MV} = 1 - \exp \left\{ -2.303 \frac{0.34\, T_K^{0.5} (h_l + h_s)}{M^{0.5}\, P^{0.25}\, G_S{}^{0.25}} \right\} \qquad (1:4)$$

where T_K = absolute temperature (^{o}K)

h_l = static liquid seal (cm)

h_s = slot opening (cm)

M = molecular weight

P = total pressure (atm)

G_S = vapour rate per slot (cm^3/sec)

Chaiyavech and Van Winkle[17] using distillation systems in a 1 inch diameter sieve plate column have suggested the following correlation of system properties which, it is claimed, is better than those of O'Connell[7] and Drickamer and Bradford[6]:

$$E_{MV} = 0.0691 \left(\frac{\sigma_L}{\mu_L U_g}\right)^{0.64} (Sc)^{0.19} (\alpha)^{0.056} \qquad (1;5)$$

where σ_L = surface tension (dynes/cm)

U_g = column velocity cm/sec

Sc = Schmidt number (viscosity/density x diffusivity)

α = relative volatility

Planovski[22], using the intuitive argument that the rate of mass transfer on a bubble cap or sieve plate is a function of the energy dissipated in the bubbling process, developed a correlation of the number of gas film transfer units against the difference between the total pressure drop and the "dry plate" pressure drop. Comparison between different systems is by a power of Schmidt number ratio. The Schmidt number Sc is the ratio of the viscosity to the product of density and diffusivity and is the mass transfer equivalent of the Prandtl number.

A correlation of Murphree liquid plate efficiency has been given by Quigley, Johnson and Harris[23] from studies of gas hold-up and bubble size on sieve plates.

Gilbert, West and Shimzu[24], using Higbie's[11] diffusion equation for both phases and a bubble size and foam density from correlations, give an equation for Murphree point efficiency on bubble cap and sieve plates.

Gerster and his co-workers[25,26,27] made an important contribution to the elucidation of plate efficiency by suggesting investigation of single-phase resistance controlling systems and a comparison of the performances of these systems through the Schmidt number. It was shown that by evaluating individual resistances and then combining them, the performance of two phase resistant systems could be predicted. It was suggested that the number of transfer units of each phase was inversely proportional to the Schmidt number to the power 0.5 for the liquid phase and 0.67 for the gas phase, a prediction which has since been substantiated by Calderbank[28].

In 1952 the American Institute of Chemical Engineers organised a five year research project, on the efficiency of bubble cap plates. A method of predicting plate efficiency was developed, based on experimental data obtained in distillation and gas absorption equipment, both industrial and academic. The complete findings of the project have been published [18,19,20] with a design manual[21] describing the rather complicated method of efficiency prediction. The method applies principally to binary distillation systems or absorption of a component between inert gas and liquid carriers, but can be applied less satisfactorarily to multicomponent systems. A description of the method which is based on Gerster's individual phase transfer unit approach, is outlined below.

It is assumed that the bubble plate design and operating conditions have been established and the physical properties including viscosity and diffusivity of both phases have been determined either experimentally or from correlations. From an estimate of the clear liquid height the mean liquid residence time is calculated. Application of this residence time in an empirical correlation with liquid diffusivity and column vapour velocity gives an estimate of the number of liquid phase transfer units. Similarily, the number of gas phase transfer units is estimated from a correlation including terms in gas diffusivity, density, viscosity and velocity, weir height and liquid rate and gradient. These transfer units are combined in the usual way with equilibrium data to give an overall number of transfer units, and hence a point efficiency.

From a consideration of the factors influencing liquid mixing an "eddy diffusivity" is deduced and converted into the dimensionless Peclet number. A graphical presentation of the solution of the diffusion equation relating point and plate efficiencies with Peclet number as a parameter, permits deduction of the Murphree plate efficiency. A correction can be applied for entrainment.

Comparison of predicted and actual efficiencies demonstrates the reliability of the method and its superiority to the less complicated correlations.

1 : 4 The effect of Column Variables on Plate Efficiency

Summarised below are the effects of column and system variables on the efficiency of both liquid and gas phase resistance controlling systems.

(i) Weir Height

This is an important variable, since an increase in liquid depth increases the contact time of the rising bubble, thus tending to increase both gas and liquid phase efficiencies. The liquid residence time on the plate is also increased, with a beneficial effect on the liquid phase efficiency. Too high a weir, however, causes an excessive pressure drop, or lowers the vapour velocity - both undesirable effects.

(ii) Vapour Velocity

An increase in vapour velocity causes greater turbulence on the plate and a greater foam depth (or vapour hold-up). These effects generally increase liquid phase efficiency through more effective contact between the phases but their effect on gas phase efficiency is not so certain since at high vapour velocities there may be much "jetting", as shown by Spells[15], with a detrimental effect on efficiency. A maximum efficiency is often found[29]. Entrainment may lower efficiency at excessive vapour velocities.

(iii) Liquid Rate

An increase in liquid rate on a plate increases the volume of liquid on the plate[29] with the result that the greater froth depth increases gas phase efficiency. This effect also tends to increase liquid phase efficiency but with the simultaneous reduction in liquid residence time on the plate, there is usually a nett reduction in efficiency. An excessively high liquid rate may set up a large hydraulic gradient with the outcome that "dead zones" may occur, or even liquid "dumping," which is more serious.

(iv) Column Temperature and Pressure

In distillation, the column temperature and pressure are related and may be varied to suit the required conditions; for example to reduce the operating temperature, the distillation can be done under vacuum. Changes in temperature and pressure affect vapour and liquid density, viscosity and diffusivity with resultant effects on the molecular diffusion rates. Investigations by Ellis, Barker and Contractor[30] into sieve plate performance at reduced pressures, show that the effect of pressure on efficiency is small, a conclusion confirmed by other workers[31,32]. No generalisations are reliable, as the effect of reduced pressure depends on the system used.

(v) Vapour viscosity has an effect on gas phase molecular diffusion, as is shown by the successful use of the Schmidt number for comparing diffusion rates, but it is unlikely to affect the gas - liquid dynamics of the plate. Liquid viscosity has been recognised as being probably the most important single factor in determining plate efficiency[6]. As with vapour viscosity, the liquid viscosity affects molecular diffusion as characterised by the Schmidt number. In addition it affects the fluid dynamics of the plate, changing liquid residence time and flow pattern, and bubble size and velocity especially at high slot velocities. This has been shown by Barker and Choudhury[33] who found a deterioration in gas phase efficiency at viscosities greater than 5 centipoises. Other workers[3,19] have claimed that the effect of liquid viscosity on efficiency can be adequately explained in terms of the associated change in diffusivity for liquid phase resistant systems.

(vi) Diffusivity

Mass transfer coefficients in both phases are controlled by the ambient physical conditions in the region of the interface and by the diffusivity of the mobile component. The relation between the mass transfer coefficient and diffusivity is discussed later in Section 1:6.

(vii) Surface Tension

Surface tension affects interfacial area in its effect on froth properties including the rate of froth breakdown, and possibly bubble size. Greater froth formation will tend to increase the plate efficiency, provided that there remains sufficient height for effective vapour - liquid disengagement, otherwise excessive entrainment may occur.

The importance of the surface tension - composition relationship has been discussed by Zuiderweg[34] and Danckwerts[35].

The presence of surface active agents has been shown to affect mass transfer rates[36] but this is not likely to occur in industrial columns.

(viii) Entrainment

It has been long recognised that liquid carried in the vapour stream to the plate above will reduce efficiency. Colburn[37] established the relation between the efficiency reduction and the amount of entrainment. Several workers[38,39,40] have reported data on entrainment, and attempted correlations between vapour velocity and plate spacing. Entrainment is proportional to approximately the third power of vapour velocity and inversely proportional to the same power of plate spacing.

(ix) Liquid "Dumping" "Weeping" or "Leakage"

This effect, of more importance to sieve plates than bubble cap plates, has probably little effect on efficiency provided it is not too severe. Despite occurring mainly near the inlet weir (where the hydraulic seal is greatest) the effect on efficiency is minimised by mass transfer which must take place during the fall of the droplet, indeed contacting devices like the Turbogrid plate operate on this principle.

(x) Component Concentration

Anomalous plate efficiencies have been found using systems in which the concentration driving force is very small, for example in very dilute solutions or near azeotropes. Van Wijk and Thijssen[96] have established that this effect is not due to inaccurate concentration measurement but that there is a reduction in the diffusion rate. Haselden and Sutherland[47] have observed this effect with the ammonia-water system and conclude that a study of the thermal effects of distillation may help to explain this anomaly.

1 : 5 Comparison of Bubble Plates

The principal commercial bubble plates are described individually and their performances compared. An excellent review of these plates is given by Freshwater[41].

(i) Bubble Cap Plate

Since its invention in 1818 by Cellier Blumenthal, this has been the most popular gas-liquid contacting plate. The commonest form is the circular cap with vertical slots mounted concentrically above the riser which is sealed into the plate. Many variations are possible with cap size and shape, and slot height and width, but they seldom result in any significant improvement over the standard design.

(ii) Sieve or Perforated Plate

Many chemical engineering texts[42,43] give adverse reports on sieve plate performance, for example a narrow stability range and high pressure drops. Until recently, therefore, when Mayfield[44] et al. showed the sieve plate in a more favourable light, its use was confined to a few traditional industries such as alcohol distilling. Plate design is fairly standard with 3/16 or 1/4 inch diameter holes punched on about 1 to 1½ inch triangular pitch. The "shower deck" plate is of similar design but with no liquid downcomers.

(iii) A.P.V. West Plate

This can be described as a form of tunnel bubble cap plate with a sieve plate immediately above it. The liquid flow is by co-ordinated reflux. It combines the performance of the sieve plate with the stability of the bubble cap at low vapour velocities.

(iv) Kuhni Plate (See Figures 1 and 2)

This plate, of Swissorigin, patented[45] in 1937, is the bubble plate used in the principal part of this work.

The plate consists of spun co-axial rings of tunnel bubble caps and gutters, the walls of adjacent gutters forming the risers inside the caps. Vapour bubbles into the liquid from serrations in the cap skirts, analogous to bubble cap slots. Distributing tubes radiating from the central downcomer convey the liquid to the periphery of the plate below. Liquid flow is thus radial from the periphery to the central well on every plate giving co-ordinated reflux. The slot area is approximately 5% of the column area.

(v) Kittel Plate

This plate consists of pairs of slotted metal trays in which, because of the angle of the slots, the vapour imparts a centrifugal or centripetal swirl to the liquid. There are no downcomers, the liquid leaking to the plate below at the centre and periphery alternately.

(vi) Koch Kaskade and Benturi Plates

In the "Kaskade" plate the liquid flows down a series of "steps" through which the gas blows horizontally, forcing the liquid against and through a perforated baffle to the next "step". The difficulty of fitting this type of plate in a circular column has been overcome by modifying the design to give horizontal plates as in the "Benturi" plate.

(vii) Shell Turbogrid Plate

This is probably the simplest gas-liquid contacting plate, consisting of parallel metal bars up to 1/2 inch apart. There are no downcomers, the

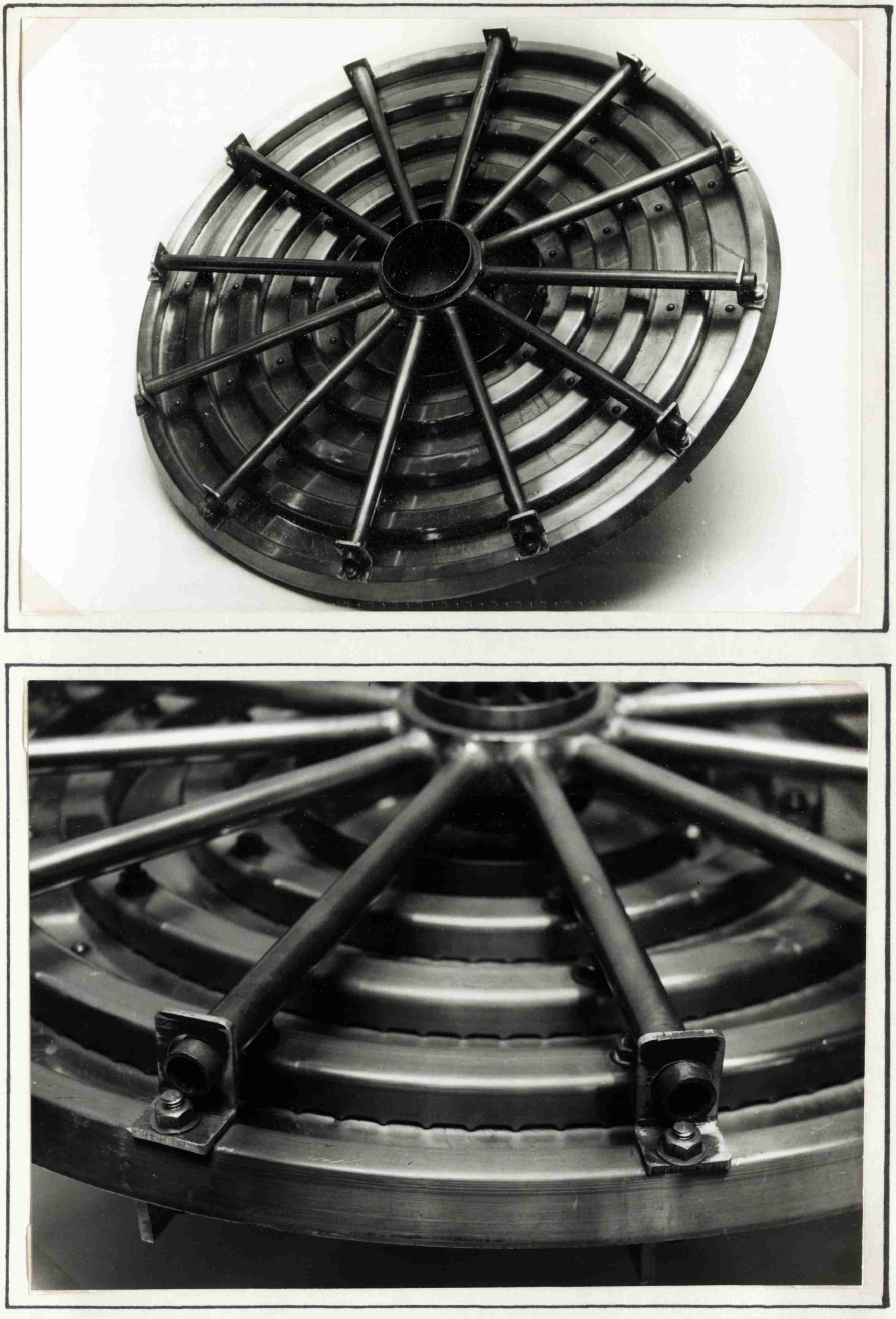

THE 30 INCH DIAMETER KUHNI PLATE

FIG 1

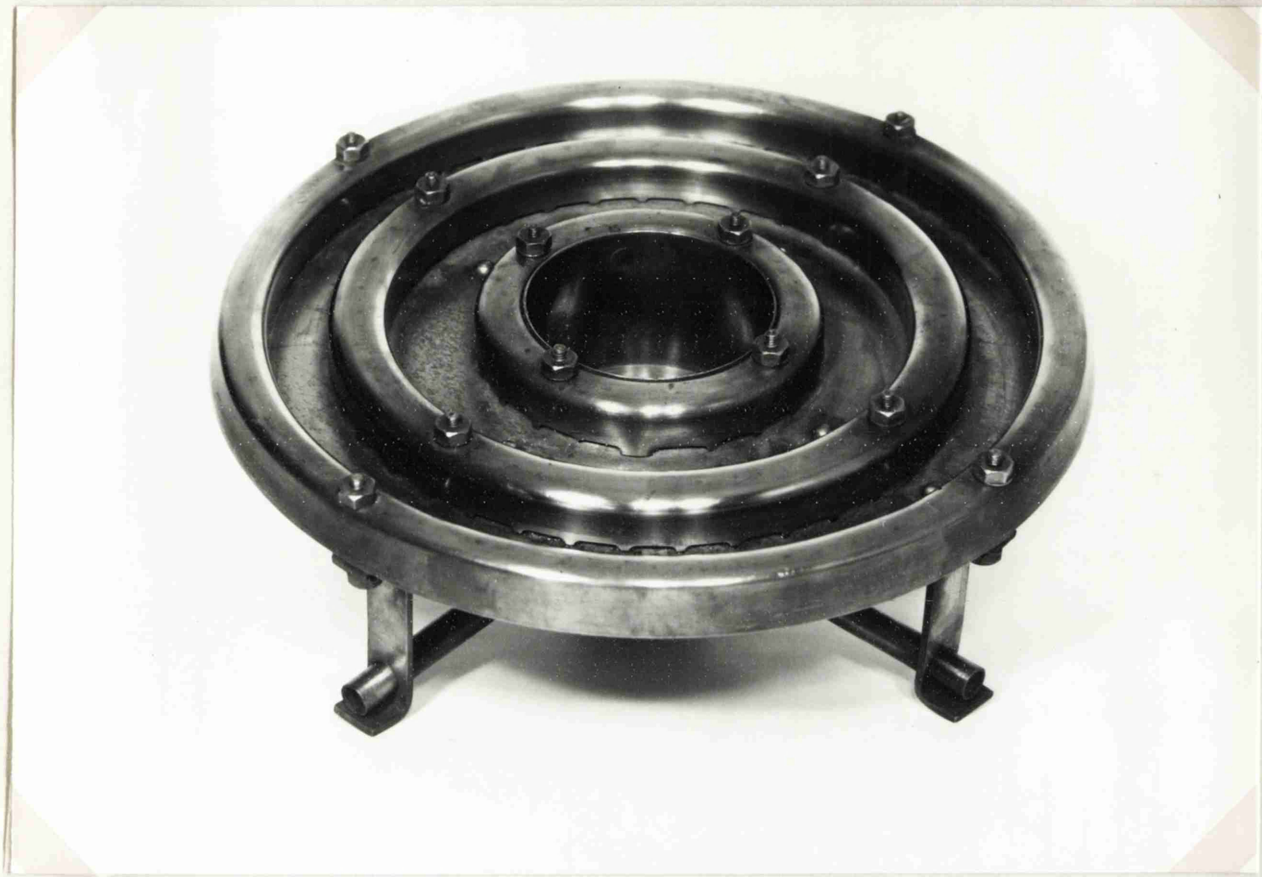

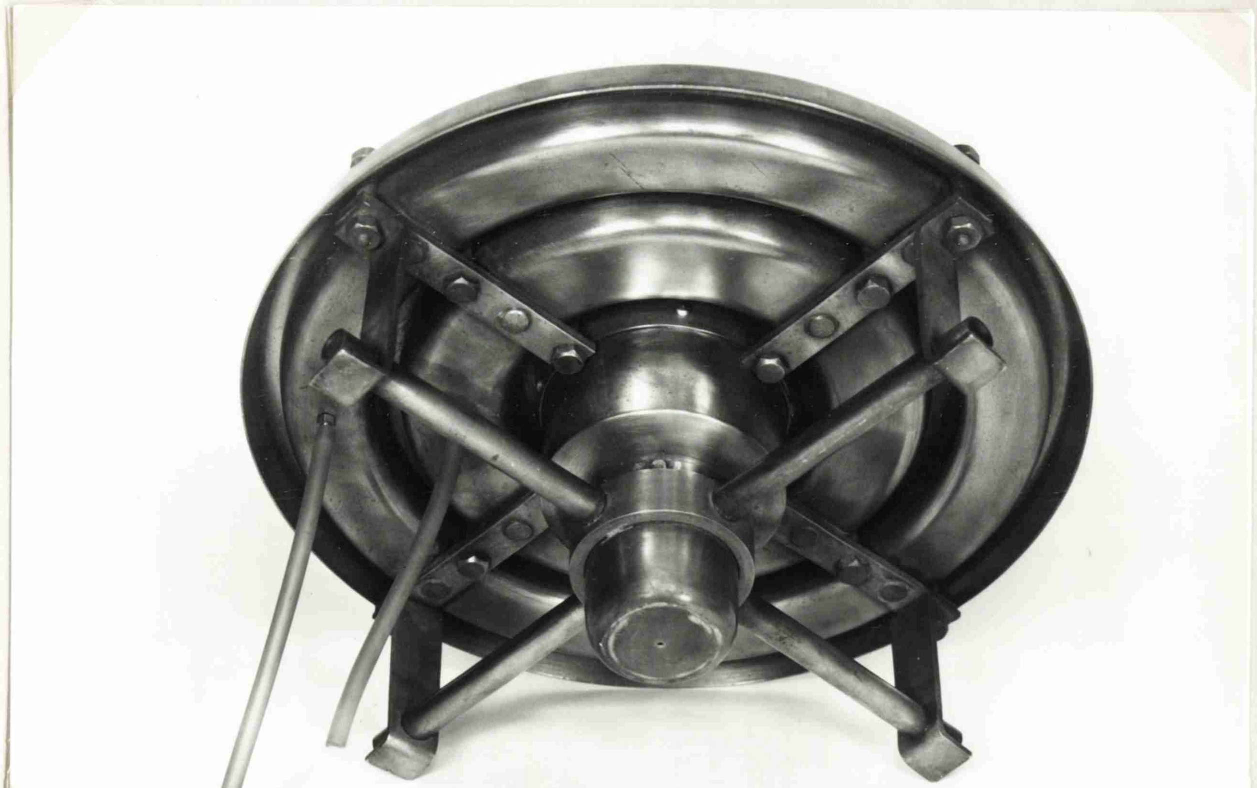

THE 12 INCH DIAMETER KUHNIPLATE, THE LOWER VIEW SHOWING THE LIQUID DISTRIBUTERS AND THE CLEAR LIQUID HEIGHT MANOMETER TAPPINGS.

FIG 2

vapour and liquid passing through the slots in opposite directions.

(viii) Jet Tray

This plate is similar to the sieve plate except that there are punched tabs instead of holes, giving the vapour a horizontal velocity in the direction of liquid flow. There are no weirs.

(ix) Plates with Moving Caps

Several plates such as the Koch "Flexitray", the "Ballast" plate and the Nutter "Float Valve" Plate, have been designed to give a greater range of plate stability by incorporating a device which reduces the "slot area" at low gas rates, thus maintaining the slot velocity. The device is usually a cap (or caps) which is raised by the momentum of the gas stream.

The Relative Performance of Bubble Plates

In recent years much attention has been paid to the sieve plate and to comparing it with the bubble cap plate which is regarded as the standard plate for comparison of performance. Mayfield *et al.*[44] showed that the sieve plate can have a greater efficiency than the bubble cap plate, and that the stability range is adequate provided the hole diameter is small enough. Small holes give a high pressure drop and high stability; large holes a low pressure drop and low stability. Jones and Pyle[46] found that sieve plate pressure drop is lower than that for a bubble cap plate, entrainment is 20% less and the capital cost 30% less. Garner Ellis and Freshwater[47] found that the liquid phase efficiencies of a sieve plate are not significantly less than that of a bubble cap plate, and that the pressure drop characteristics are better.

In general it can be stated that the sieve plate, which is increasing in popularity as more design data become available, will give better performance than the bubble cap plate at reduced cost.

Much less information is available on the performance of the other less common plates, though much work has been done in Birmingham University evaluating and comparing plate performance, and much data reported at a recent symposium on distillation organised by the Institution of Chemical Engineers[102].

Garner *et al*[48,47] found that the Kaskade plate compares favourably with the bubble cap plate especially at high vapour velocities where high efficiency is maintained and pressure drop is still relatively low. The pressure drop characteristics of the Kaskade plate are excellent.

The rather complicated gas-liquid flow characteristics of the Turbogrid plate have been elucidated by Garner, Ellis and Bershadsky[49], who showed that the pressure drop across the Turbogrid plate is very low and depends on the phase of operation. In a later study Garner, Ellis and Freshwater[47] found that the liquid film efficiency of the Turbogrid is lower than that of bubble cap plate and has a very narrow range of even relatively high efficiency. The gas film efficiency is, however, superior to that of the bubble cap plate over a fairly wide range. Majeweski[105] has confirmed that in general plate efficiencies are lower, but shows that this is no real disadvantage, since the permissible plate spacing is much less.

The Kuhni plate is claimed to give a very high efficiency maintained over a wide range of vapour rates because of the high slot velocity and the coordinated reflux. At low vapour rates the inner troughs cease to bubble, the high slot velocity being maintained near the periphery. The pressure drop is, however, relatively high.

It is claimed by Pollard[50] that the Kittel plate has a lower pressure drop than the bubble cap plate with comparable efficiency, and a capital and installation cost about 25% less. Zuiderweg,[101] et al. showed that the liquid flow system could break down, especially with larger diameter plates, with a detrimental effect on efficiency. Stanislaus and Smith[100] suggest that the Kittel plate is most suitable for vacuum distillation owing to its low pressure drop.

Robin[51], in an assessment of the Glitsch "Ballast" plate, which has two sets of moving caps, shows it to have a greater operating range than the bubble cap plate. The efficiency and pressure drop are comparable to that of a bubble cap plate. Stanislaus and Smith[100] and Zuiderweg et al.[101] showed that the "Flexitray" has slightly better efficiency and pressure drop characteristics than the bubble cap plate with a longer range of operating conditions.

The jet tray has been shown by Forgrieve[98] to give efficiencies equal to those of a bubble cap plate. The advantage of the jet tray is its higher capacity, permitting either higher throughputs in existing columns or a reduction in cost and size for planned columns.

Dummet[104] has shown the performance of the A.P.V. West plate to be superior to that of a bubble cap plate. Efficiencies are higher, partly because of the co-ordinated reflux and pressure drops are equivalent to the bubble cap plate. The principal advantage is the long range of plate stability. The plate is capable of modification for special operating conditions such as vacuum fractionation.

In general it can be stated that the performances of distillation or gas absorption plates with liquid downcomers is roughly equivalent, the traditional bubble cap plate being the least, and the sieve plate the most attractive in both performance and cost.

Plates without downcomers are not so flexible, but may be excellent for special purposes, such as vacuum distillation, where their unique performance characteristics are desirable.

1 : 6 Mass Transfer Theory

(i) Whitman Two Film Theory

In 1923 Whitman[52] introduced the "Two Film" theory of mass transfer, which postulates laminar fluid films on both sides of the interface. It is assumed that equilibrium between the phases exists at the interface, which itself provides no resistance to mass transfer. The rate of mass transfer is controlled by the molecular diffusion rate through the film. Fick's First Law[53] is assumed to apply, the rate thus being proportional to concentration difference and diffusivity, and inversely proportional to film "thickness".

Deduction of the common mass transfer equations from Fick's Law can be found in any standard Chemical Engineering text[54]. These equations for gas-liquid mass transfer are given below.

$$N_A = K_l \bar{a} (x_L - x_i) = K_g \bar{a} (y_i - y_G) \qquad (1;6)$$

Where N_A = mass transfer rate of the diffusing component (lb mol/hr)

K_l = liquid film mass transfer coefficient (ft/hr)

K_g = gas film mass transfer coefficient (ft/hr)

$\bar{a}$ = interfacial area (ft.^{2})

x_L = concentration of the mobile component in the liquid phase (lb mol/ft^3)

y_G = concentration of the mobile component in the gas phase liquid (lb mol/ft^3)

x_i = concentration of the mobile component at the liquid interface (lb mol/ft^3)

y_i = Concentration of the mobile component at the gas interface (lb mol/ft^3)

It can be shown that if $y_i = \bar{m}.x_i$, $\bar{m}$ being a dimensionless Henry's Law constant, (lb mol/ft.^{3} per lb mol/ft.^{3})

$$N_A = K_G \bar{a} (\bar{m}x_L - y_G) = K_L \bar{a} (x_L - y_G/\bar{m}) \qquad (1;7)$$

where K_G = "Overall" gas film mass transfer coefficient ft/hr.

K_L = "Overall" liquid film mass transfer coefficient ft/hr.

and $$\frac{1}{K_G} = \frac{1}{K_G} + \frac{\bar{m}}{K_l} \qquad (1;8)$$ and $$\frac{1}{K_L} = \frac{1}{K_l} + \frac{1}{\bar{m}Kg} \qquad (1;9)$$

Thus $$K_L = \bar{m} K_G \qquad (1;10)$$

The gas "film" mass transfer coefficients can be expressed as above as "lb mol/ft.^{2} hr. (lb mol/ft.^{3} concentration difference)" which reduces to "ft./hr.". Alternatively they can be expressed in terms of partial pressures of the diffusing component as "lb mol/ft.^{2} hr. atm". If this second system is used the Henry's Law Constant has the dimensions atm ft.^{3}/lb. mol, gas phase concentrations being expressed as partial pressures.

Confirmation that the overall resistence to mass transfer is the sum of two individual resistances has been provided by Sherwood[55].

According to the Two Film theory, the mass transfer coefficient should be directly proportional to the diffusivity of the mobile component. This is disproved by experimental studies on gas film controlled mass transfer on wetted wall columns and with bubbling systems[108, 109]. It has been found that

$K_g \propto D_G^b$ where D_G is the gas diffusivity.

Gerster[25] and Calderbank[28] suggest that b = 0.67

Studies of liquid film controlled mass transfer, experimentally difficult owing to ripples on wet surfaces, have shown that a similar relationship holds as in gas film controlled mass transfer.

If $K_l \propto D_L^{b'}$, where D_L is the licuid diffusivity, then several workers suggest[110, 111, 95] that $b' = 0.5$ to 0.67.

(ii) Penetration Theory

In 1936 Higbie[11] proposed the "Penetration Theory" of mass transfer through liquid films. This theory, which is based on the contacting of liquid surface elements with rising bubbles, regards the mass transfer process as an unsteady state build-up of diffusing material into regularly renewed liquid surface elements. It is claimed that in most gas-liquid contacting operations, insufficient time is available for achievement of steady state film diffusion. The mass transfer coefficient will therefore depend on the time of contact of the element and on the diffusivity to the power 0.5.

$$\text{i.e. } K_l \propto \sqrt{\frac{D_L}{t_c}} \qquad (1;11)$$

where t_c is the contact time (sec.)

Danckwerts[65] has since suggested that the contact time "t_c" is better replaced by a rate of surface renewal "s" giving the equation

$$K_l \propto \sqrt{D_L . s} \qquad (1;12)$$

where s is the rate of surface remewal.

It has been suggested[18] that the Penetration Theory may apply to the gas phase and this is supported by gas absorption data.

Maroudas and Sawistowski[130] in a study of liquid-liquid mass transfer have concluded that local gradients of solute concentration near the interface cause interfacial "eruptions" with resultant turbulence and "induced" surface renewal. This "induced" surface renewal is thought to control the rate of mass transfer rather than random eddies. Surface renewal rates of 100 per second were found.

(iii) Other Developments

It has been suggested that the two theories above are not incompatible, but complementary. Toor and Marchello[56] suggest that if the unsteady state build-up of material in the interfacial region continues for long enough, then steady state diffusion may become effective. This will be commonest in fluids of low Schmidt number and where contact time between the phases is long.

Thus, the penetration theory will apply initially in the mass transfer process, but under certain conditions steady state diffusion may follow, giving an overall value greater than 0.5 to the power of the diffusivity.

Kishinevskii and Mochalova[103] have suggested that under the very turbulent conditions often found in vapour liquid contacting equipment eddy diffusivity becomes important in determining mass transfer rates. Garner & Porter[99] have pointed out that effective diffusivities of 2 to 3 times the molecular diffusion are required to explain some plate efficiencies. Calderbank and Korschinski[90] have found effective diffusivities up to 70 times the molecular diffusivity.

(iv) Diffusivity

In mass transfer theory, accurate data on gas and liquid diffusivity are essential but often scarce.

Theoretical studies of diffusion in the gaseous state based on the Kinetic theory have resulted in successful, semi-empirical gas diffusivity correlations such as those proposed by Gilliland[57] Hirschfelder[58], Fair and Lerner[59] and Wilke[60].

Application of similar methods to the liquid state have not been so successful. Diffusivities have been found experimentally by methods such as those of Johnson and Babb[61] and Davidson and Cullen[62]. Correlations have been proposed by Wilke and Chang[63] and Ibrahim and Kuloor[64].

1 : 7 Liquid mixing on Bubble Plates

The effect of liquid mixing on Murphree plate efficiency can be considerable when the liquid composition changes markedly from inlet to outlet; indeed, Murphree plate efficiencies of over 100% may be encountered.

Unless the degree of mixing is known and can be expressed mathematically, either complete mixing or no mixing must be assumed, both of which will give erroneous results. Mixing always occurs on gas absorption plates and it is, therefore, not justifiable to assume either complete mixing or no mixing.

The value of the Murphree plate efficiency thus depends on two separate factors. Firstly, the mass transfer coefficient and the contact time and area of the phases control the efficiency at any point. Secondly, the degree of liquid mixing on the plate controls the liquid concentration distribution over the plate and hence the distribution of concentration driving forces. Thus, assuming the point efficiency to be constant over the whole plate, the plate efficiency which depends on the overall mass transfer rate, will depend on the point efficiency and on the distribution of concentration driving forces as determined by the degree of liquid mixing.

The first mathematical treatment of mixing on a bubble plate was by Kirschbaum[42] who postulated a number of hypothetical "perfectly mixed pools" of liquid, the degree of mixing being characterised by the number of such pools. A plate with "plug flow" would have an infinite number of pools, a perfectly mixed liquid mass, one pool.

Gatreaux and O'Connell[66] derived the relationship between the number of "pools" and the Murphree plate and point efficiencies. This "pool" concept, although a considerable advance on the previous alternatives of plug flow or complete mixing, does not represent the true physical conditions on the plate.

Oliver and Watson[67] devised a liquid recirculation concept in which a fraction of the outlet liquid is assumed to be recycled to the inlet. Johnson and Marargozis[68] suggested that the prime cause of mixing is liquid splashing upstream and downstream of each bubbling centre.

Another approach which has received much attention recently is the eddy diffusion concept of mixing. This has been developed by Rukinshtein[69] and Gerster[19] and is similar in principle to theories of fluid mixing in pipes and vessels. The degree of mixing is assumed to be proportional to the concentration gradient and an "eddy diffusivity" is postulated as the proportionality constant. This concept is more realistic than the pool concept but still does not take into account stagnant pockets of liquid or "short circuiting" which probably exist on bubbling plates.

Tracer techniques have been used to determine the degree of mixing on bubbling plates[106, 107, 19]. These methods all give a residence time distribution of the liquid from which the degree of mixing, the liquid hold-up and the mean residence time can be calculated. Danckwerts[70] first elucidated the concept of residence time distributions and subsequent work by Levenspeil and Smith[71], Van der Laan[72] and Werner and Wilhelm[73] has made it possible to characterise mixing by a dimensionless parameter, the Peclet number, which is the ratio of the tray length to the "mixing" length or alternatively the ratio of the froth velocity to the "eddy diffusion" velocity.

The Peclet number Pe is defined as

$$Pe = \frac{Z\ V}{D_E} = \frac{Z^2}{D_E\ tm} \qquad (1;13)$$

where Z is the tray length (ft.)

V is the froth velocity (ft./sec.)

D_E is the eddy diffusivity (ft.^{2}/sec.)

tm is the mean liquid residence time (sec.)

For a rectangular plate the equation relating the variance, σ^2, of the concentration-time curve at the outlet caused by an injection of tracer at the inlet, to the Peclet number was derived by Vander Laan[72].

$$\sigma^2 = \frac{2}{Pe^2}\ (Pe - 1 + e^{-Pe}) \qquad (1:14)$$

The relationship between the Murphree vapour point and plate efficiencies and the Peclet number was derived at the University of Delaware[19]. It is shown graphically in Figure 3.

On a radial flow plate the froth velocity is not constant and a mean Peclet number must be used. This is obtained by replacing the froth velocity by the ratio of path length to residence time in the definition of the Peclet number. No equations exist in the literature relating the Peclet number to the variance for radial flow plates and such an equation was derived as part of this work

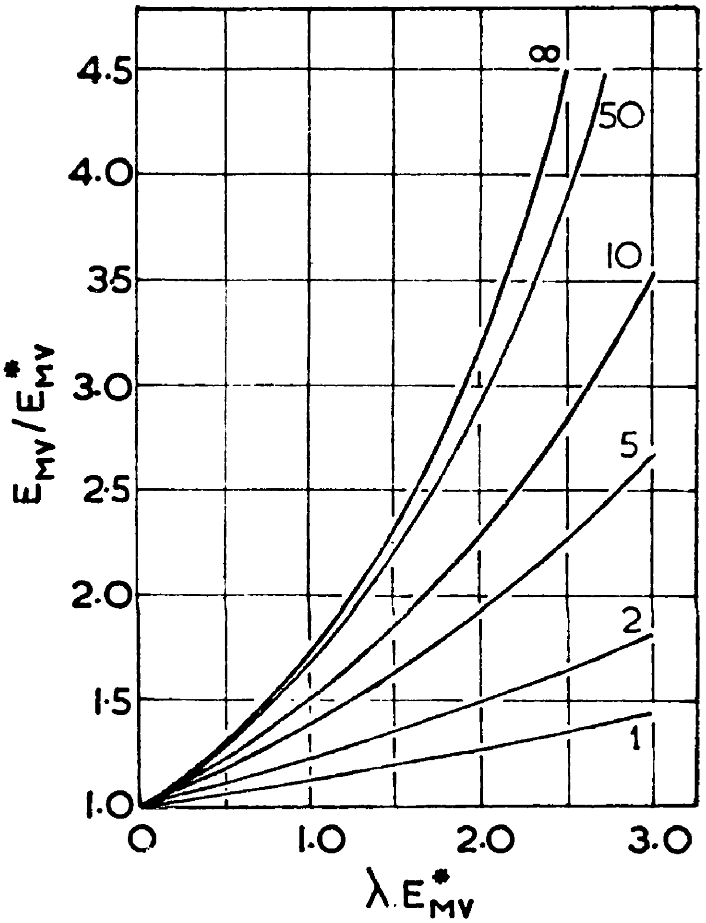

PARAMETER IS PECLET NUMBER Pe

RELATIONSHIP BETWEEN PLATE AND POINT EFFICIENCY AS A FUNCTION OF THE PECLET NUMBER

FIG 3

Mass transfer and liquid mixing on a gas-absorption plate

Consider a gas absorption plate with a liquid rate of L_p ft.^{3}/hr and vapour rate of G_p ft.^{3}/hr with inlet and outlet liquid and vapour concentrations of x_1 and x_2 and y_1 and y_2 lb.mol/ft.^{3} respectively. Let the liquid path length be Z ft. Assume that y_1 the inlet vapour concentration is constant over the plate area. This plate is shown diagrammatically below.

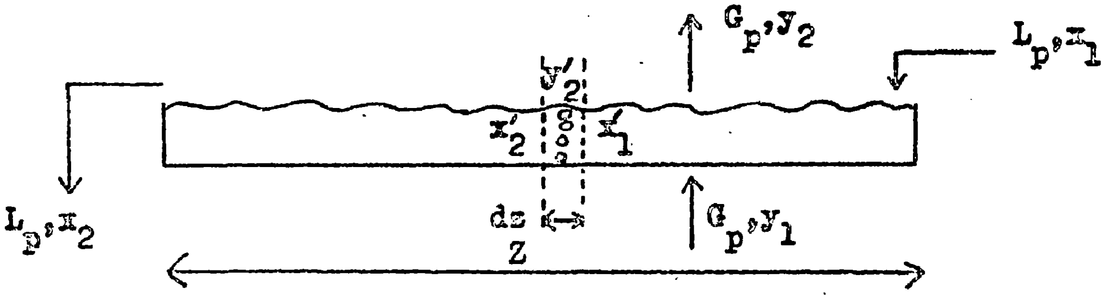

Murphree efficiencies are defined as below

(i) Murphree vapour plate efficiency $E_{MV} = \dfrac{y_2 - y_1}{y_e - y_1}$ (1:15)

(ii) Murphree vapour point efficiency $E^*_{MV} = \dfrac{y'_2 - y_1}{y'_e - y_1}$ (1;16)

(iii) Murphree liquid plate efficiency $E_{ML} = \dfrac{x_1 - x_2}{x_1 - x_e}$ (1;17)

(iv) Murphree liquid point efficiency $E^*_{ML} = \dfrac{x'_1 - x'_2}{x'_1 - x'_e}$ (1;18)

where $y_e = \bar{m}.x_2$ and $x_e = y_2/\bar{m}$, $y'_e = \bar{m}.x_2$, and $x'_e = y_2/\bar{m}$;

and where $\bar{m}$ is a dimensionless Henry's Law constant (lb.mol/ft.^{3} per lb.mol/ft.^{3}) and y'_2, x'_1, and x'_2 represent the conditions at a bubbling point.

Consider the mass transfer at a bubbling point.

Let the volume of vapour passing through this point be $G_P \frac{dz}{z}$ ft.^{3}/hr.

Let each bubble have a volume V_b ft.^{3}, an area a_b ft.^{2} and a residence time in the froth t_b seconds.

Then the total area existing at this point $= \frac{dz}{z} \frac{G_P a_b}{V_b} t_b$ ft^2

(and the total area on the plate $= G_P a_b t_b/V_b$ ft.^{2} $= a_P$ ft.^{2})

Now $V_b . dy = K_G . a_b .(y_e - y)\, dt$

∴ Integrating this equation between limits of $y = y_1$ $t = 0$ and $y = y_2'$ $t = t_b$ gives

$$\ln \left\{ \frac{(y_e - y_1)}{(y_e - y_2')} \right\} = K_G \ a_b \ t_b/V_b$$

$$\therefore \quad -\ln \ (1 - E^*_{MV}) = K_G \ a_b \ t_b/V_b$$

But $a_b . t_b/V_b = a_P/G_P$ $\quad \therefore -\ln (1 - E^*_{MV}) = \frac{K_G \, a_P}{G_P} = \frac{K_G \, a}{G_V}$

where a = interfacial area per ft.^{2} of plate area.

G_V = vapour rate in ft.^{3}/ft.^{2} plate area. hr.

Similarly $-\ln (1 - E^*_{ML}) = \frac{K_L \, a_P}{L_P} = \frac{K_L \, a}{L_V}$ (1;19)

where L_V liquid rate in ft.^{3}/ft^2 hr.

Chilton and Colburn[3] defined the transfer units, N_G and N_L :-

$$N_G = \frac{dy}{(1 - y)(y_e - y)}, \quad N_L = \frac{dx}{(1 - x)(x - x_e)} \qquad (1;20) \ \& \ (1;21)$$

These are "overall" transfer units and are the combination of individual "film" transfer units N_g and N_l. The following relationships can be derived:

$$N_g = \frac{k_g\ a}{G_V} \qquad N_l = \frac{k_l\ a}{L_V} \qquad N_G = \frac{K_G\ a}{G_V} \qquad N_L = \frac{K_L\ a}{L_V}$$

(1;22) to (1;25)

$$1/N_G = 1/N_g + \lambda/N_l \quad \text{and} \quad 1/N_L = 1/N_l + 1/\lambda N_g$$

$$\text{and } N_L = \lambda N_G \quad \text{where} \quad \lambda = \bar{m}.\ G_V/L_V$$

Integration of the equations defining transfer units is simplified for diffusion in dilute solution as the terms $(1 - y)$ and $(1 - x)$ may be taken as unity. This is justifiable for the humidification and oxygen desorption systems where y and x have maximum values of approximately 1.5×10^{-2} and 2×10^{-5} mol fractions respectively.

On a gas absorption plate three possible liquid mixing conditions exist,

(i) Complete or Perfect Mixing

(ii) Plug Flow or No Mixing,

(iii) Partial Mixing

These three conditions will be discussed separately.

(i) Complete Mixing

The liquid concentration on the plate is constant at the value x_2 thus all parts of the plate are equivalent and y_2' the outlet point vapour concentration equals y_2 the mean concentration.

$$\text{Thus } E_{MV} = \overset{*}{E}_{MV} = 1 - e^{-N_G} \qquad (1;26)$$

Expressing the mass transfer in liquid terms it can be shown that[19]

$$N_L = E^*_{ML}/(1 - E^*_{ML}) \qquad (1;27)$$

(ii) Plug Flow

By integrating conditions at a point over the whole plate the following equations can be derived:[19]

$$E^*_{MV} = \frac{1}{\lambda} \ln (1 - \lambda E_{MV}) \quad \text{or} \quad E_{MV} = \frac{1}{\lambda} (e^{\lambda E^*_{MV}} - 1)$$

or by expanding the series $e^{\lambda E^*_{MV}}$

$$E_{MV} = E^*_{MV} + \frac{\lambda}{2!} \cdot E^{*2}_{MV} + \frac{\lambda}{3!} \cdot E^{*3}_{MV} + \ldots\ldots \text{etc.}$$

Thus it can be seen that $E_{MV} > E^*_{MV}$ and can have values $< 100\%$ depending on the value of λ

$$\text{Also} \quad N_L = -\ln (1 - E_{ML}) \qquad (1;28)$$

(iii) Partial Mixing

This is the condition under which all gas absorption plates operate, the other two conditions of complete mixing and plug flow being of theoretical interest only as the extremes of liquid mixing. It is impracticable to use liquid point efficiencies in partial mixing studies, indeed the use of such efficiencies is rarely justifiable in view of their doubtful theoretical basis. All calculations are done using vapour plate and point efficiencies and it is thus necessary to convert vapour efficiencies to liquid efficiencies and vice-versa. This is achieved by the following equations which are derived from mass balances over the plate.

$E_{MV} = E_{ML} \Big/ \left[E_{ML} + \lambda(1 - E_{ML})\right]$ and rearranging, (1;29)

$$E_{ML} = \lambda E_{MV} \Big/ \left[\lambda E_{MV} + (1 - E_{MV})\right] \qquad (1;30)$$

Identical equations hold for point efficiencies i.e.

$$E^*_{ML} = \lambda E^*_{MV} \Big/ \left[\lambda E^*_{MV} + (1 - E^*_{MV})\right] \qquad (1;31)$$

An equation relating plate and point vapour efficiencies has been derived [19] in terms of the Peclet Number. This equation is very complicated and is always used in the graphical form shown in Figure 3.

1 : 8 Bubble Dynamics

In elucidating the mass transfer characteristics of a bubble plate, a knowledge of bubble dynamics is essential in that the bubble dynamics determines bubble size, shape, velocity, oscillation and internal circulation.

The earliest work was by Sugden[9] whose equation for bubble diameter was obtained by equating buoyancy and surface tension forces at an orifice under near-static conditions. It was soon realised[75,76] that at higher gas velocities Sugden's equation did not apply. In 1946 Geddes[8] attempted a correlation of plate efficiency using bubble sizes based on Sugden's static equation. This aroused interest in bubble mechanics and much work followed on bubble formation, the behaviour of rising bubbles and mass transfer from bubbles.

Reviews of the literature on bubble formation are given by Hughes, Handlos, Evans and Maycock[78] and Davidson and Schuler[79]. The current theories on bubble formation are outlined below.

It is impossible to correlate bubble diameter and velocity against orifice diameter and gas velocity, completely in one equation as with increasing gas velocity the bubbling mechanism passes through several different phases. At low gas velocities, bubble diameter is correlated by Sugden's equation[9,82,77,84]. As the gas velocity increases the bubble frequency increases, bubble diameter remaining substantially constant[77,80,82]. A critical frequency is reached at about 15 to 20 bubbles per second at which the frequency remains constant and increasing velocity increases bubble diameter[28,81,82,86]. At still higher gas velocities a gas jet forms which breaks up into bubbles of a variety of sizes[81,83].

In the constant frequency regime chain bubbling occurs, that is, there is no substantial gap between successive bubbles since the rising velocity is not sufficient to separate them[85,28].

The submergence of the orifice or slot may affect bubble formation since a bubble may burst at the liquid surface before having disengaged from the gas source thus giving a direct discharge to the vapour space[15,16].

Surface tension has little effect on bubble formation in the constant frequency regime[85,23] but is important at lower gas velocities.

Viscosity has little effect at low gas velocities[84] but at high velocities the bubble diameter is largely determined by the disengagement period during which the bubble "neck" seals and which depends on the liquid viscosity[87,79]. Thus viscous liquids tend to give larger bubbles.

Orifice diameter plays an important part in determining bubble diameter. In the low gas velocity regime the bubble diameter is proportional to the cube root of the orifice diameter[23]. Orifice diameter, in determining gas velocity also influences the regime in operation. Most of the work on bubble formation has been done on horizontal circular orifices as in sieve plates. In bubble cap plates the "effective" orifice diameter depends on the slot opening which in turn depends on the gas velocity.

Surface Area on Bubble Plates

Chu *et al*[93] measured the surface area and contact time of bubbles from a slot and elucidated the dependence of these quantities on gas velocity, slot size and submergence and surface tension. A high speed cine technique was used and the analysis of the film was very tedious. Calderbank[91,92] measured the surface area of bubbles in an agitated tank and on a sieve plate by a light transmission technique. This method is superior to that of Chu permitting quick measurement and assessment of surface area. Correlations for interfacial area on a sieve plate are given. Calderbank, Evans and Rennie[94] devised a similar optical reflection method for determination of surface areas and a gamma ray absorption technique for measurement of foam density. Calderbank and Moo Young[95] used these methods in determination of interfacial area on sieve plates.

Internal Circulation of Bubbles

It has been shown by Bond and Newton[88] that below a critical diameter, about 1 to 2 mm, drops or bubbles behave like perfect spheres with no internal circulation. Internal circulation affects rising velocity, oscillation, surface renewal and hence heat and mass transfer to the bubble.

Garner and Hammerton[74] observed internal circulation in bubbles by traces of ammonium chloride and showed the importance of the presence of surface active agents.

Calderbank and Karchinski[90] and later Calderbank[92] showed that rates of heat and mass transfer to circulating and non-circulating bubbles are quite different, presumably owihg to the increased rate of surface renewal in the circulating bubbles.

Garner and Hammerton[89] in tests on bubbles of diameter up to 0.8 cm. concluded that up to a diameter of 0.4 cm. mass transfer rates were those expected of a non-circulating sphere. Above 0.4 cm the data suggested internal circulation of the bubbles.

1 : 9 Approach to the Problem

The aim of this work was to determine the operating characteristics, including plate efficiency and pressure drop, of two sizes of Kuhni plate and to suggest improvements in design.

Through the generosity of two local firms, Blairs Ltd, (the manufacturers) and the British Dyewood Coy Ltd two Kuhni plates were provided of 30 inch and 12 inch diameter. The 12 inch diameter plate is the smallest plate available and the 30 inch plate the largest that could be comfortably accommodated in the available laboratory space.

Plate efficiency characteristics can be determined by either distillation or gas absorption systems. A distillation system would have required a considerable amount of auxiliary heat exchange equipment and preferably a column with several plates. In addition, it was felt that an investigation of mass transfer on a bubble plate is easier with gas absorption systems where thermal and other complicating effects do not exist to the same extent.

It has been established[25] that plate efficiency characteristics depend on the distribution of mass transfer resistance between the gas and liquid phases. It was thus decided to use one gas absorption system with the controlling resistance in the gas phase and one with the controlling resistance in the liquid phase.

The humidification of air was chosen as the gas phase resistant system principally because the materials required, air and water, are readily available and cheap. The alternative of using a very soluble gas, such as ammonia was discarded because of the difficulty, inconvenience and expense of using such a gas on a large scale.

The choice of a liquid phase resistant system is usually confined to the absorption or desorption of a slightly soluble gas in a liquid. The liquid chosen is usually water for convenience and in this work oxygen was chosen as the gas in preference to carbon dioxide, nitrogen or any other slightly soluble gas owing to the ease with which it can be determined volumetrically.

For a complete elucidation of the liquid phase resistant system a knowledge of the residence time characteristics of the liquid on the plate is necessary. The efficiency depends on the degree of liquid mixing on the plate, and the liquid hold-up and mean residence time are important in determining plate efficiency. It was decided to determine the residence time characteristics by a tracer technique for the 30 inch plate.

The small liquid hold up on the 12 inch plate makes accurate residence time determination, by tracer methods, difficult, so liquid hold-up was measured by clear liquid height manometers fitted to the plate floor. As a check on the reliability of this method for determining liquid hold-up, clear liquid height measurements were made on the 30 inch plate and compared with the residence time data.

Liquid viscosity has been recognised as a very important factor in determining plate efficiency since it affects both the mass transfer rates and the fluid dynamics of the plate It was decided to obtain data on the dependence of both liquid and gas phase resistant system efficiencies on liquid viscosity and to determine the effect of liquid viscosity on the fluid dynamics of the plate by residence time methods. A viscosity-increasing agent was selected for addition to water which has little effect on the other physical properties of water. The effects of this agent on the solubility and diffusivity of oxygen in water, the density and water vapour pressure were also determined.

Plate pressure drop on the Kuhni plate is reputedly high and this was confirmed by experiment. Attempts were made to improve plate performance on the 30 inch plate by increasing the slot area, thus reducing pressure drop, and by increasing the weir height.

Whenever possible tests were designed on a factorial basis to obtain the maximum amount of information from the results.

SECTION 2

DESCRIPTION AND DESIGN OF THE EXPERIMENTS

2 : 1 The Humidification System

This method requires a knowledge of the inlet and outlet air humidities and the equilibrium humidity. Two methods are generally used, one described by Gerster Bonnet and Carmody[25], the other by Garner and Freshwater[29].

(i) Gerster's Method, (Outlet hygrometer)

In this method both the inlet and outlet humidities are measured by wet and dry bulb hygrometers and the equilibrium humidity taken as the saturation humidity at the water temperature, which is constant and equal to the inlet air wet bulb temperature.

The main criticism of this method is that the outlet humidity is artificially raised by evaporation of entrained water between the plate and the hygrometer. A baffle to remove the entrainment provides a wetted surface to the air stream causing additional humidification. Gerster introduced a correction for this effect, which amounted to 1% to 2% in the efficiency.

(ii) Garner and Freshwater's Method (Solution Evaporation)

In this method the inlet humidity is measured by a hygrometer and the equilibrium humidity taken as the saturation humidity at the outlet air dry bulb temperature. This temperature was chosen since it could not be assumed that conditions were adiabatic.

A dilute (2 - 5%) solution of sodium carbonate in water is used in the system and the outlet humidity deduced by measuring the amount of water evaporated during the test. The principle is that water is lost by evaporation but solution by entrainment. The amounts of water lost by each method can be found from mass balances.

Let W_1 and W_2 be the initial and final weights of solution, (lb)
C_1 and C_2 be the initial and final concentrations of solute
W_E be the weight of solution entrained during the test (lb)
W_V be the weight of water evaporated during the test (lb)

By mass balances on the water and solute:

$$W_1 - W_2 = W_E + W_V \tag{2:1}$$

$$W_1 C_1 = W_2 C_2 + W_E (C_1 + C_2)/2 \tag{2:2}$$

These two equations can be solved for W_E and W_V

The use of the average of C_1 and C_2 for the effective concentration of the entrainment infers that the concentration of the solution increases linearly with time. This assumption is justifiable only if C_1 and C_2 are not different by more than 10%. This necessitates using a very large water reservoir unless water is added continuously to maintain a constant solute concentration.

The advantages of using this procedure of adding water continuously are that a small reservoir can be used, the effect of the solute on the system properties is constant and the solution temperature is more constant. This method, which was devised in the course of this work, was found to give greater accuracy.

In calculating the evaporation and entrainment the amount of water added to the reservoir is added to the left hand side of equation (2:1) and the equations solved as before.

Garner and Freshwater's method is more accurate than Gerster's if constant conditions can be maintained for about 5 hours, the duration of a test.

It was decided to do tests by both methods and compare the results. These are given in Figure 38, where the points represent the sodium carbonate solution evaporation efficiencies and the lines the outlet psychrometer efficiencies and it can be seen that there is very little difference. Gerster's method was chosen for the remaining tests, its main advantages being that more tests could be done in a given time and that the inlet humidity need only remain constant for about 30 minutes compared with 5 hours for the other method, an important consideration since the inlet air humidity could not be controlled.

(iii) Psychrometric Data

Inlet and outlet humidities were measured by forced draught wet and dry bulb psychrometers. The air velocity of 20 ft/sec. past the wet bulb was sufficient to make radiation effects negligible[118]. The accuracy of the thermometers was ± 0.1F.

Humidities were deduced from the following equation:-

$$H = H_S - 1.72 (T_d - T_w) \qquad (2:3)$$

where H = the air humidity in grains water per pound of dry air

H_S = the saturation humidity at the wet bulb temperature (Gr/lb) (found from data in the IHVE Guide 1955[112])

T_d = the dry bulb temperature, °F

T_w = the wet bulb temperature, °F

The constant 1.72 is from data of Lewis[113] and is the ratio

$$\frac{0.26 \times 7{,}000}{\lambda_W}$$

where 0.26 is the ratio of mass and heat transfer coefficients for evaporation of water,

λW is the latent heat of evaporation of water at the mean wet bulb temperature, taken as 1,058 BTU/lb (59°F)

(iv) Calculation of Efficiency

Efficiencies were deduced using the equation,

$$E_{MV} = \frac{H_2 - H_1}{H_e - H_1} \qquad (2:4)$$

where H_1 = the inlet humidity, grains/lb. dry air

H_2 = the outlet humidity, grains/lb. dry air.

H_e = the equilibrium humidity, grains/lb. dry air.

The equilibrium humidity was taken as the saturation humidity at the mean water temperature. It was found that once conditions had stabilised the inlet and outlet water temperatures differed by less than 0.5°F and the outlet wet bulb temperature differed by less than 0.2°F from the outlet water temperature.

(v) Heat Balance on the Humidification System.

A heat balance readily shows that the inlet air is heated by 6 to 12° F by the blower, depending on the air rate and the ambient temperature. Also, one of the psychrometers blew the air across the thermometers and a slight heating effect of the blower was noted. Since the inlet air was sampled before it passed through the blower the air enthalpy indicated by the inlet psychrometer was lower than that of the air entering the column. Tests on the systems showed conditions to be adiabatic for both the 12 inch and 30 inch plates. A specimen heat balance is given in Appendix A:2 .

2 : 2 The Oxygen Desorption System

It was decided to pass the feed water to the plate down a packed column containing oxygen under slight pressure (3 p.s.i.g.) to increase the oxygen content from the equilibrium concentration of 10 parts per million (p.p.m.) to 30 to 40 p.p.m. On the plate this excess oxygen was partly desorbed from the water by the air stream.

The efficiency of desorption was deduced from the equation

$$E_{ML} = \frac{X_1 - X_2}{X_1 - X_e} \qquad (2{:}5)$$

Where X_1 = the inlet water dissolved oxygen content (p.p.m.)

X_2 = the outlet water dissolved oxygen content (p.p.m.)

X_e = the equilibrium dissolved oxygen content (p.p.m.)

The equilibrium oxygen content was deduced from data in the International Critical Tables[114] and is taken as the oxygen content in equilibrium with air saturated with water vapour at the mean water temperature and the atmospheric pressure. The oxygen solubility data can be given by the equation.

$$H_{O_2} = (2.486 + 0.0554\,(T' - 10)) \times 10^7 \qquad (2{:}6)$$

where H_{O_2} = the Henry's Law Constant (mm Hg)

T' = the temperature °C

Dissolved oxygen contents were measured by the Winkler method (Appendix C).

It was found that the oxygen content of the inlet water decreased steadily during a test by about 2 p.p.m. per hour. This was attributed to nitrogen desorbing from the water in the oxygenation tower and reducing the partial pressure of the oxygen. The error thus caused by assuming the nitrogen content of the inlet water to be that in equilibrium with air is less than 0.1% and was neglected.

2 : 3 Selection of Viscosity - Increasing Agents

It was decided to determine the effect of changes in liquid viscosity on both gas phase and liquid phase resistance controlling systems and on residence time distributions. To enable the maximum amount of information to be obtained a substance was required that increased the viscosity of water with as little effect as possible on density, oxygen solubility or vapour pressure. "Cellofas B", the sodium salt of carboxy methyl cellulose manufactured by I.C.I., was chosen in preference to sugar or glycerol, the usual agents. The effects of "Cellofas B" on the properties of water were examined and are described in Appendix D. As can be seen the effect on density and water vapour pressure are negligible so that "Cellofas B" is thus preferable to sugar both as regards properties and cost. Jordan[127] has shown that the oxygen diffusivity characteristics of both sugar and glycerol solutions are irregular which would complicate the elucidation of the effect of viscosity on plate efficiency. In the liquid residence time tests, discussed in Section 2:4, sugar was used to change the water viscosity because of the effect of the salt tracer on the viscosity of "Cellofas B" solutions. It was found that even a trace of electrolyte reduced the viscosity of "Cellofas B" solutions considerably, presumably because of the break up of the inter-molecular bonds. The effect of electrolytes on the viscosity of sugar solutions on the other hand is very small. Potassium chloride was, however, chosen as the tracer in preference to sodium chloride which was used for the tests with water since the effect of the potassiumion is less than that of the sodium ion.

2 : 4 Selection of Liquid Residence Time Method

To establish the residence time distribution in a fluid system some property of the inlet fluid must be changed either suddenly or continuously and this property measured at the outlet. The effect of the change should be as small as possible on the dynamics of the system. The commonest property chosen is conductivity which can be easily changed by addition of small quantities of electrolyte and has the advantage that it is easily convertible to an electrical output which can be recorded.

Several methods have been used in determining residence time distributions. The tracer can be injected instantaneously giving the familiar skew Gaussian concentration-time graph at the outlet, the concentration rising to a maximum then falling off to the original base line. A steady flow of tracer can be fed to the system then suddenly stopped and the gradual reduction in tracer concentration at the outlet recorded. This method[106] gives the "cumulative distribution" function direct, that is, the integrated form of the concentration - time curve. Conversely a steady flow of tracer can be started and the build up to steady outlet concentration recorded. A more elaborate method[107] is to inject tracer at the inlet with sinusoidally varying concentration at constant frequency and record the concentration amplitude at the outlet. Another method is to inject tracer continuously near the outlet and measure the tracer concentration at points nearer the inlet. This method is suitable for plates with a long liquid path length.

It was decided that the simplest procedure, that of injecting a pulse of tracer at the inlet, was most suitable. The tracer chosen was saturated sodium chloride solution and an injector was devised which would inject about 1 cc. of this solution over a very short period of time (<0.1 second) into an inlet to the plate on the periphery. The injector contained a pair of platinum wires (suitably connected to the recording circuit) which would enable an input time signal to be recorded.

A circuit which recorded the input time signal and the outlet conductivity continuously was constructed and is described in Section 3:5.

The problem of measuring the outlet conductivity as near to the plate outlet as possible was solved by constructing a cell on the inner wall of the outlet weir. The outlet water thus flowed over the weir and made immediate contact with the cell. Two parallel platinum wires mounted 1/4 inch apart and mounted round the inside of the weir formed the cell. Provided the distance between the wires is constant, the relationship between the quantity of tracer between the wires and conductivity is as follows:

$$K' = A + BQ \qquad (2:7)$$

where K' is the conductivity, A and B are constants and Q is the mass of tracer between the wires. This equation was confirmed by operating the plate with solutions of known concentration and measuring the resultant conductivity.

It is a reasonable and necessary assumption that the liquid between the wires is constantly changing and has the same concentration as the bulk of the liquid flowing over the weir. The effect of air bubbles carried over the weir is to give a "wavy" line on the chart. The amplitude of the deviation was normally less than 10% of the conductivity reading.

It is likely that the number of bubbles interfering with the operation of the cell is approximately constant throughout a test and their overall effect can be neglected. It was noted that the "base line" conductivity depended on both the gas and liquid rates, this effect being attributed to differing degrees of interference by bubbles.

From the outlet tracer concentration curve the mean residence time of the liquid on the plate, the liquid hold-up and the degree of mixing can be deduced. Appendix B gives the derivation of the equations used in determining these quantities.

The system selected will therefore record the degree of radial mixing of the tracer and give the residence time distribution of the liquid flowing across the plate. It will, however, give no indication of the degree of lateral mixing. To accomplish this by conductivity means would require a very elaborate apparatus thus a simpler method of continuously injecting dye at an inlet point and observing the "spread" of dye was devised. A 5% solution of "Wool Green" dye in water was injected at about 1 cc. per second at the plate periphery through a narrow copper tube. When conditions had stabilised a photograph was taken from a height of 5 feet above the plate, using a red filter. Photographs were taken at a variety of air rates, water rates and injection points and they are discussed later in Section 5:5

2 : 5 Alterations in Plate Design

By comparison with other bubble plates the Kuhni plate has a high pressure drop and a low weir height.

The total plate pressure drop can be regarded as the sum of three component pressure drops.

(i) Dry plate pressure drop.

(ii) Hydrostatic pressure drop or clear liquid height.

(iii) "Residual" pressure drop.

The "residual" pressure drop is a combination of the effects of inertial forces and surface tension. This analysis of plate pressure drop is an over-simplification since all the effects causing the pressure drop do not necessarily act simultaneously during the bubbling cycle, but it is, however, sufficiently accurate for the purposes of this work. The Kuhni plate, despite its low weir height and correspondingly low clear liquid height has a relatively high pressure drop, attributable to the small slot area causing a high "dry plate" pressure drop. It was decided to increase the slot area of the 30 inch plate and determine the resultant effect on pressure drop and efficiency. This was achieved by raising the annular rings of the plate and is discussed later in Section 3:10.

The effect of increasing the weir height is generally to increase both pressure drop and gas phase efficiency. It was decided to determine the effect of this change on pressure drop and efficiency of the 30 inch plates

Since most industrial gas absorption and distillation systems are "gas film" controlling, the humidification efficiency was used although a complete appraisal of the effect of alterations in plate design would require liquid "film" efficiency tests as well.

2 : 6 Properties of Solutions of "Cellofas B" in Water

In the humidification tests the humidities depend on the vapour pressure of the water on the plate. The addition of a solute such as "Cellofas B" will reduce this vapour pressure and affect the psychrometric data. It is essential that the magnitude of this effect be known by measuring the vapour pressure of "Cellofas B" Solutions.

In the oxygen desorption tests the effect of increasing viscosity is not only to change the fluid dynamics of the plate but possibly also to change the oxygen solubility and the mass transfer coefficient through a change in oxygen diffusivity. The effect of "Cellofas B" on oxygen solubility and diffusivity in water was unknown and it was decided to obtain some data for this system. The effect of "Cellofas B" on solution density, viscosity, vapour pressure, oxygen solubility and diffusivity is described in Appendix D.

The measurement of the diffusivity of such a system is rather difficult, different methods giving conflicting results. Several methods are available for determining diffusivity. Measuring diffusion rates through porous discs[121] is complicated by the necessity to calibrate the disc at each viscosity with systems of known diffusivity and equal viscosity. Other methods such as capillary diffusion[123] or diffusion through quiescent interfaces[122] suffer from the time involved for each determination and the difficulty of analysing such small quantities of liquid. Wetted wall methods have the disadvantage that rippling has a marked and uncertain effect on mass transfer rates. A considerable advance in methods of determining the diffusivity of slightly soluble gases has been made by Davidson & Cullen[62] who devised a method in which the liquid flows over the surface of a sphere in an enclosed chamber and the rate of gas absorption measured directly by metering the gas. This method gives repeatable results and is relatively quick and easy. It was thus chosen for these determinations and is described in Appendix D.

SECTION 3

DESCRIPTION OF THE APPARATUS

The performances of a 12 inch and a 30 inch diameter Kuhni plate have been investigated. These plates were incorporated in separate plants which will be discussed individually. The general design of both plates and plants is described, followed by the modifications required for humidification, oxygen desorption and residence time tests.

3 : 1 Design of the 30 inch Diameter Kuhni Plate

Photographs and a drawing of the plate are given in Figures 1 and 4. The plate was constructed in 17 S.W.G. copper with brass supporting angle and copper and brass bolts. There were three annular tunnel bubble caps at diameters of 13.19, 18.32 and 23.42 inches. These caps were 0.95 inch high and 1.18 inches broad with slots 3/32 inch deep by 9/16 inch long spaced 1/8 inch apart. There was a total of 614 slots giving a total slot area of 30.06 square inches which represents 4.25% of the column cross sectional area.

The outer ring had slots on the inside and was sealed on the outside to the column wall. The central weir had an internal diameter of 9.37 inches and was 2.56 inches deep at that diameter, tapering to a 2.75 inch internal diameter downcomer. The weir height was 0.95 inch and the liquid path length 10.2 inches.

The inlet distributing well which would have acted as a seal pot for the plate above had 12 radial 5/8 inch bore copper tubes sloping down to the periphery at an angle of 1° to the horizontal. Flush tappings were made in the floors each of each of the four troughs and connected to "clear liquid height" manometers.

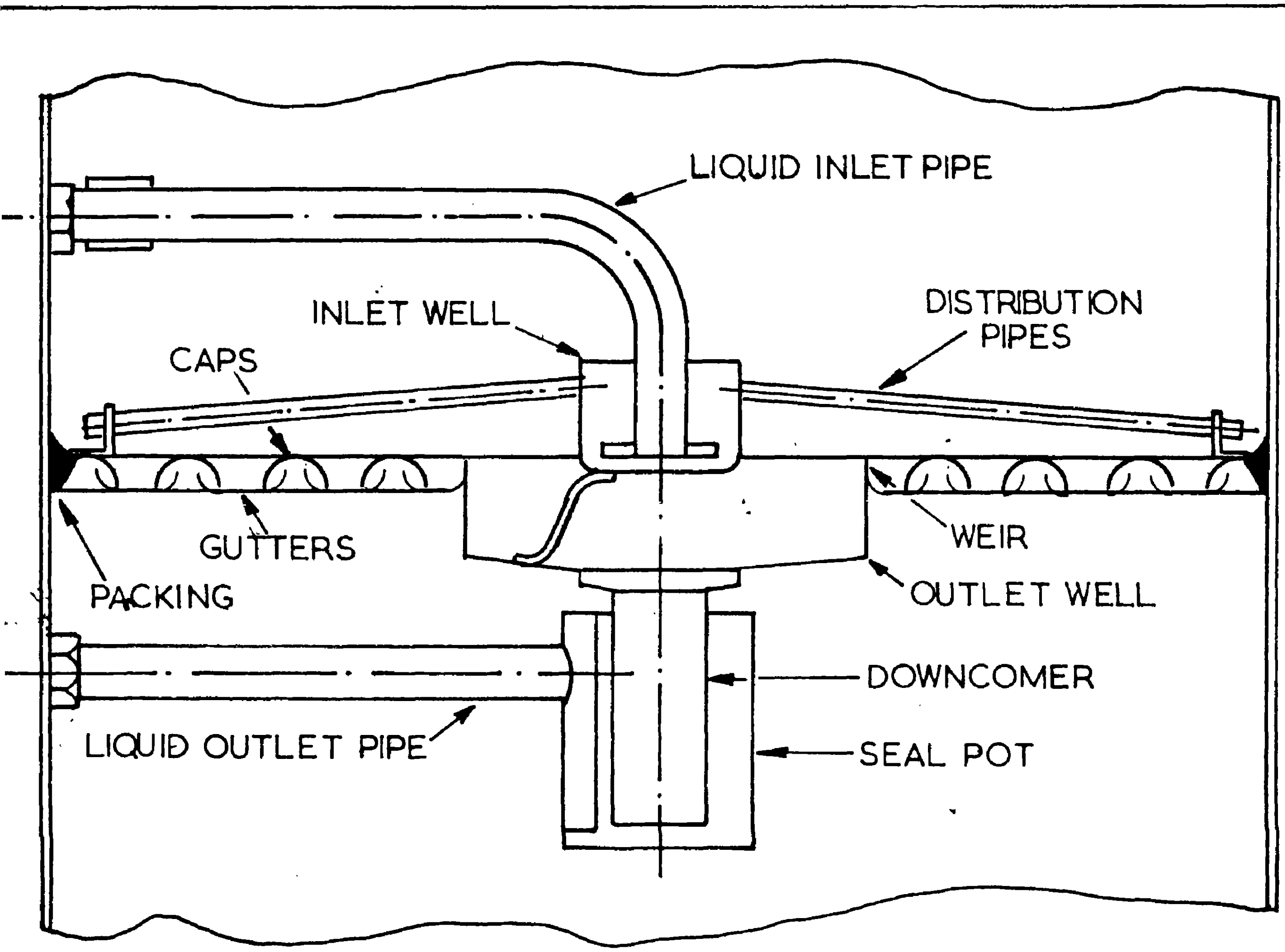
LIQUID INLET PIPE
INLET WELL
DISTRIBUTION PIPES
CAPS
GUTTERS
WEIR
PACKING
OUTLET WELL
DOWNCOMER
LIQUID OUTLET PIPE
SEAL POT

SIDE ELEVATION SCALE - 1 to 5

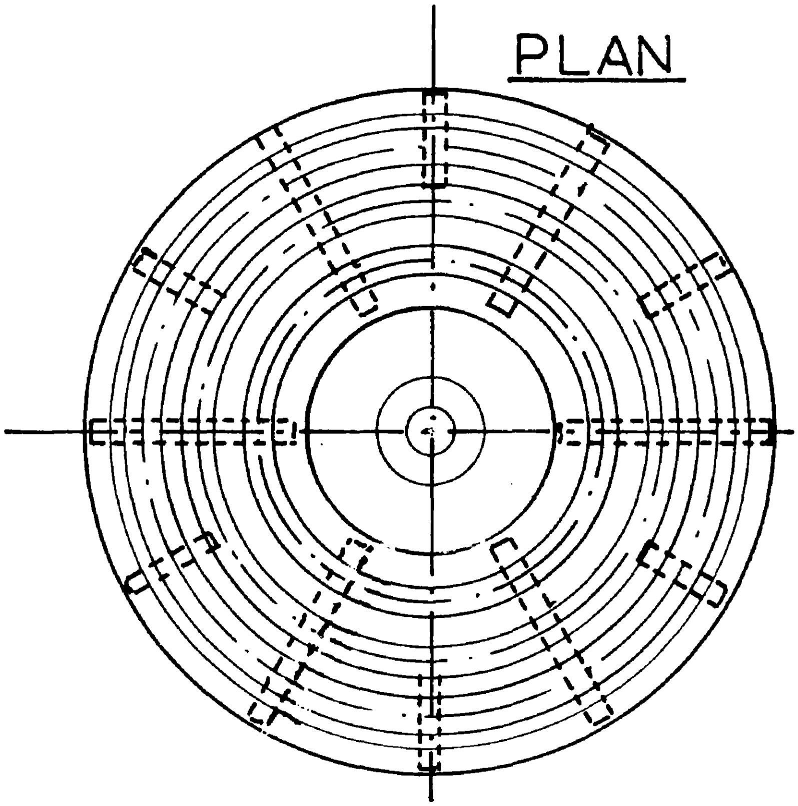

THE
30 INCH DIAMETER
KUHNI
DISTILLATION
PLATE

FIG 4

3 : 2 General Design of the 30 inch Kuhni Plate Plant

The general arrangement of the plant is illustrated in Figure 5. A Keith Blackman centrifugal fan capable of delivering 25,000 cubic feet of air per hour at 6 inches water head was driven by a 5 h.p. electric motor. Air was drawn to the fan inlet through 8 inch diameter ducting in which an orifice meter and a butterfly control valve were fitted. From the fan outlet the air passed to the base of the galvanised steel test column through a steam heater which was not used in the present work.

After passing through the plate the air was discharged to the atmosphere outside the laboratory by a length of 8 inch diameter flexible ducting. The top of the test column was constructed in 1/4 inch thick "Perspex". A drainage hole was provided in the base plate of the column.

Water was pumped from a 22 gallon galvanised steel tank by a Stuart-Turner centrifugal pump, capable of delivering 720 gallons of water per hour at 5 feet head, through a control valve to a "Rotameter" reading from 50 to 500 gallons per hour. From the "Rotameter" the water was piped to the central inlet well of the plate. The outlet water passed down the central downcomer to a seal pot and through the outlet pipe which returned it to the water tank.

The Kuhni plate was sealed into the test column by asbestos cord and putty packing. A "Perspex" window was built into the column wall above the plate for observation of froth heights, a scale engraved on this window and a scale fitted in the central well being viewed simultaneously to avoid

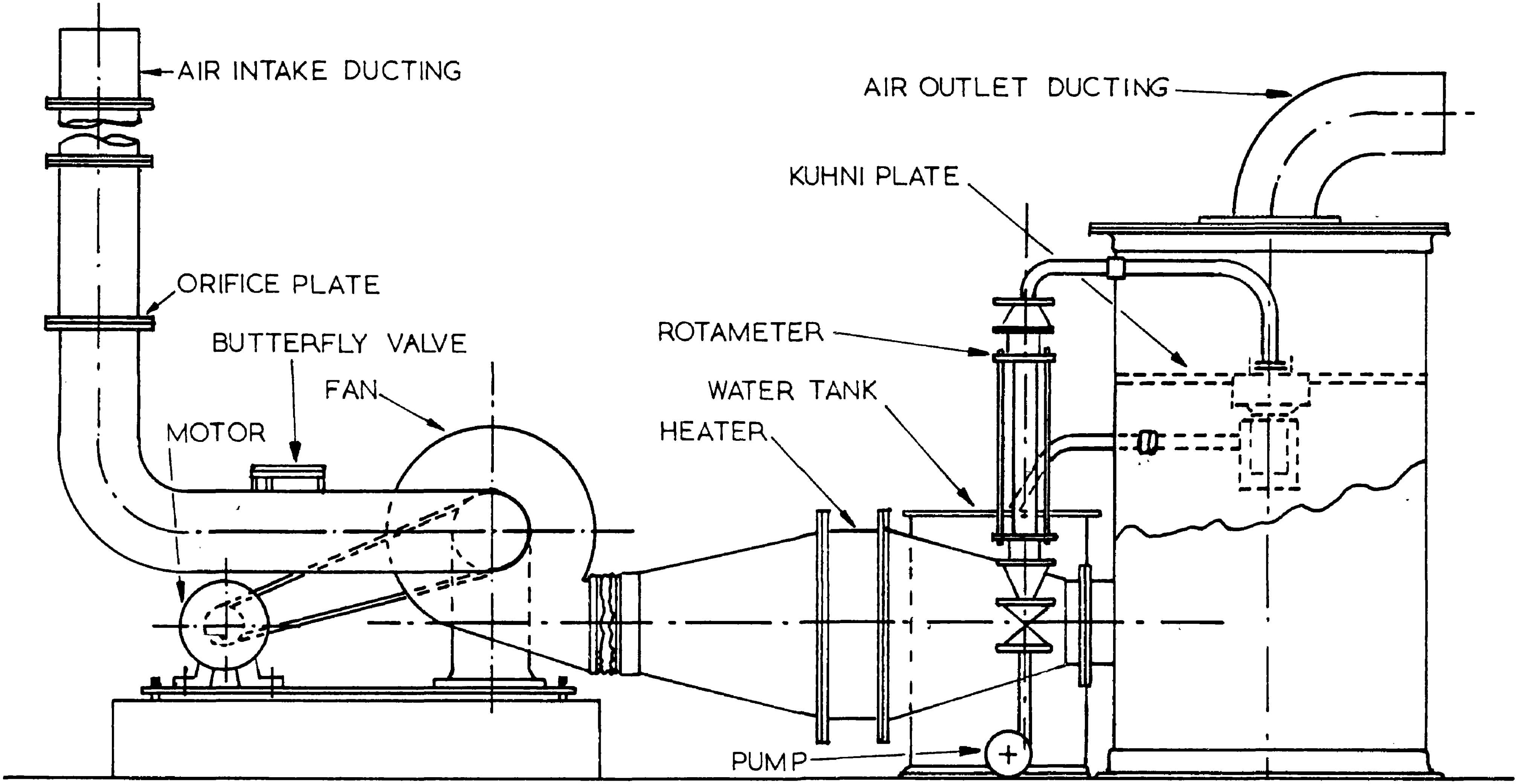
AIR INTAKE DUCTING
AIR OUTLET DUCTING
KUHNI PLATE
ORIFICE PLATE
BUTTERFLY VALVE
ROTAMETER
FAN
WATER TANK
MOTOR
HEATER
PUMP

FIG 5 GENERAL ARRANGEMENT 30 INCH KUHNI PLATE PLANT

parallax errors.

Air flow was measured by a 4.714 inch diameter sharp edged orifice plate with D and D/2 tappings in the 8 inch diameter inlet duct. The pressure differential was measured by an "Askania" micromanometer. The calibration for this meter was taken from B.S.1042 (1943).

The Kuhni plate pressure drop was indicated on a U tube water manometer.

On the water circuit temperatures were measured before and after the plate by thermometers accurate to ± 0.1°F.

3 : 3 Modifications for Humidification Tests (30 inch Plate)

The inlet air humidity was measured continuously by blowing a sample stream, taken from the entrance to the inlet duct, across the bulbs of dry and wet bulb thermometers, both accurate to ± 0.1°F, at a velocity of approximately 20 feet per second. A sample of the outlet air was drawn from the outlet duct and passed through a similar psychrometer. A drawing of one of these electrically driven psychrometers is given in Figure 6.

In the humidification tests in which sodium carbonate solution was evaporated a constant level device was fitted to the water tank to replenish the water as it evaporated and thus maintain the sodium carbonate solution concentration constant. This is shown in Figure 7.

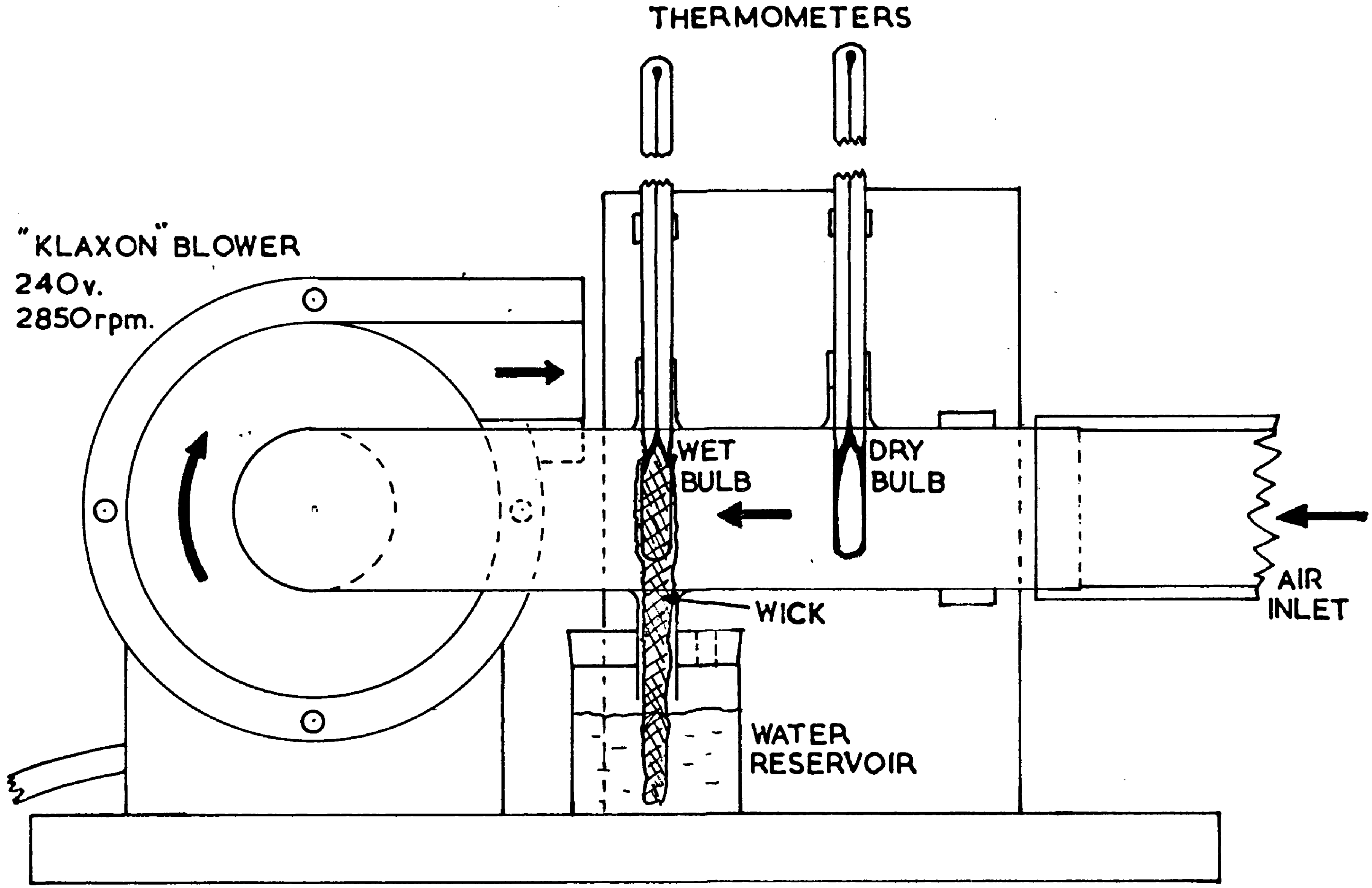
THERMOMETERS
"KLAXON" BLOWER
240v.
2850rpm.
WET
BULB
DRY
BULB
WICK
WATER
RESERVOIR
AIR
INLET

FORCED DRAUGHT WET & DRY BULB PSYCHROMETER – FIG 6

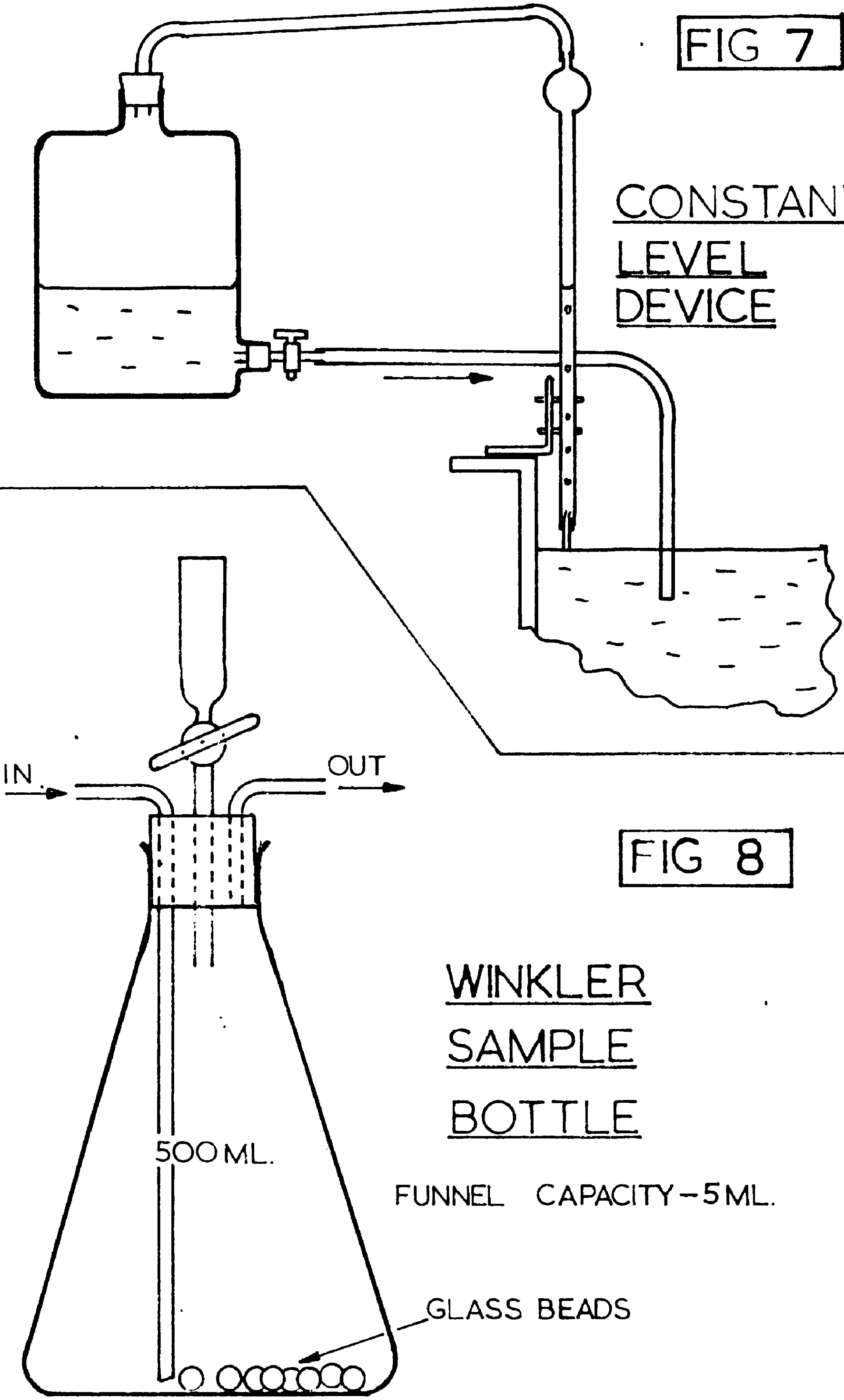
IN.
OUT
500 ML.
GLASS BEADS

FIG 7

CONSTANT LEVEL DEVICE

FIG 8

WINKLER SAMPLE BOTTLE

FUNNEL CAPACITY – 5 ML.

3 : 4 Modification for Oxygen Desorption Tests (30 inch plate)

Drawings of the oxygenation equipment and sample bottles are given in Figures 8 and 9.

The feed water was sprayed into the top of a 9 inch diameter oxygen absorption column containing a 4 foot bed of "Tellerette" polythene packing. Oxygen was fed to the tower from a pressure cylinder at a controlled rate. The oxygen-rich water was raised from the foot of the column to a 1 gallon glass settling tank 4 feet above the plate. From this tank the water flowed through a level-regulating tap to the central inlet well of the plate.

A sample stream of the inlet water was siphoned continuously from the settling tank through a sample bottle and a "Rotameter" which read from 0.2 to 2 gallons per hour. A sample of the outlet water was similarily taken from the outlet pipe, both sample streams draining to the main water tank.

FIG 9

OXYGEN ABSORPTION APPARATUS

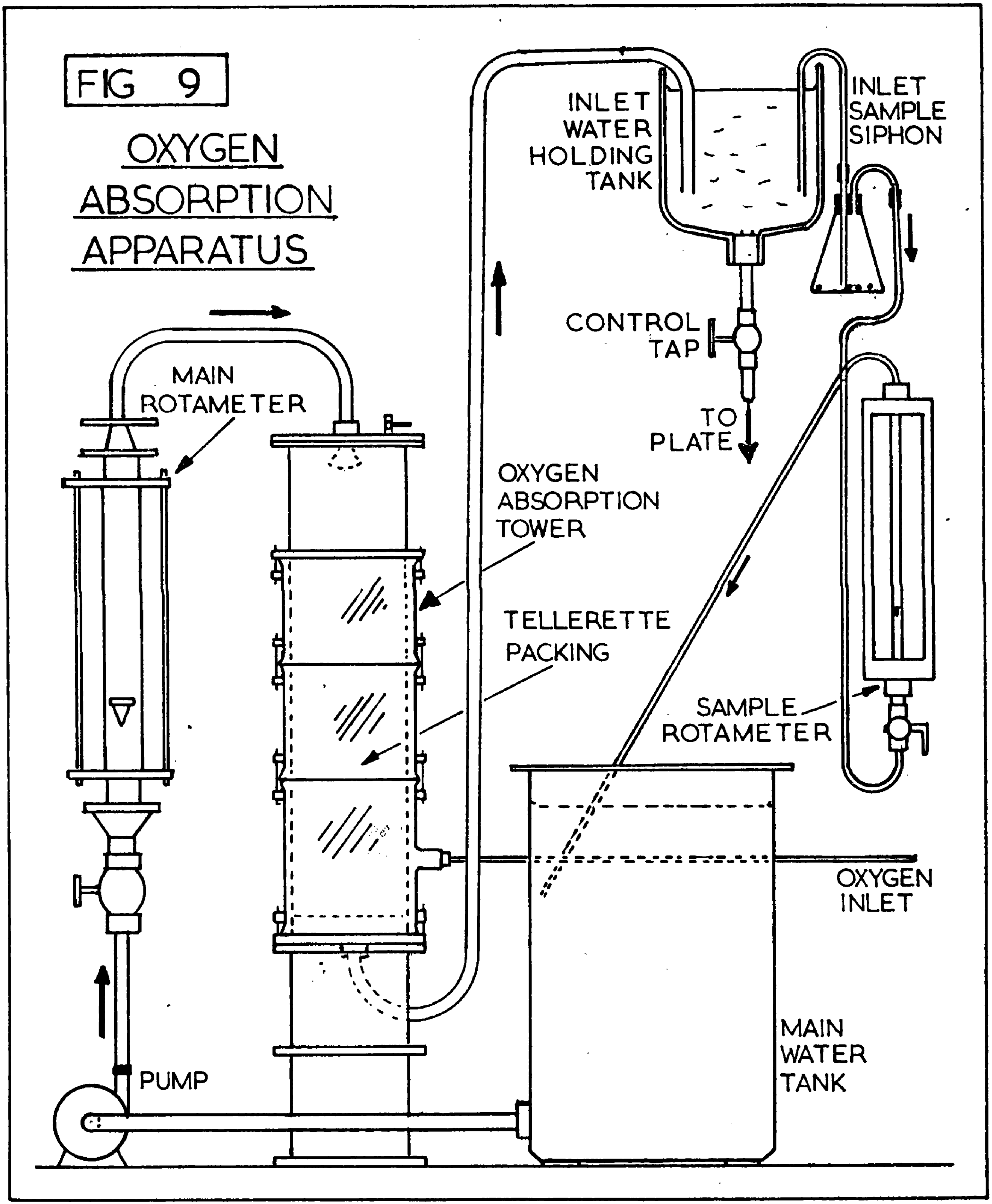
INLET WATER HOLDING TANK
INLET SAMPLE SIPHON
CONTROL TAP
TO PLATE
MAIN ROTAMETER
OXYGEN ABSORPTION TOWER
TELLERETTE PACKING
SAMPLE ROTAMETER
OXYGEN INLET
MAIN WATER TANK
PUMP

3 : 5 Modifications for Residence Time Tests (30 inch plate)

As discussed earlier (Section 2:4) it was decided to obtain residence time distributions by injecting tracer instantaneously at the plate periphery and measuring the conductivity of the outlet water immediately it passed over the outlet weir.

The injection device is shown in Figure 10. A hand bulb blower was connected to the side arm and the device primed with 1 cc. of saturated salt solution added by a pipette through the ground glass joint. With the stopper in position the solution could be ejected by compressing the hand bulb. As the solution left the device it momentarily made electrical contact between two suitably placed platinum wires, this registering as the input time signal on the recorder chart. The design of the device prevented dripping after ejection.

The conductivity cell is shown in Figure 11. It consisted of two parallel 24 inch lengths of 24 S.W.G. platinum wire 1/4 inch apart, held in position by "Perspex" formers attached to the weir by 6.B.A. bolts. Paper impregnated with "Araldite" epoxy resin adhesive insulated the wires from the weir. One end of each wire was connected to the recording equipment by screened cable.

The cell formed one arm of an unbalanced resistance bridge circuit operating at 10 volts, 1,000 cycles per second A.C. Output from this bridge was rectified, amplified and recorded on a Kelvin-Hughes single channel Mark 5B Recorder with a chart speed of 2.5 cm per second. Teledeltos chart paper 5 cm wide was used in which the trace was burned by a 300 volt arc at the point of the pen. A general circuit diagram is given in Figure 13.

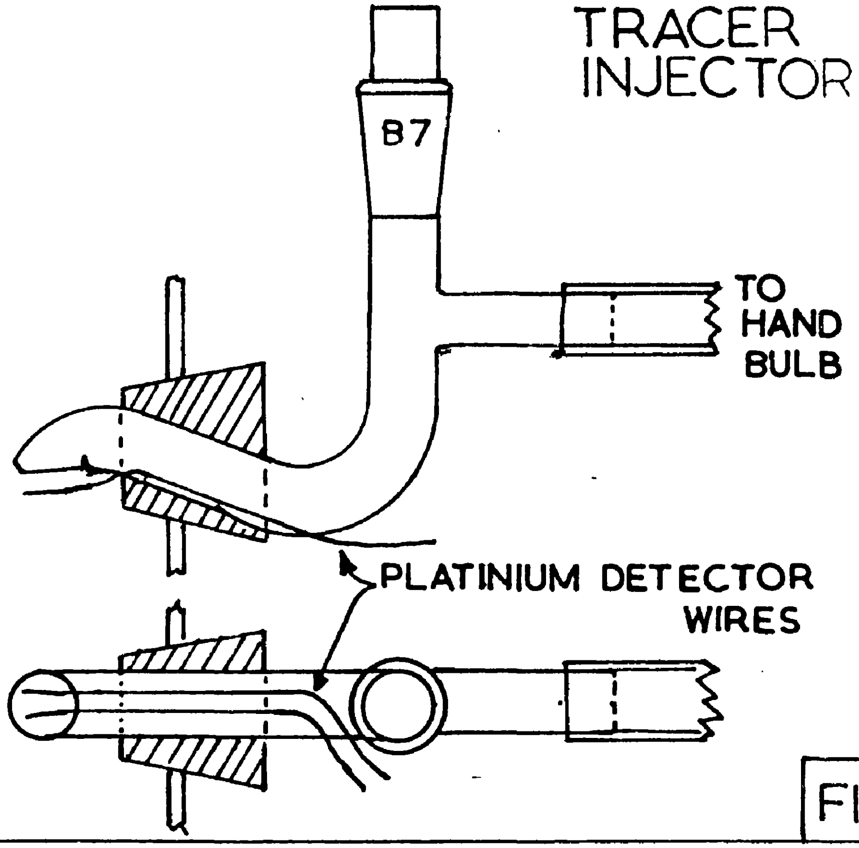
B7
TO HAND BULB
PLATINIUM DETECTOR WIRES

TRACER INJECTOR

FIG 10

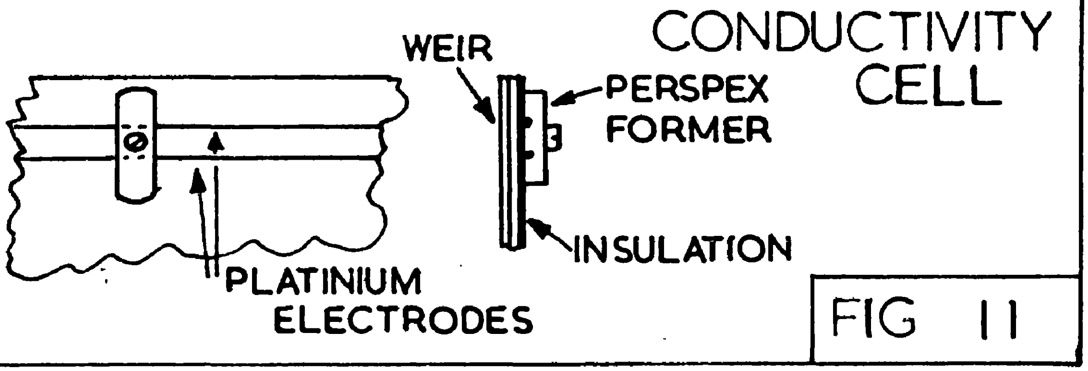
WEIR
PERSPEX FORMER
INSULATION
PLATINIUM ELECTRODES

CONDUCTIVITY CELL

FIG 11

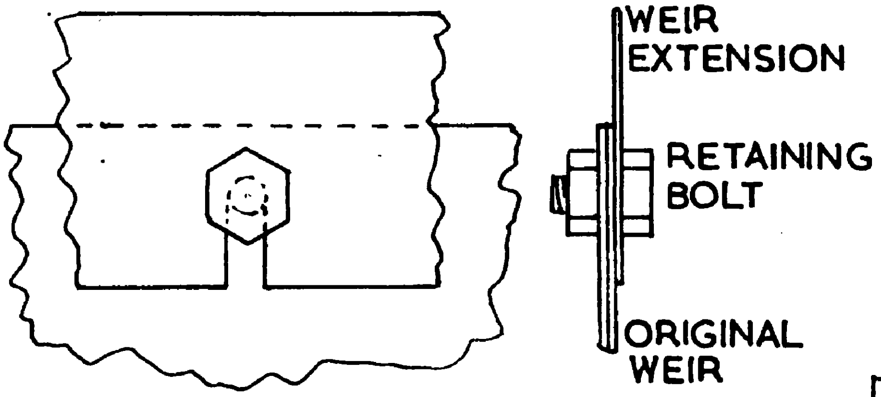
WEIR EXTENSION
RETAINING BOLT
ORIGINAL WEIR

WEIR EXTENSION

FIG 12

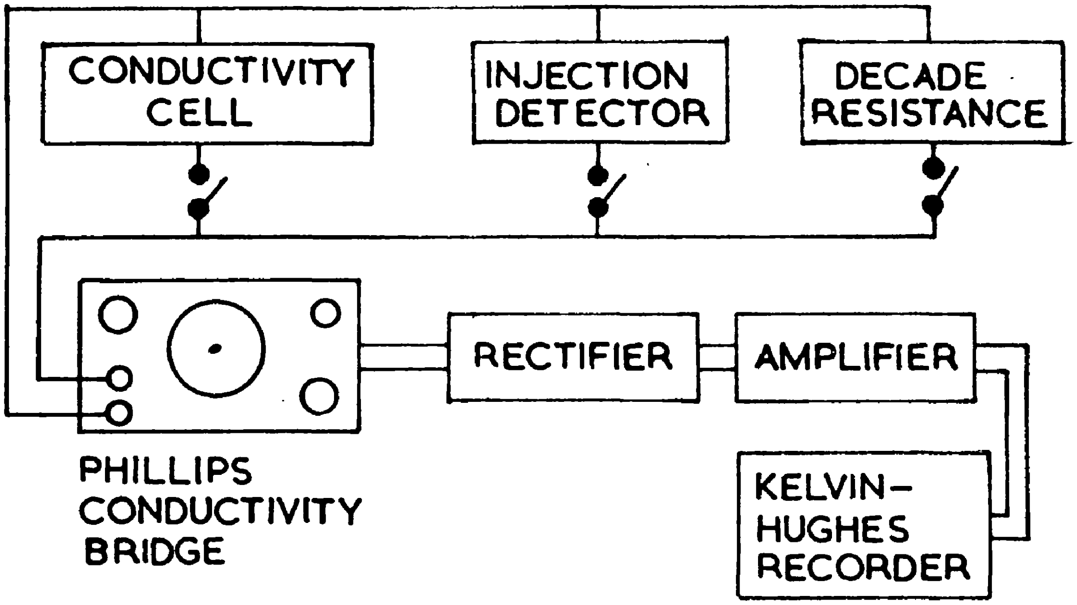
CONDUCTIVITY CELL
INJECTION DETECTOR
DECADE RESISTANCE
RECTIFIER
AMPLIFIER
PHILLIPS CONDUCTIVITY BRIDGE
KELVIN-HUGHES RECORDER

GENERAL CIRCUIT DIAGRAM

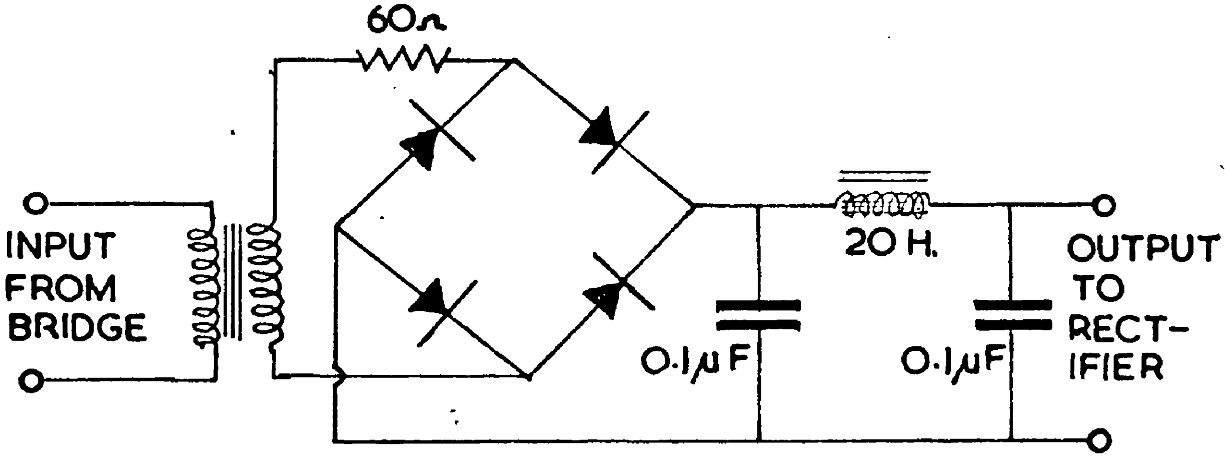
60Ω
INPUT FROM BRIDGE
20 H.
0.1μF
0.1μF
OUTPUT TO RECT-IFIER

RECTIFIER CIRCUIT DIAGRAM

FIG 13

A Phillips Conductivity Bridge PR9500 which included a source of 1,000 c/s .A.C. was modified by removing the electronic indicator valve EM 34 and the input to this value amplified by a 6C4 triode. The output from this valve which was dependent on the "out of balance" of the bridge circuit and hence on the resistance of the cell. This output was "stepped up" by a small transformer and rectified by silicon rectifiers. The circuit diagram of the rectifier is given in Figure 13. Output from this rectifier (2 volts DC maximum), was amplified by a Kelvin Hughes Type 6 Amplifier designed for use with the Recorder.

Zero could be set on the chart by a bias control on the amplifier and sensitivity could be adjusted by controls on both the amplifier and the bridge. The system could thus record a wide range of cell resistances. A decade resistance box (1 to 10,000 Ω) could be switched into the circuit for calibration purposes.

Had the outlet water, containing salt, been returned to the tank the conductivity "base line" would have changed during the course of a test. The outlet water was therefore discharged to the drain and the water in the main tank continuously made up by water from the main water supply. In the tests using sugar solution it would have been too expensive to discharge sugar solution to waste so a second tank was installed from which solution could be pumped to the main tank. This alteration meant that during a test, sugar solution was pumped from the main tank, across the plate, to the second tank, and on completion of the test the accumulated water was pumped back to the main tank where it was mixed before the next test by an electric stirrer.

3 : 6 Design of the 12 inch Diameter Kuhni Plate

Photographs and a drawing of the plate are given in Figures 2 and 14.

This plate was also constructed mainly in 17 S.W.6. Copper. There was only one annular tunnel bubble cap at a diameter of 7.86 inches. As in the 30 inch plate the outer ring had slots in the inside and in addition there was an inner ring of slots on the outside of a tunnel cap, the inside of which formed the weir. The caps were 0.82 inches high and the middle cap in 0.79 inches broad.

The total slot area was 6.80 square inches which represents 6.01% of the column cross sectional area.

The weir had an internal diameter of 3.35 inches and a height above the plate floor of 0.82 inches.

The inlet distributing well had radial 3/8 inch internal diameter copper tubes sloping down to the periphery of the plate.

Two flush tappings were fitted to the plate floors for measurement of clear liquid height on external U-tube manometers.

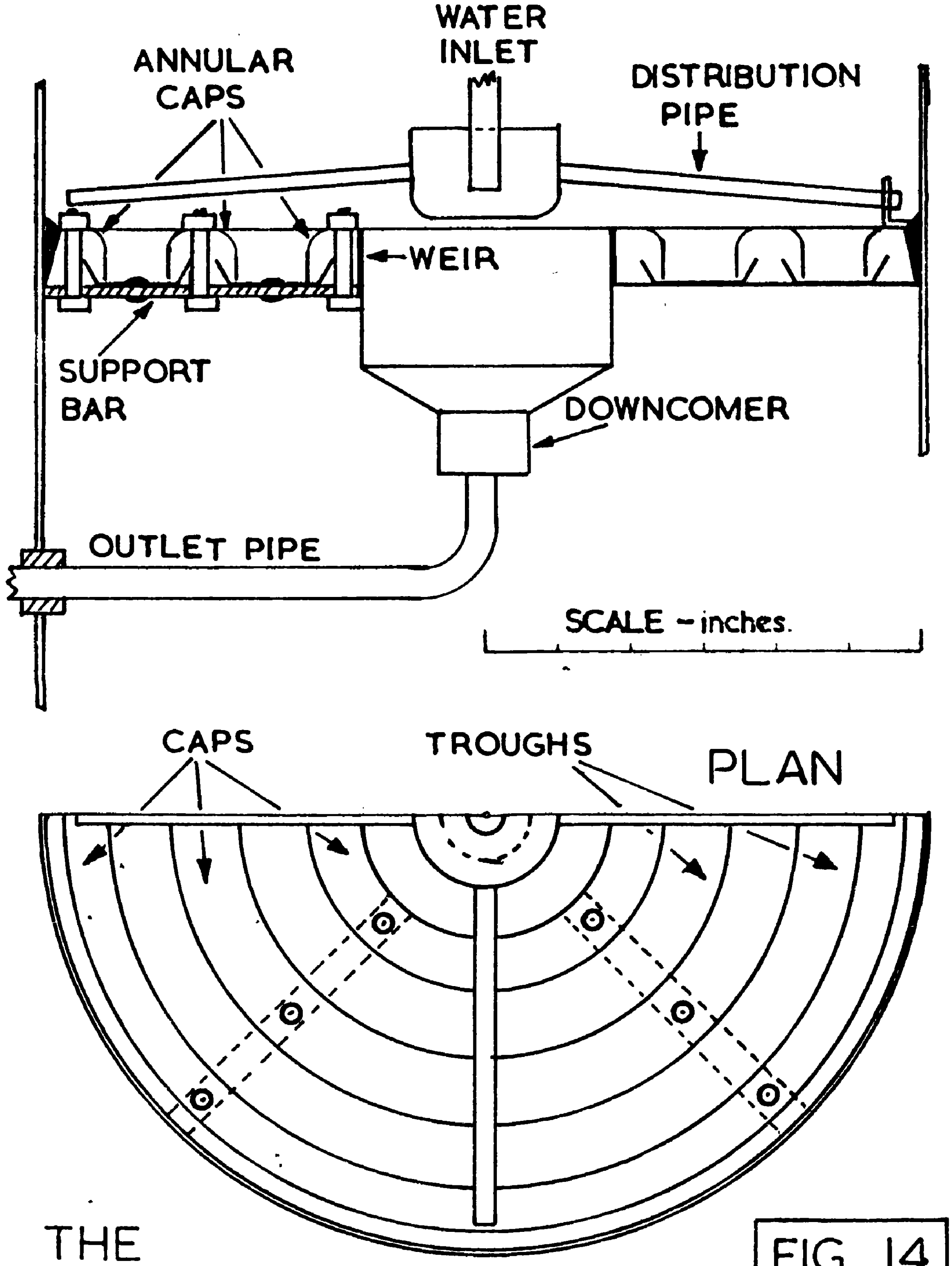
WATER INLET
ANNULAR CAPS
DISTRIBUTION PIPE
WEIR
SUPPORT BAR
DOWNCOMER
OUTLET PIPE
SCALE – inches.
CAPS
TROUGHS
PLAN

FIG 14

THE
12 INCH DIAMETER
KUHNI DISTILLATION PLATE

3 : 7 General Design of the 12 inch Kuhni Plate Plant

The general arrangement of the plant is illustrated in Figure 15.

A Keith Blackman forge blower, capable of delivering 5,000 cubic feet of air per hour at 12 inches water head, was driven by an A.C. electric motor. Air was drawn to the fan inlet through 12 feet of 6 inch diameter flexible ducting. A butterfly valve at the fan outlet controlled the air flow which was measured by an orifice meter. The air entered the base of the 12 inch diameter copper test column in which the Kuhni plate was sealed. This column had "Perspex" windows above and below the plate. A length of 4 inch diameter flexible ducting conducted the outgoing air to the discharge point.

Water was pumped from a 10 gallon tank by a Stuart Turner centrifugal pump to the plate through one of two "Rotameters" arranged in parallel each with a control valve. Control was also achieved by a by-pass back to the tank, The "Rotameter" range was from 5 to 200 gallons per hour. The outlet water flowed by gravity back to the tank.

The sharp edged orifice plate had D and D/2 tappings with an orifice diameter of 2.000 inches, the pipe diameter being 4 inches. The calibration of this orifice plate was taken from B.S.1042 (1943). Manometers indicated the pressure drop across the orifice plate and the Kuhni plate.

Thermometers accurate to ± 0.1°F were fitted in the water circuit before and after the plate.

FIG 15

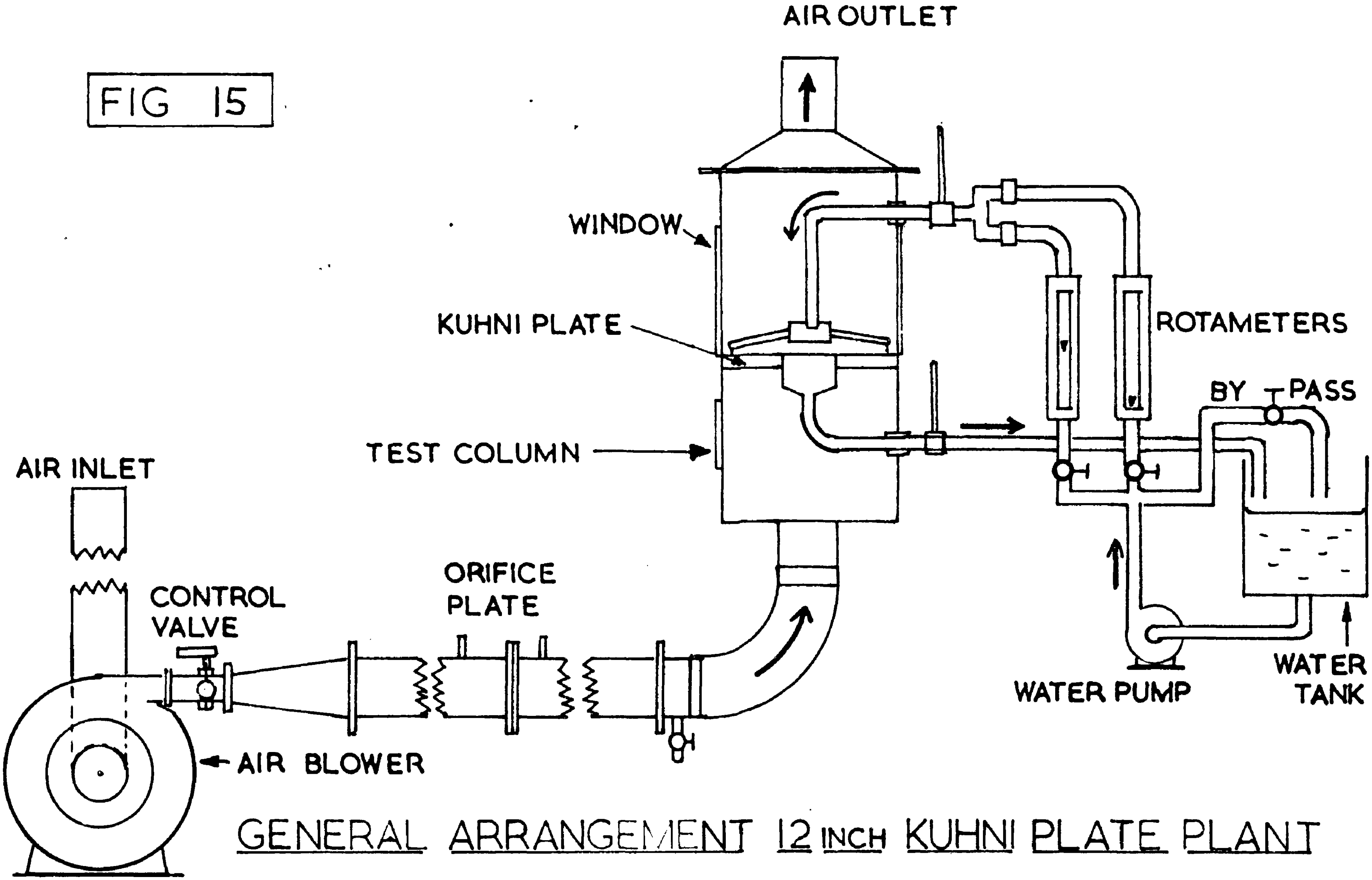
AIR OUTLET
WINDOW
KUHNI PLATE
TEST COLUMN
ROTAMETERS
BY PASS
AIR INLET
CONTROL VALVE
ORIFICE PLATE
WATER PUMP
WATER TANK
AIR BLOWER

GENERAL ARRANGEMENT 12 INCH KUHNI PLATE PLANT

3 : 8 Modifications for Humidification Tests (12 inch Plate)

The wet and dry bulb psychrometers used in the 30 inch plate tests were installed at the air inlet and outlet.

3 : 9 Modifications for Oxygen Desorption Tests (12 inch Plate)

The oxygenation tower and settling tank used in the 30 inch plate tests were used and the sampling apparatus and procedure repeated.

3 : 10 Alterations in Plate Design (30 inch Kuhni Plate)

(i) Slot Area

The slot area of the 30 inch plate is 30.06 in.^{2}, there being a total of 614 slots each with an area of 0.0489 in.^{2}. This area corresponds to 4.25% of the column cross sectional area. The slot area can be increased without permanently altering the plate design by raising the annular rings. Washers were placed between the shoulder of the holding bolts and the annular rings. To prevent the bolts and rings slipping to their original position the bolt heads were soldered to the brass angle which supports the rings and troughs.

Details of the slot areas formed by adding the 0.040 in thick brass washers are given in Figure 16. As can be seen the effect of one washer is not to raise the rings by the full 0.040 in. as there is a gap of 0.030 in. between the bolt shoulders and the rings. The amount by which the rings were raised varied slightly (± 0.008 in.) over the plate, the figures in Figure 16 being averages. Measurements were made by a clock-gauge micrometer with the plate on a surface plate.

(ii) Weir Height

The weir height of the plate was raised by inserting a copper collar in the outlet well. The height of the collar above the existing weir could be varied, the collar being fixed to the weir by bolts as shown in Figure 12.

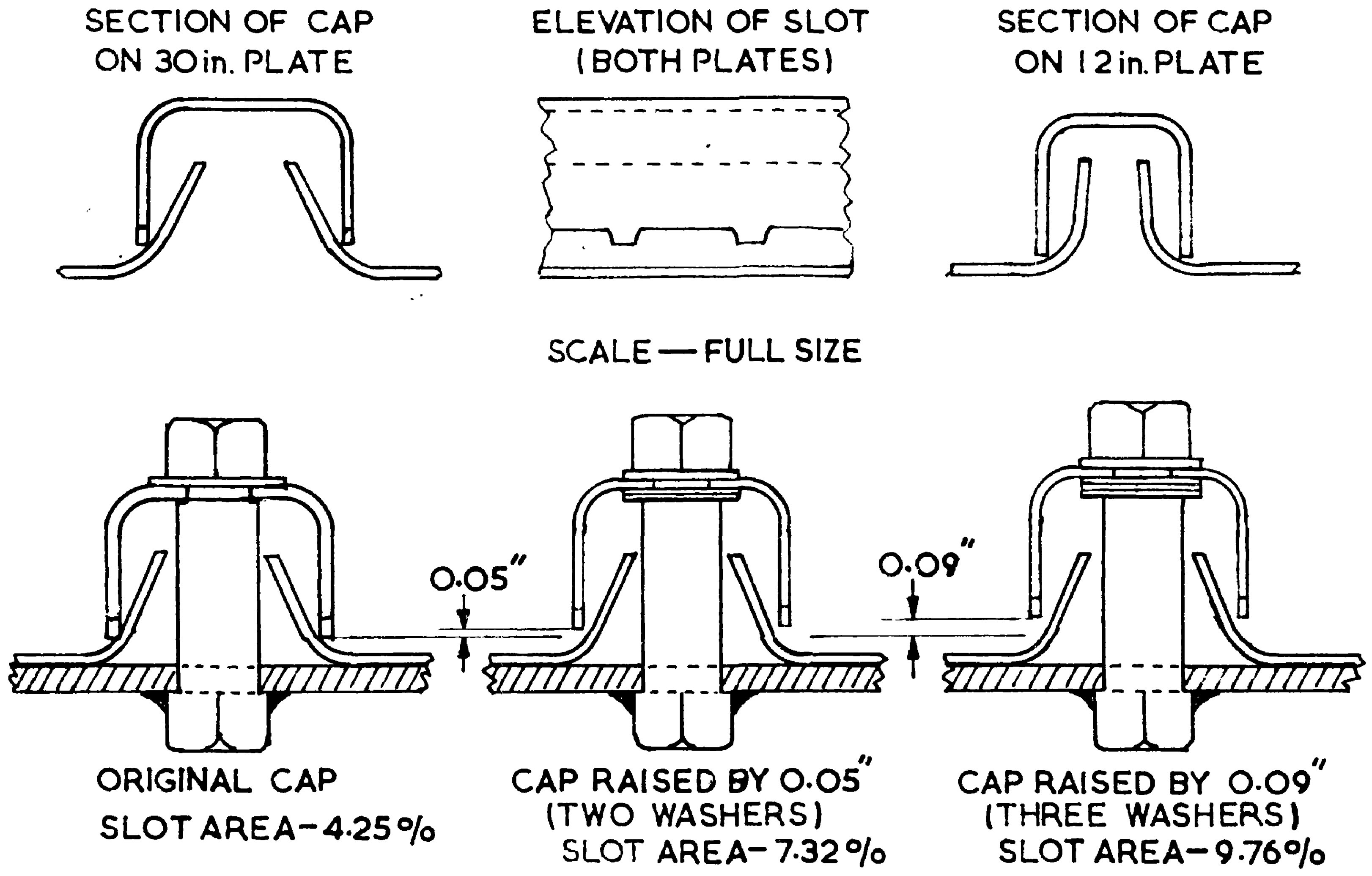
SECTION OF CAP
ON 30in. PLATE
ELEVATION OF SLOT
(BOTH PLATES)
SECTION OF CAP
ON 12in. PLATE
SCALE — FULL SIZE
0.05"
0.09"
ORIGINAL CAP
SLOT AREA – 4.25%
CAP RAISED BY 0.05"
(TWO WASHERS)
SLOT AREA – 7.32%
CAP RAISED BY 0.09"
(THREE WASHERS)
SLOT AREA – 9.76%

DETAILS OF CAPS AND SLOTS OF 12" AND 30" KUHNI PLATES AND CAP RAISING ON THE 30" PLATE

FIG 16

SECTION 4

EXPERIMENTAL PROCEDURE

4 : 1 Humidification tests on both Kuhni Plates

As discussed previously (Section 2:1), two methods were used to determine humidification efficiency, the "sodium carbonate solution evaporation" method and the "outlet psychrometer" method. A description of both methods is given, the former being applied only to the 30 inch Kuhni plate. The procedure for the "outlet psychrometer" method was the same for both plates.

(i) "Sodium Carbonate Solution Evaporation Tests"

About 50 lb. of dilute (1%) Sodium carbonate solution was weighed to an accuracy of ± 0.05 lb. A sample was estimated volumetrically for sodium carbonate concentration by titration against standard acid. The solution was added to the water tank which had been previously drained. At a noted time the air and solution flows were started and quickly adjusted to the required values. The inlet psychrometer was started and checked to ensure that the wick was clean and wet. The constant level device which added water to the tank to maintain the solute concentration constant was filled.

At ten-minute intervals the following readings were taken:

(a) Inlet wet and dry bulb temperatures.

(b) Solution inlet and outlet temperatures.

(c) Plate Pressure Drop.

In addition the solution rate and the air rate were continually adjusted to the desired values, the froth height, the weight of water added to the constant level device and the barometric pressure noted.

When about 25 lb. of water had been evaporated and replaced through the constant level device (in 4 to 8 hours) the test was stopped at a noted time The system was completely drained, the liquid on the plate and in the outlet well being syphoned out and the combined solution weighed. A sample of the solution was estimated volumetrically.

The mean values of the inlet humidity and the solution temperatures were calculated and, with the other data, used to determine the plate efficiency and entrainment as shown in the specimen calculation in Appendix A .

(ii) "Outlet Psychrometer Tests"

The air and water rates were adjusted to the required values and the psychrometers checked and started. After a stabilising period of twenty minutes the following readings were taken at one minute intervals for ten minutes.

(a) Inlet wet and dry bulb temperatures.

(b) Inlet water temperature.

(c) Outlet wet and dry bulb temperatures.

(d) Outlet water temperature.

If there had been no significant change (± 0.3°F) in any of these variables during the test period the readings were averaged. If a significant change had taken place the run was repeated. In addition the orifice plate pressure drop, Rotameter reading, plate pressure drop, froth height, and the barometric pressure were noted. A specimen calculation of the efficiency is given in Appendix A .

4 : 2 Humidification Tests on 30 inch Kuhni Plate using "Cellofas" Solutions

The procedure for these tests was similar to the "outlet psychrometer" tests with water, but with two modifications.

(i) The liquids used were dilute (< 1%) solutions of "Cellofas B" in water, of viscosity 2 cP, 4 cP, 8 cP and 16 cP. These solutions were prepared by dissolving the granulated solid in hot water and mixing the resultant solution thoroughly by an electric stirrer with sufficient water in the tank to give the required viscosity. For details of the concentration-viscosity relationship see Appendix D. Samples of the solution were taken at regular intervals for viscosity determination, using the procedure in BS. 188 (1957) and the solution concentration suitably adjusted when necessary to maintain the viscosity within 5% of the required value.

(ii) The Rotameter was calibrated for each viscosity level and the liquid rates suitably adjusted to give the required flow.

With those two modifications the procedure was identical to that described in Section 4:1(ii).

4:3 Oxygen Desorption Tests on both Kuhni Plates

The Oxygen absorption tower was filled with oxygen from a cylinder by displacement of water. The air and water rates were adjusted to the required values. By trial and error adjustment of the oxygen cylinder valves the rate of oxygen addition to the absorption tower was made equal to the rate of oxygen absorption in the tower, this equivalence being shown by the attainment of a constant water level at the base of the tower. Adjustment of the tap on the pipe leading from the glass tank to the plate kept the water level in the tank constant.

The two sample bottles were connected up and the inlet and outlet streams sampled continuously. The inlet sample flow was adjusted to 2 gallons per hour, a rate sufficient to scavenge the sample bottle every 4 minutes. This "bleed off" was compensated for in choosing the water rates.

When conditions has stabilised for about 20 minutes the water inlet and outlet temperatures were taken at 1 minute intervals for 10 minutes. The orifice plate pressure drop, the "Rotameter" readings, the plate pressure drop and the barometric pressure were also noted.

The sample bottles were disconnected, care being taken to avoid enclosing air bubbles. Reagents were added to the bottles and the oxygen content estimated volumetrically by a modified Winkler method as described in Appendix C.

The plate efficiency was deduced as shown in Appendix A.

4 : 4 Oxygen Desorption Tests on 30 inch Kuhni Plate using "Cellofas" Solutions

The procedure for these tests was similar to the oxygen desorption tests using water.

Dilute solutions of Cellofas B made up to and maintained at the required viscosities, (2 cP, 4 cP, 8 cP and 16 cP), were used, regular viscosity determinations being made.

The dissolved oxygen determination had to be considerably modified because of the interference of the "Cellofas". This is discussed in Appendix C, and involved the buffering of the sample solutions to a pH of 8.

4 : 5 Liquid Residence Time Tests on 30 inch Kuhni Plate

Two series of tests were done, firstly with water and secondly with sugar solutions of viscosity 2 cP, 4 cP, 8 cP and 16 cP. These tests are described separately.

(i) Tests using water

The water and air flows were started and adjusted to the required values. Unlike the previous efficiency tests the water did not flow in closed circuit but was pumped to waste, the tank being continuously replenished from the water main. The electrical recording apparatus was switched on and a "heating up" period of 20 minutes allowed. By switching the decade resistance box into circuit the pen reading could be adjusted to the required range of conductivities. This was achieved by setting the decade box at (say) 5,000 ohm and balancing the bridge circuit to give zero output at maximum sensitivity. Zero was set on the chart at this output and the sensitivity adjusted to give a full scale reading when the resistance of the decade box was zero. The chart was thus calibrated in terms of resistance, (or conductivity). Calibration graphs were prepared for each balance resistance used and are given in Appendix F. The balance resistance was chosen to be greater than the cell resistance with water flowing.

The injector was filled with 1 cc. of concentrated salt tracer solution and the stopper replaced. The air and water rates were checked and the chart motor started with the conductivity cell and injection detector switched into circuit. Tracer solution was ejected by compressing the hand bulb, the momentary contact formed in the detector giving a "kick" on the chart trace, the detector was switched out of circuit to avoid any interference with the cell reading. After a few seconds the conductivity of the cell increased to a maximum then gradually decreased to the original base line. When it was certain that the base line had been reached the chart motor was switched off and the test details noted on the chart.

Each run was repeated three times and the data averaged. This was done by taking a minimum of 20 readings from the charts at constant time increments, starting with the injection signal as zero time, such that these readings covered the whole period of conductivity change. The chart readings from each repeat test were averaged, converted to conductivities, and the "base" line conductivity subtracted from each. The mean residence time and mixing parameters were deduced as shown in Appendix A.

(ii) Tests using Sugar Solutions

As explained previously (Section 2:3) it had been hoped to do these tests with solutions of "Cellofas B" but the effect of salt tracer solution on the viscosity of these solutions necessitated the use of sugar solutions to increase the liquid viscosity.

The sugar solutions were made up to the required viscosity and maintained at that viscosity, a periodic check being made. As with the "Cellofas" solutions the Rotameter required recalibration for each viscosity level. The principal difference between the water and sugar solution tests was that in the former the outlet water contaminated with salt tracer was discharged to the drain whereas for the sugar solution tests, such a procedure would have been prohibitively expensive.

The outlet sugar solution was discharged to a second tank and on completion of each test the collected solution was pumped back to the main tank where the resultant solution was thoroughly mixed. As a result the "base line" conductivity varied from test to test but not during a test. Potassium chloride solution was used as the tracer, as its effect on the viscosity of sugar solutions is less than sodium chloride. Apart from these modifications the procedure adopted was identical to that for the water tests.

Each test was duplicated and the results calculated as for the water tests. A specimen calculation is given in Appendix A.

SECTION 5

DISCUSSION OF THE RESULTS

5 : 1 Residence Time and Liquid Hold-Up Tests with Water

The mean residence time of the liquid on a plate, (tm sec.) and the volume of liquid hold-up on the plate (V_L gall.) are related as follows

$$V_L = 0.49 \text{ tm } L_M/3{,}600, \qquad (5;1)$$

where L_M is the liquid flow rate (lb./ft.^{2} hr)

Of the two quantities, residence time and hold-up, the hold-up is probably the more fundamental, in that the volume of liquid on the plate depends on the resistance to flow across the plate, the resultant hydraulic gradient and the volume of the gas bubbles in the froth. The residence time can best be regarded as a function of the liquid hold-up and the liquid flow rate.

From Figure 17, showing the hold-up characteristics for air and water, it can be seen that the water hold-up is a function of both air and water rates. An increase in water rate causes a greater hold-up because of the increased hydraulic gradient and outlet weir crest height. The grater hold-up is also indicated by the plate pressure drop data in Figure 23 and by the clear liquid height measurements in Figure 24. These clear liquid height measurements are mean values deduced from the "clear liquid heights" of the four channels between the tunnel caps by weighting the four readings in proportion as the area of each channel. The percentage areas of the channels were 36, 29, 22 and 13, reading from the periphery inwards.

The effect of an increase in air rate is generally a reduction in water hold-up, due to the increased violence with which the air stream propels the water across the plate.

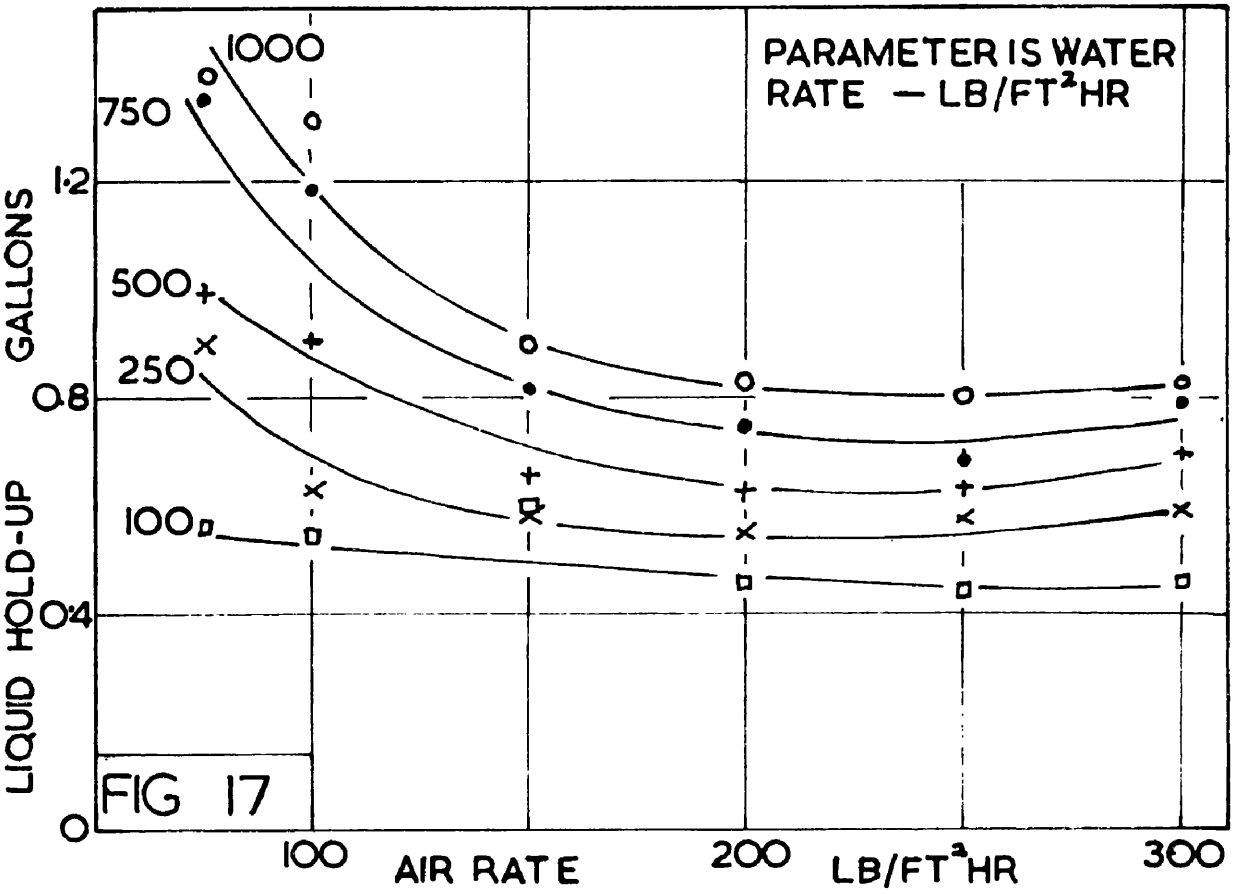
PARAMETER IS WATER RATE — LB/FT²HR
1000
750
500
250
100
LIQUID HOLD-UP GALLONS
0
0·4
0·8
1·2
100
200
300
AIR RATE
LB/FT²HR

FIG 17

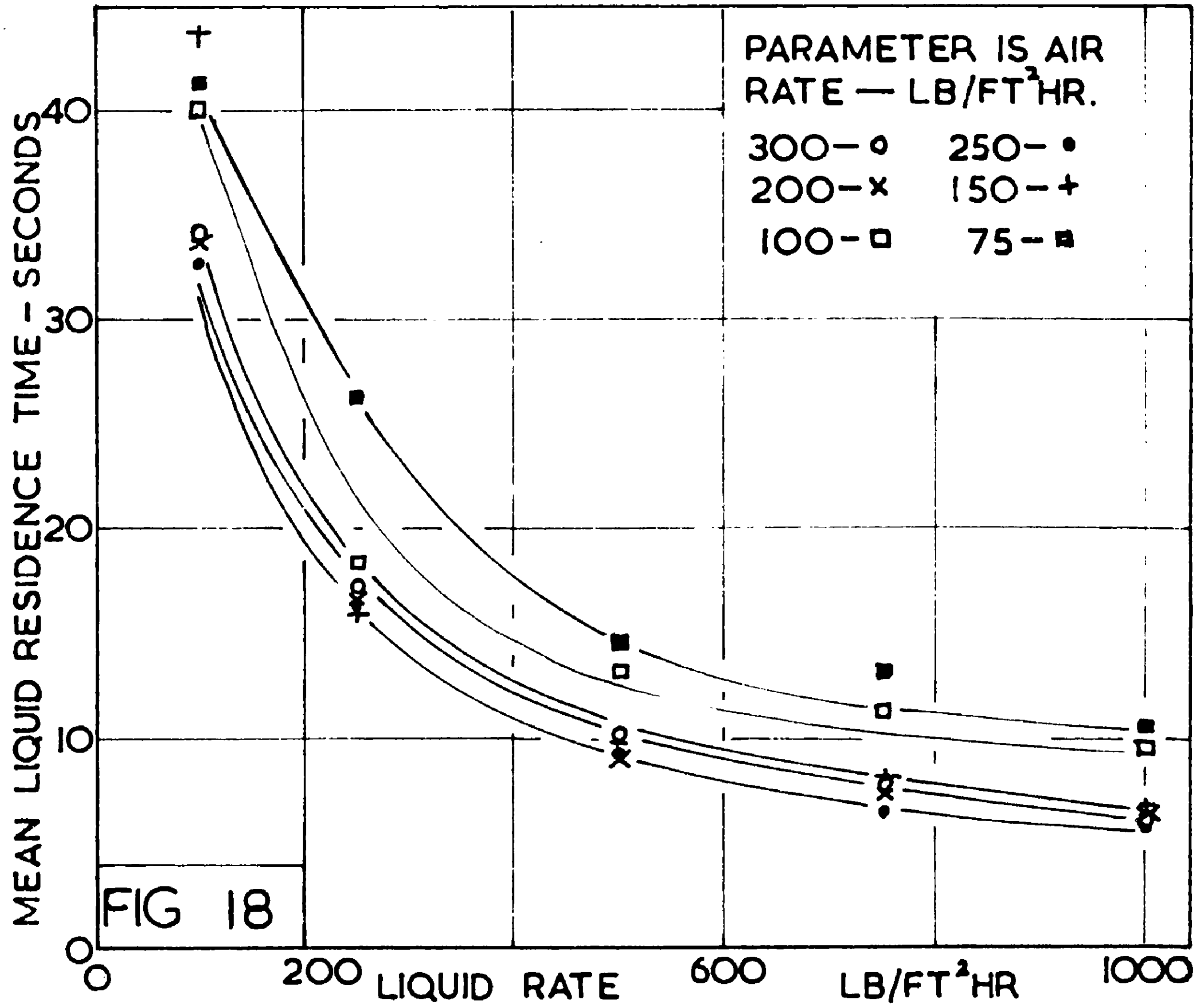
PARAMETER IS AIR RATE — LB/FT²HR.
300 — ○
250 — ●
200 — ×
150 — +
100 — □
75 — ■
MEAN LIQUID RESIDENCE TIME - SECONDS
0
10
20
30
40
0
200
600
1000
LIQUID RATE
LB/FT²HR

FIG 18

Comparison of Figure 17 showing the water hold-up and Figure 24 showing the clear liquid height shows that between air rates of about 220 and 300 lb./ft.^{2} hr. the water hold-up increases on an average by about 5% while the clear liquid height continues to fall and appears to be "levelling out" at 300 lb./ft.^{2} hr. This anomaly is probably caused by the increased volume of water held as droplets in the space immediately above the froth since this volume will not be indicated by the clear liquid height manometers. It was noticeable that the amount of water in this space increased markedly at high air rates and the entrainment losses plotted in Figure 39 support this observation.

Calculation of the volume of water on the plate from clear liquid height measurements is unreliable because of this effect and also because of the difficulty of estimating the effect of the cap volume since the froth density may not be constant in a vertical direction. The volume of water on the plate is about 10 to 25% greater than the volume estimated from clear liquid height measurements. For example, at 500 lb./ft.^{2} hr. water rate and 200 lb./ft.^{2} hr.(air rate) the water hold-up is 0.62 gall as against 0.51 gall estimated from the clear liquid height of 0.44 in.

Figure 18 shows the residence time of the water as a function of air rate with water rate as parameter. The graph indicates the marked increase in residence time at water rates less than 500 lb./ft.^{2} hr. This increase in residence time is of great importance in determining the oxygen desorption efficiency and will be discussed in greater detail later.

A rough correlation is given below for residence time which applies to air rates from 75 to 250 lb./ft.^{2}hr. As an approximation residence times above 250 lb./ft.^{2} hr. can be taken as equal to the residence time at 250 lb./ft.^{2}hr. Hold-up data can be estimated from the equation below and the equation at the beginning of this section, (5:1).

Correlation

$$tm = 590/L_M^{0.55} - 0.045\, G_M \qquad (5;2)$$

where tm = mean residence time (sec.)

L_M = water rate (lb./ft.^{2}hr)

G_M = air rate (lb./ft.^{2}hr)

5 : 2 Residence Time and Liquid Hold-Up Tests with Viscous Solutions

The residence time and hold-up of aqueous sugar solutions of viscosity 2, 4, 8 and 16 cP were determined at all combinations of four liquid rates and three air rates.

If the viscosity of a liquid flowing across a bubbling plate is increased the hydraulic gradient increases, the height of the weir crest increases and the amount of splashing decreases. It is to be expected that more viscous liquids will resist the tendency to be thrown into the air space, reducing entrainment and also the flow due to splashing. Barker and Choudhury[33] found that the entrained droplet size increased at high viscosities and that above 5 cP a reduction in entrainment took place.

The results of the tests are shown in Figures 19, 20 and 21. Each figure gives the hold-up data at one air rate, liquid rate being the parameter. There is very little difference between the 300 lb./ft.^{2}hr and 200 lb./ft.^{2}hr. (air rate) graphs. Both show a steady but slight increase in hold-up with increasing viscosity. The graph at an air rate of 100 lb./ft.^{2}hr (Figure 19) is quite different in form, the liquid hold-up increasing more rapidly especially at high liquid rates. The reason for this irregularity of the hold-up at low air rates is almost certainly that the inner trough of the plate ceased to bubble, no liquid being displaced by air bubbles. Since this air rate is very low by commercial standards this effect is of academic interest only, except in demonstrating that the plate has a fairly high "turn-down" ratio.

The differences in hold-up between viscosities of 1 cP and 16 cP, at

FIG 19

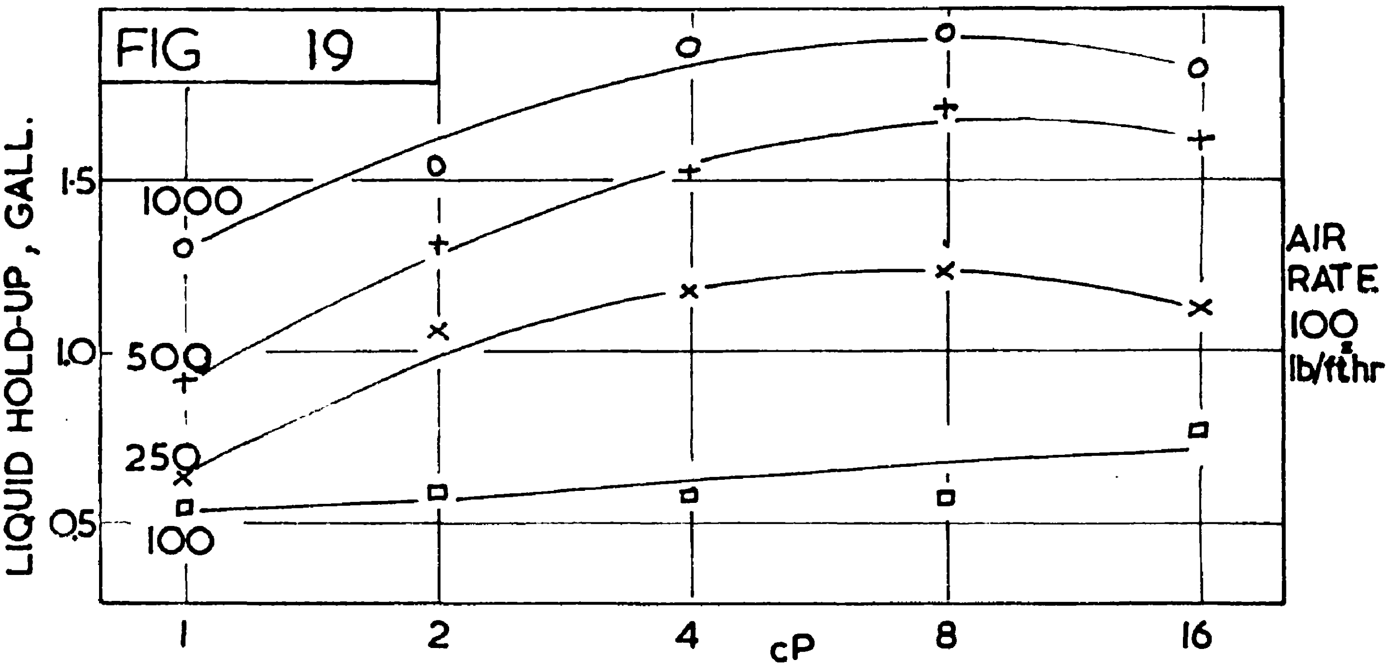

FIG 20

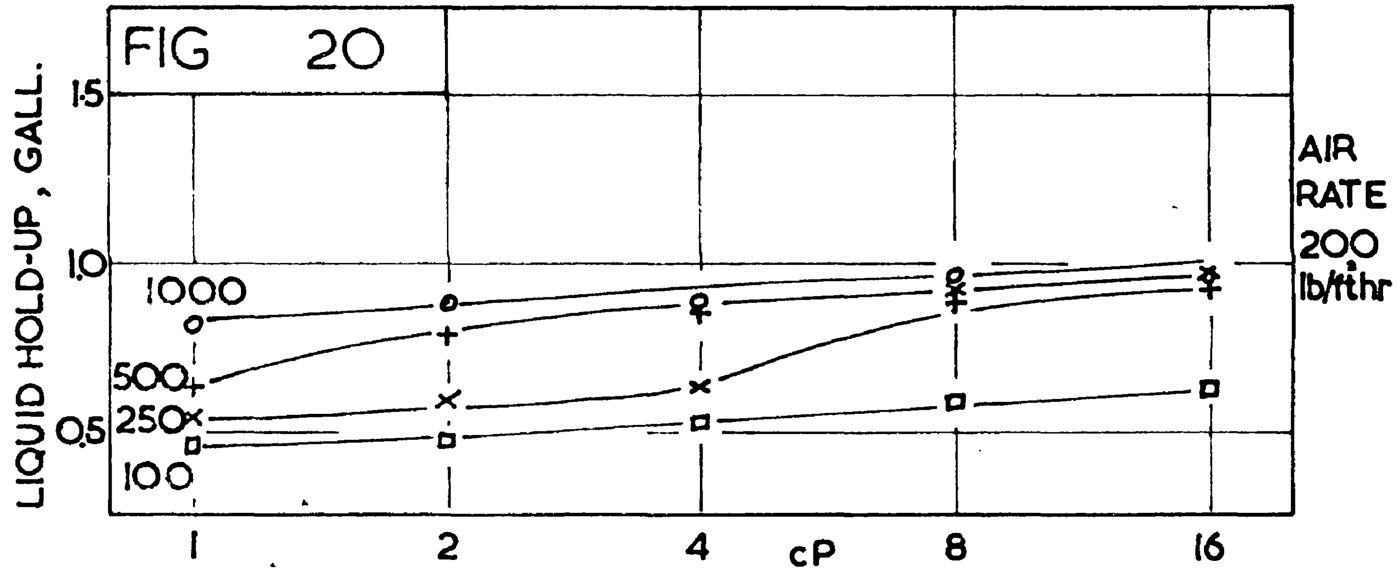

FIG 21

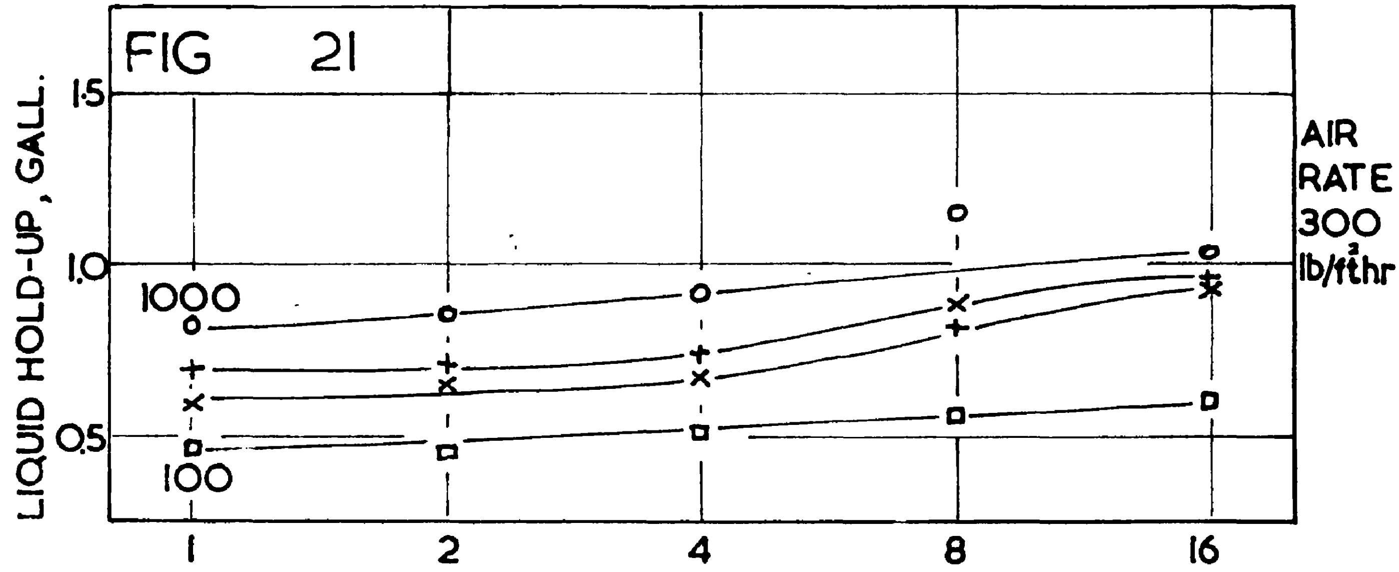

LOG. VISCOSITY — CENTIPOISE.

PARAMETER IS WATER RATE — LB/FT²HR

given air and liquid rates, are remarkably similar for the conditions in which the inner ring is bubbling. The increase varies from 0.2, to 0.4 gall. and has an average value of 0.24 gall. This is used later in correlating the hold-up.

It is noticeable from Figures 20 and 21 that the curves at liquid rates of 250 and 500 lb./ft.^{2}hr, have an inflexion between 4 and 8 cP. where the hold-up increases sharply. The 100 lb./ft.^{2}hr (air rate) curve shows no such inflexion. This sudden rise in hold-up is difficult to explain, but it may be associated with a change in the bubbling mechanism. In the humidification and oxygen desorption tests a change in efficiency characteristics was noted in this region. This is discussed in greater detail in later sections.

Since the liquid hold-up increases with increasing viscosity the residence time also increases accordingly. The increase in residence time is more marked at high liquid rates as can be seen from Figure 22; at the liquid rate of 1,000 lb./ft.^{2}hr. the increase in residence time is negligible. The sudden increase in residence time between 4 and 8 cP is again noticeable.

Summarising the effects of viscosity on liquid hold-up and residence time it has been shown that different characteristics occur depending on whether or not the inner trough is active.

If the inner trough is not bubbling, the hold-up increases considerably with increasing viscosity, especially at high liquid rates.

If the inner trough is bubbling, the hold-up has been shown to increase by an average of 0.24 gall. of water for the change in viscosity from 1 cP to 16 cP. Certain anomalies have been observed in the 4 cP to

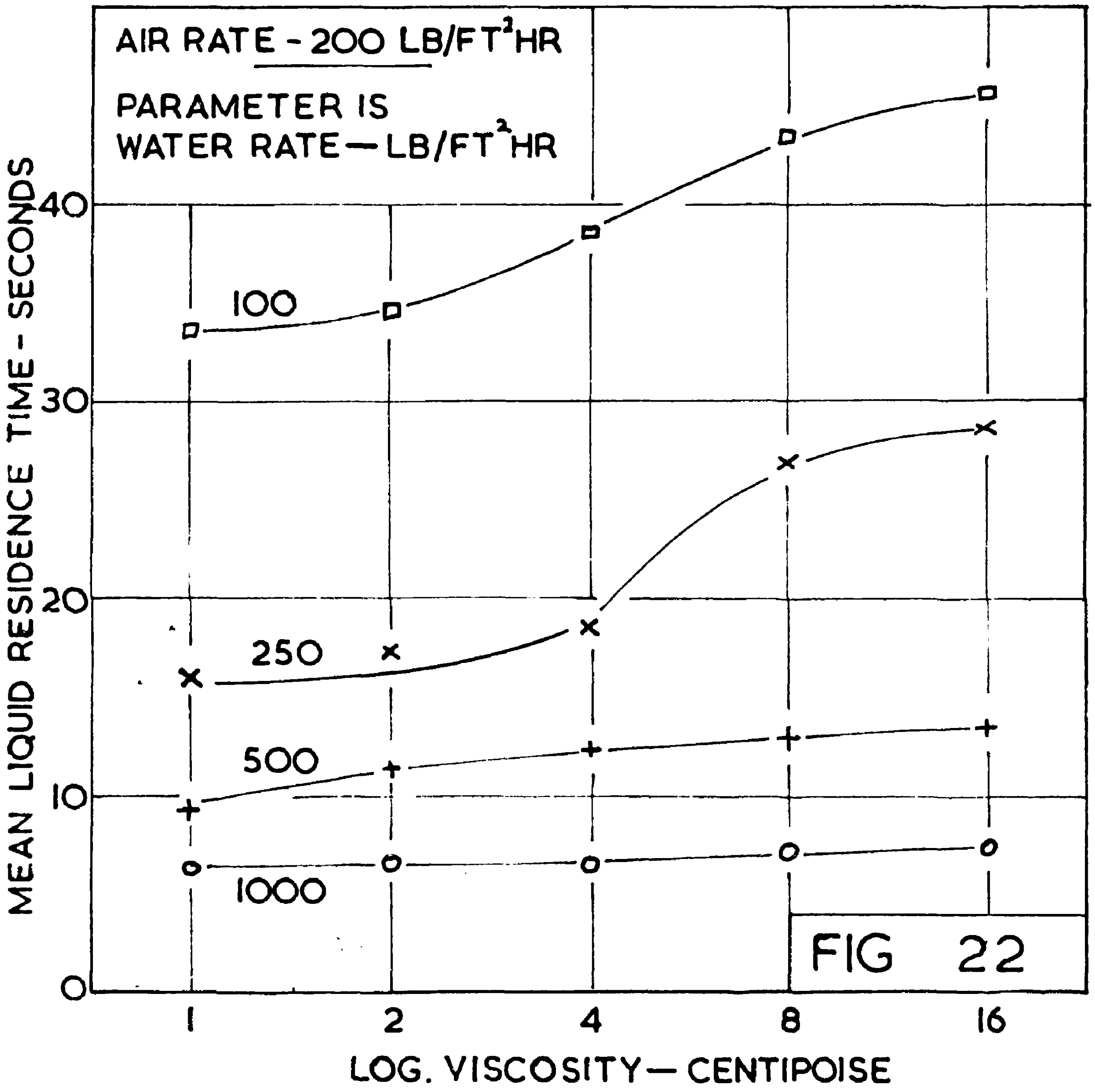
AIR RATE - 200 LB/FT²HR
PARAMETER IS
WATER RATE—LB/FT²HR
100
250
500
1000
MEAN LIQUID RESIDENCE TIME - SECONDS
0
10
20
30
40
1
2
4
8
16
LOG. VISCOSITY— CENTIPOISE

FIG 22

8 cP region but their effect is small. The liquid residence time also increases but the amount of the increase varies considerably depending on the liquid rate.

An approximate correlation for the increase in hold-up with increasing viscosity is given by equation (5;3) below. This is applicable only to conditions when the inner trough is active.

$$V_L = V_{L(1\ cP)} + 0.2 \log \mu. \qquad (5;3)$$

where V_L = volume of liquid hold-up (gall.)

$V_{L(1\ cP)}$ = volume of liquid hold-up at 1 cP and identical operating conditions (gall.)

μ = Viscosity (cP)

A correlation for hold-up at 1 cP has been given earlier, (equations (5:1) & (5:2)).

Differences between Sugar and "Cellofas B" Solutions

It is unfortunate that these tests could not have been done with "Cellofas B" solutions since there are some differences between the properties of sugar and "Cellofas B" solutions. The principal difference is in density where for example solutions of sugar and "Cellofas B" of viscosity 16 cP differ in density by 23%. The density and viscosity characteristics of these two solutions are given in Figures 87 and 90 in the Appendix.

It is unlikely that the greater density of the sugar solutions has a marked effect on the hold-up characteristics, although the greater inertia of the sugar solutions may affect the bubbling mechanism slightly.

It should be noted that all viscosities are stated as absolute viscosities (centi-Poises) rather than as kinematic viscosities (centi-Stokes). This is in accordance with current chemical engineering practice although in discussions on fluid drag and inertia the kinematic viscosity is possibly more relevant. "Cellofas B" solutions, being so dilute with densities close to 1 g/cc. have absolute and kinematic viscosities almost exactly numerically equal.

5 : 3 Pressure Drop and Froth Height Tests

The plate pressure drop can be considered as the sum of three terms, the "dry plate" pressure drop, the "hydraulic" pressure drop and the "residual" pressure drop. The "residual" pressure drop is small enough to be neglected in this analysis. This model is an approximation since these component pressure drops do not necessarily act simultaneously.

Figure 23 shows the pressure drop characteristics of the 30 inch plate. The effect of an increase in air rate or water rate is to increase the plate pressure drop. An increased water rate gives a greater volume of water on the plate with a correspondingly higher "hydraulic" pressure drop while an increased air rate gives a greater "dry" pressure drop.

A criticism of the Kuhni Plate has been that the dry plate pressure drop is too high, mainly because of the small slot area which amounts to only 4.25% of the column area. Subsequent tests discussed in Section 5:11 showed that this pressure drop could be reduced by increasing the slot area.

The dashed line in Figure 23 is the difference between the plate pressure drop at a water rate of 1000 lb./ft.^{2}hr and the dry plate pressure drop. It can be seen to vary from 0.7 to 1.3 inches of water. This quantity, which approximates to the hydraulic pressure drop is lower at high air rates owing to the lower volume of liquid on the plate at these air rates. This is demonstrated by the clear liquid height graph in Figure 24. Another factor causing the high values of the hydraulic pressure drop at low air rates is the inactivity of the inner trough. This results in a lower "effective" slot area and a correspondingly

FIG 23

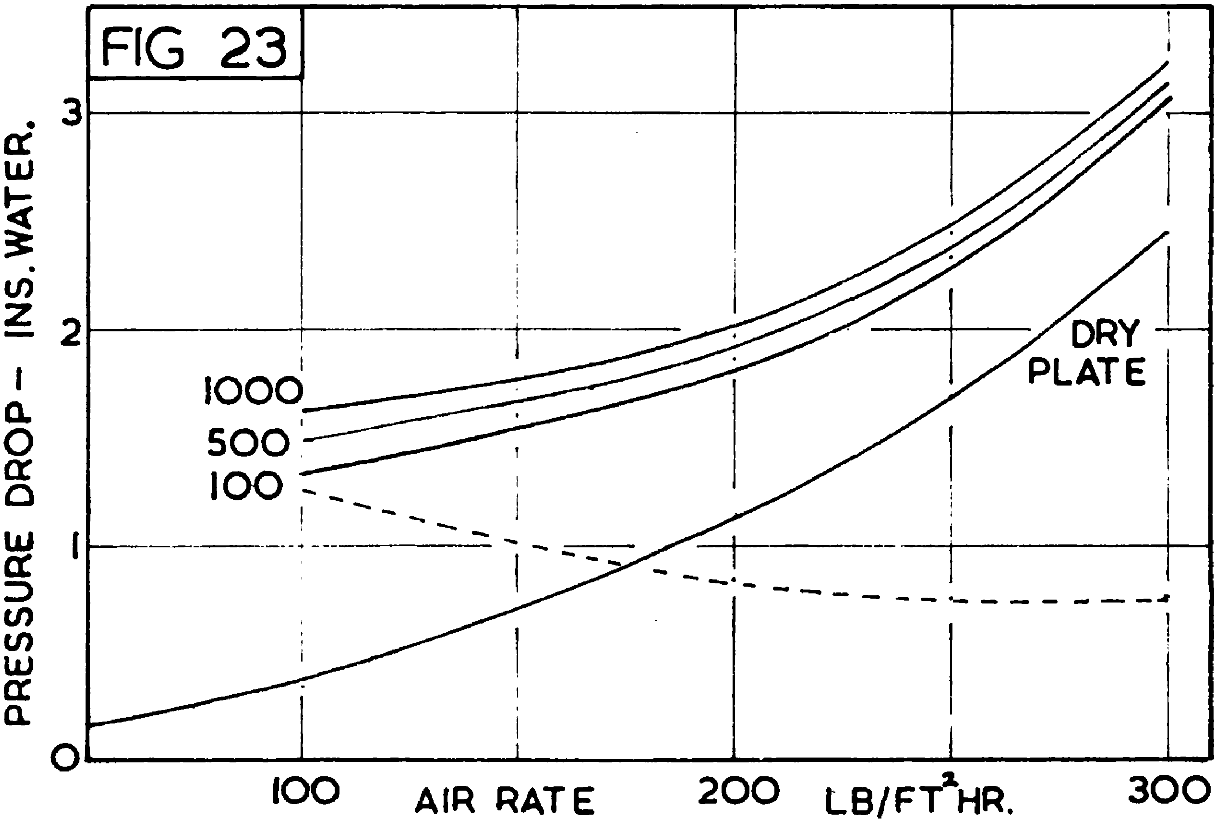

FIG 24

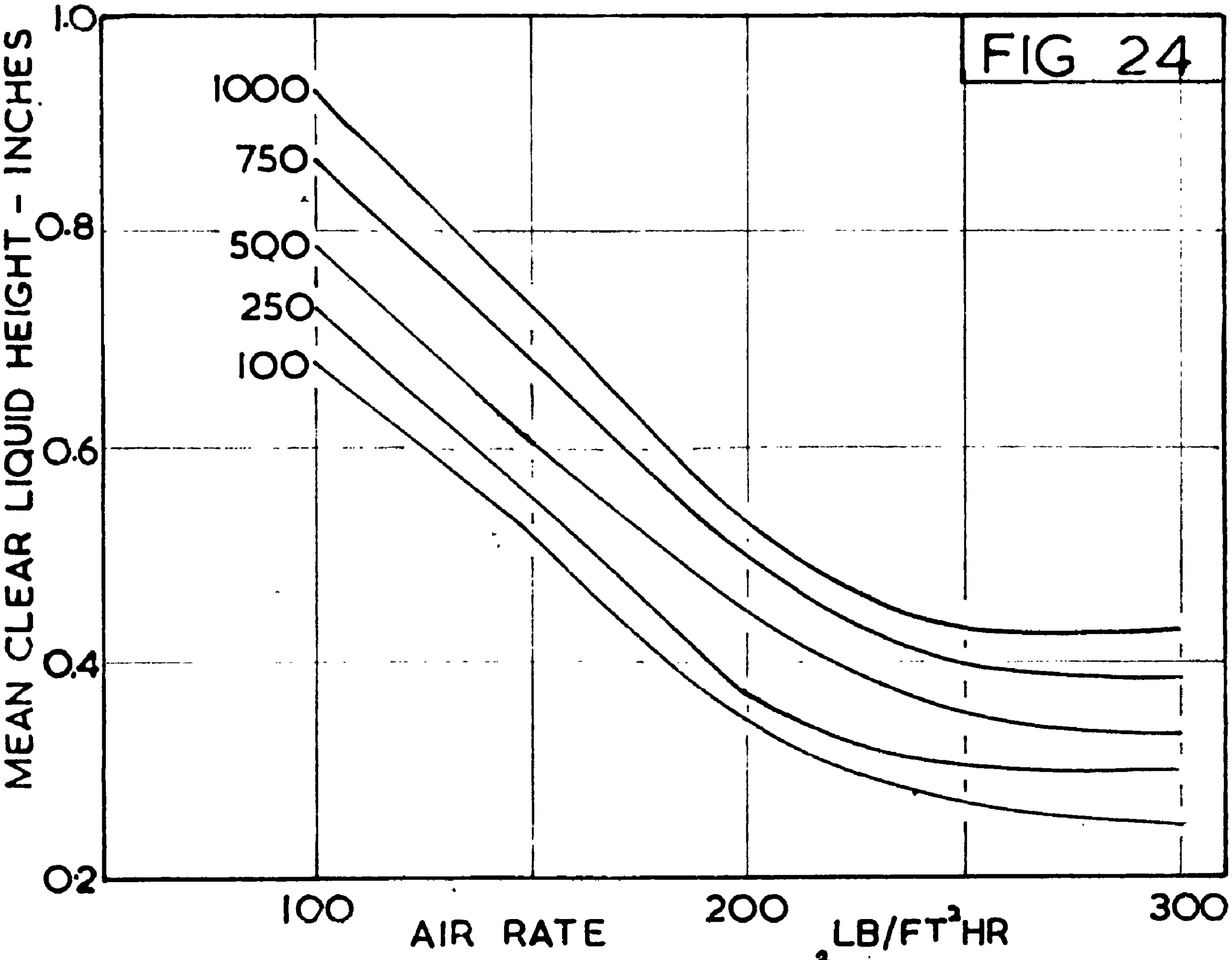

PARAMETER IS WATER RATE — LB/FT²HR

higher "dry plate" pressure drop. It is thus misleading to subtract the "dry plate" pressure drop from the plate pressure drop when some of the slots are inactive.

The froth height characteristics for the original 30 inch plate and the modified plate with weir heights of 1.5 and 2.0 inches are given in Figures 25, 26 and 27. The froth height on most bubble plates depends primarily on the gas rate, increasing considerably with increasing gas rate. The Kuhni Plate with its low weir height and different slot design behaves very differently and the froth height can be seen to be virtually independent of the air rate and dependent only on the water rate and weir height. Froth heights are very difficult to estimate, different workers obtaining different estimates from the same operating condition. It is largely a matter of opinion where the froth height should be measured and it is a mistake to place too much reliance on these estimates.

It is difficult to explain why the froth height should decrease with increasing air rate at the higher weir heights but it may be a result of a lower water hold-up on the plate. The data at weir heights of 1.5 and 2.0 inch in Figures 26 and 27 are used later in Section 5:11.

It is convenient to correlate the plate pressure drop (ΔP (plate)) as the sum of the two component pressure drops, dry plate pressure drop ($\Delta P(\text{dry})$) and hydraulic pressure drop, ($\Delta P(\text{hyd})$).

$$\Delta P(\text{dry}) = 1.30\, G_M^{1.72} \times 10^{-4} \text{ inches of water} \qquad (5;4)$$

$$\Delta P(\text{hyd}) = 7.01\, G_M^{-0.53} \cdot L_M^{0.105} \text{ inches of water} \qquad (5;5)$$

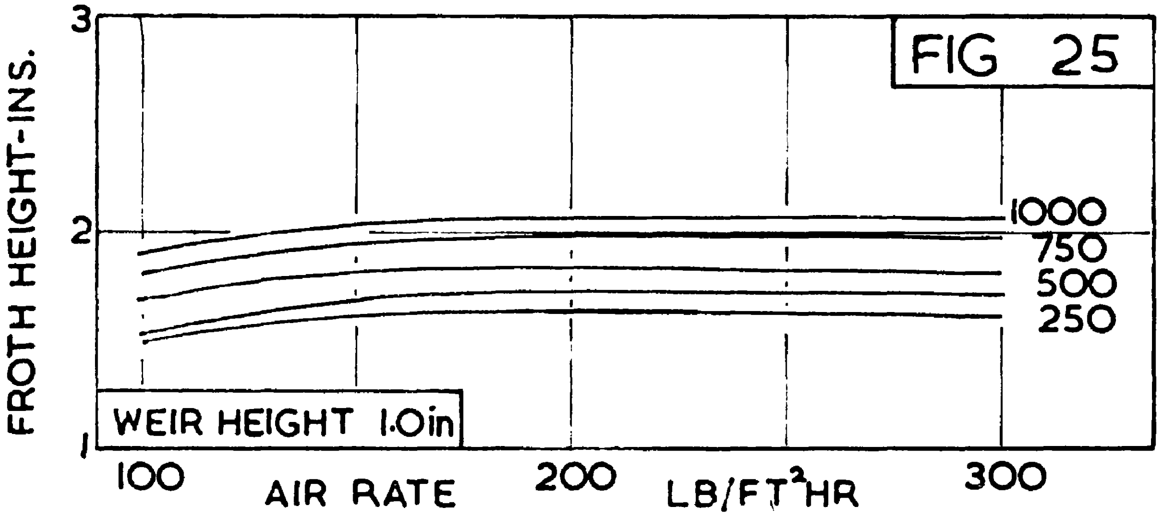

FIG 25

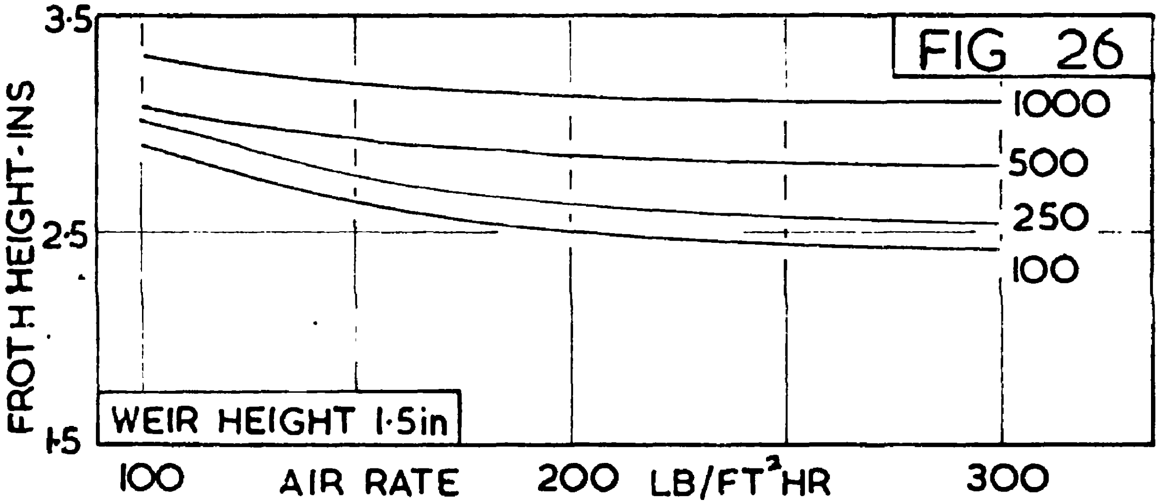

FIG 26

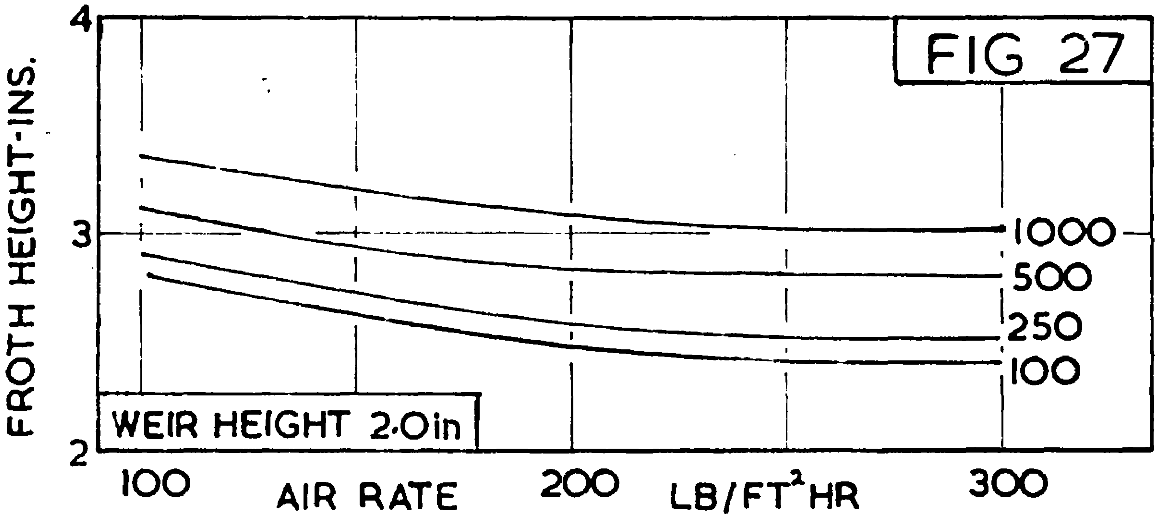

FIG 27

PARAMETER IS WATER RATE – LB/FT^{2}HR

$\Delta P(\text{plate}) = \Delta P(\text{dry}) + \Delta P(\text{hyd})$ inches of water (5;6)

Where G_M = air rate (lb./ft.^{2}hr)

L_M = water rate (lb./ft.^{2}hr)

A correlation is given below for froth height with the original plate with a 1 inch weir height.

$$F.H. = 1.55 + 5.\,L_M.\,10^{-4} \qquad (5;7)$$

where F.H. = Froth height (in.)

L_M = Water rate (lb./ft.^{2}hr)

5 : 4 Liquid Mixing Tests with Water

As has been discussed in the Introduction, equations exist relating the variance of the outlet time-concentration curve and the Peclet number, Pe, on rectangular distillation plate. It was necessary to derive the corresponding equation for radial flow plates and this is done in Appendix B. The equation is as follows:

$$\sigma^2 = \frac{\left(\frac{q}{p}\right)^4 \frac{(1+\alpha)^2}{(\alpha-2)} - \frac{(1-\alpha)^2}{(\alpha+2)}}{\left[\left(\frac{q}{p}\right)^2 (1+\alpha) + (1-\alpha)\right]^2} \quad \text{and} \quad Pe = 4\alpha \frac{(q-p)}{(q+p)} = \frac{(q-p)^2}{D_E . tm.}$$

ie. equations 6:5, 6:6, and 6:7.

where σ^2 = dimensionless normalized variance

q = peripheral radius of the plate (ft.)

p = radius of the outlet weir (ft.)

tm = mean liquid residence time (sec.)

α = ratio $qV_1/2D_E$

and where V_1 = froth velocity at the periphery (ft./sec.)

D_E = eddy diffusivity (ft.^{2}/sec.)

Using the above equations values of the Peclet number and the eddy diffusivity were calculated for each tracer injection test and are plotted in Figures 28 and 29.

The Peclet Numbers obtained very from 10 to 30 a fairly, small variation. The Peclet Numbers obtained at the University of Delaware on bubble cap trays varied from 0.4 to 50. Smoothed values of the

FIG 28

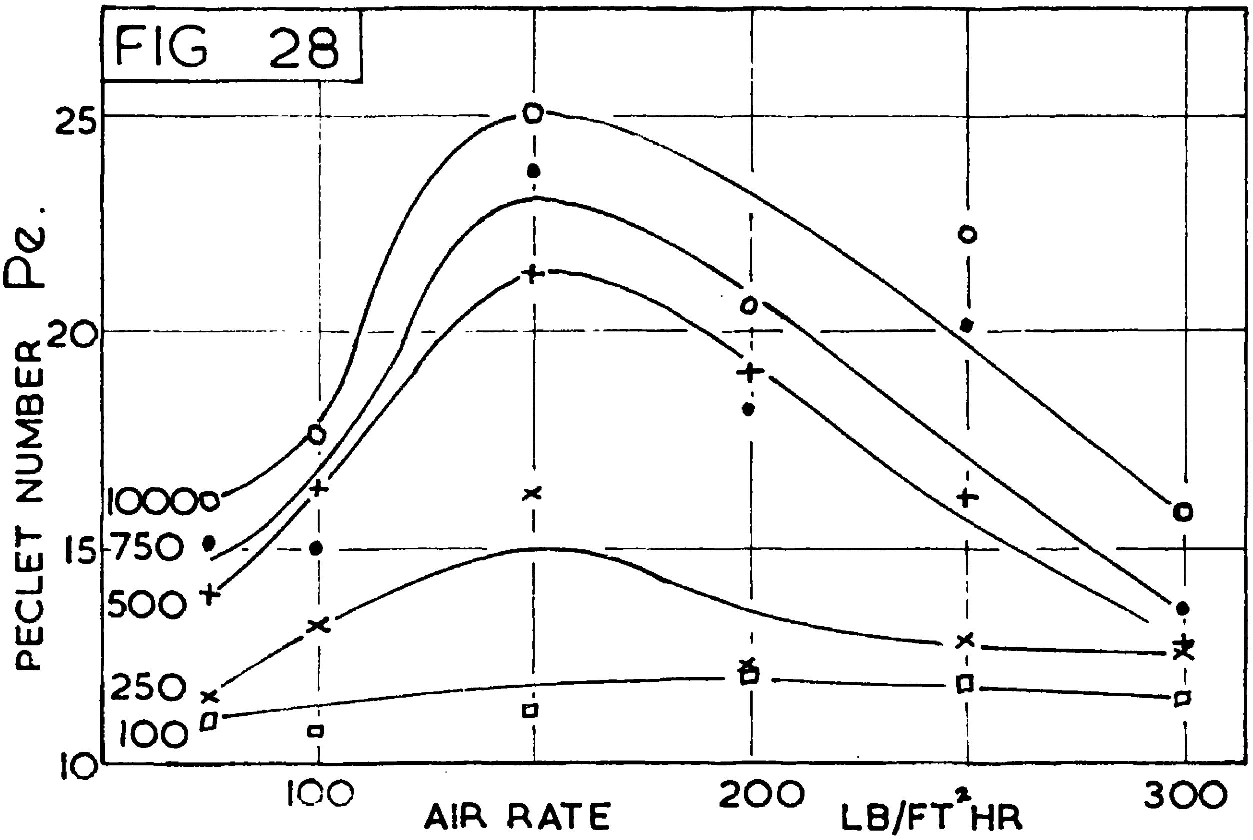

FIG 29

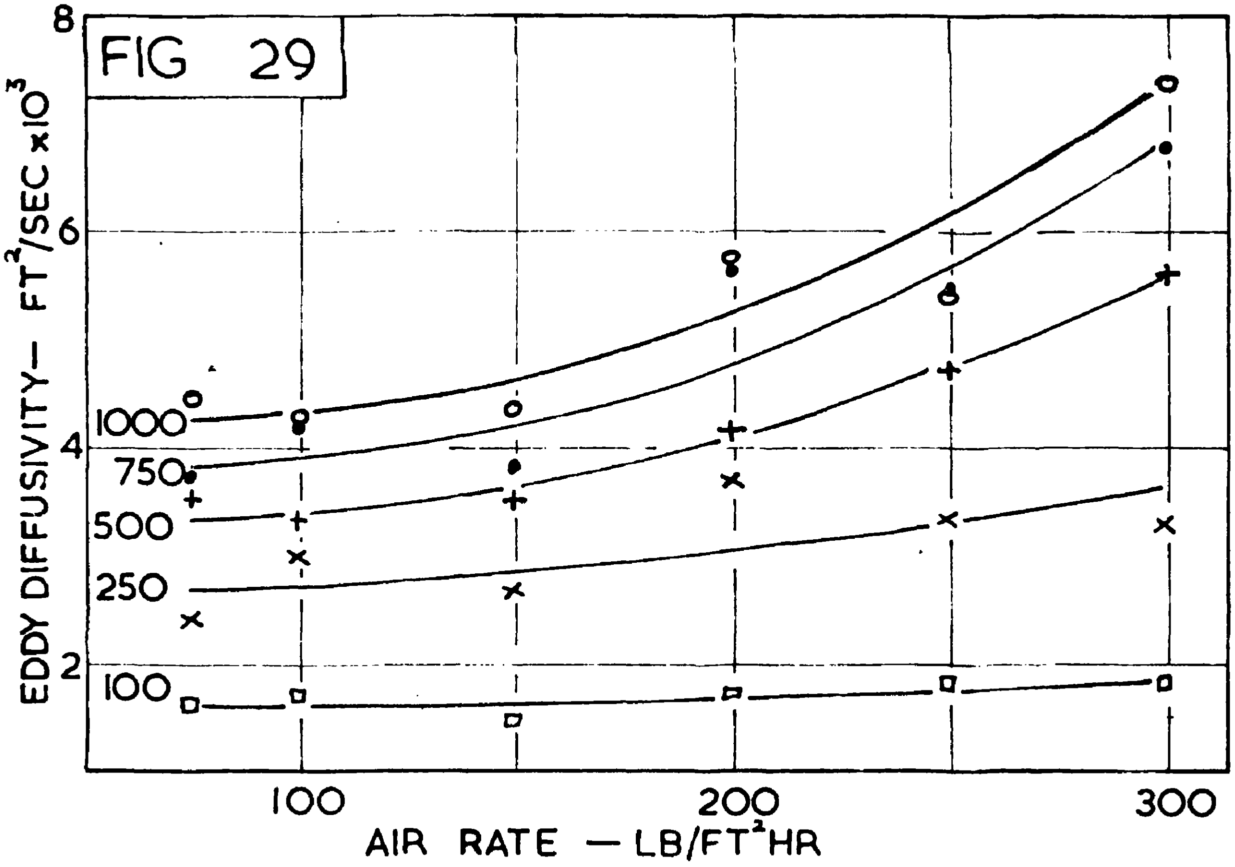

PARAMETER IN BOTH FIGURES IS WATER RATE, LB/FT^{2}HR
1000— ○ ; 750— ● ; 500— + ; 250— × ; 100— □

Peclet number taken from Figure 28 were used in calculating the number of transfer units in the oxygen desorption tests.

Figure 29 shows that the eddy diffusivity increases with increasing air and water rates. At low water rates the effect of air rate is negligible. It has been suggested[19] that the eddy diffusivity is a function of the froth height only. From Figures 25 and 29 it appears that froth height and eddy diffusivity may well be related, since the form of the curves is similar.

The increase in eddy diffusivity occurring at high air and water rates does not, however, support this theory since air rate has very little effect on froth height on the Kuhni Plate. Gilbert[107] has concluded that gas rate has no significant effect on eddy diffusivity apart from its effect on froth density. The Kuhni Plate with its very low froth height and weir height may be unique in this respect.

It is interesting to compare the values of the eddy diffusivities on the Kuhni Plate with those obtained by other workers. Eddy diffusivities in this work varied from .0015 to .0075 $ft.^2/sec$. The Delaware tests[19] on bubble cap plates gave diffusivities from .02 to .21 $ft.^2/sec$. Gilbert obtained diffusivities from .02 to .11 $ft.^2/sec$. The explanation of the much lower eddy diffusivities obtained on the Kuhni plate is that the liquid and gas rates used are lower than those of bubble cap plates and the low weir height and froth heights of the Kuhni plate do not permit the same degree of back mixing as on other plates. In addition the design of the annular caps is such that it is unlikely that much liquid diffuses back over these caps owing to the relatively high froth velocities over the caps. On a bubble cap plate, liquid is able to flow back in eddys between caps whereas on the Kuhni plate the caps act almost as "non return" valves.

If the A.I.Ch.E. Bubble Tray Design Manual[21] correlation for eddy diffusivity is applied to the Kuhni Plate fair agreement is obtained considering that the correlation is not strictly applicable to conditions on the Kuhni Plate. For example, at a water rate of 250 lb./ft.^{2}hr and an air rate of 300 lb./ft.^{2}hr the observed eddy diffusivity is 0.0033 ft.^{2}/sec. The figure obtained from the correlation is 0.0020. It is unfair to apply a correlation to conditions outside its "terms of reference" but its application in this instance shows that the low eddy diffusivities on the Kuhni Plate are probably a result of the weir height and the operating conditions and that a conventional plate operating under similar conditions would give similarily low eddy diffusivities.

The form of the curves in Figure 28 of the Peclet Number is the result of the irregular form of the residence time (or liquid hold-up) curves. The Peclet number is inversely proportional to the liquid residence time which is in turn proportional to the liquid hold-up at a constant liquid rate. As a result the high values of the liquid hold-up occurring at low gas rates reduce the Peclet Number under these conditions forming a maximum in the curve. This maximum (which corresponds to a minimum degree of mixing) was confirmed by dye injection tests on the degree of lateral mixing. These tests are discussed in Section 5;5.

5 : 5 Dye Injection Tests with Water

These tests were done to study the degree of lateral mixing on the plate. Dye was injected continuously into the froth and when conditions had stabilised a photograph was taken. Some typical results are shown in Figure 30, A to I.

The first series A, B and C in Figure 30 show the effect of changing the air rate at a constant water rate of 500 lb./ft.^{2}hr. It can be seen that the photos at 300 and 100 lb./ft.^{2}hr (A & C) have a greater degree of lateral mixing than the centre photo at 200 lb./ft.^{2}hr. This suggestion of a minimum mixing condition is substantiated by the discussion in the previous section. In Photo "C" the inner trough is not bubbling and there is considerable lateral mixing in it. The "diffussion angle" is less than 180°. It can be seen that the plate caps are almost equally visible in the three photos indicating the constancy of the froth height.

The second series D, E and F show the effect of changing the liquid rate at a constant air rate of 200 lb./ft.^{2}hr. There is very little difference in mixing between D and E, i.e. 1,000 and 500 lb./ft.^{2}hr (water rate). Photo F shows a slightly greater degree of mixing which is to be expected from the previous mixing discussion.

It is interesting to note the effect of the increase in froth height, in making the plate features almost invisible in D. The froth height of D is 2.0 inches, while that of F is 1.6 inches.

The third series, G, H and I were taken at a water rate of 500 lb/ft2 hr. and an air rate of 200 lb./ft.^{2}hr. injecting the tracer at different points on the plate. Photo E of the last series in Figure 30 shows the condition with the tracer injected at the edge of the plate, G, H and I show the tracer injected into the troughs, successively nearer to the outlet weir. The injection pipe can be seen as a white line on the photos. It is immediately apparent from H and I that very little back mixing occurs from the inner two troughs. This is probably a result of the relatively higher froth velocity nearer to the centre of the plate Photo G, however, shows a fair amount of back mixing, associated with the lower froth velocity nearer to the periphery, which suggests that the bulk of the liquid mixing on the plate occurs in this region.

FIG 30

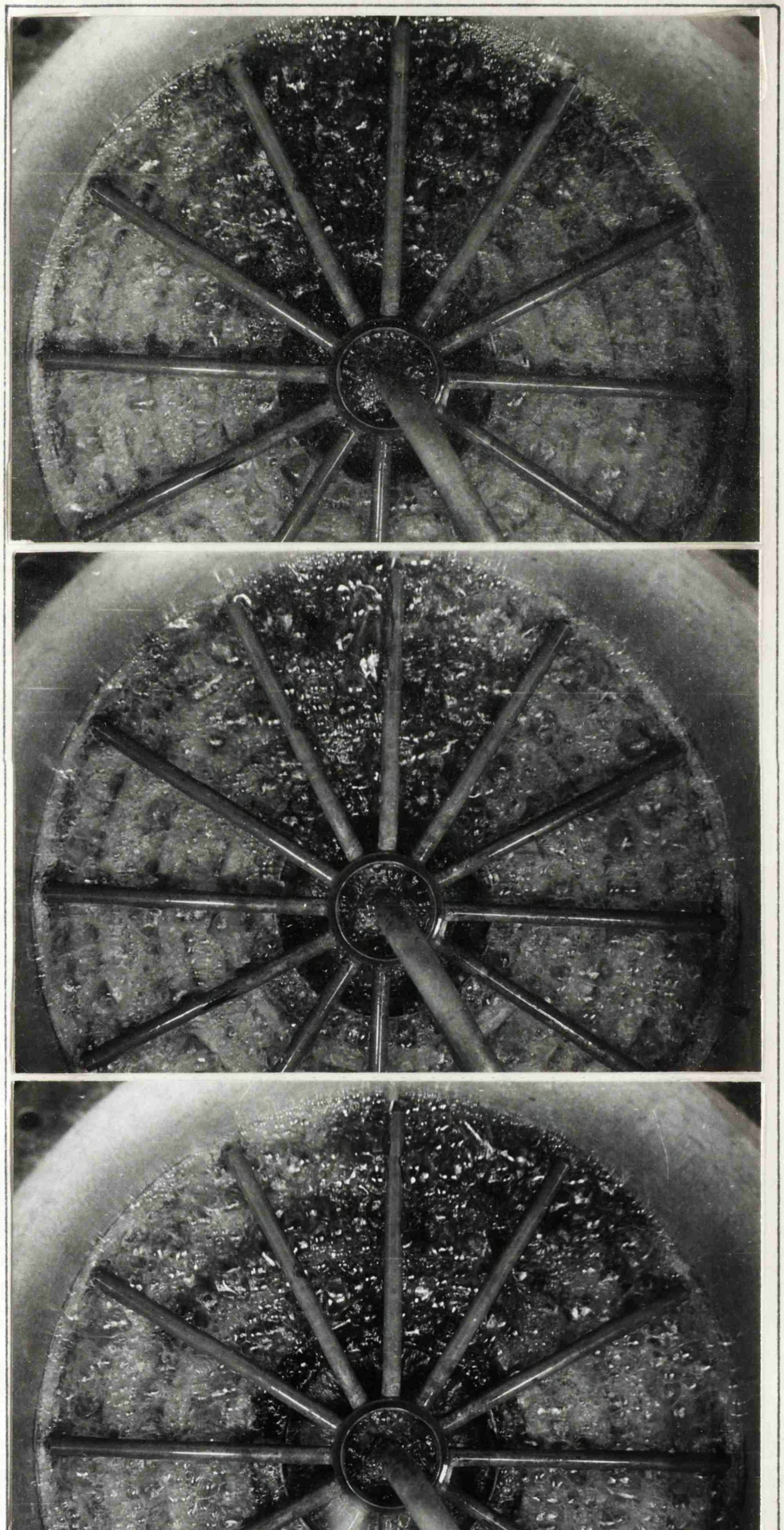

A

G_M — 300

L_M — 500

B

G_M — 200

L_M — 500

C

G_M — 100

L_M — 500

FIG 30

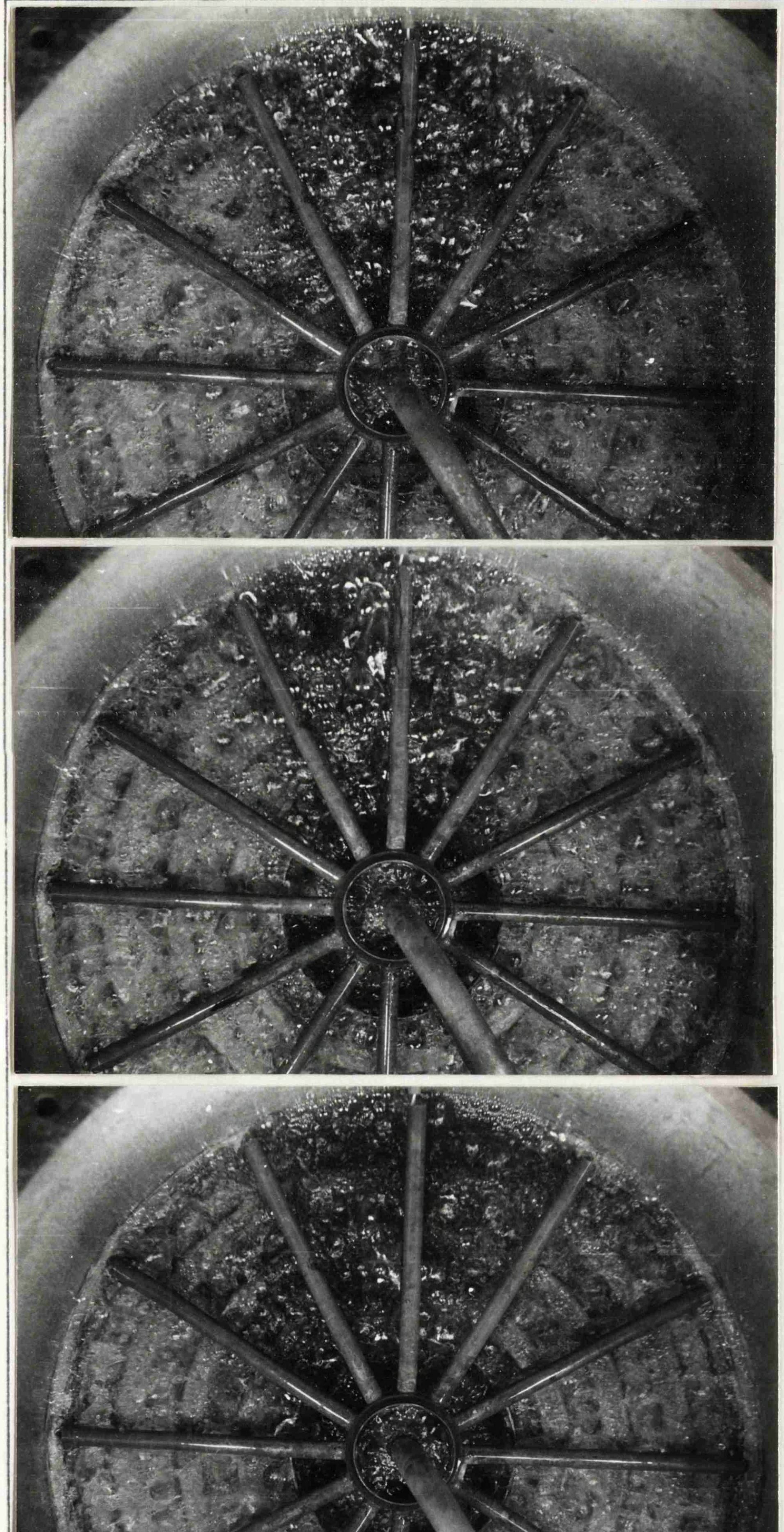

D

$G_M - 200$

$L_M - 1000$

E

$G_M - 200$

$L_M - 500$

F

$G_M - 200$

$L_M - 100$

FIG 30

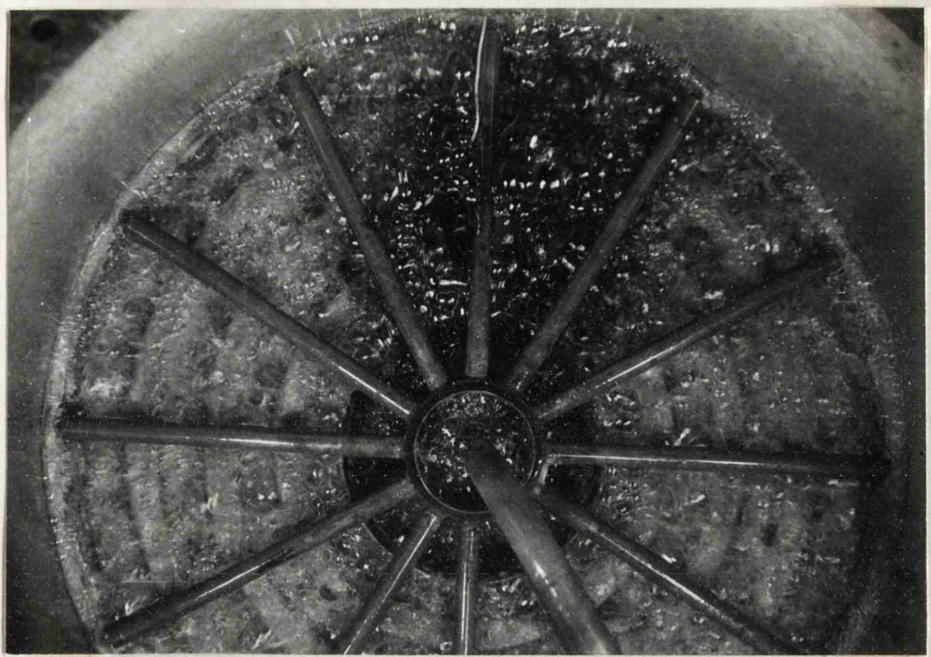

G

G_M — 200

L_M — 500

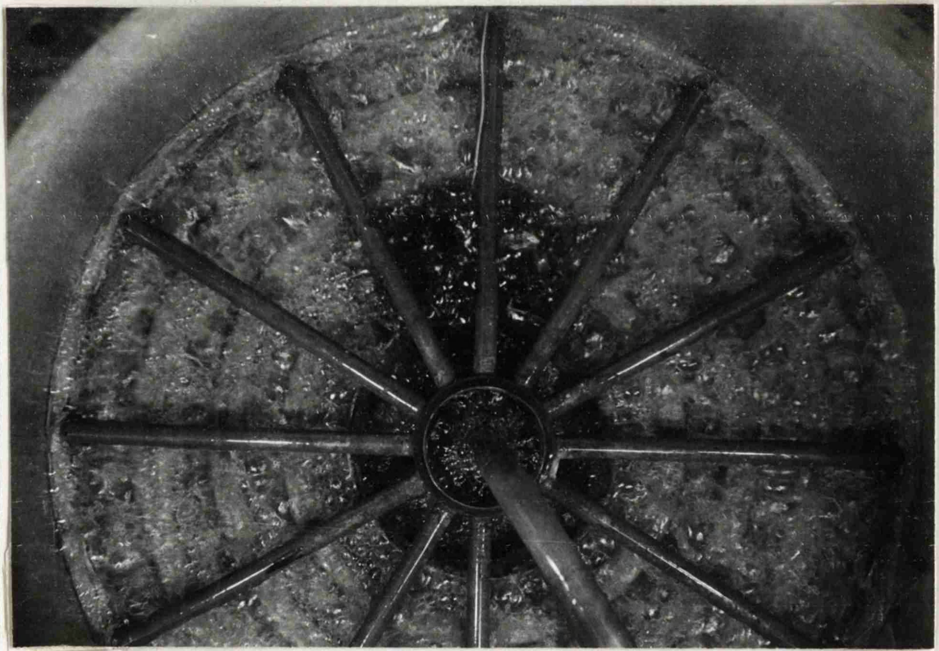

H

G_M — 200

L_M — 500

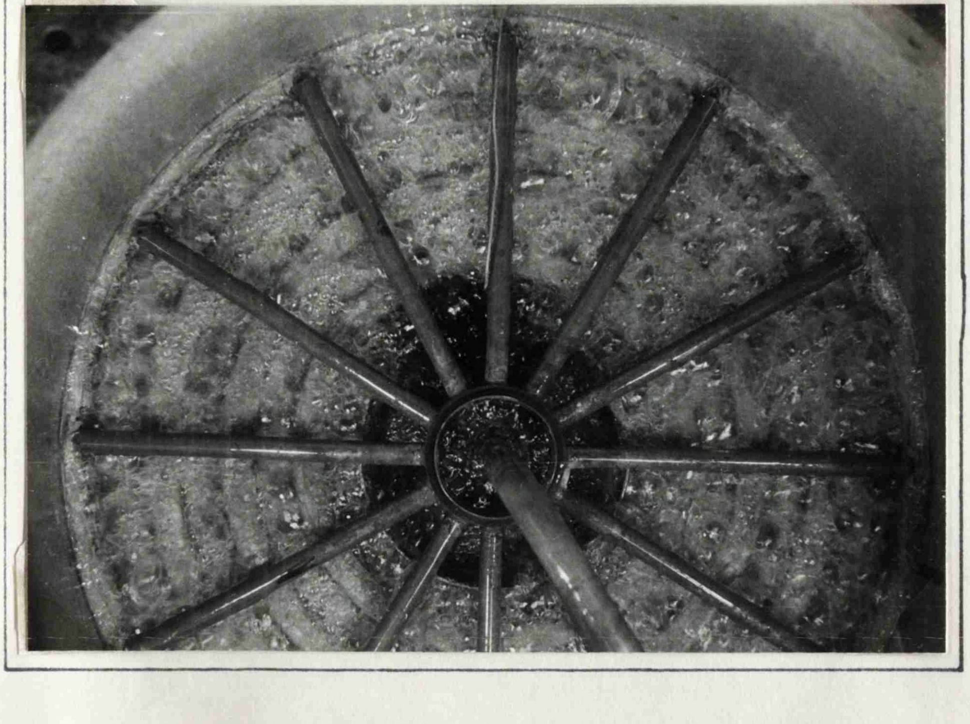

I

G_M — 200

L_M — 500

5 : 6 Liquid Mixing Tests with Viscous Solutions

As part of the A.I.Ch.E. Research Programme[19] the effects of liquid density, viscosity and surface tension on eddy diffusivity were investigated. Only four tests were done to determine the effect of these variables singly and it was concluded that eddy diffusivity was independent of all three. More searching tests on the effect of liquid viscosity using the steam-water system led to the same conclusion.

The results of the series of tests on the Kuhni Plate at viscosity levels of 2, 4, 8 and 16 cP are shown in Figures 31, 32 and 33 as eddy diffusivities and in Figures 34, 35, 36 and 37 as Peclet numbers.

Figures 31, 32 and 33 show the eddy diffusivity plotted against viscosity at air rates of 100, 200 and 300 lb./ft.^{2}hr. respectively. An increase in eddy diffusivity of approximately 30% between 1 and 2 cP is apparent and thereafter there is a fall in eddy diffusivity to 16 cP. The increase is to be expected since the eddy diffusivity appears to be a function of the volume of liquid on the plate. The reduction is probably due to increasing sluggishness slowing down the rate of mixing of the liquid.

The overall effect is, however, small in the range of viscosities investigated.

The graphs of the Peclet numbers show that they are almost independent of all the variables investigated. Of the 48 tests only 2 Peclet numbers were outwith the range 10 to 15. This result is largely coincidental since the conditions under which the eddy diffusivities are highest are those under which the liquid residence times are lowest and these two effects, appearing as a product in the Peclet number, cancel out. This constancy of the mixing parameter is of some importance in the analysis of the oxygen desorption results, to be discussed later.

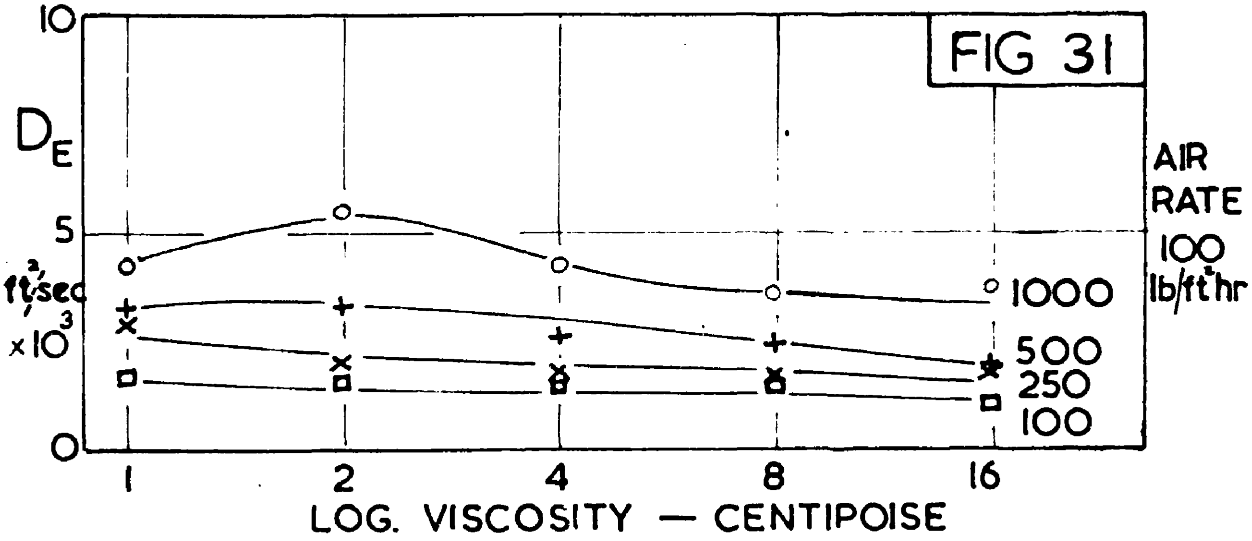
FIG 31

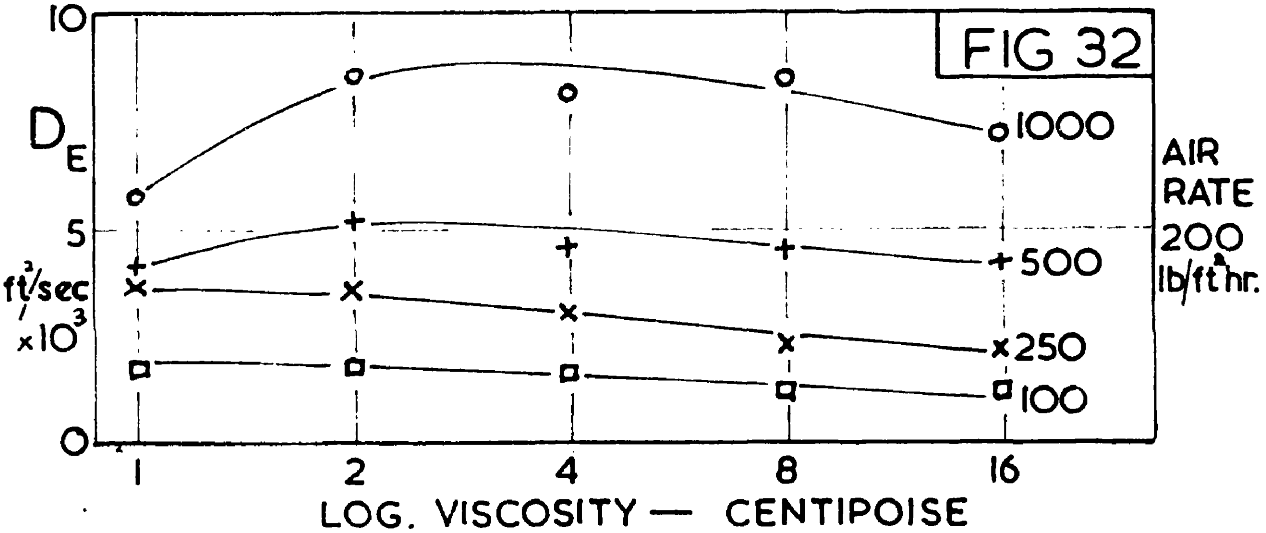
FIG 32

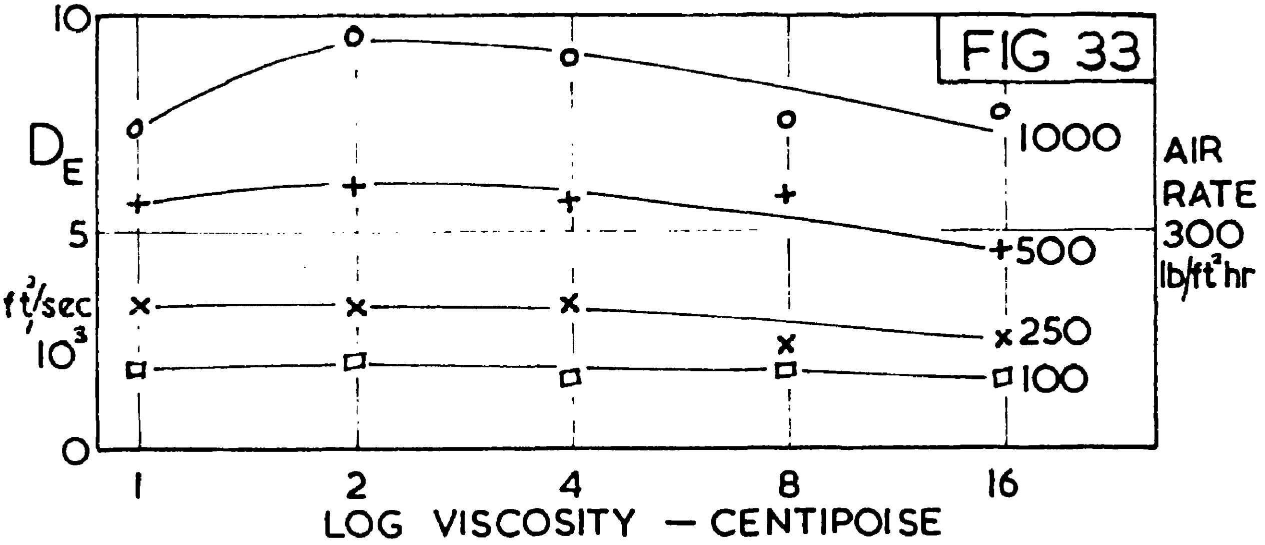
FIG 33

PARAMETER IS WATER RATE — LB/FT^2HR

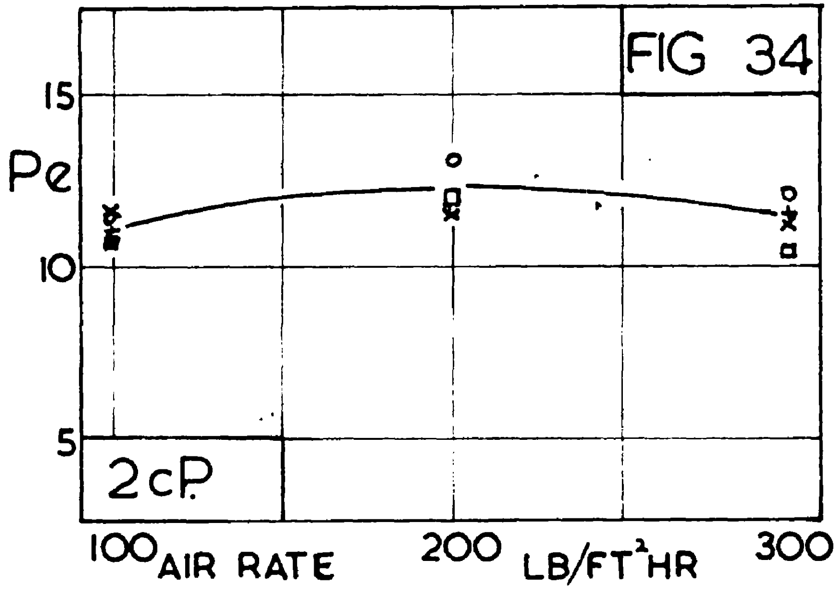
FIG 34

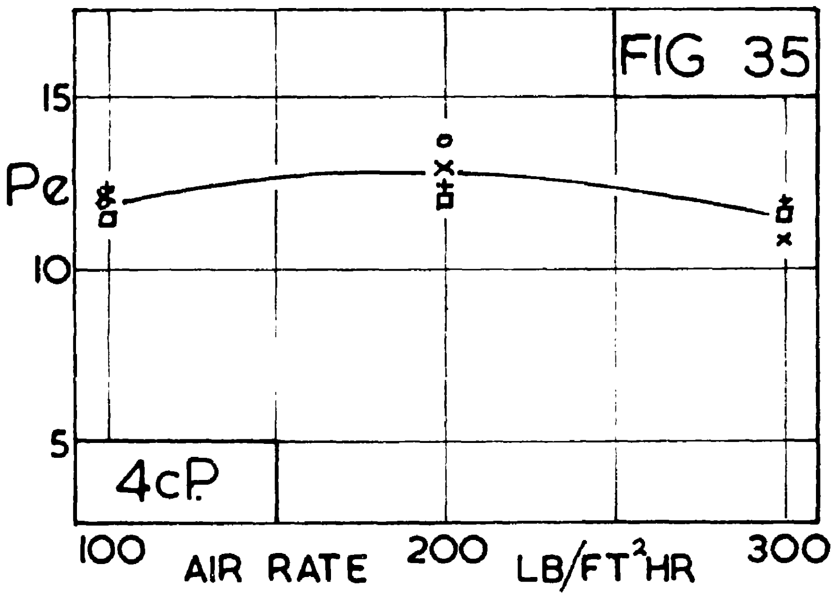
FIG 35

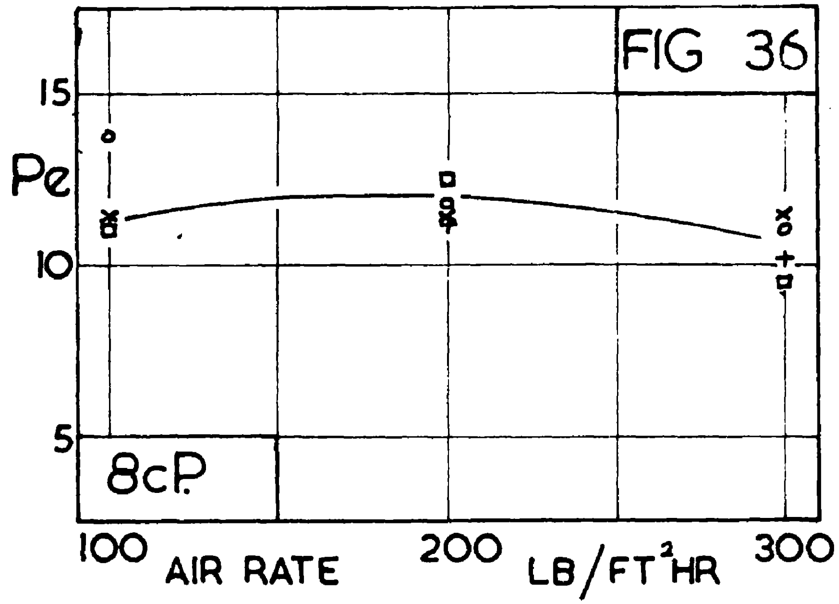
FIG 36

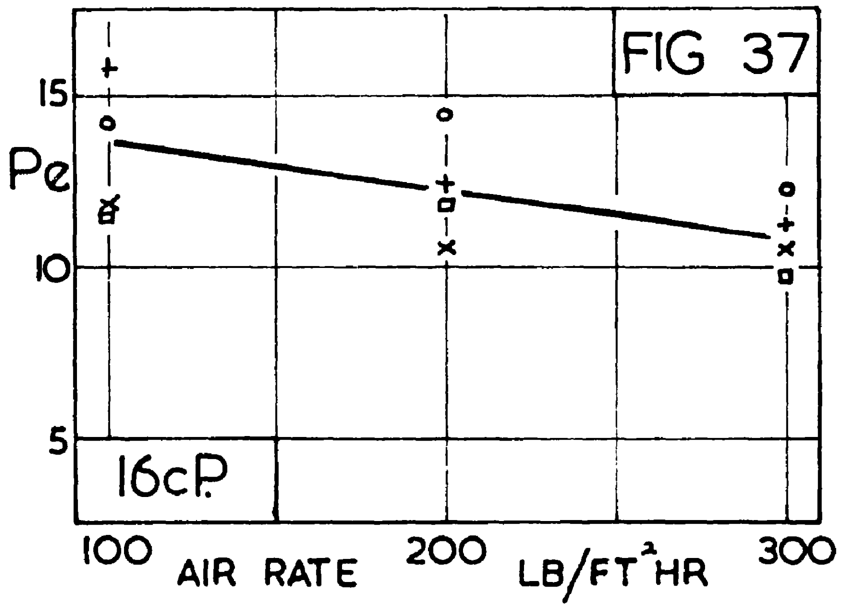
FIG 37

PARAMETER IS WATER RATE - LB/FT²HR - 1000— o ; 500— + ; 250— x ; 100— □.

5 : 7 Gas Phase Efficiency Tests with Water

Figure 38 shows the efficiencies obtained on the 30 inch plate using the two methods of humidification efficiency determination. The solution evaporation method gives less accurate results than the outlet psychrometer method, the points showing a fairly wide scatter. It was hoped that the effect of evaporation of entrained water in the air stream leaving the plate would be indicated by higher efficiencies in the outlet psychrometer tests, especially at high air rates but the results are not sufficiently accurate to draw any such conclusion.

Entrainment data obtained in these tests are given in Figure 39. These data must not be confused with plate to plate entrainment which would be greater and dependent on the plate spacing. The amount of entrainment lost during a test is remarkably small and is always less than 15% of the "gross evaporation" due to evaporation and entrainment. If the entrainment correlation for a bubble cap plate published by the A.I.Ch.E. Research Committee[21] is applied to the Kuhni Plate the predicted entrainment is far greater than that actually occurring. It appears that the Kuhni plate despite its very high slot velocities, corresponding to the slot area of 4.25% of the column area, has low entrainment characteristics. This advantage is probably necessary and may be offset by the very low plate spacings used commercially. For example, a typical plate spacing for a 12 inch plate is 4.0 inches and a 30 inch plate 5.1 inches.

As a result of the low entrainment characteristics the use of the outlet psychrometer method is more justifiable than it would be for a

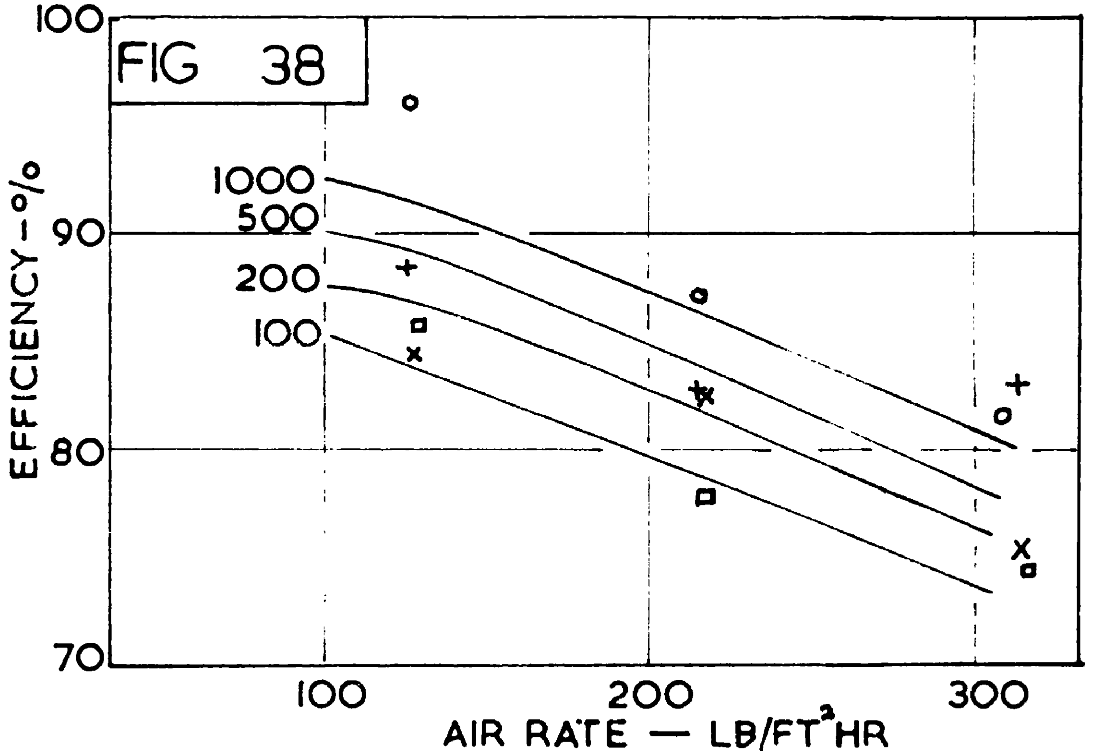

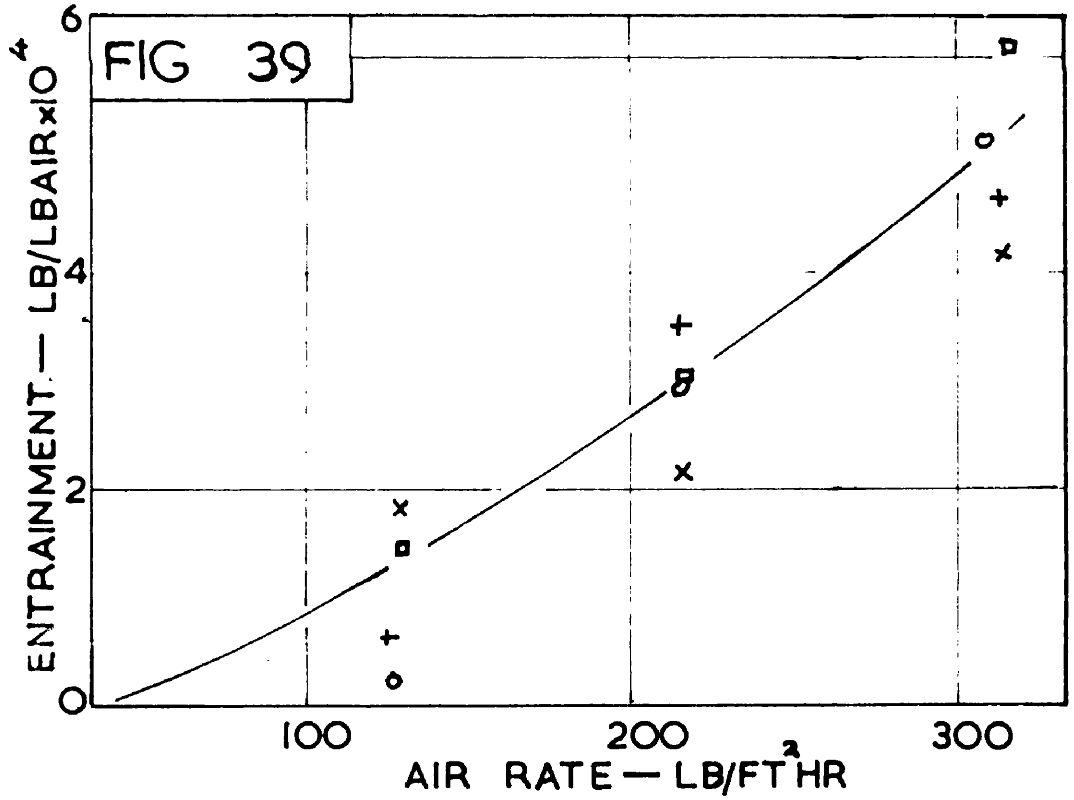

PARAMETER IN BOTH FIGURES IS WATER RATE
1000 — ○ : 500 — + : 200 — × : 100 — □ (LB/FT²HR)

bubble cap or sieve plate, especially since the air rates used in the present work are relatively low by comparison with those used in bubble cap columns.

The deduction of the maximum probable error for the two humidification methods is given in Appendix G and the high value of 10.7% for the solution evaporation method is to be expected from the wide scatter of the data in Figure 38. The reason for this large error is primarily that the increase in humidity is measured indirectly by a method involving an accurate knowledge of the air rate. The scatter of the data can be partly attributed to the variation in inlet humidity and temperature during the test. The inlet air was drawn from the atmosphere of the laboratory and varied in absolute humidity by up to 10% and in temperature by up to 10°F. For these reasons and the greater convenience and accuracy (maximum probable error 4.5%), the outlet psychrometer method was preferred for the later tests.

Figure 40 shows the gas phase efficiency characteristics and the qualitive conclusions can be immediately drawn that an increase in efficiency is brought about by either increasing the water rate or decreasing the air rate. The dashed line indicates the conditions under which the inner trough stops bubbling, at conditions to the left of this line the inner trough is inactive.

The effect of an increase in water rate is to increase the water hold-up on the plate as has been discussed in Section 5;1. The increased hold-up of water causes an increase in the froth height with the result that there is a greater air hold-up on the plate with a corresponding increase in contact time between the phases. The air hold-up can be

FIG 40

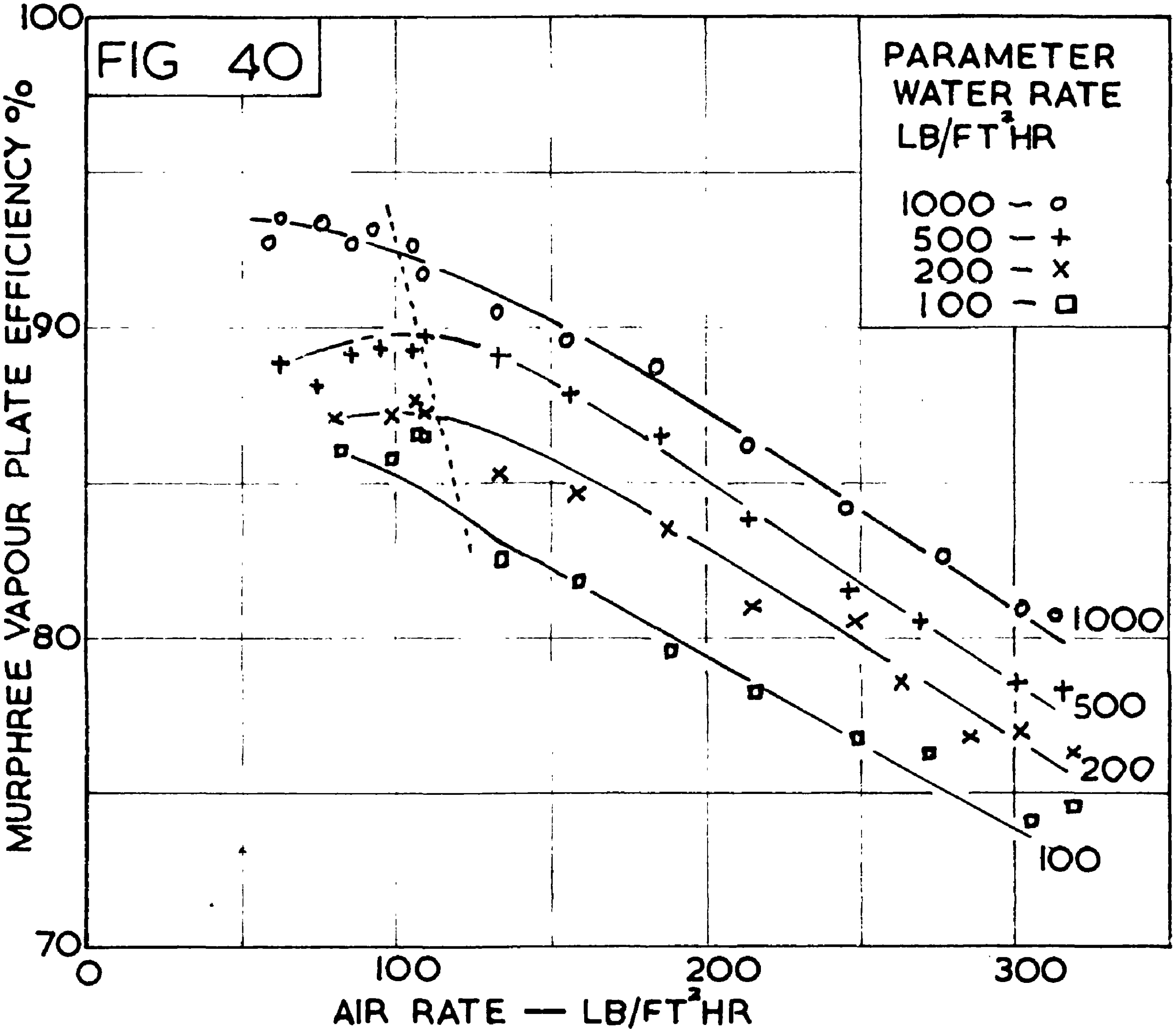
PARAMETER
WATER RATE
LB/FT^{2}HR
1000 — o
500 — +
200 — x
100 — □
MURPHREE VAPOUR PLATE EFFICIENCY %
100
90
80
70
0
100
200
300
AIR RATE — LB/FT^{2}HR
1000
500
200
100

calculated by subtracting the water hold-up from the froth volume, taking into account the volume of the caps. From the air hold-up and the air flow rate an estimate can be made of the residence time of the air in the froth.

To analyse the data further it is necessary to convert the efficiencies to transfer units and then to values of K_Ga, the product of the gas film mass transfer coefficient and the interfacial area per square foot of column cross sectional area. The quantity "a" is thus dependent on the froth height and should not be confused with the quantity often used in similar work, namely the interfacial area per unit volume of froth.

Figure 41 shows K_Ga plotted against air rate with water rate as parameter. The values of K_Ga show a remarkable variation in the range of operating conditions studied. It is certain that the interfacial area "a" increases as the air hold-up increases and this explains part of the change in K_Ga, but the air hold-up depends relatively little on the air rate whereas K_ga is very dependent on the air rate.

Table(vii) in the Tabulated Results gives air hold-up and residence time data, and a specimen calculation of these quantities is given in Appendix A (v). Figure 42 shows this data in graphical form.

It can be readily seen from this figure that an increase in water rate results in an increased air residence time. For example, at an air rate of 200 lb./ft.^{2}hr the effect of increasing the water rate from 100 to 500 then 1,000 lb./ft.^{2}hr is to increase the air residence time from

FIG 41

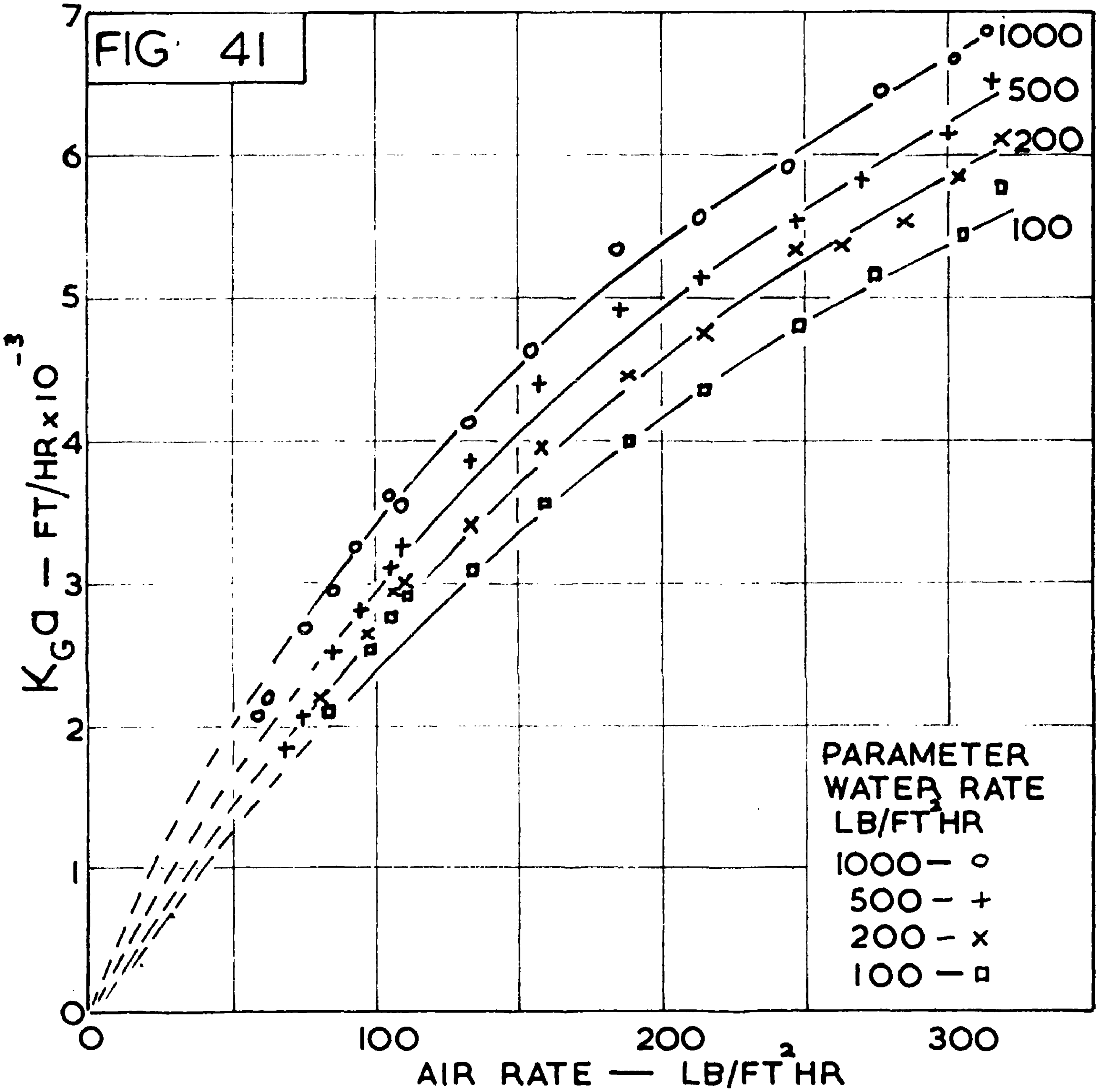

$K_G a$ — FT/HR × 10^{-3}
0
1
2
3
4
5
6
7
0
100
200
300
AIR RATE — LB/FT^2 HR
1000
500
200
100
PARAMETER
WATER RATE
LB/FT^2 HR
1000 — ○
500 — +
200 — ×
100 — □

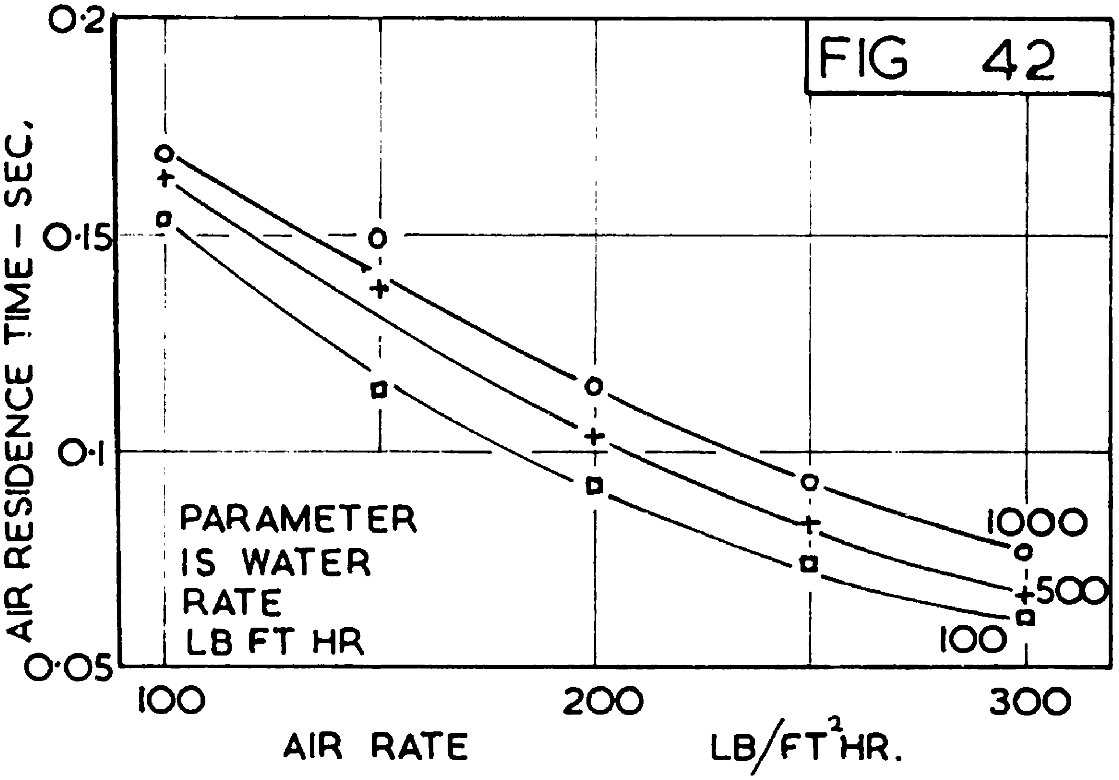

FIG 42

AIR RESIDENCE TIME - SEC.
0·2
0·15
0·1
0·05
100
200
300
AIR RATE
LB/FT²HR.
PARAMETER
IS WATER
RATE
LB FT HR
1000
500
100

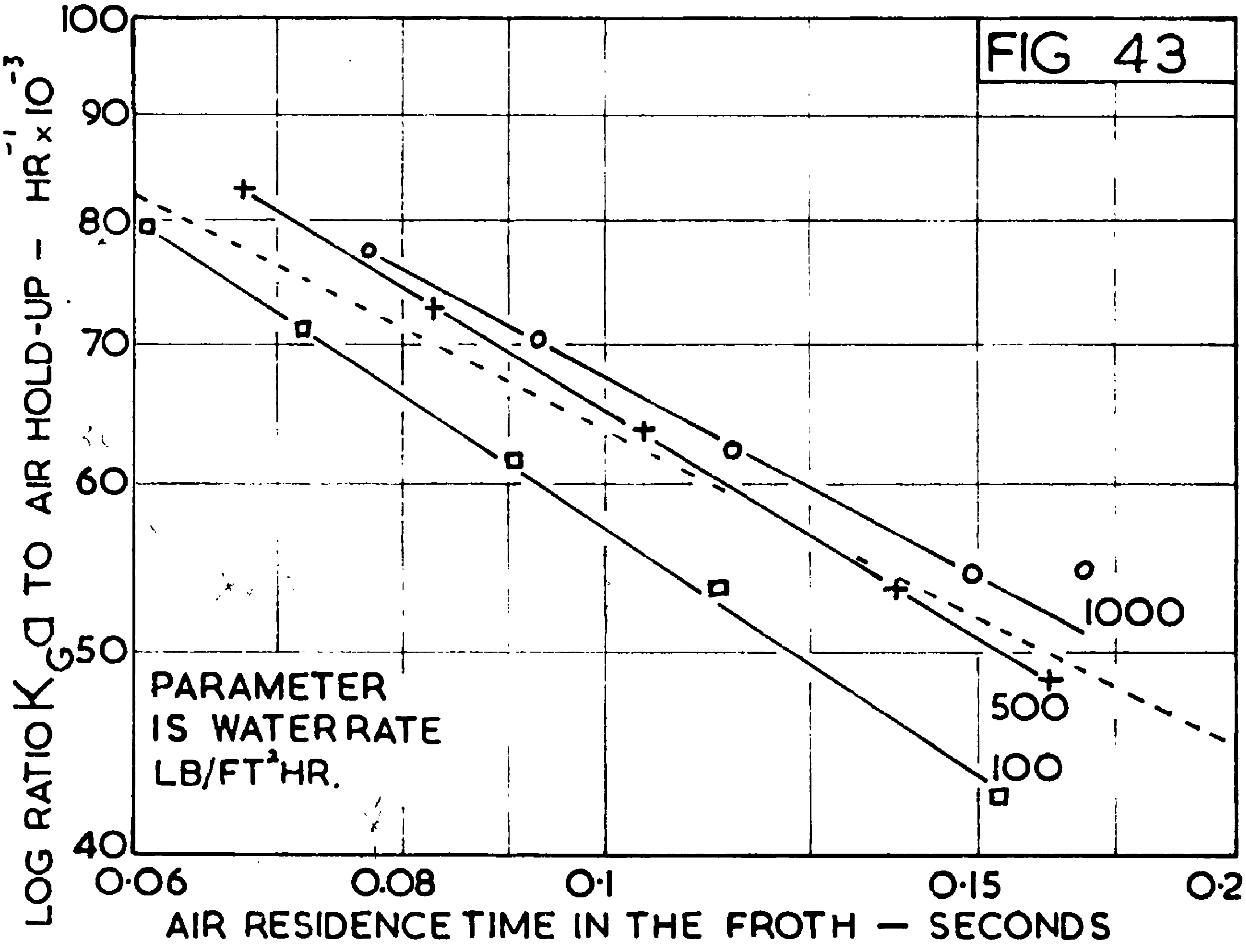

FIG 43

LOG RATIO K_Ga TO AIR HOLD-UP - $HR^{-1} \times 10^{-3}$
100
90
80
70
60
50
40
0·06
0.08
0·1
0·15
0·2
AIR RESIDENCE TIME IN THE FROTH — SECONDS
PARAMETER
IS WATER RATE
LB/FT²HR.
1000
500
100

0.091 to 0.104 then 0.115 seconds.

The effect of an increase in air rate is always to reduce the efficiency. This is a result of the lower air residence time at high air rates and also probably of increased "jetting" or "leakage" taking place at these high air rates. Figure 42 shows that at a water rate of 500 lb./ft.^{2} hr. the effect of increasing the air rate from 100 to 300 lb./ft.^{2}hr. is to reduce the air residence time from 0.163 to 0.067 seconds.

Chu et al[93] have shown that at slot submergences less than 2.5 inches the interfacial area per unit volume of vapour in a froth is constant.

Thus it is a fair assumption that "a" is nearly proportional to the air hold-up. This would be exact if bubble diameters and shapes were constant. Thus the ratio, K_Ga/(Air hold-up per ft.^{2} of plate area) will be nearly proportional to K_G and will be a useful quantity in estimating the effect of air and water rates on K_G. Figure 43 shows this ratio plotted against air residence time with water rate as parameter. The residence time was chosen for plotting purposes since the Penetration Theory of mass transfer applied to the gas phase predicts a relationship between K_G and the residence time "t_c" of the form.

$$K_G \propto t_c^{-0.5} \qquad (5;8)$$

In Figure 43 the dash line has an equation of the Penetration Theory form above and it can be seen that it follows the data remarkably closely.

The fact that the parameter curves do not coincide suggests that there may be more "jetting" at low water rates, which is to be expected from the observations of Spells and Bakowski[15,16].

Other complicating factors which preclude exact analysis of the data are that mass transfer must occur in the space immediately above the froth, that mass transfer to the air stream or jet in the immediate vicinity of the slot may be of the type investigated on wetted walls and thus dependent on the air velocity and friction with the result that equations derived on the basis of mass transfer from bubbles only will never exactly describe the very complicated processes taking place on a bubbling plate.

The data in Figure 43 are, however, sufficiently close to the "Penetration Theory line" to add support to the suggestion[18] that this theory may apply to gas phase mass transfer on a bubbling plate.

Garner and Porter[99], in an analysis of gas phase mass transfer from bubbles conclude that the relationship between the number of gas phase transfer units, the diffusivity D_G, the contact time t_c and the bubble radius r is as follows:

$$N_G = 0.52 + D_G \cdot \pi^2 \cdot t_c / r^2 \qquad (5:9)$$

Where D_G t_c and r are in consistent units.

This is based mass transfer to a sphere under unsteady state conditions. The Kuhni Plate data do not fit an equation of this type which is not surprising since the low weir height, the high slot velocity and the "jetting" largely invalidate the use of the model system on which equation 5;9 is based.

A correlation of the transfer units N_G against air rate (G_M lb./ft.^{2}hr.) and water rate (L_M lb./ft.^{2}hr.) is given below:

$$N_G = 4.4 \quad G_M^{-0.32} \cdot L_M^{0.14} \qquad (5;10)$$

5 : 8 Gas Phase Efficiency Tests with Viscous Solutions

The gas phase efficiency of the 30 inch Kuhni Plate was measured at viscosities of 2, 4, 8 and 16 cP, twenty tests being done at each viscosity level. The results are given in Figures 44, 45, 46 and 47.

The water vapour pressure tests on "Cellofas B" solutions described in Appendix D(ii) showed that the lowering of the vapour pressure was negligible and that the psychrometric data for pure water could thus be used. Any changes in the humidification characteristics are therefore not attributable to changes in the water vapour pressure.

Comparison of these four graphs shows little change in the efficiency "characteristics" with respect to air and water rates, but there is, however, a considerable change in the absolute value of the efficiency for each viscosity level. There is a steady rise in efficiency from 1 cP to 8 cP then a fall to 16 cP where the efficiencies are slightly lower than for water at 1 cP. The increase in efficiency from 1 to 8 cP varies from 6 to 12% and is very roughly equivalent to a 50% increase in the number of transfer units.

Figures 48 and 49 show this maximum plotted as K_Ga instead of efficiency, the maximum being most pronounced at high liquid rates.

A comparable series of tests was done by Barker and Choudhury[33] with sugar solutions on a 5 ft. diameter bubble cap tray. These authors found that the efficiency remained nearly constant up to a viscosity of 4 cP, above which it decreased steadily to the maximum viscosity investigated, 16.8 cP. The decrease in efficiency from 1 cP to 16 cP was very large, being from 80% down to 42% or in transfer units from 1.61 to

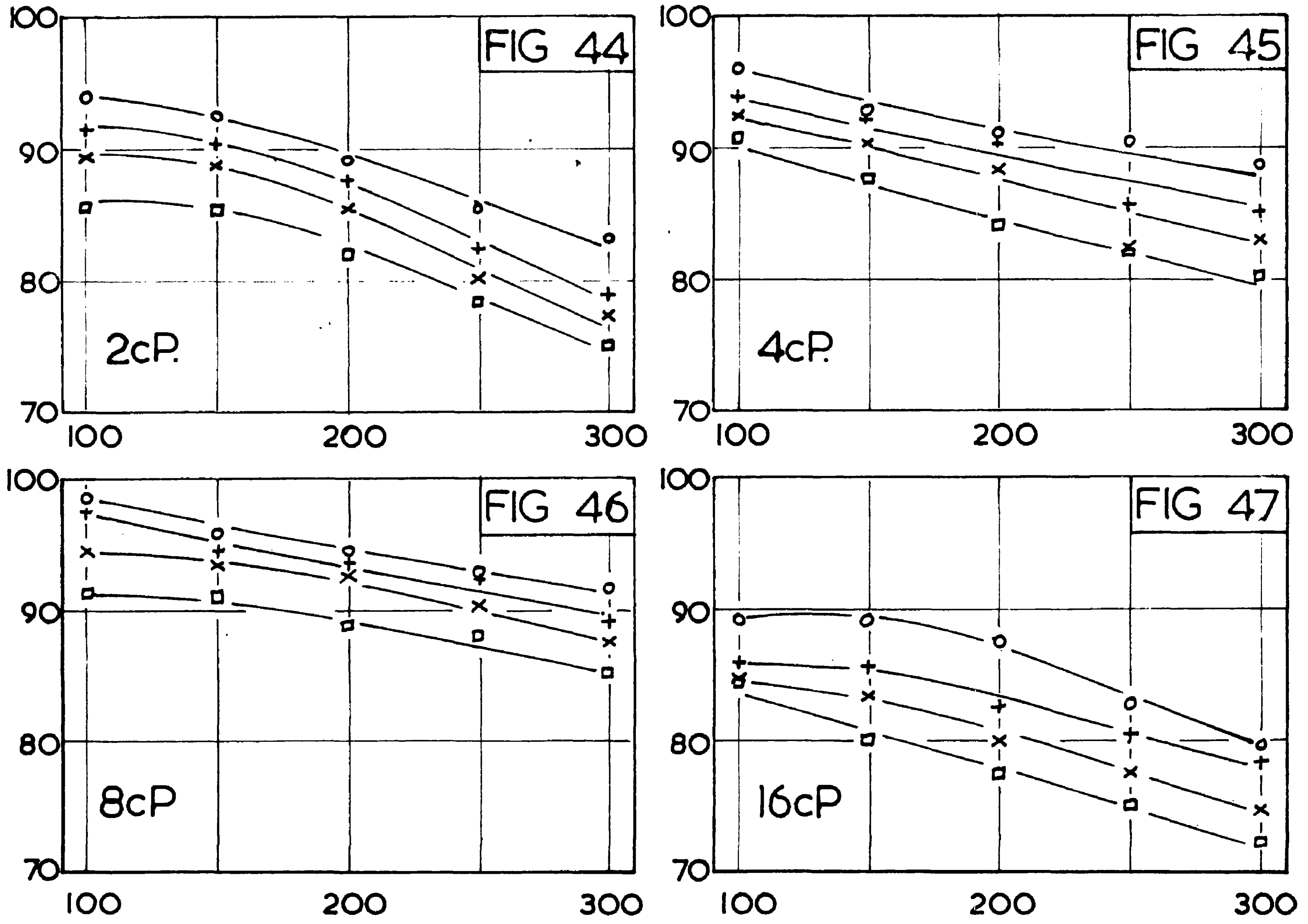

MURPHREE VAPOUR PLATE EFFICIENCY % AS A FUNCTION OF AIR RATE, LB/FT^{2}HR, AT VISCOSITIES OF 2, 4, 8 & 16cP.
PARAMETER IS LIQUID RATE LB/FT^{2}HR 1000—o ; 500—+ ; 200—x ; 100—□ .

FIG 48

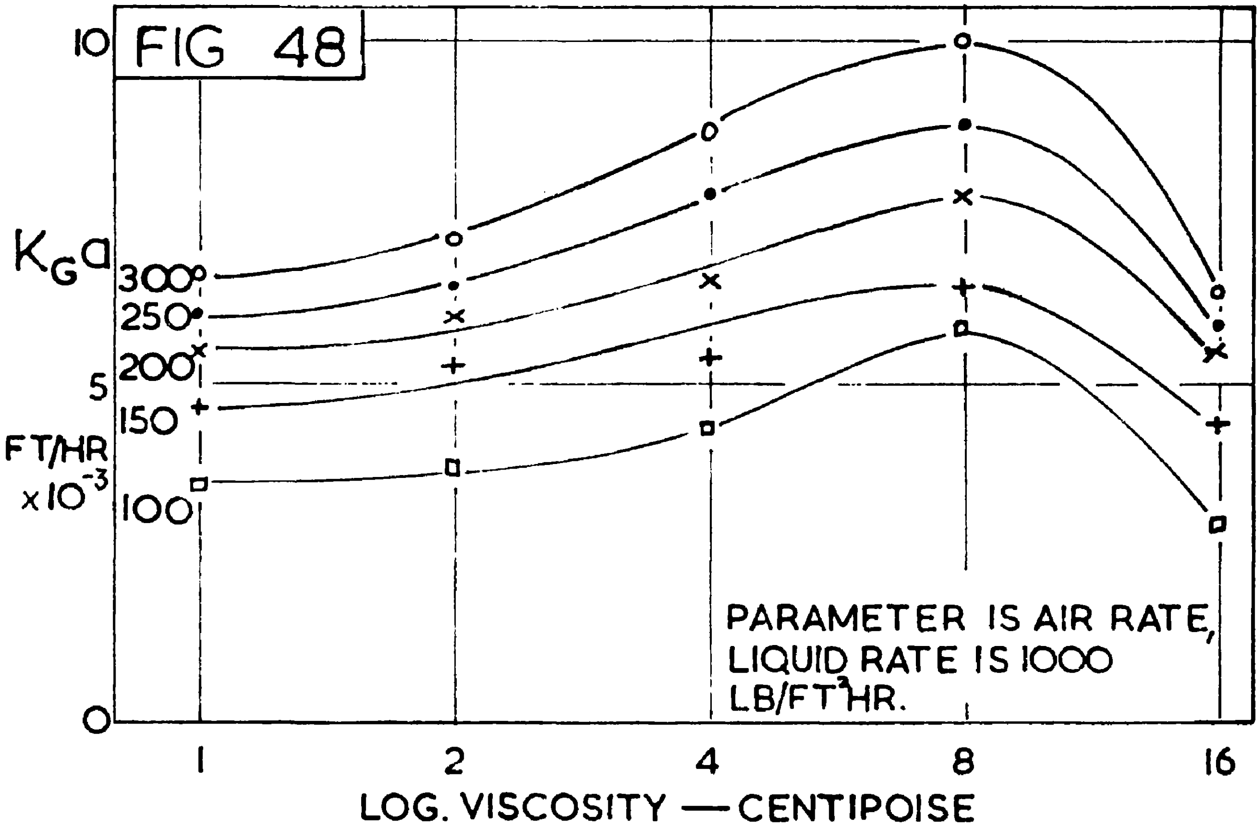

PARAMETER IS AIR RATE, LIQUID RATE IS 1000 LB/FT²HR.

FIG 49

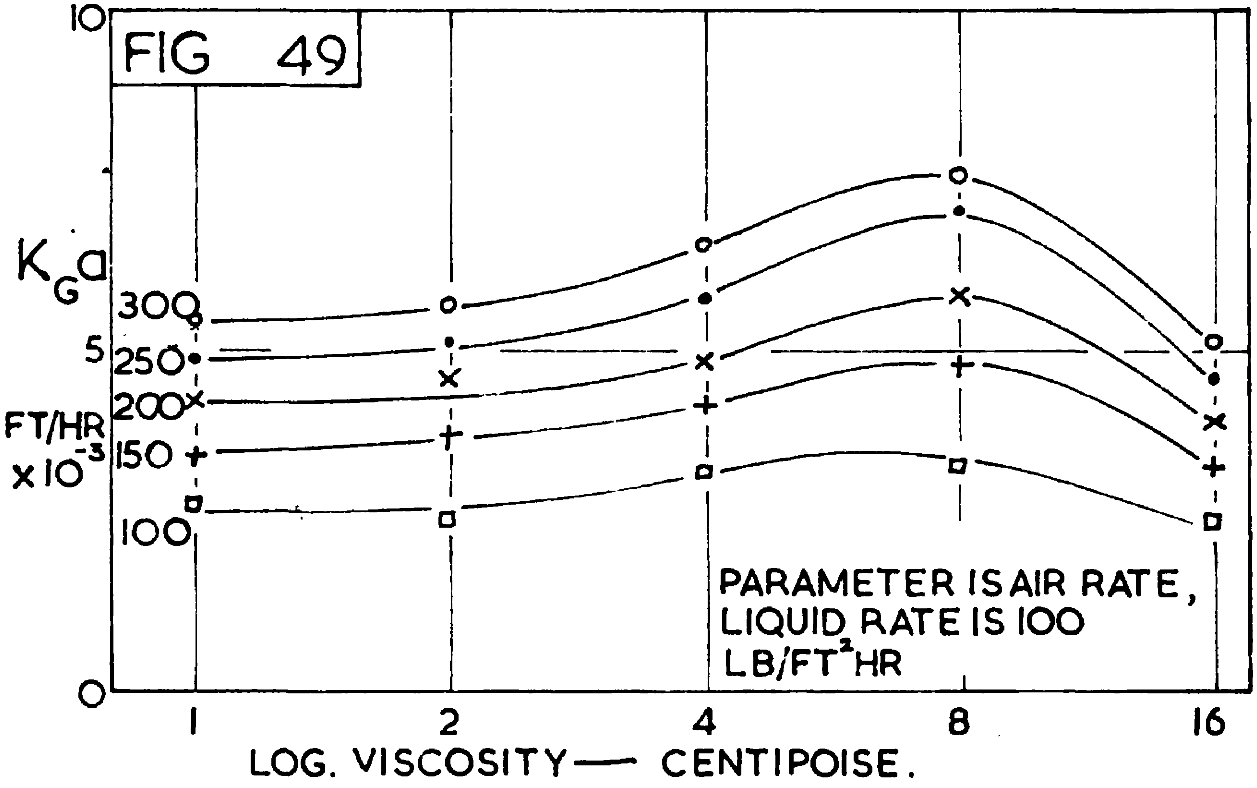

PARAMETER IS AIR RATE, LIQUID RATE IS 100 LB/FT²HR

0.60, a 63% decrease. This decrease was explained by the larger bubble size occurring at high viscosities and the reduction in froth height. The difference between Barker and Choudhury's results and the author's is probably attributable to the difference in liquid submergence between the plates. The Kuhni Plate has a weir height of 1 inch compared with 3.4 inches for the 5 ft. bubble tray. This lower liquid seal must affect the bubbling characteristics, particularly with regard to "jetting" or "leakage" of the air through the liquid.

As part of the A.I.Ch.E Research Programme on tray efficiencies at the University of Michigan[18] the efficiency of vapourisation of cyclohexanol into nitrogen was determined at viscosities from 12 cP to 25 cP. It was found that the efficiency increased with increasing viscosity although the froth height remained substantially constant. The weir height in these tests was 1.5 inches.

A thorough examination of the effect of viscosity on bubble formation, rise and bursting would be necessary to elucidate the reasons for these efficiency characteristics. The most convenient method of examining these phenomena is the use of high speed cine filming of a bubbling slot, as has been done by Spells and Bakowski[15,16]. Some exploratory tests of this nature were done recently[129] in these laboratories using a "Perspex" model section of the Kuhni Plate but the technical difficulties encountered prevented many definite conclusions being reached.

These tests were not strictly comparable to conditions on an operating Kuhni Plate since only one slot was used in all but one of the tests. The liquid seal is greater when only one slot is active and there is also interference between neighbouring and facing slots. Discrete bubbling was observed at only the lowest air rates, equivalent to about 100 lb./ft.^{2}hr. The bubble diameter was of the order of 2 cm. At this air rate bubble frequency and size varied while at higher air rates "surging" rather than bubbling took place and direct "jetting" or leakage" was observed. Interference between facing bubbling slots was observed in the one film in which two slots were used.

It is impossible, at present, to satisfactorily explain the efficiency characteristics obtained in these tests but it is interesting to speculate on the probable effects which liquid viscosity has on gas phase mass transfer.

Davidson[79] found that at high viscosities bubble size was largely determined by the time taken for the "neck" of the bubble to close during formation. At high viscosities the "neck" closes more slowly and more gas passes into the bubble before disengagement from the slot. On the Kuhni Plate it was observed that at high viscosities some bubbles grew so large that they burst at the surface before disengagement, causing "jetting". It was also observed that at high viscosities bubbles were larger and fewer in number.

The rising velocity of bubbles in viscous liquids is reduced, giving a longer residence time but it is doubtful whether this is applicable to the Kuhni Plate with its low liquid seal. Measurements of froth height at high viscosities on the Kuhni Plate showed very little difference from the froth heights for water.

It was observed, by use of the high speed filming technique, that at high air rates on the Kuhni Plate a jet of air formed at the slot, which continuously discharged air in "surges" rather than as descrete bubbles. This may be peculiar to the Kuhni Plate with its low slot area and high slot velocities. It may be that at high viscosities the discharge from such a jet is different in form since the fluid drag of the liquid is greater and the liquid is moving more sluggishly, resisting both the expansion of bubbles formed at the jet and the penetration of the jet through the body of the liquid.

The effects discussed in the last few paragraphs have all dealt with the surface area between the phases and not with the mass transfer coefficients at the surfaces. It at first appears unlikely that a change in viscosity of the liquid phase will affect the rate of mass transfer from the surface of the liquid, there being no liquid "film" resistance. If, however, the liquid and gas are moving then a change in liquid viscosity must affect the interfacial friction and hence the mass transfer coefficient. The rate of "circulation" of the gas in the vicinity of the interface is dependent on the corresponding "circulation" rate in the liquid phase because of the fluid drag (or friction). The rate of "surface renewal" as postulated by Danckwerts[65] is a function of this "circulation" rate and since the rate or surface renewal is an important factor in determining the mass transfer coefficient it is to be expected that circulation in the liquid phase will have an effect on the gas "film" mass transfer coefficient.

Another effect of liquid viscosity will be on the properties of the froth. It is to be expected that the viscosity will partly determine the thickness of bubble skins and their tendency to burst. No marked effect, however, has been observed on froth height and the effect of viscosity on froth properties may thus be slight.

It appears that the only firm conclusion to be drawn from the tests discussed in this section is that the state of knowledge of the effects of liquid viscosity on bubbling on a gas absorption plate is not sufficient to explain the results of these tests or the results of other workers. The differing form of results obtained by using different systems and different plates suggests that plate efficiency is a complex function of liquid viscosity. Several mechanisms whereby liquid viscosity may affect gas "film" resistant mass transfer have been discussed and a combination of these may be responsible for the results obtained.

5 : 9 Liquid Phase Efficiency Tests with Water

Analysis of liquid phase mass transfer on a bubbling plate is in many respects more difficult then gas phase mass transfer. The primary difference is that while the gas can be assumed to move through the froth in "plug flow" in the form of bubbles or jets, with an estimable contact time, the liquid, being the continuous phase in the froth, flows through the froth relying on chance encounters with gas bubbles for mass transfer. The contact time of a gas bubble is equivalent to its residence time in the froth but the contact time of a liquid element is only loosely related to its residence time in the froth.

The problem is further complicated by the uncertainty of the mechanism of liquid flow round a bubble. Higbie[11] assumed that the contact time of an element of liquid with a bubble is the bubble diameter divided by the bubble velocity, that is, the time for the element to move from top to bottom of the bubble. Even if this were a proven fact, it is of little practical use unless bubble diameters and rising velocities are known. Even then the bubble diameters may not be constant and the bubbles may not be spherical.

The Kuhni Plate, with its low weir height is more complicated since the bubbles, being of approximately the same diameter as the weir height[129], can not be regarded as simulating Higbie's model. The principal contact time between liquid elements and the gas probably occurs during bubble formation. The concept of random surface renewal, depending on liquid eddies as postulated by Danckwerts[65], is more readily applicable since it involves no terms in bubble diameter. In addition to these difficulties the effect of liquid mixing must be determined and allowed for in the estimation of mass transfer rates from plate efficiency data.

As a result of these factors it is impossible to analyse the oxygen desorption results to the same extent as the humidification results without a more detailed knowledge of bubble dynamics.

The approach adopted in this discussion is to consider firstly the plate efficiency results, then the effect of liquid mixing on these efficiencies and finally the fundamental mass transfer data obtained from the reduction of plate data to point data using the mixing parameter the Peclet number, obtained in the liquid mixing studies.

Discussion of Plate Efficiency Data

The plate efficiency data are shown in Figures 50 and 51 which are cross plots of each other. The efficiency at a water rate of 100 lb./ft.^{2}hr is almost independent of air rate and has a value of approximately 96%. Increasing the water rate always causes a decrease in efficiency presumably because of the shorter residence time of the water on the plate. Increasing the air rate increases the efficiency probably because of the greater air hold-up in the froth and the greater turbulence in the froth.

It was thought at first that the maximum value of the plate efficiency of approximately 96%, towards which the efficiency curves seem to tend, represented the equilibrium conditions and that the calculations or analyses were in error. A thorough check of all possible errors was made and it was concluded that the data are correct, the 96% efficiency level being a maximum value less than equilibrium. Subsequent tests using "Cellofas B"

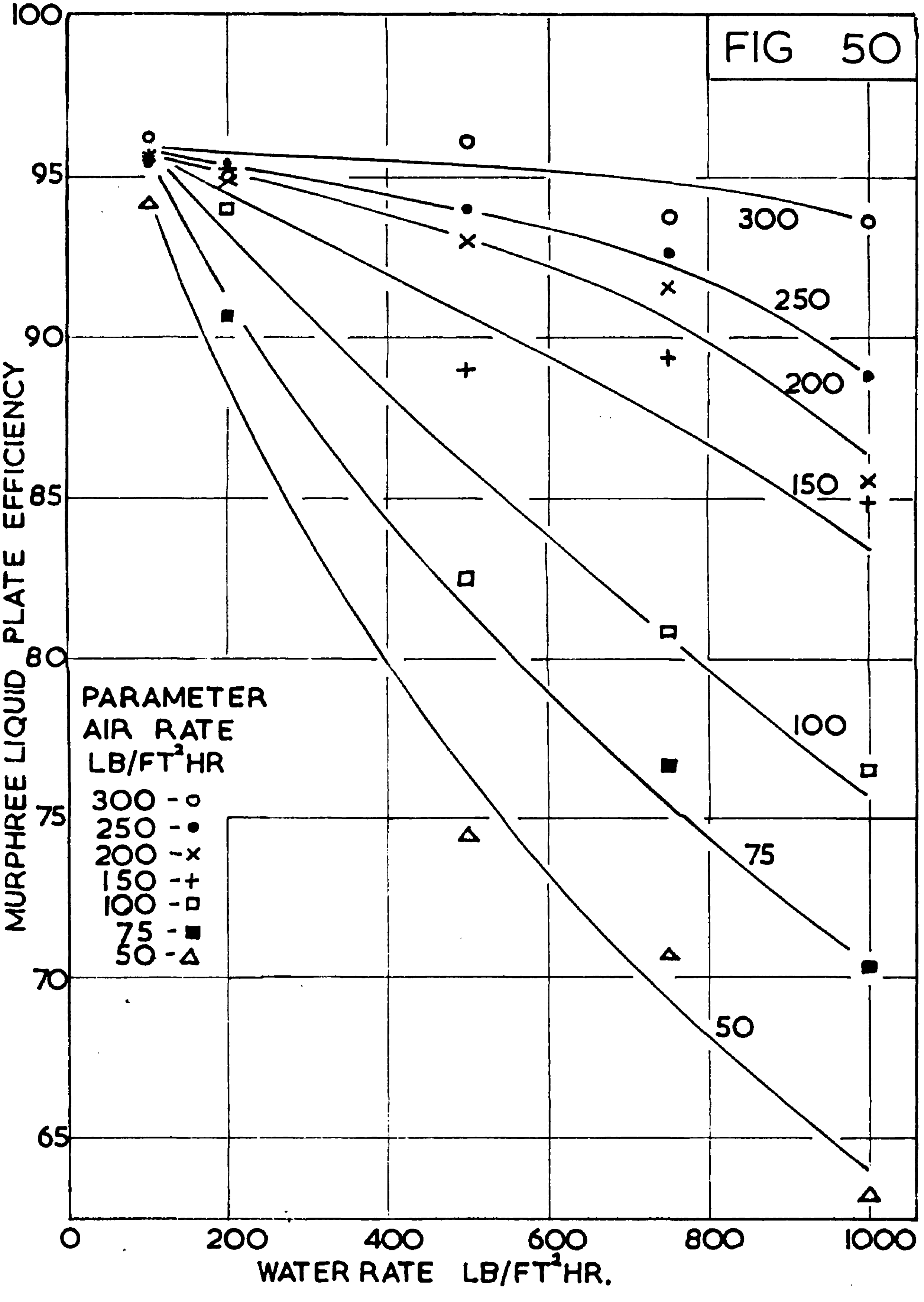

FIG 50

MURPHREE LIQUID PLATE EFFICIENCY
WATER RATE LB/FT²HR.
100
95
90
85
80
75
70
65
0
200
400
600
800
1000
300
250
200
150
100
75
50
PARAMETER
AIR RATE
LB/FT²HR
300 - ○
250 - ●
200 - ×
150 - +
100 - □
75 - ■
50 - △

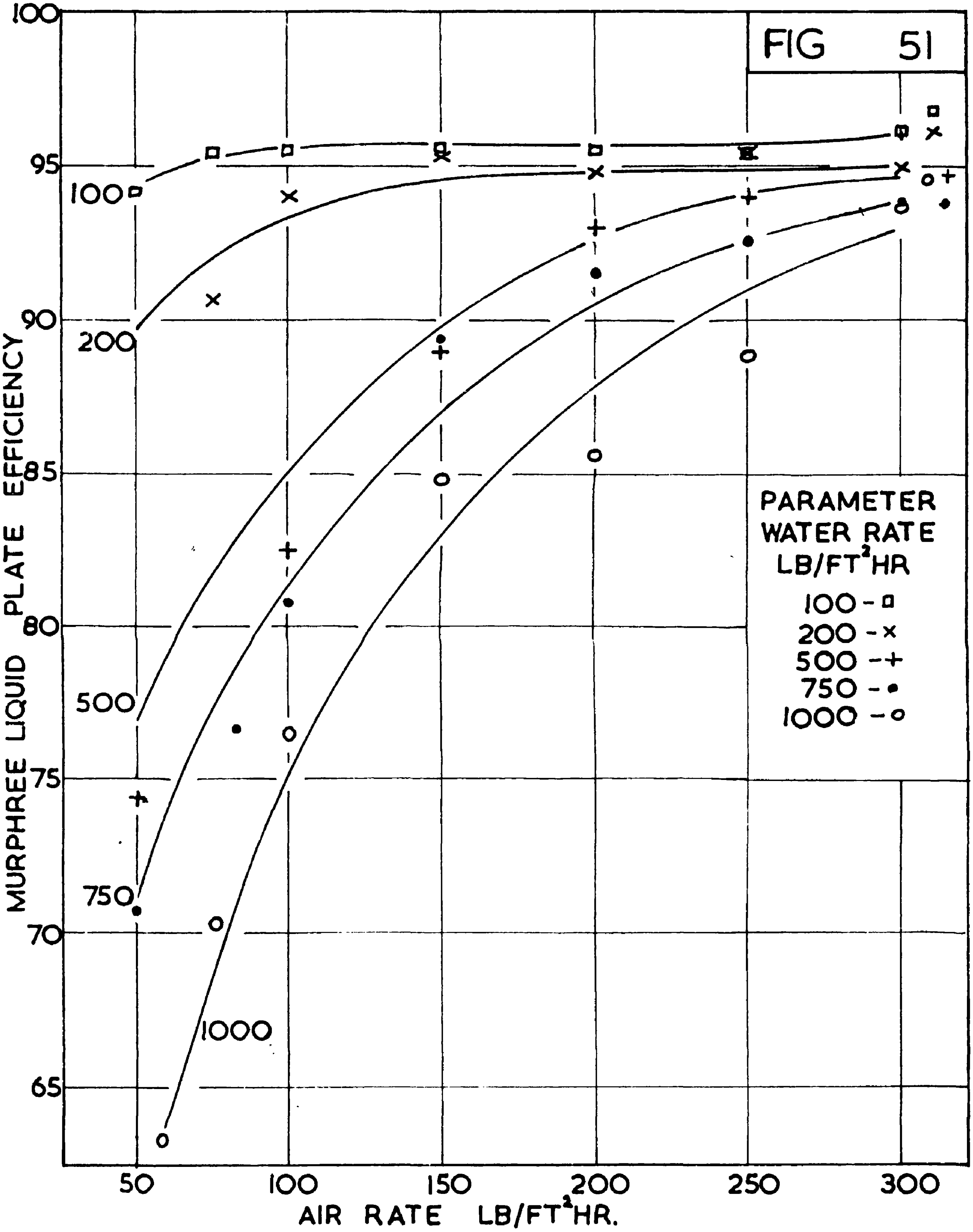
FIG 51
MURPHREE LIQUID PLATE EFFICIENCY
AIR RATE LB/FT²HR.
100
95
90
85
80
75
70
65
50
100
150
200
250
300
100
200
500
750
1000
PARAMETER
WATER RATE
LB/FT²HR
100 - □
200 - ×
500 - +
750 - ●
1000 - o

solutions gave several efficiencies over 96% which confirms this conclusion.

Efficiency characteristics of this form are not uncommon in liquid phase studies, a maximum efficiency being obtained over a range of gas rates[18].

Discussion of Liquid Mixing

As has been discussed in the Introduction, the Murphree liquid plate efficiency depends not only on the mass transfer rates but on the degree of liquid mixing on the plate.

For example, if the mass transfer coefficient, interfacial area and contact time gave an approach to equilibrium equivalent to 3 transfer units, then the Murphree plate efficiency would be 95% if there was no liquid mixing (plug flow) but only 75% if there was complete mixing. The equations for these conditions have been given in the Introduction, Section 1;7. It is thus essential that information is available on the degree of liquid mixing if the effect of operating conditions on mass transfer rates are to be studied from plate efficiency data.

The process of converting Murphree liquid plate efficiencies to transfer units described below is rather complicated.

(i) Conversion of liquid plate efficiency E_{ML} to vapour plate efficiency E_{MV}.

This is achieved using equation (1;29)

$$E_{MV} = E_{ML}\Big/\left[E_{ML} + \lambda(1 - E_{ML})\right] \quad \text{where} \quad \lambda = \overline{m}\,.G_V/L_V$$

(ii) Conversion of vapour plate efficiency E_{MV} to vapour point efficiency E^*_{MV}.

If the mixing parameter, the Peclet number, obtained from the residence time distribution data is applied to the equation relating plate and point vapour efficiency derived in the University of Delaware Report[19] the point efficiency can be found. In practice it is easier to use the equation in its graphical form shown in Figure 3. This graph is a plot of E_{MV}/E^*_{MV} against λE^*_{MV} with Peclet number as parameter and is designed for the conversion of E^*_{MV} to E_{MV}. The reverse process (E_{MV} to E^*_{MV}) is difficult on this graph since E^*_{MV} occurs in both ordinate and abscissa. To facilitate the conversion of plate to point efficiency the original data in the University of Delaware Report were replotted in the form shown in Figure 52, in which E^*_{MV}/E_{MV} is plotted against λE^*_{MV}.

(iii) Conversion of vapour point efficiency E^*_{MV} to liquid point efficiency E^*_{ML}.

This is achieved by equation (1;31)

$$E^*_{ML} = \lambda E^*_{MV}/[\lambda E^*_{MV} + (1 - E^*_{MV})]$$

(iv) Conversion of liquid point efficiency E^*_{ML} to transfer units N_L.

The data could have been considered in terms of liquid point efficiencies but it is more convenient and more theoretically sound to use transfer units as obtained from equation (1;27)

$$N_L = E^*_{ML}/(1 - E^*_{ML})$$

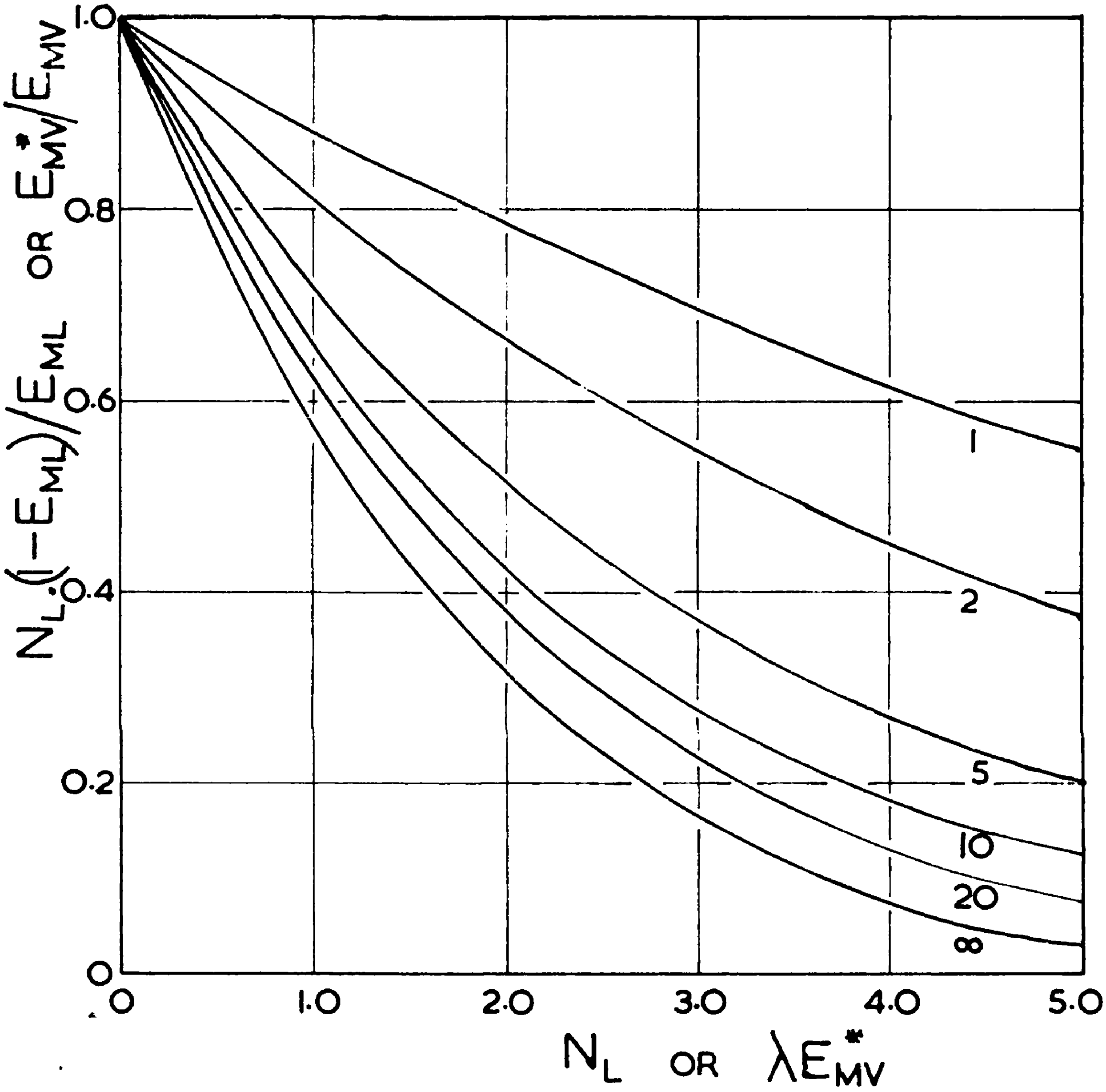

RELATIONSHIP BETWEEN MURPHREE LIQUID PLATE EFFICIENCY AND THE NUMBER OF LIQUID "FILM" TRANSFER UNITS WITH PECLET NUMBER AS PARAMETER

FIG 52

(v) Conversion of transfer units N_L to mass transfer group K_La.

This is achieved by equation (1;25)

$$N_L = K_La/L_V$$

Owing to the large value of λ,(10^5) the above equations can be simplified and combined in a form more suitable for application to Figure 52.

The ordinate in Figure 52 is E^*_{MV}/E_{MV} and this can be shown to equal $N_L\ (1 - E_{ML})/E_{ML}$ when λ is large compared with unity. Also $\lambda\ E^*_{MV}$, the abscissa equals N_L when λ is large. These alternative quantities are shown in Figure 52. To obtain a number of transfer units corresponding to E_{ML} and Pe, a line is drawn through the origin of Figure 52 of gradient $(1-E_{ML})/E_{ML}$. The intersection of this line and the Peclet number parameter line gives on the abscissa the corresponding value of N_L.

The effect of a large Peclet number (corresponding to little mixing) is to give a value of N_L similar to that in equation (1;28) for plug flow.

$$N_L = -\ln(1 - E_{ML})$$

In general the values of N_L are between 10 and 30% greater than the "plug flow" transfer units as defined above. The effect of the mixing on the Kuhni Plate is thus to reduce the effictiveness of mass transfer by approximately 20% from the maximum value obtained when no mixing occurs.

The use of the equation derived in the University of Delaware Report[19] and shown graphically in Figure 52 is not strictly correct for the radial flow Kuhni Plate since the equation was derived for a rectangular cross flow plate. An attempt was made to derive and solve the equation for the Kuhni Plate but it was found that the time required for solution of this equation would be very considerable. It was felt that the error in applying the mean Peclet number to the existing equation would be slight and would not justify the time required for solution of the radial flow equation.

Discussion of Mass Transfer Data

Figure 53 shows the data in the form of transfer units plotted against air rate. The curves are of the same form as the efficiency plot in Figure 51 and show the maximum value attained of approximately 4 transfer units.

It is unfortunate from the experimental point of view that the Kunhi Plate has such high oxygen desorption efficiencies since errors in the data above an efficiency of 90% become magnified in the conversion to transfer units owing to the use of the quantity $(1-E_{ML})$. For example an error of 1% at an efficiency of 95% gives an error in the transfer units of 20% whereas at 80% the effect of a 1% error is 7% in the transfer units. As a result the accuracy of the transfer unit data is lower at high plate efficiencies. Ideally, therefore, a system should be chosen with an efficiency range below 85%.

A lineor relationship has been suggested[19] between the number of transfer units N_L, and the liquid residence time in the froth, for residence times below 15 seconds. The theoretical basis for this suggestion is that the liquid contact time with the gas will be a function of its residence time in the froth. Figure 54 shows the transfer unit data plotted

FIG 53

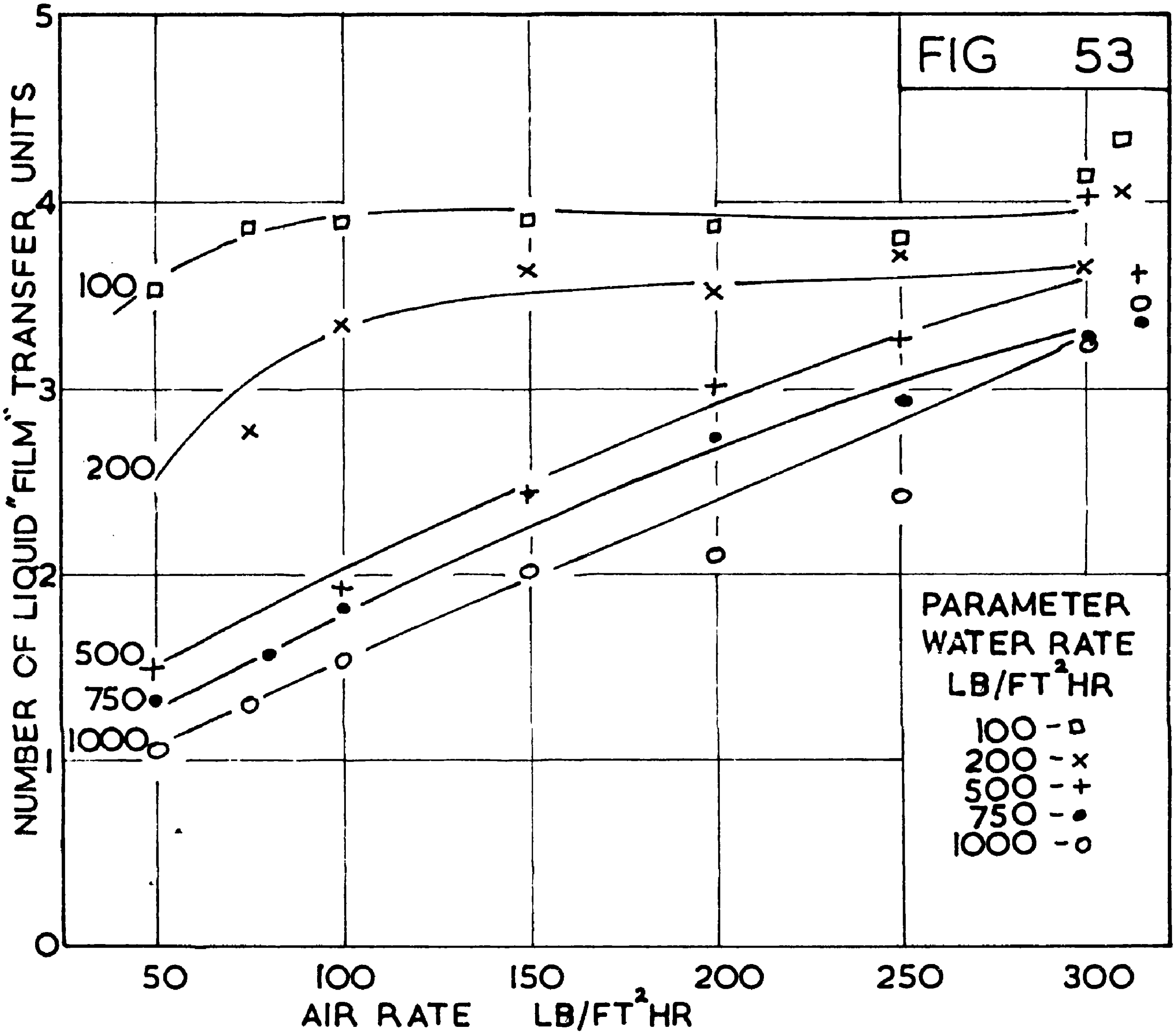

NUMBER OF LIQUID "FILM" TRANSFER UNITS
AIR RATE LB/FT² HR
0
1
2
3
4
5
50
100
150
200
250
300
100
200
500
750
1000
PARAMETER
WATER RATE
LB/FT² HR
100 - □
200 - ×
500 - +
750 - ●
1000 - ○

against water residence time with air rate as parameter and it can be seen that an increase in residence time is always associated with an increase in the transfer units, confirming the basis of the above suggestion. There are insufficient data to prove the suggested linear relationship below 15 seconds but it appears that there may be a relationship of this form. The air rate parameter curves show that at high air rates the rate of mass transfer is greater owing to the more effective contact between the phases and possibly a greater degree of liquid turbulence and surface renewal.

At low air rates where the inner trough is not bubbling it is misleading to attempt to correlate the water residence time with the transfer unit data since a considerable proportion of the residence time is spent in this trough with no air-water contact by bubbles.

Figure 55 shows the data in the form of the group $K_L a$. As in the humidification data the quantity "a" is the interfacial area per square foot of plate area. The effect of increased air rate on $K_L a$ can be adequately explained in terms of the probable increase in "a" and possible also in K_L , owing to the greater turbulence.

It is less easy to explain the effect of the water rate on $K_L a$. It has been shown that an increase in water rate increases the froth height and air hold-up with a probable increase in "a", the interfacial area. This accounts for part of the dependence of $K_L a$ on water rate but it appears that the water rate also influences the value of K_L.

For example at an air rate of 200 lb./ft.^{2} hr. the effect of

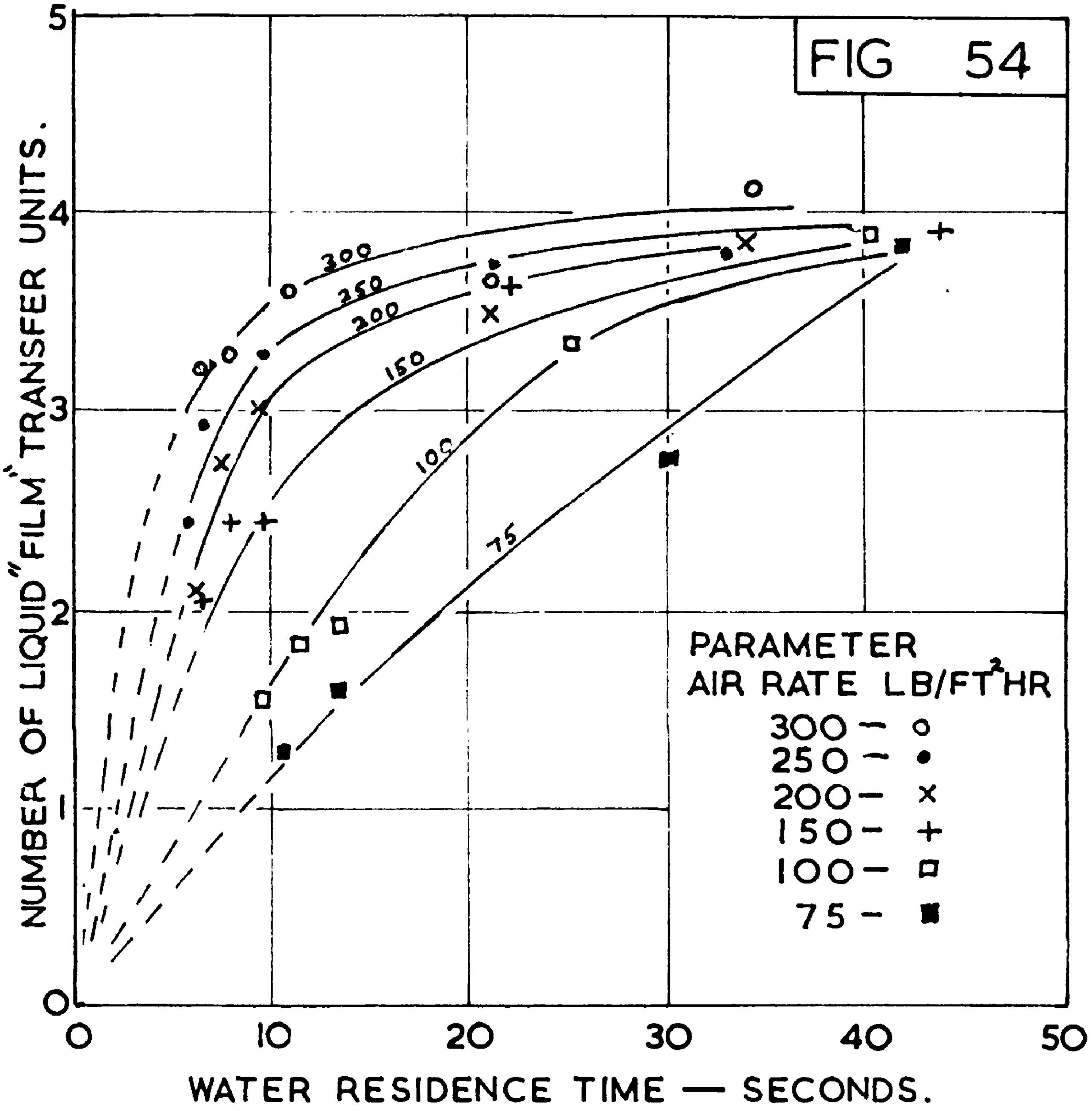
FIG 54
NUMBER OF LIQUID "FILM" TRANSFER UNITS.
WATER RESIDENCE TIME — SECONDS.
0
1
2
3
4
5
0
10
20
30
40
50
300
250
200
150
100
75
PARAMETER
AIR RATE LB/FT²HR
300 — ○
250 — ●
200 — ×
150 — +
100 — □
75 — ■

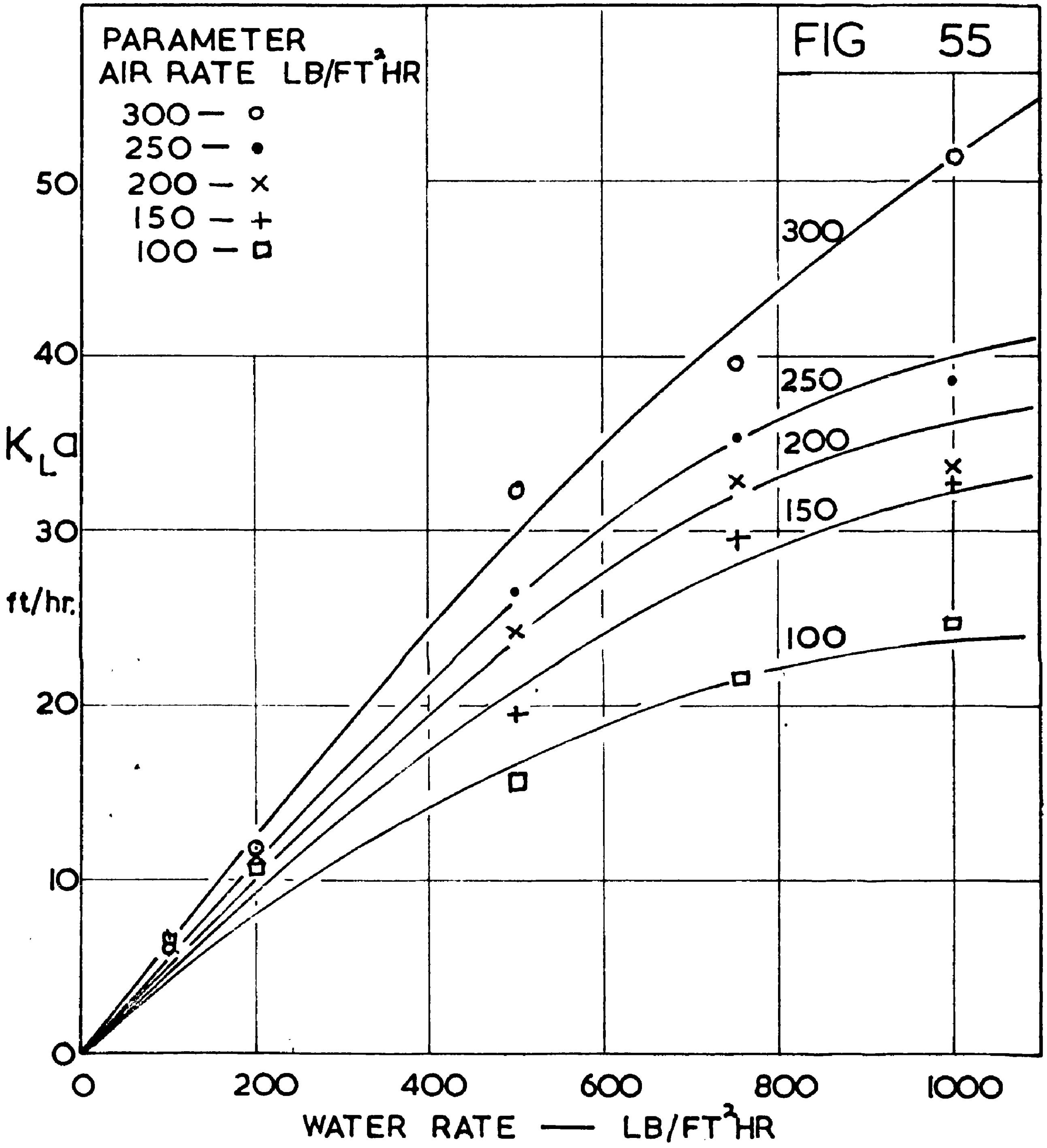

FIG 55

PARAMETER
AIR RATE LB/FT² HR
300 — ○
250 — ●
200 — ×
150 — +
100 — □
300
250
200
150
100
$K_L a$
ft/hr.
0
10
20
30
40
50
0
200
400
600
800
1000
WATER RATE — LB/FT² HR

increasing the water rate from 100 to 1,000 lb./ft.^{2}hr is to increase K_La from 6.2 to 33.6 ft./hr., a 440% increase. The corresponding increase in air hold-up is 27% which is very unlikely to be associated with a 440% increase in "a". The increase in Kga under these conditions is 31%.

A possible explanation is that the increased water velocities on the plate cause a greater turbulence in the liquid phase resulting in a higher rate of surface renewal of the water. Danckwerts has suggested[65] that such an increase in the rate of surface renewal will increase the mass transfer coefficient K_L. In the above example the mean water velocity (the path length divided by the residence time) increases from 0.025 ft./sec. to 0.14 ft./sec. an increase of 460%. It is likely that there is a corresponding increase in the turbulence, rate of internal circulation and rate of surface renewal. Figure 56 shows K_La plotted against the mean water velocity and an approximately linear relationship is evident.

It can be concluded from this discussion that in a liquid phase resistant system the effect of an increase in gas rate is generally to increase the rate of mass transfer and hence the liquid plate efficiency owing to the more effective contact between the phases. The effect of an increase in the liquid rate is more complicated since it increases the mass transfer coefficient and the interfacial area but decreases the contact time of the liquid with the gas. The overall effect of an increase in liquid rate is, however, a reduction in efficiency.

A correlation of K_La in terms of air and water rates is given below.

$$K_L a = 3.45 . (G_M + 133) . L_M^{0.845} \times 10^{-4} \qquad 5:11.$$

G_M and L_M being the air and water rates in lb./ft.^{2} hr.

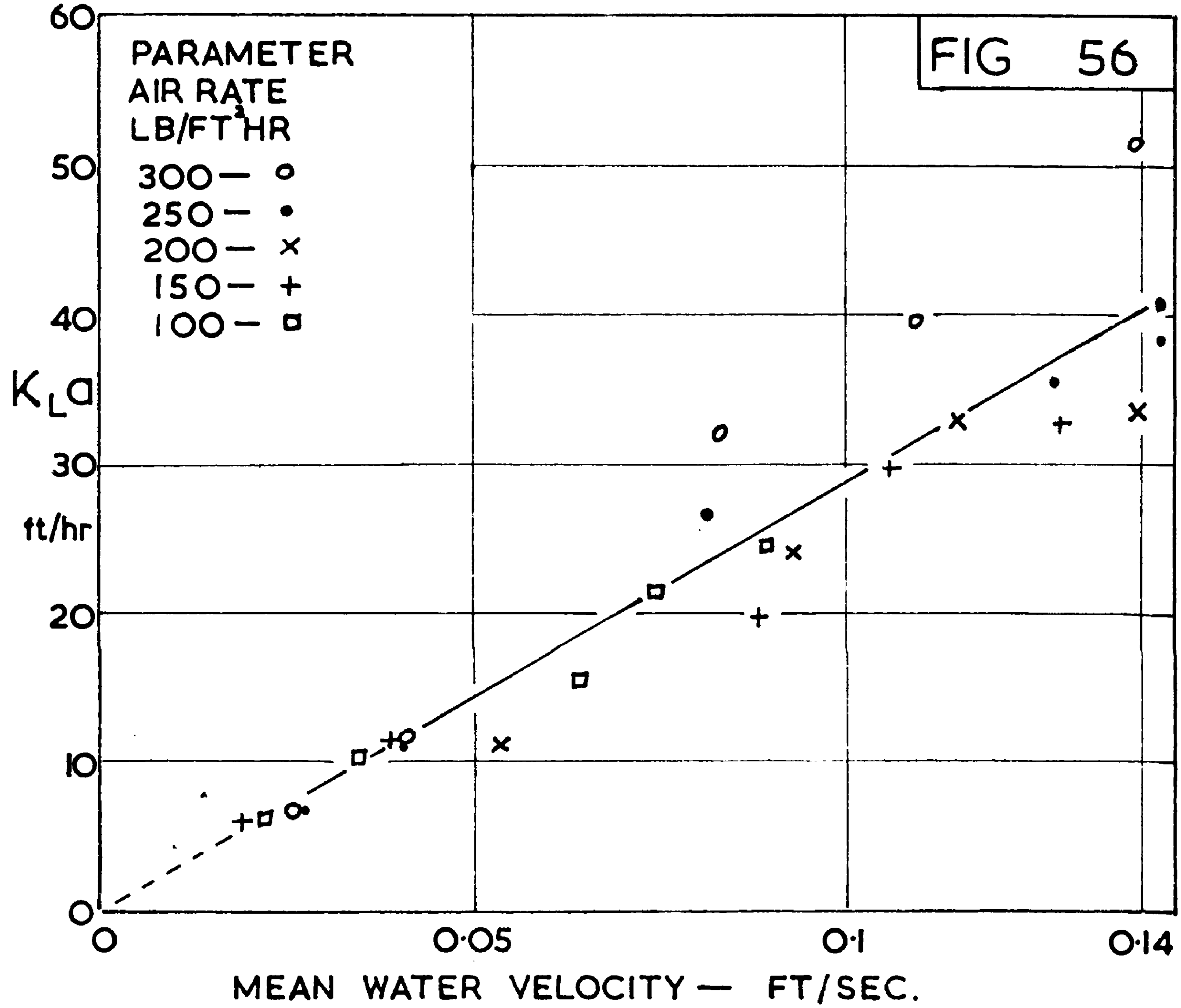
FIG 56
PARAMETER
AIR RATE
LB/FT²HR
300 — ○
250 — ●
200 — ×
150 — +
100 — □
K_L a
ft/hr
0
10
20
30
40
50
60
0
0·05
0·1
0·14
MEAN WATER VELOCITY — FT/SEC.

5 : 10 Liquid Phase Efficiency Tests with Viscous Solutions

Oxygen desorption efficiencies were measured at four viscosity levels, 2, 4, 8 and 16 cP., sixteen tests being done at each level. Using the same procedure as in the tests with water, plate efficiency data were converted to "point" data, allowing for the effect of liquid mixing. The data are presented in the form of transfer units and as the group K_La.

It is shown in Appendix D that the addition of "Cellofas B" to water has no detectable effect on the solubility or diffusivity of oxygen in water in the range of concentrations used. Any changes in mass transfer rates due to the addition of "Cellofas B" cannot, therefore, be attributed to changes in the molecular diffusivity or solubility of the oxygen. Although the molecular diffusivity is not affected the eddy diffusivity at the interface may be affected and a change in the "effective" diffusivity, as discussed by Kishinevskii and Mochalova[103] and Garner and Porter[99], may result.

Walter and Sherwood[3], using the carbon dioxide-water-glycerol system investigated the effect of liquid viscosity on liquid point efficiency. It was found that a change in viscosity from 1 to 4 cP. caused a 50% reduction reduction in K_L. Jordan[127] has shown that the corresponding decrease in diffusivity is 43%. The liquid seal in these tests was 1.82 inches.

The Final Report of the University of Michigan[18] gives data for the desorption of carbon dioxide from water at 0.9 cP. and cyclohexonal from 20 to 100 cP., the viscosity being controlled by the operating temperature. It was concluded that at all but the highest viscosities, (90 cP.), the effect of liquid viscosity could be adequately explained by the associated change in diffusivity. The variations in mass transfer rate were correlated by an equation of the form:

$$K_L \propto D_L^{0.5} \qquad (5;12)$$

From Figures 57, 58, 59 and 60 it can be seen that there is no marked change in the form of the efficiency curves which are similar to those in Figure 51, the corresponding data for water. The same general conclusions regarding the effects of gas and liquid rates on the water system can thus be applied to these more viscous systems. Some difference in the absolute values of the efficiencies are apparent, the 2 and 4 cP graphs having higher efficiencies than the 8 and 16 cP graphs.

Figures 61 and 62 show K_La plotted against the viscosity with air and water rates as parameters. Again these graphs are similar to the corresponding humidification graphs. As with the humidification system the maximum value is difficult to explain. The factors which influence the humidification efficiency, which were discussed in Section 5;8, i.e. bubble size, rising velocity, formation mechanism, internal circulation, froth stability and jetting will also influence the oxygen desorption efficiency though probably to a different degree and in a different way.

The most obvious reason for the increase in efficiency with increasing viscosity in the range 1 to 4 cP is the increase in liquid residence time in the froth, which will be associated with an increase in contact time and hence an increase in the number of transfer units.

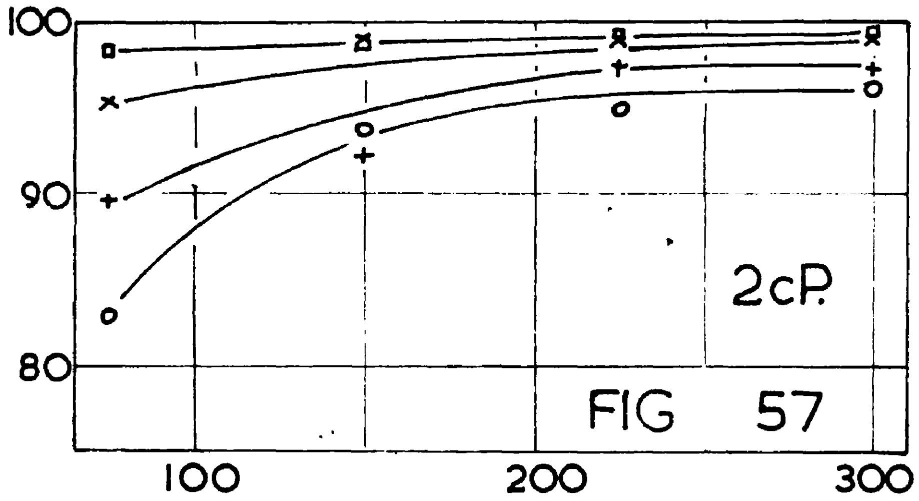

FIG 57

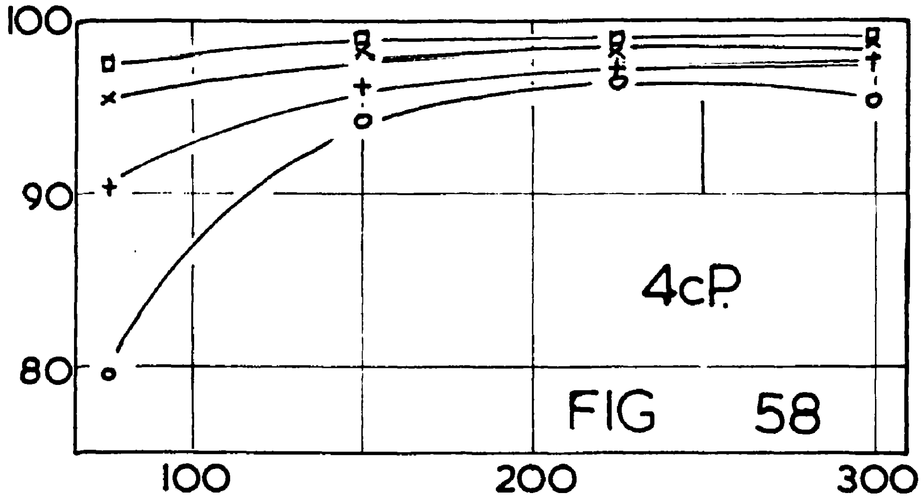

FIG 58

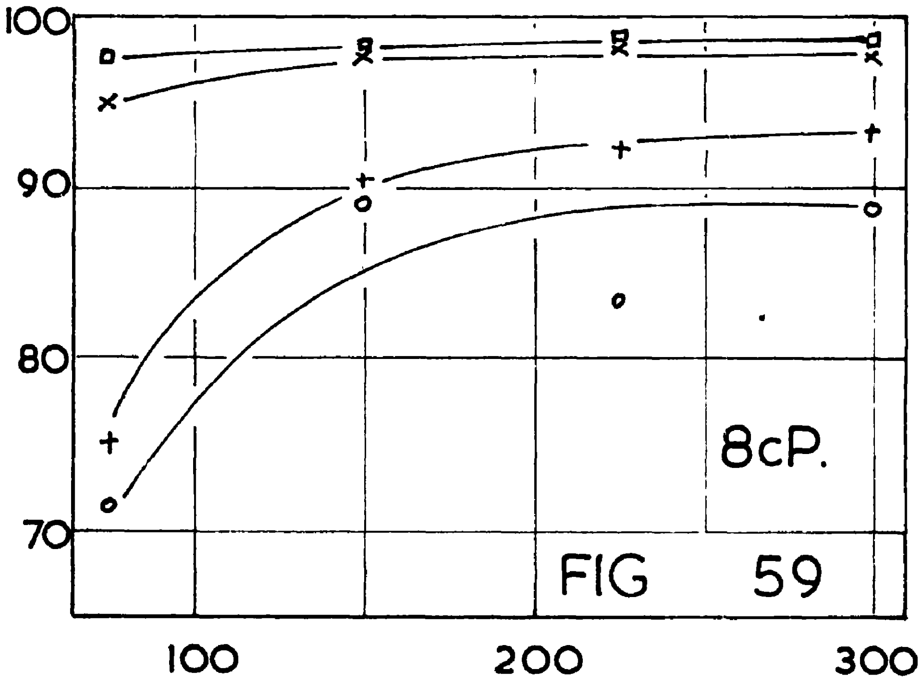

FIG 59

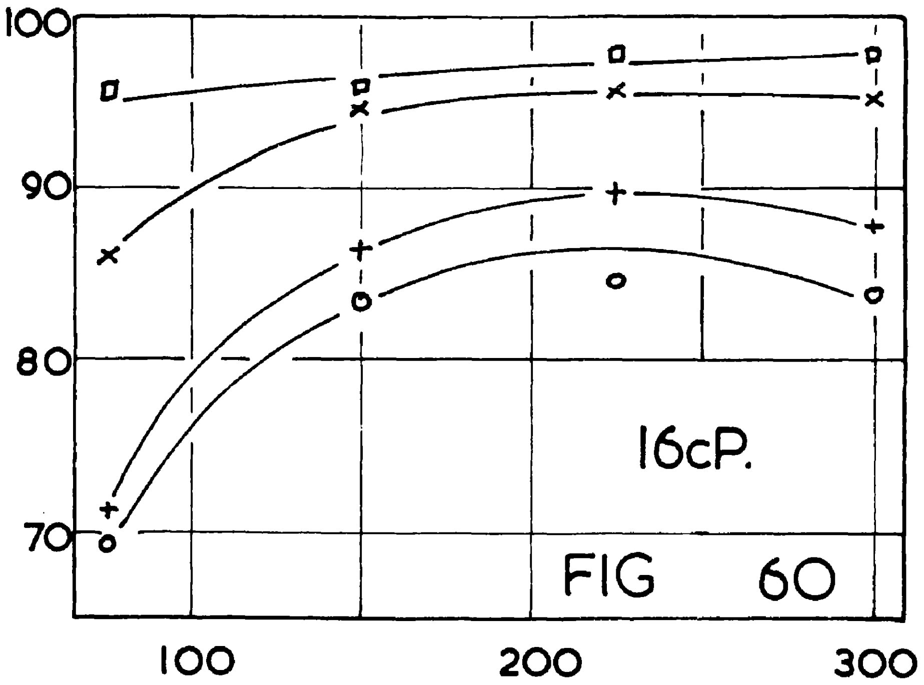

FIG 60

MURPHREE LIQUID PLATE EFFICIENCY % AS A FUNCTION OF AIR RATE, LB/FT^{2}HR,
AT VISCOSITIES OF 2,4,8 & 16cP.
PARAMETER IS LIQUID RATE LB/FT^{2}HR 100—□; 200—×; 500—+; 1000—○.

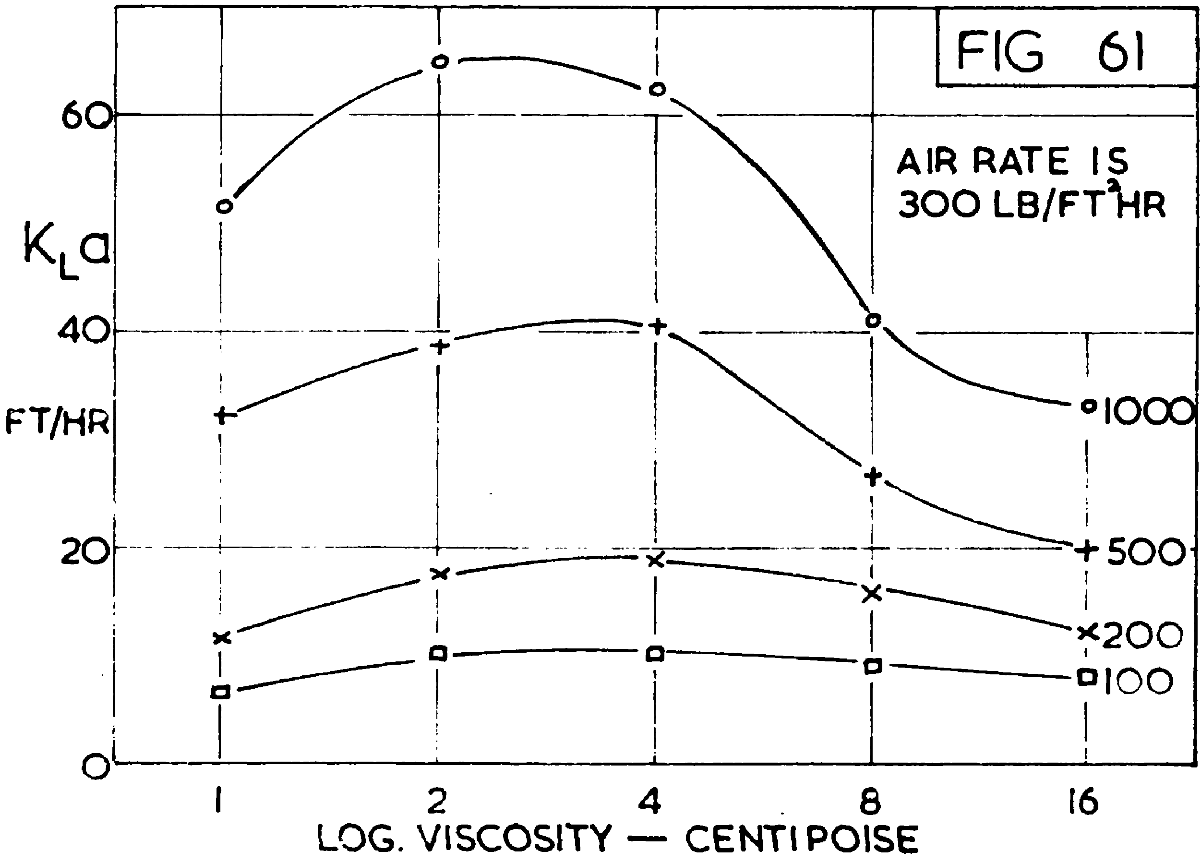

FIG 61

AIR RATE IS
300 LB/FT²HR
K_La
FT/HR
60
40
20
0
1
2
4
8
16
LOG. VISCOSITY — CENTIPOISE
1000
500
200
100

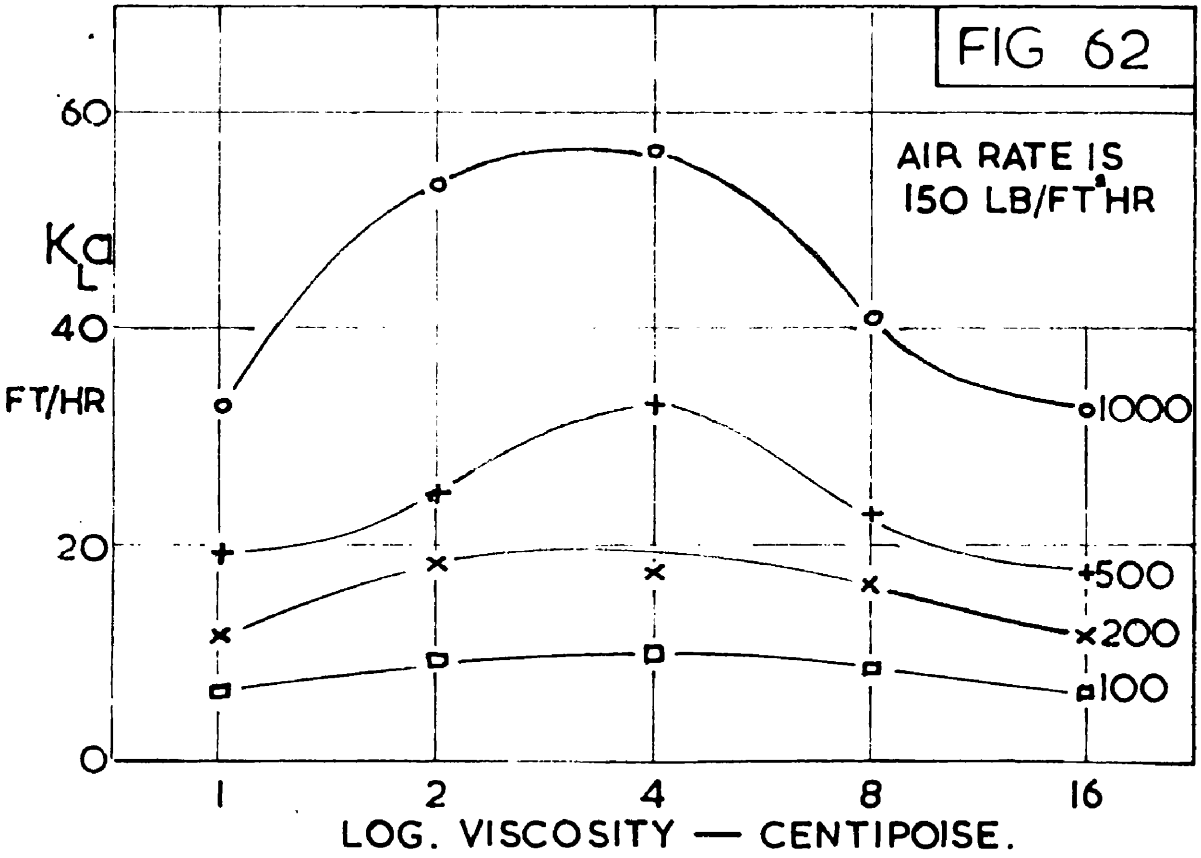

FIG 62

AIR RATE IS
150 LB/FT²HR
K_La
FT/HR
60
40
20
0
1
2
4
8
16
LOG. VISCOSITY — CENTIPOISE.
1000
500
200
100

This increase in residence time is, however, small compared with the increase in transfer units and although it provides an explanation for part of the increase the principal cause of the increase must lie elsewhere.

One striking difference between the humidification and oxygen desorption efficiencies is that the maximum values of K_Ga and K_La occur at different viscosities. The fact that, between 4 and 8 cP, K_Ga is still increasing while K_La is decreasing points to an effect of viscosity on K_L which is not acting on K_G, or vice-versa. An effect which could explain this anomaly is the "damping" effect of viscosity on the eddy diffusivity near the interface, with a resultant decrease in the rate of surface renewal and the mass transfer coefficient. Increasing viscosity, therefore, will tend to reduce the mass transfer coefficient in the liquid phase, the decrease in K_La starting at a lower viscosity than that of K_Ga.

It is, however, unwise to attempt too detailed an explanation with the meagre information available at present. Until a more complete knowledge of the effects of liquid viscosity on bubbling mechanism is available it is impossible to predict or explain these phenomena adequately.

It is interesting to note the absolute value of the ratio K_Ga/K_La. This dimensionless ratio varies from 100 to 600 in the present work. It has been suggested[19] that if the Penetration Theory applies to the gas phase as well as to the liquid phase, as the results of the humidification studies seem to indicate, then the ratio K_Ga/K_La will be of the same order as $(D_G/D_L)^{0.5}$. Data from ammonia absorption and oxygen desorption on the same plate tended to confirm this suggestion. The diffusivity of oxygen in water at 15°C is 6.39×10^{-5} ft.^{2}/hr.[62] and that of water vapour in air at the same temperature as 0.925 ft.^{2}/hr.[114]. The ratio D_G/D_L has therefore the value 14,500 and the ratio $(D_G/D_L)^{0.5}$ the value 120. This latter value is within the range of K_Ga/K_La values obtained in this work. It thus appears that the relationship between K_G and D_G, and K_L and D_L is of the form predicted by the Penetration Theory applied to both phases.

The two film steady state theory would have predicted the K_Ga/K_La ratio to be approximately

$$14{,}500 \times \frac{(\text{liquid "film" thickness})}{(\text{gas "film" thickness})}$$

If this is true then the gas "film" is 25 to 150 times "thicker" than the liquid film, a very unlikely condition.

5 : 11 Tests with Varying Weir Height and Slot Area

As described in Section 2:5 it was decided to determine whether changes in the slot area would improve the pressure drop characteristics and to determine the resultant effect on efficiency. It was also decided to investigate the effect of increasing the weir height. The humidification efficiency of the 30 inch plate was determined at three weir heights and three slot areas and all combinations of these variables.

The weir heights chosen were,

(i) Existing weir height of approximately 1 in. - i.e. 1 in. total height
(ii) An extension in height of 1/2 in. - i.e. 1½ in. total height
(iii) An extension in height of 1 in. - i.e. 2 in. total height

The slot areas chosen were,

(i) 4.25% (existing)
(ii) 7.32%
(iii) 9.76%, the area being expressed as a percentage of the column area.

Twenty tests were done at each combination of the above variables, that is, on the original plate and eight other plate conditions. The efficiency results are given in Figures 63 to 71.

Effect of Weir Height

As was expected an increase in weir height, by increasing the froth height and hence the air residence time in the froth, increases the plate efficiency. Figure 72 shows the increase in the gas phase transfer units at an air rate of 200 lb./ft.^{2}hr. with water rate as parameter. The increase is very slight at low water rates. As can be seen from Figure 73

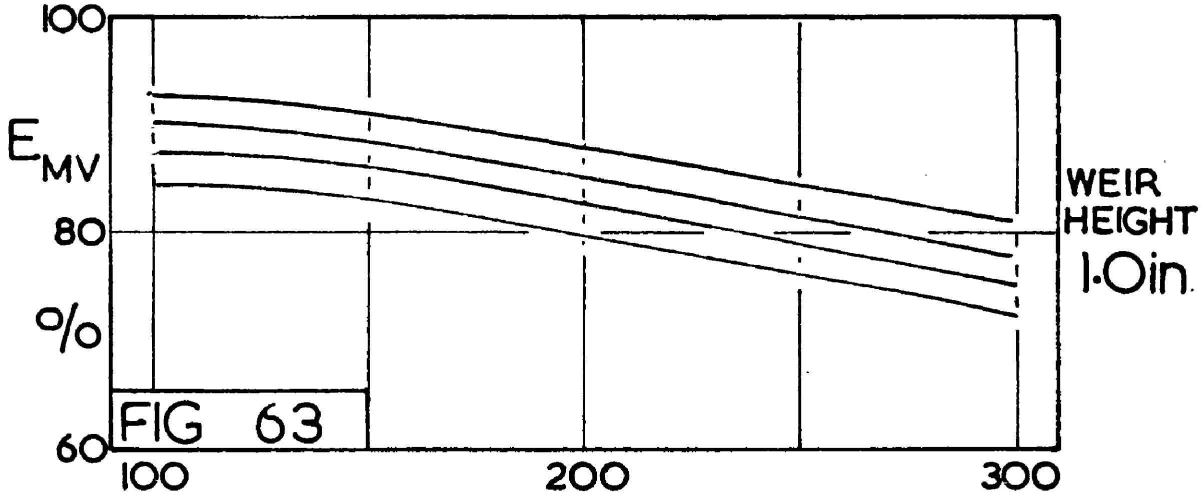

FIG 63

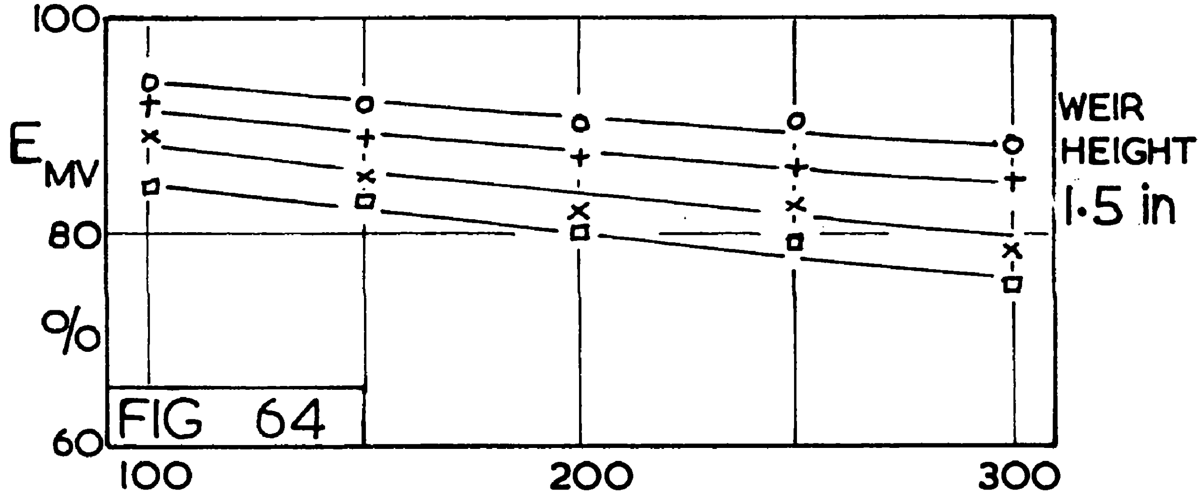

FIG 64

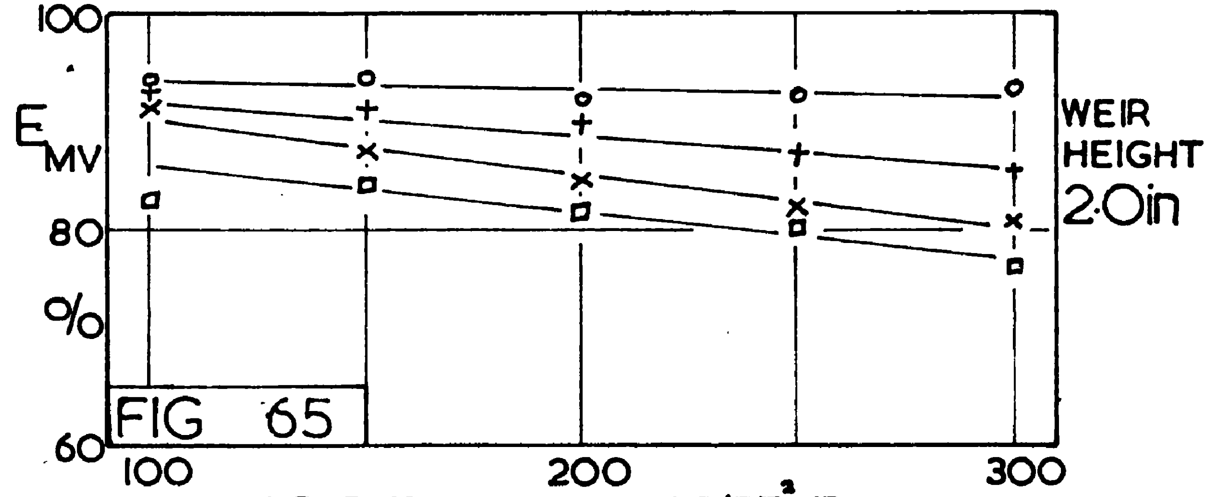

FIG 65

AIR RATE — LB/FT^{2}HR

30in KUHNI PLATE — SLOT AREA — 4·25 %

PARAMETER IS WATER RATE, LB/FT^{2}HR.
1000 – ○ 500 – + 250 – × 100 – □

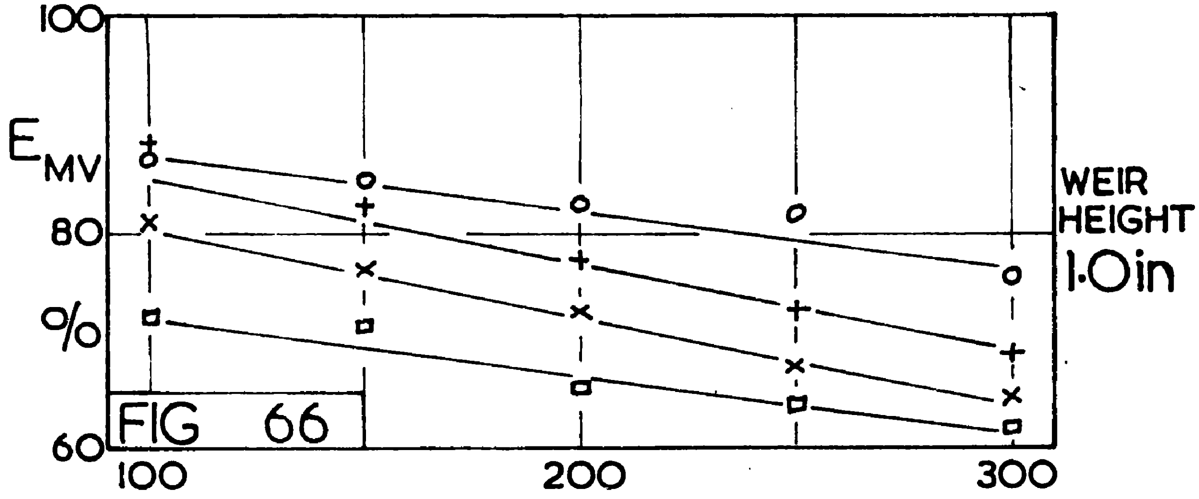

FIG 66

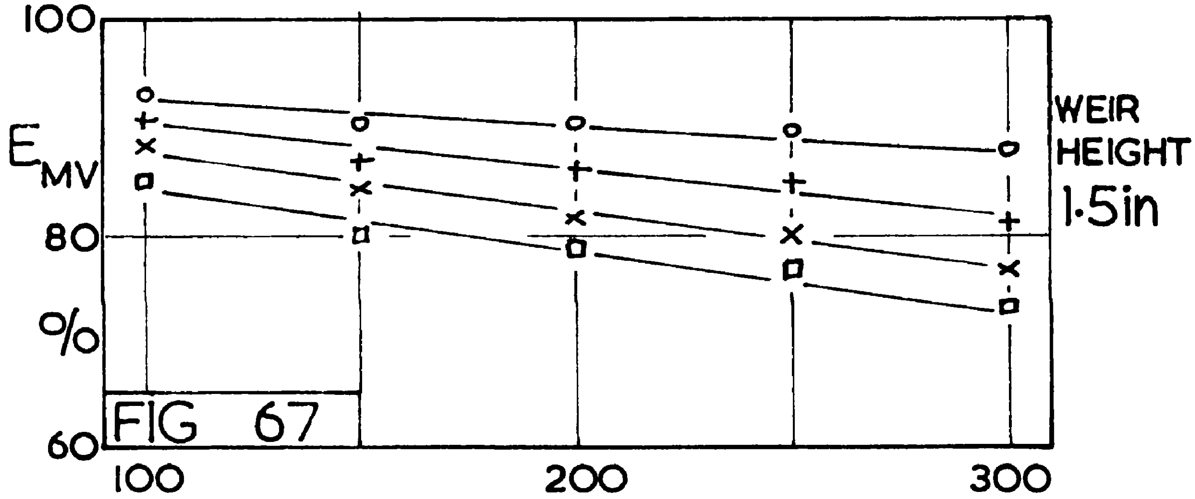

FIG 67

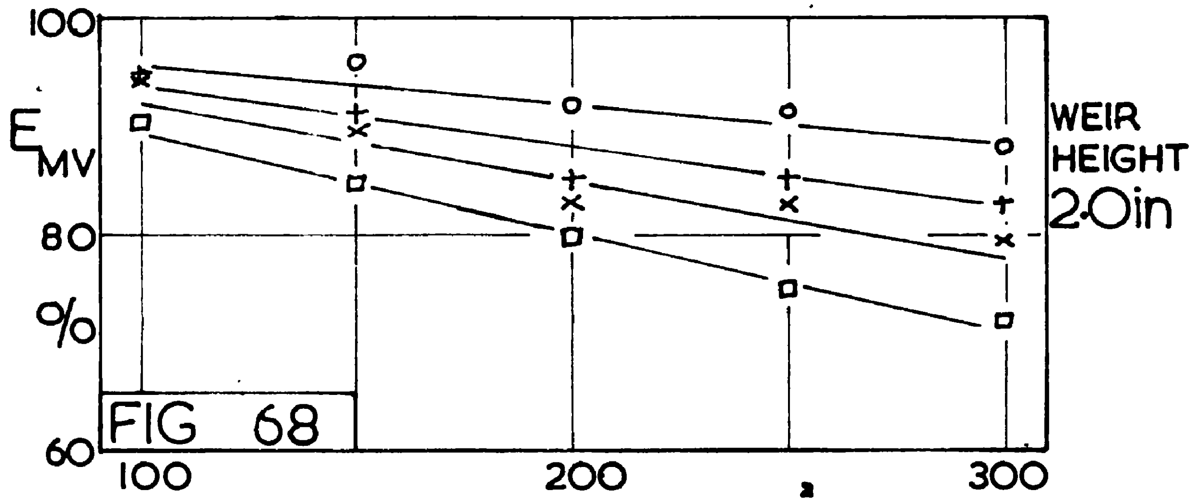

FIG 68

AIR RATE — LB/FT^{2}HR

30in KUHNI PLATE — SLOT AREA – 7·32 %

PARAMETER IS WATER RATE LB/FT^{2}HR.
1000 – o 500 – + 250 – x 100 – □

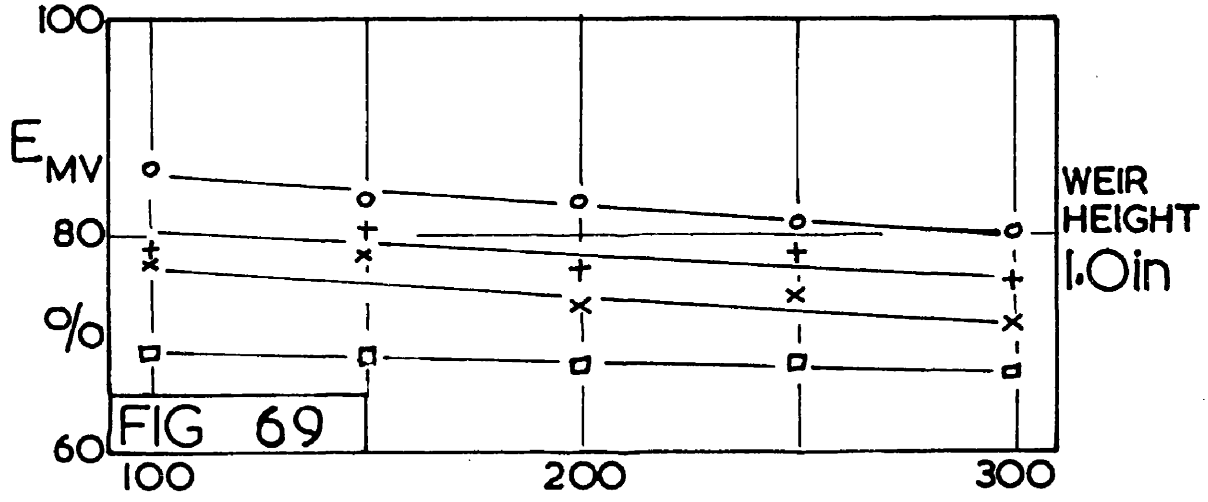

FIG 69

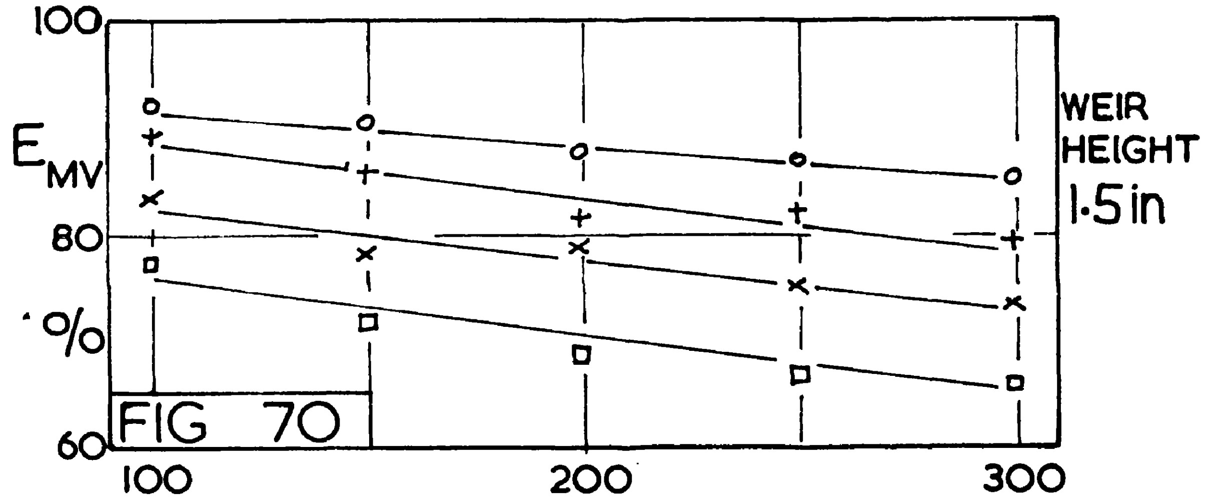

FIG 70

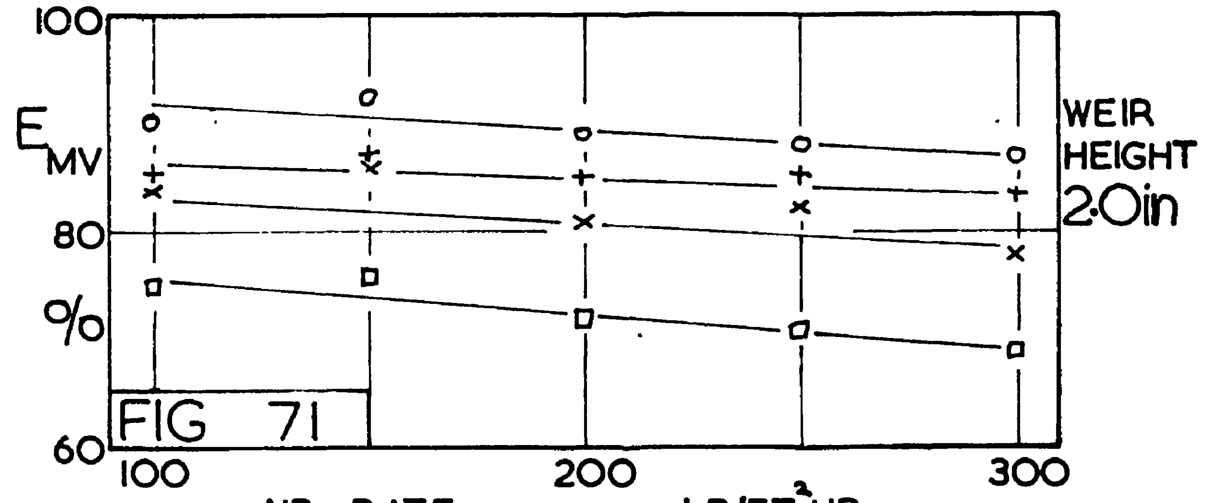

FIG 71

AIR RATE — LB/FT^{2}HR

30in KUHNI PLATE — SLOT AREA-9.76%

PARAMETER IS WATER RATE - LB/FT^{2}HR.
1000 — ○ 500 — + 250 — × 100 — □

FIG 72

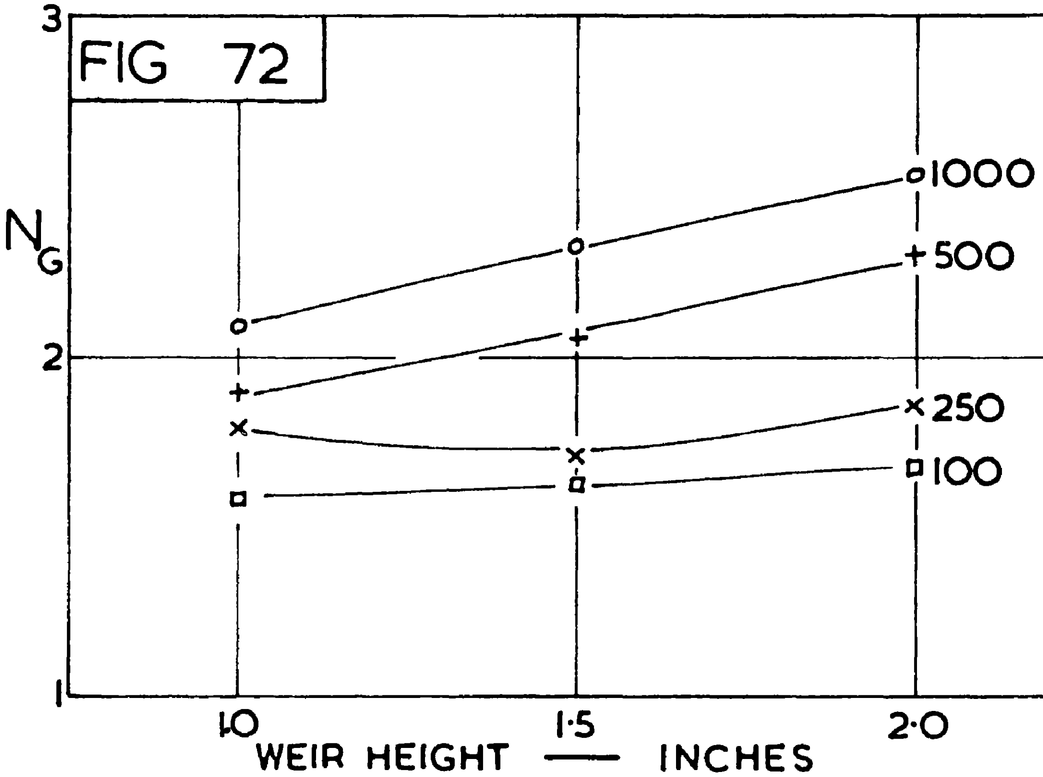

FIG 73

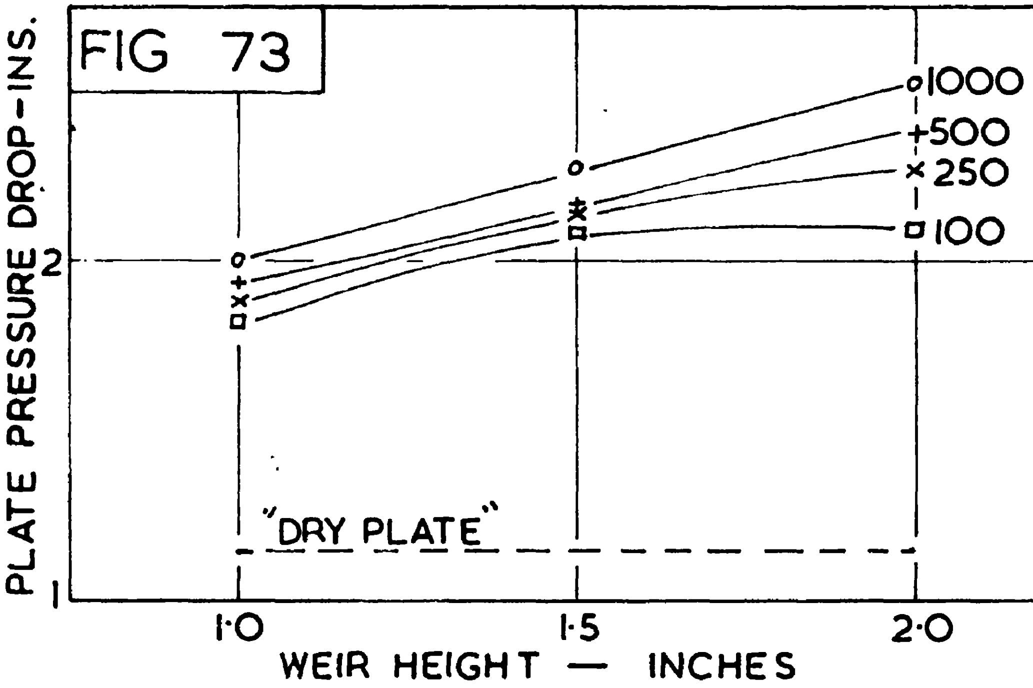

AIR RATE IS 200 LB/FT^{2}HR
PARAMETER IS WATER RATE – LB/FT^{2}HR

there is an associated increase in plate pressure drop.

There can be little doubt that the increase in efficiency is attributable to the greater froth height, with the resultant increase in air residence time and interfacial area. The effect of increasing the weir height is thus similar to the effect of increasing the water rate, as was discussed earlier with reference to the humidification efficiency characteristics of the 30 in. plate. In that discussion it was shown that the group K_Ga varied greatly with the operating conditions and while changes in the interfacial area "a" may account for part of this variation, the most important contribution to these changes came from "K_G". It was further shown that K_G depends on the air residence time in the froth, as is predicted by the Penetration Theory and that the relationship between K_G and the residence time is of the form predicted by that theory.

To test if an increase in weir height gives the increase in mass transfer predicted by the Penetration Theory it is necessary to estimate the air hold-up in the froth and thus the residence time. The air hold-up was obtained by subtracting the water hold-up from the froth volume. No water hold-up data were available from water residence time tests so an estimate was made by adding a volume of water equivalent to the increase in clear liquid height to the volume of water on the plate with no weir extension. It was felt that this procedure is likely to be more accurate than estimating the water hold-up from the clear liquid height only. It has been shown earlier that such a procedure is liable to give considerable errors.

As in the previous discussion an attempt was made to show the effect of air residence time on K_G alone, by using the K_Ga/(air hold-up per ft.^{2} of plate area) ratio to eliminate approximately the variation in "a". Figure 74 shows K_Ga/(air hold-up) plotted against the air residence time. The curves are the same form as those for the original plate which suggests that the Penetration Theory may well apply to gas phase resistant mass transfer on a gas absorption plate.

As with the original plate the froth height was found to be relatively independent of air rate and primarily dependent on water rate. The froth height is generally between 0.5 and 1.0 inches greater than the weir height ahd is shown in Figures 25, 26 and 27 in Section 5;3.

Effect of Slot Area

Carey et al[4] have suggested that the number of transfer units of a bubble cap plate is inversely proportional to the cube root of the slot width. This is probably a result of coarser bubbling, the larger bubbles having a smaller surface area to volume ratio.

In the tests on the Kuhni Plate the slot area was increased by raising the caps and thus increasing the slot height but it is probable that the effect of increasing the slot height on the Kuhni Plate is similar to that of increasing the slot width on a bubble cap plate. One important difference in this respect between the bubble cap and the Kuhni Plate is that the slots of a bubble cap are "open" to an extent dependent on the gas rate whereas the slots of the Kuhni Plate, being only 3/32 in. high are probably either completely open or completely closed.

The most important feature of the increase in slot area is the considerable reduction in dry plate pressure drop. If the passage of air through the plate was frictionless, the pressure drop at a given air rate

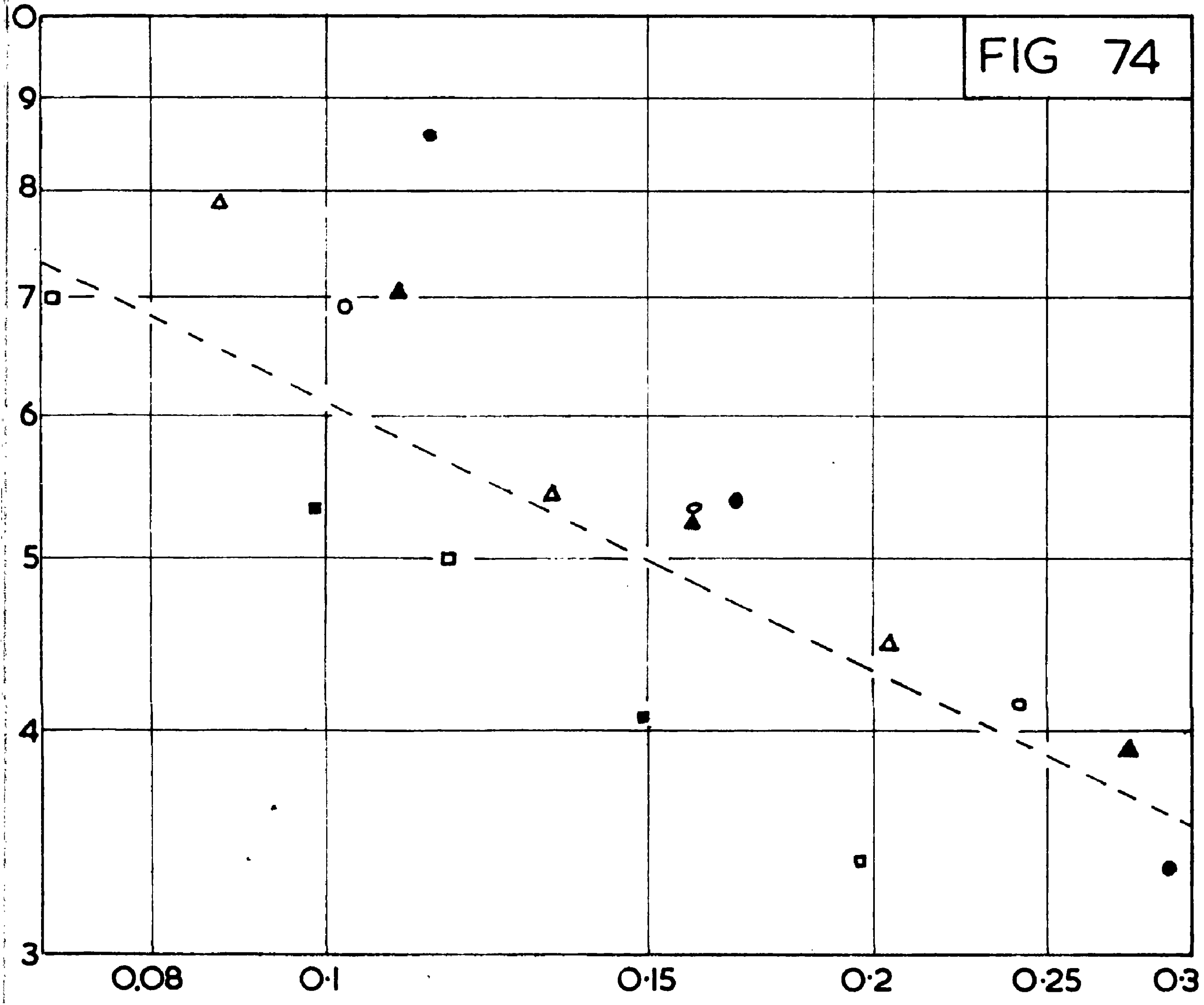

PLOT OF THE RATIO "$K_G a$" TO THE "AIR HOLD-UP PER UNIT PLATE AREA" (ORDINATE) AGAINST AIR RESIDENCE TIME IN THE FROTH IN SECONDS (ABSCISSA), (LOG-LOG).

PARAMETERS ARE WEIR HEIGHT, INS & WATER RATE, LB/FT²HR

1·5 INCH — 1000— ○ ; 500— △ ; 100— □ :

2·0 INCH — 1000— ● ; 500— ▲ ; 100— ■ .

would be inversely proportional to the fourth power of the slot area thus even a small increase in slot area causes a marked reduction in pressure drop. Figure 75 shows the dry plate pressure drops and it can be seen that the pressure drops at 9.76% and 7.32% are about 25% and 60% respectively of the pressure drop at 4.25%, the original slot area. This reduction in dry pressure drop is very desirable and gives a considerable reduction in the plate pressure drop.

It is noticeable that the 9.76% line on Figure 75 is still higher than the 12 inch plate line even although the 12 inch plate has a slot area of 6.01%. The reason for this is that the riser design is different, the riser of the 30 inch plate being close to the slot and restricting the air flow. A change in riser design would probably be beneficial.

Figure 76 shows the efficiency data obtained with the three slot areas at a water rate of 1,000 lb./ft.^{2}hr. As can be seen the efficiency tends to drop to a constant value or even to show a slight minimum. At an air rate of 100 lb./ft.^{2} hr there is a continuous drop in efficiency whereas at 300 lb./ft.^{2}hr there is a minimum value. The corresponding pressure drop data in Figure 77 show the considerable reduction in plate pressure drop associated with the increase in slot area.

It is difficult to explain all these effects without a sounder knowledge of the bubbling mechanism and the effect which slot area changes have on that mechanism. It is still more difficult to correlate these changes in efficiency at all accurately and to predict the efficiencies at other slot areas. It appears, however, that the efficiency although reduced is not seriously reduced and that the benefits with respect to pressure drop greatly outweigh the disadvantages of lower efficiency.

FIG 75

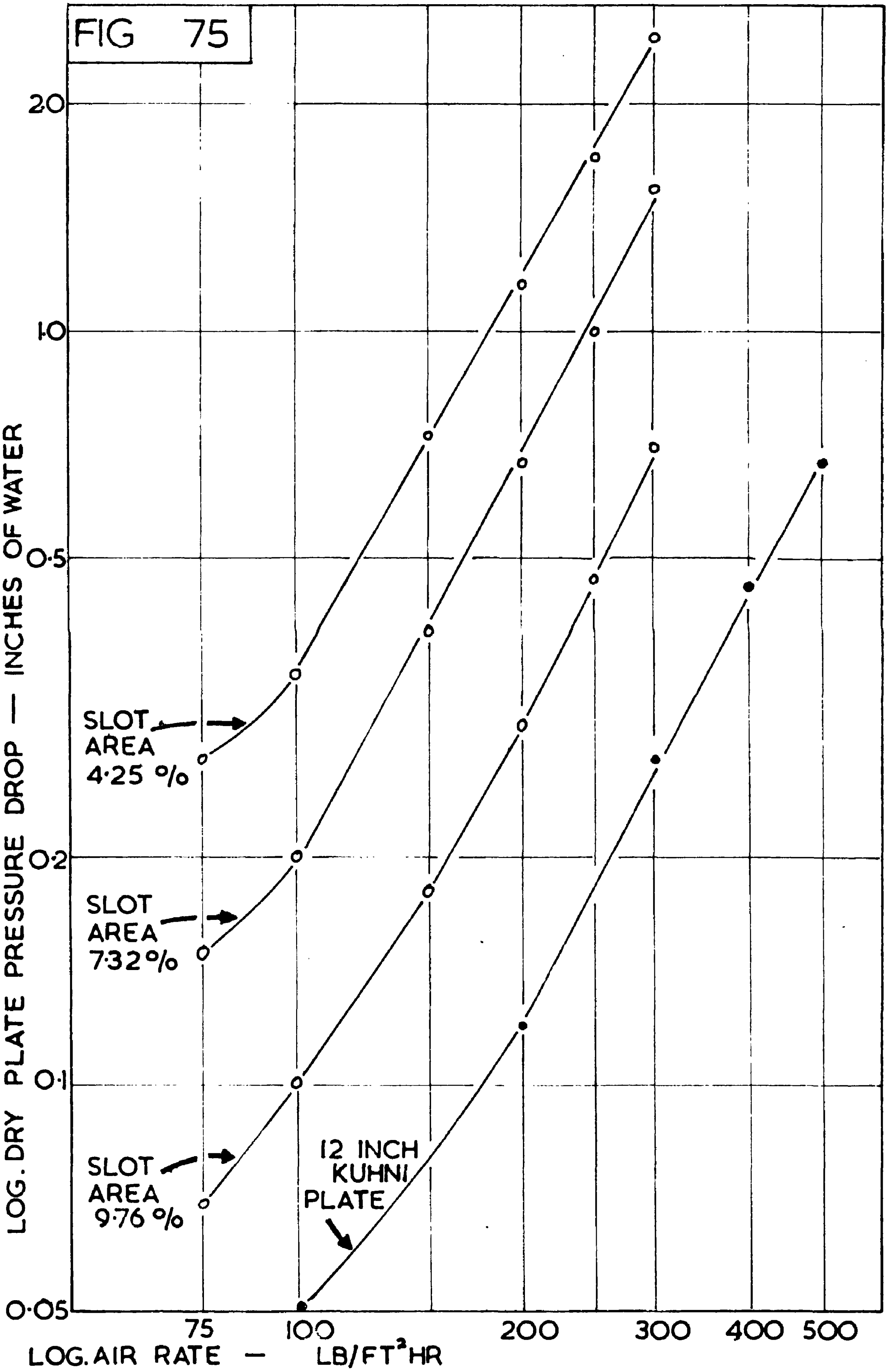

2·0
1·0
0·5
0·2
0·1
0·05
75
100
200
300
400
500
LOG. DRY PLATE PRESSURE DROP — INCHES OF WATER
LOG. AIR RATE — LB/FT² HR
SLOT AREA 4·25 %
SLOT AREA 7·32 %
SLOT AREA 9·76 %
12 INCH KUHNI PLATE

FIG 76

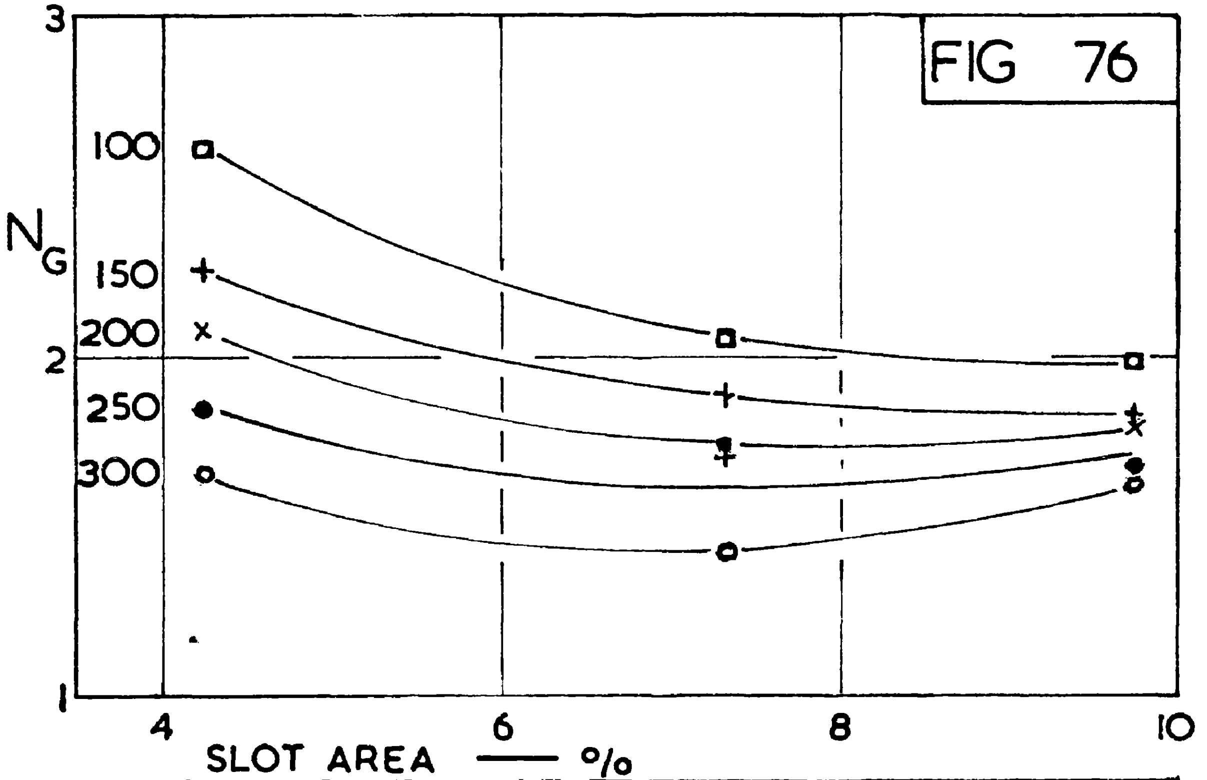

FIG 77

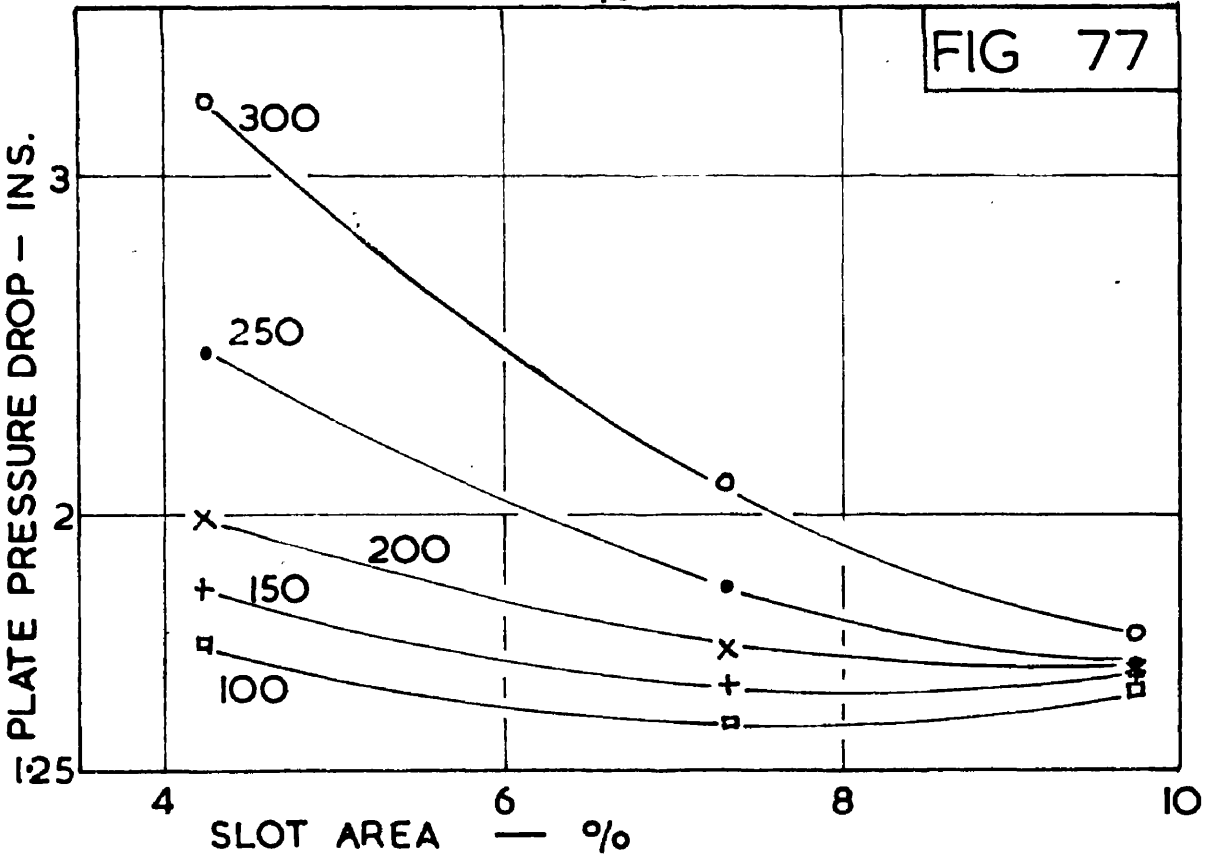

WATER RATE IS 1000 LB/FT^{2}HR
PARAMETER IS AIR RATE – LB/FT^{2}HR

An effect of increased slot area which was noted but not measured was an increase in entrainment which possibly gave artificially high efficiencies, especially at high air rates. The question whether this effect would necessitate increased plate spacing or other measures to reduce entrainment can only be answered by a study of plate to plate entrainment.

Interaction between Slot Area and Weir Height

The previous discussion in this section describes the effect of a change in either slot area or weir height. It is generally inadvisable to assume that the effect of a combination of variables of this type is a simple addition of the two effects.

A statistical analysis was done using data from all nine plate conditions. The data were taken from the efficiency graphs and were four efficiencies taken at the combinations of water rates of 100 and 1,000 lb./ft.^{2}hr and air rates of 100 and 300 lb./ft.^{2}hr. The efficiencies were converted into transfer units and the data analysed statistically to test for interactions between the four variables, air rate, water rate, weir height and slot area.

The results indicated that there is an interaction between air rate slot area and weir height which can be interpreted as meaning that changing the slot area has a different effect on efficiency with different air rates and with different weir heights. The variable effect of air rate was noted in the previous section and investigation of the graphs shows that for example at a weir height of 1.5 in. and increase of slot area from 4.25% to 7.32% has very little effect whereas a further increase to 9.76% produces a marked reduction in efficiency especially at low water rates.

The statistical analysis and study of the graphs suggest that the bubbling mechanism may depend on the air rate, the slot area and the submergence and that transitions from bubbling to jetting may occur under conditions dependent on these three variables.

Conclusions on Plate Alterations

The reason for determining the effect of changes in weir height and slot area on the performance of the Kuhni Plate was that it might be possible to suggest improvements in design, especially with regard to these two design variables. In deciding whether a particular change in design is beneficial, both efficiency and pressure drop must be considered. A useful quantity in this respect is the "pressure drop per theoretical plate" (P.D.P.T.P.) which is equivalent to the ratio of pressure drop to efficiency. It would, however, be misleading to use this quantity alone in determining the desirability of a given design since the capital cost of a distillation or gas absorption column depends largely on the number of plates required which is a function of efficiency alone for a given throughput. Thus a particular design with a low "P.D.P.T.P." may be precluded by virtue of the number of plates required.

Figure 78 shows the "P.D.P.T.P." plotted against weir height with slot area as parameter at operating conditions of 1000 lb./ft^{2}hr. water rate and 300 lb./ft.^{2}hr air rate. The 7.32% and 9.76% slot area curves are far lower than that of the existing plate showing the desirability of

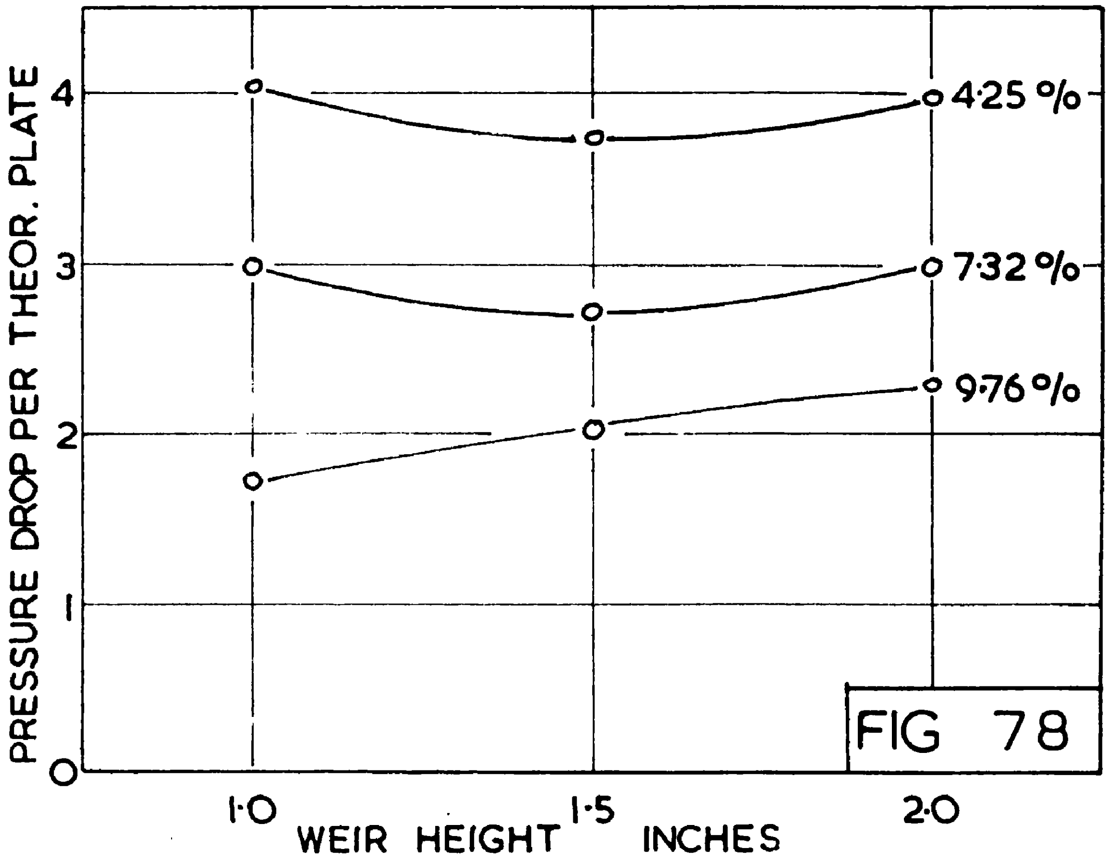

FIG 78

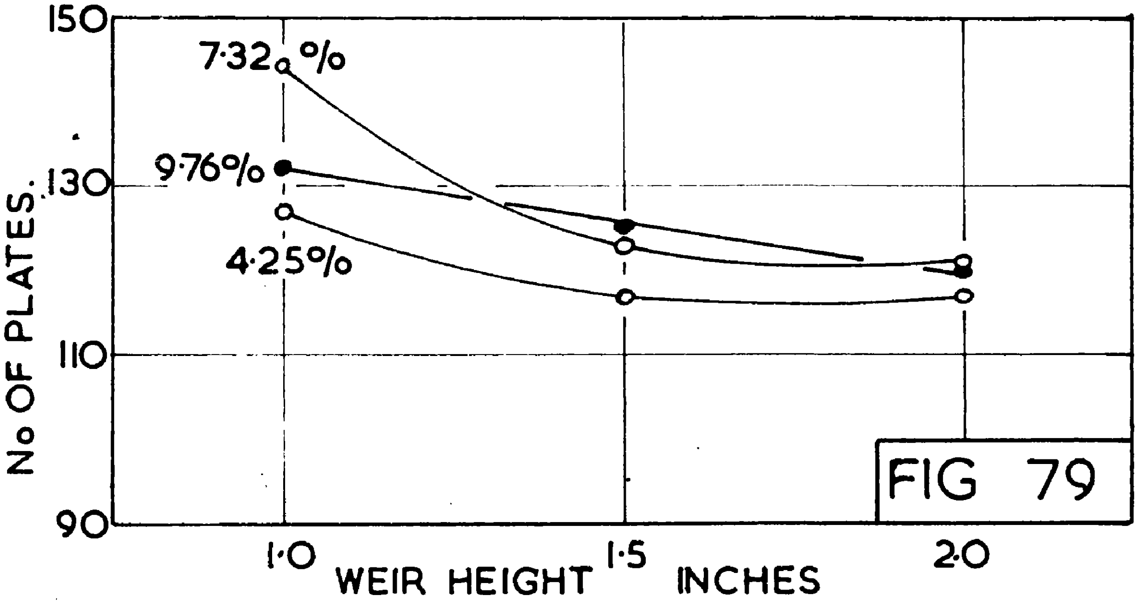

FIG 79

PARAMETER IS SLOT AREA
AIR RATE 300 LB/FT^{2}HR
WATER RATE 1000 LB/FT^{2}HR

increasing the slot area. At lower air rates where the dry plate pressure drop is less it can be shown that the curves are closer but the higher slot area is still desirable.

It can be seen from Figure 78 that weir height has no marked effect on the "P.D.P.T.P.". This is not unexpected since an increase in weir height causes increases in both efficiency and pressure drop.

Figure 79 shows the desirability of using a higher weir height in a plot of the reciprocal of efficiency against weir height. The ordinate, the reciprocal of efficiency can be regarded as the number of plates required to effect a separation corresponding to 100 theoretical plates, assuming that operating conditions are identical throughout the column and that the column efficiency equals the plate efficiency. It is apparent from this figure that there is a steady drop in the number of plates required with increasing weir height, a very beneficial effect.

In conclusion, it has been shown that a considerable improvement in plate design could be made by increasing the slot area to about 10% of the column area. An increase in weir height is also desirable to compensate for the reduction in plate efficiency caused by the increased slot area and to reduce the number of plates required. Further tests are necessary to determine the effect of these changes on liquid "film" efficiency and it is probable that increased slot area will reduce the liquid "film" efficiency owing to the coarser bubbling and that increased weir height will increase the liquid "film" efficiency owing to the increased liquid residence time on the plate. It would also be advisable to establish the magnitude of any changes in plate to plate entrainment and if this becomes excessive to reduce entrainment by increasing the plate spacing and/or the liquid seal.

5 : 12 Tests on the 12 inch Diameter Kuhni Plate

The efficiency of the 12 inch plate was determined using humidification and oxygen desorption systems together with pressure drop and clear liquid height data. No residence time or mixing tests were done on the 12 inch plate, owing to the difficulty of measuring such short residence times. Some tests were carried out by Dunn[128] on the effect of changing the outlet weir height and the surface tension of the water on the humidification efficiency. The results of these tests are also discussed.

(i) Pressure Drop, Clear Liquid Height and Froth Height

Figure 80 shows the pressure drop data plotted against air rate with water rate as parameter. The dry plate pressure drop is shown in this figure and also on a log-log plot in Figure 75. Comparison of the dry plate pressure drops in Figure 75 shows the 12 inch plate to have a dry pressure drop of approximately 12% of the original 30 inch plate at equivalent air rates. The reasons for this lower pressure drop are that the slot area of 12 inch plate is greater (6.01% against 4.25%) and that the design of the risers of the 12 inch plate offers less resistance to the passage of air. This latter effect is shown in Figure 16 where the caps are compared. As can be seen, the riser of the 12 inch plate is clear of the slot whereas the riser of the 30 inch plate is very close to the slot.

The "wet" plate pressure drop lines are seen to be substantially parallel, the higher pressure drops being associated with higher hydraulic gradients and weir crests. The reason for the tendency for the pressure drop to fall from air rates of 100 to 200 lb./ft.^{2} hr is that in

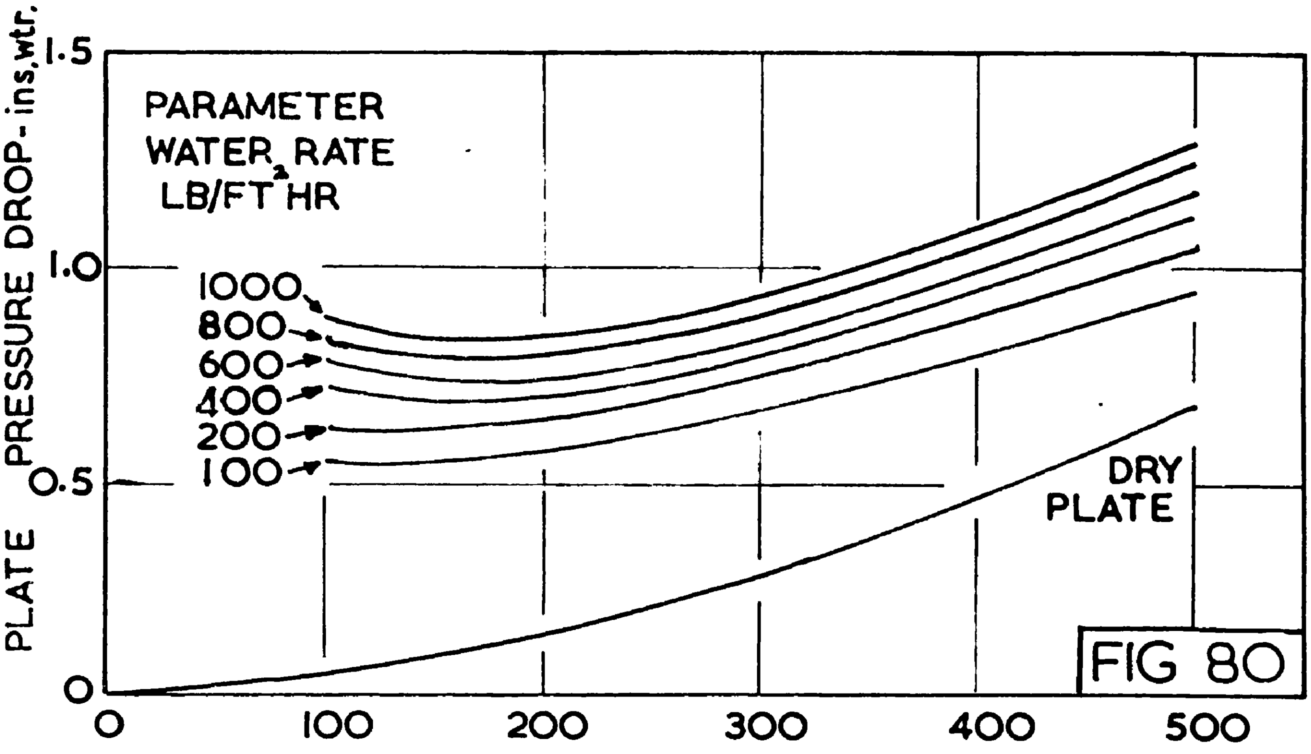

FIG 80

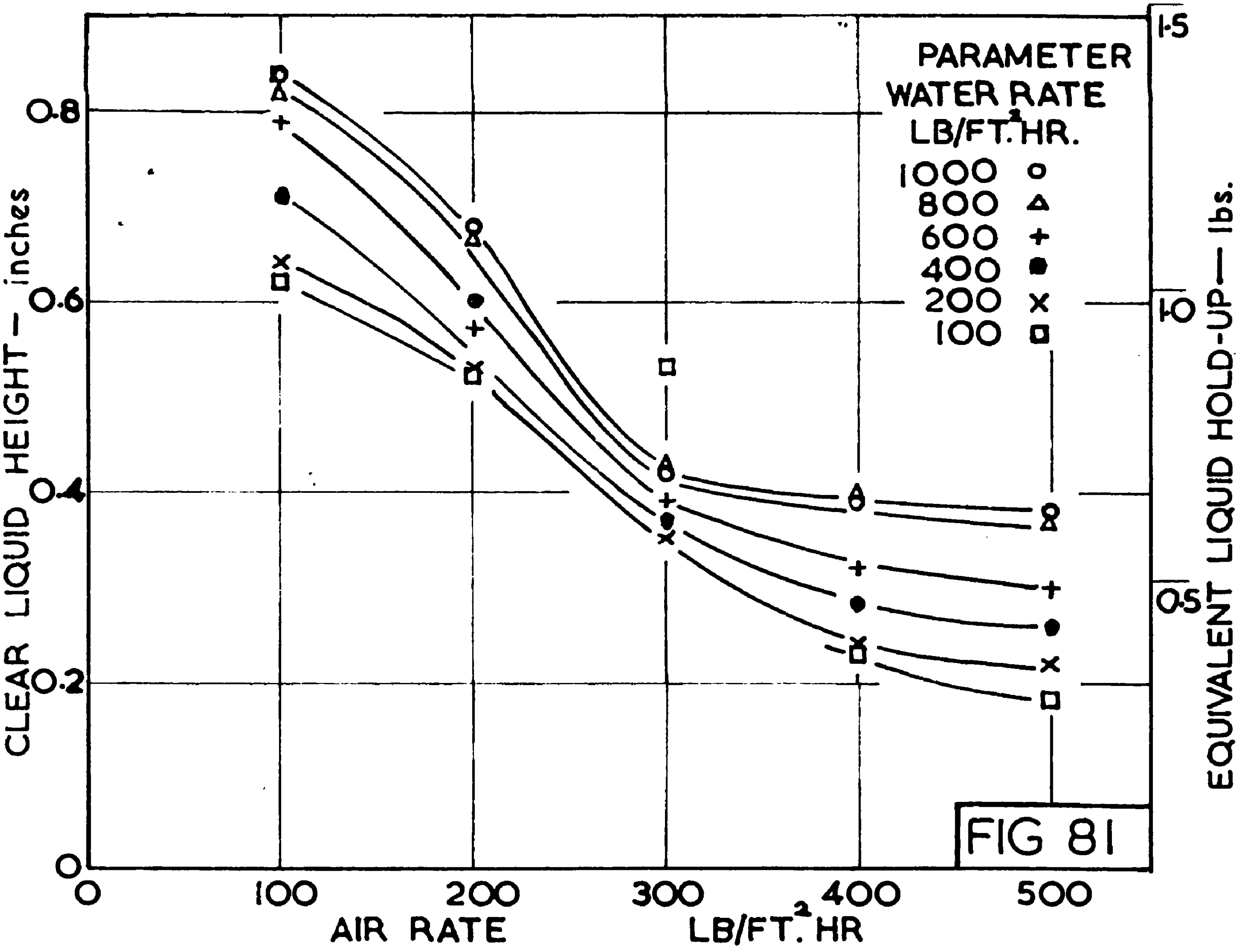

FIG 81

12 inch KUHNI PLATE

this region only the outer trough is bubbling, the effective air velocity through the slots which are active being higher than is indicated by the dry pressure drop curve. Above 250 lb./ft.^{2} hr (air rate) the dry pressure drop curve is nearly parallel to the "wet" pressure drop curves which suggests that correlation of the "wet" pressure drop should be possible by summing the dry pressure drop and a water seal, dependent on the water rate. Such a correlation is given below.

$$\text{Dry pressure drop} = 4.56 \times G_M^{1.92} \times 10^{-5} \text{ in water} \qquad (5;13)$$

$$\text{Water seal} = 0.325 + 0.315 \times L_M . 10^{-3} \text{ in water} \qquad (5;14)$$

Where G_M is the air rate in lb./ft.^{2}hr and L_M the water rate in lb./ft.^{2}hr.

The total pressure drop is the sum of the two components correlated above.

The clear liquid height measurements were converted to a mean value by weighting the individual readings in proportion to the area of the respective troughs. The resultant data are shown in Figure 81. The sharp increase in clear liquid heights below an air rate of 300 lb./ft.^{2}hr is attributable to the flooding of the inner trough. The curves are similar to the data for the 30 inch plate. It is interesting to compare the liquid hold-up per unit area for the two plates. Owing to the lower weir height of the 12 inch plate (0.79 in. against 0.99 in.) the hold-up is less. For example at 1,000 lb./ft.^{2}hr water rate and 300 lb./ft.^{2}hr air rate the hold-up on the 30 inch plate calculated from the clear liquid height is 4.9 lb. or 1.00 lb./ft.^{2} whereas the hold-up on the 12 inch plate is 0.68 lb. or 0.865 lb./ft.^{2}. The respective clear liquid heights are 0.43 inches (30 inch plate) and 0.42 inches (12 inch plate). The difference in liquid hold-up per unit area is thus not substantial. The importance of this fact will be discussed later in this section.

It proved very difficult to make froth height measurements on the 12 inch plate. Estimations of the froth height indicated that it remained fairly constant at about 0.3 inches above the weir height. No stable froth formed, the air passing through the water as jets rather than as bubbles.

Gas Phase Efficiency

Figure 82 shows the humidification efficiency results plotted against air rate with water rate as parameter. The two dashed lines show the corresponding efficiencies on the 30 inch plate. In general the efficiency of the 12 inch plate is lower and less variable than that of the 30 inch plate. The lower efficiency may be attributed to the lower weir height but the previous discussion in this section has shown that the liquid hold-up differences between the plates are not substantial. Probably the lower efficiencies are due to the lower froth height with the associated reduction in air residence time in the froth. The bubbling mechanism appeared to be different, more "jetting" taking place and this may also have caused the lower efficiencies. The relative constancy of the efficiency with air rate is probably a result of the "jetting" tendency and the inactivity of the inner trough at air rates less than 250 lb./ft.^{2}hr.

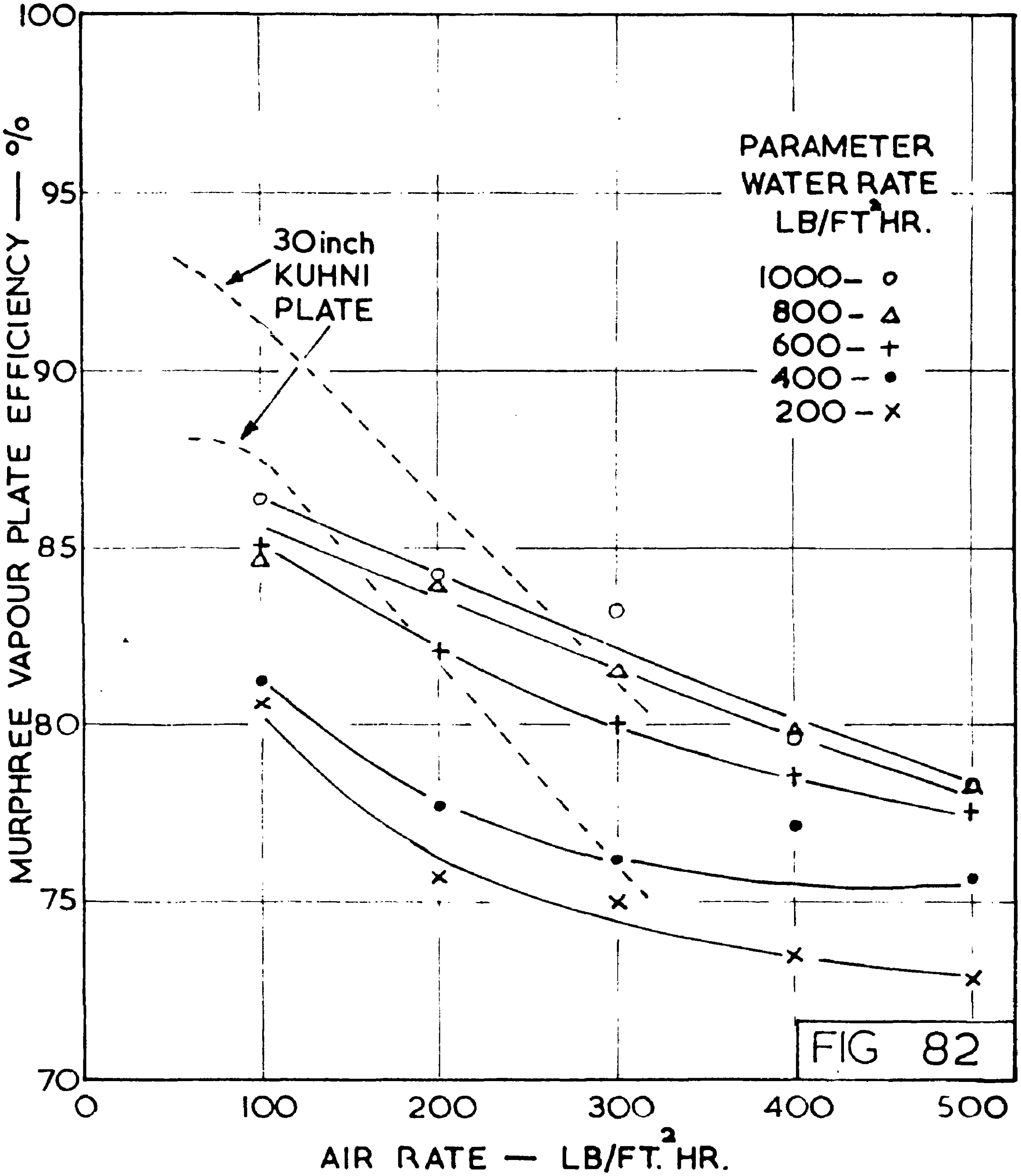

FIG 82

12 inch KUHNI PLATE

HUMIDIFICATION EFFICIENCY

Liquid Phase Efficiency

The plate efficiency results are shown in Figure 83. Since no mixing data were available for the 12 inch plate it was impossible to convert the plate efficiencies to point efficiencies. The efficiency characteristics are slightly different from the characteristics of the 30 inch plate. The efficiencies show a slight maximum at 400 lb./ft.^{2}hr (air rate) but are substantially constant in the region 300 to 500 lb./ft.^{2}hr. There is a sharp drop in efficiency associated with the inner trough ceasing to bubble at 250 lb./ft.^{2} hr. At the highest water rate of 1,000 lb./ft.^{2}hr the maximum efficiency is over 10% lower than the maximum efficiency at the lowest water rate of 100 lb./ft.^{2}hr. This is in sharp contrast to the 30 inch plate where the plate efficiency at 300 lb./ft.^{2}hr (air rate) is almost independent of water rate. The efficiencies are, in general, lower than those of the 30 inch plate.

There can be little doubt that the reasons for the lower efficiencies are that the liquid hold-up on the plate is less, the water flowing over only two bubbling troughs (or only one at air rates less than 250 lb./ft.^{2}hr) compared with four on the 30 inch plate. The less effective gas-liquid contacting as indicated by the lower humidification efficiencies will also contribute to the lowering of efficiencies.

Effect of Increasing the Weir Height

The humidification efficiencies obtained by Dunn[128] are generally higher than those obtained by the author and several efficiencies greater than 100% were obtained. This discrepancy has been attributed to the system being non-adiabatic and to a certain amount of humidification taking place in the air ducting. Weir height extensions of 0.5, 1.0, 1.5 and 2.0 inches were used. The froth heights were again low, varying from 0.2 to 1.0 inches above the weir.

Figure 85 shows the data obtained at a water rate of 400 lb./ft.^{2}hr and demonstrates the expected rise in efficiency. Pressure drop and clear liquid height also increased by an amount suggesting a froth density of approximately 0.5.

Effect of Decreasing Surface Tension

Dunn determined the humidification efficiency of the 12 inch plate at surface tensions of 50, 60 and 72 dynes per cm. using "Teepol" solutions. Considerable difficulty was encountered in keeping the surface tension constant. At surface tensions less than 50 dynes per cm. excessive foaming occurred and even at 50 dynes per cm. the froth height was often greater than the normal plate spacing of 4 inches. Figure 84 shows the increase of efficiency with surface tension decrease. The reason for the increase in efficiency is the greater froth stability and height. The increased surface area presumably overcomes any increase in mass transfer resistance due to the surface active agent. It was found that the pressure plate drop was higher at low surface tensions probably as a result of the considerable froth volume generated.

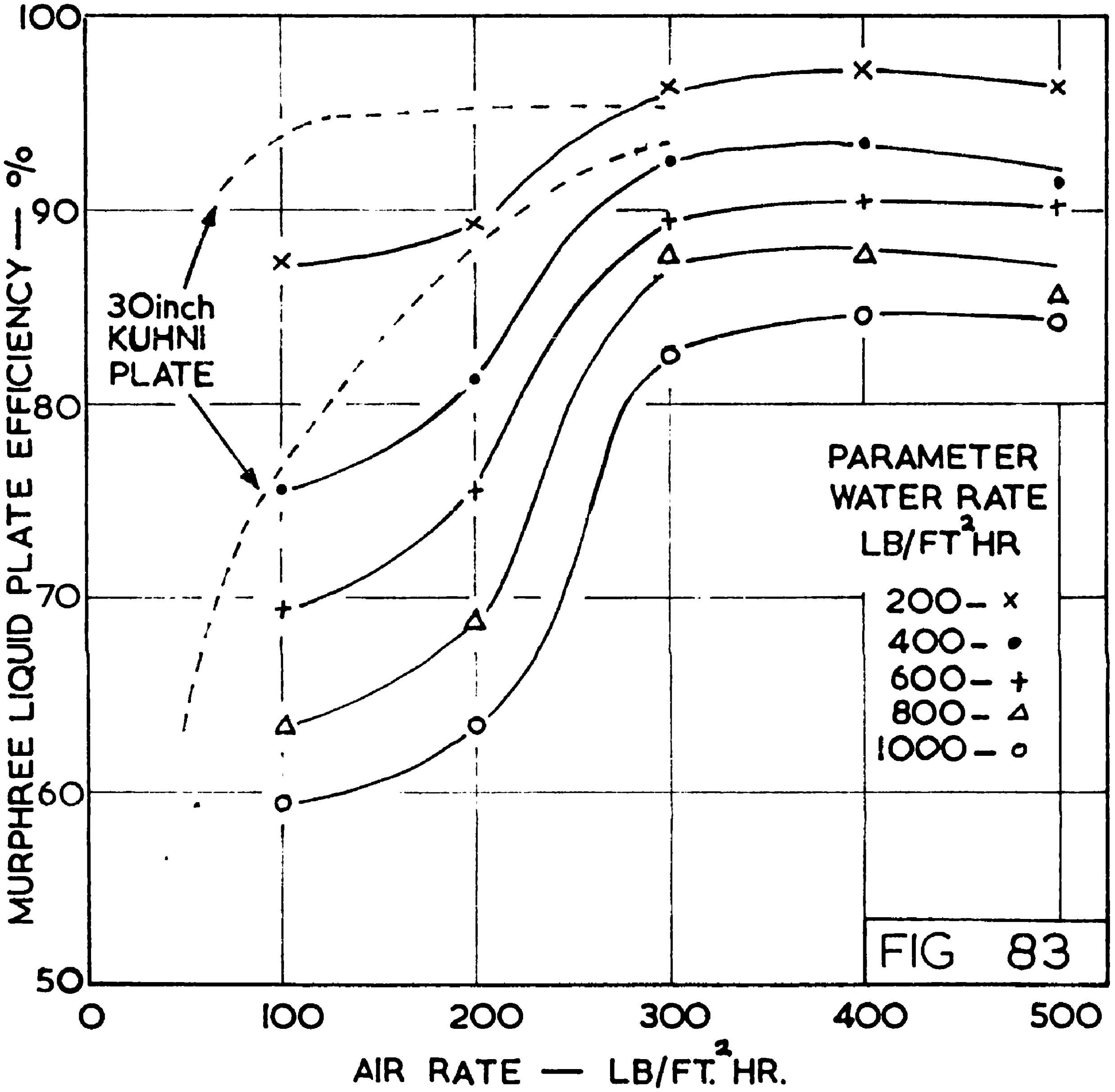

FIG 83

12inch KUHNI PLATE

OXYGEN DESORPTION EFFICIENCY

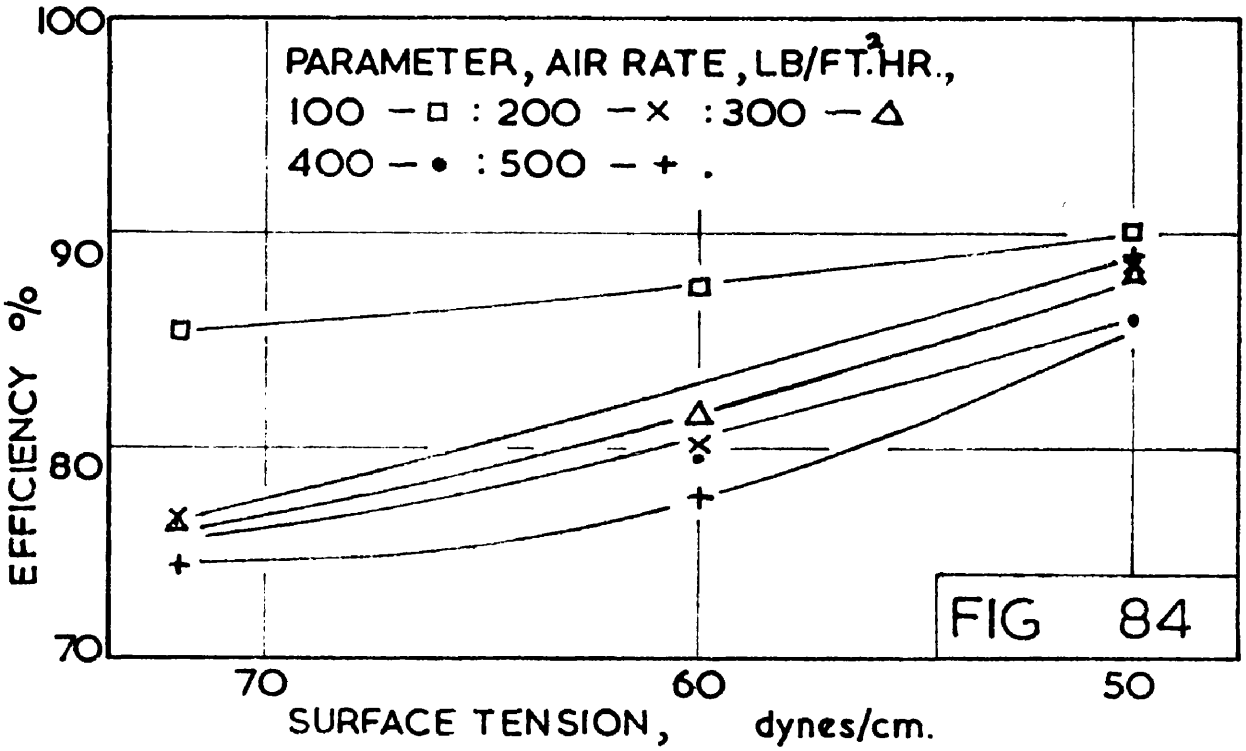

FIG 84

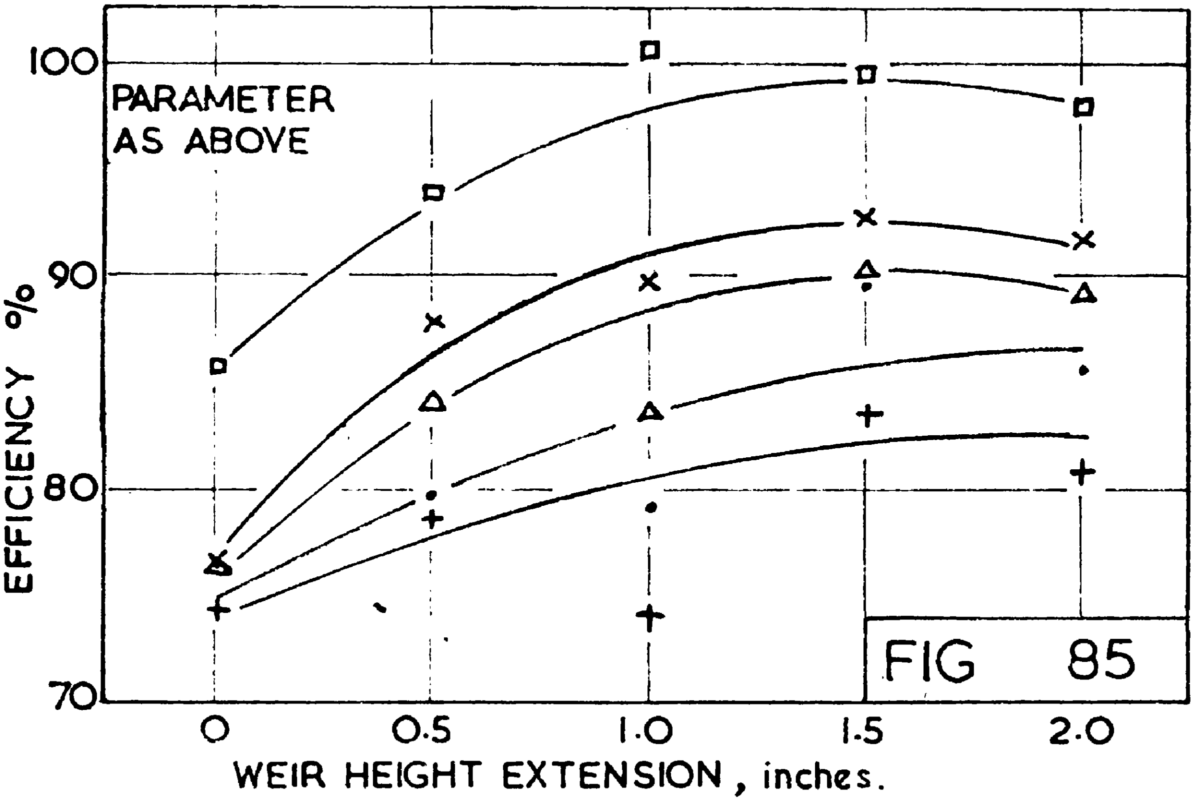

FIG 85

HUMIDIFICATION EFFICIENCY OF THE 12 INCH KUHNI PLATE AS A FUNCTION OF SURFACE TENSION AND WEIR HEIGHT AT A WATER RATE OF 400 LB/FT²HR., WITH AIR RATE AS PARAMETER

5 : 13 Comparative Performance of the Kuhni Plate and Other Bubble Plates

(i) Throughput and Pressure Drop

The 30 inch Kuhni Plate was tested at water rates up to 1,000 lb./ft.^{2}hr. (490 gall./hr.) and air rates up to 320 lb./ft.^{2}hr (1.2 ft./sec.) while the corresponding figures for the 12 inch plate were 1,000 lb./ft.^{2}hr. (79 gall./hr) and 500 lb./ft.^{2}hr (1.8 ft./sec.). These maximum throughputs were limited by the outputs of the blowers and pumps, the plate pressure drop and the permissible throughput of the liquid downcomers and distributers.

The water rate of 1,000 lb./ft.^{2}hr was the maximum flow which the distributers could handle, which is low in comparison with other bubble plates which can handle liquid rates exceeding 10,000 lb./ft.^{2}hr. Since only one plate of each diameter was studied no information is available on the column flooding liquid flow rate. Work is at present being done on this problem and the results indicate that the maximum liquid flow rate for the 12 inch column is 1,500 lb./ft.^{2}hr.

The air rate on the 30 inch plate of 1.2 ft./sec. was the maximum obtainable with the present blower and at this air velocity the plate pressure drop varied between 3.0 and 3.3 inches of water depending on the water rate. A typical pressure drop for a bubble cap or a sieve plate is between 1 and 2 inches of water[29]. As has been discussed in Section 5;11 the high pressure drop of the Kuhni plate can be reduced by altering the slot design and this is very desirable to bring the pressure drop characteristics of the Kuhni Plate into line with other plates. The 12 inch Kuhni Plate showed much better pressure drop characteristics but even then the vapour velocities are low.

It is desirable, from the point of view of capital cost of a column to keep the diameter as small as possible by having a high vapour velocity. Bubble cap and sieve plate columns operate at vapour velocities up to 5 ft./sec. and a recent Russian publication[131] describes a column with vapour velocities up to 13 ft./sec. The maximum vapour velocity is usually limited by the entrainment characteristics but no information is at present available on plate to plate entrainment characteristics of the Kuhni Plate.

At present therefore, the Kuhni Plate compares unfavourably with other bubble plates as regards throughput and pressure drop. Alterations in plate design will almost certainly improve its performance but even then it is unlikely that it will be as attractive as the cheaper sieve plate.

(ii) Efficiency

The efficiency characteristics of the Kuhni Plate are very good in the range of operating conditions studied. This is probably attributable to the high slot velocity giving very effective contact between the phases. The low weir height would be expected to give a low efficiency and tests showed that higher efficiencies could be obtained with higher weir heights. It is probable that the high slot velocity compensates for the low weir height but unfortunately it is obtained at the expense of a high plate pressure drop. For example a typical pressure drop per theoretical plate for a bubble cap plate[29] is 2.2 inches of water at a vapour velocity of 1.0 ft./sec, while the figure for the Kuhni Plate under similar conditions is 3.7 inches.

SECTION 6

APPENDIX

APPENDIX A

(i) Specimen Calculation of Solution Evaporation Test No.A1

Test Data

Air rate	307.2 lb./ft.^{2}hr
Water rate	1,000 lb./ft.^{2}hr
Duration	300 minutes

Initial weight of solution W_1	52.3 lb
Final weight of solution W_2	49.2 lb.
Weight of water added W_A	27.1 lb.
Initial titration C_1	30.23 cc. acid
Final titration C_2	29.71 cc. acid
Average inlet humidity H_1	52.13 gr./lb. dry air
Average inlet water temperature	61.75°F
Average outlet water temperature	61.60°F

Solution of the following equations for W_E, the weight of water entrained and W_V the weight of water evaporated (lb.) gives the values below.

$$W_1 - W_2 + W_A = W_E + W_V \qquad (2;1)$$

$$W_1 C_1 = W_2 C_2 + W_E \ (C_1 + C_2)/2 \qquad (2;2)$$

$$\therefore \ W_E = 3.93 \text{ lb.} \qquad W_V = 26.31 \text{ lb.} = 184,200 \text{ grains}$$

Total weight of air used during test = 307.2 x 300 x 4.90/60 = 7,526 lb.

Weight of moisture in this air = 52.13 x 7,526/7,000 = 56.03 lb.

$\therefore$ Total weight of dry air = 7,470 lb.

$\therefore$ Increase in humidity $(H_2 - H_1)$ = 18420°/7470 = 24.66 gr/lb.dry air

Mean solution temperature = 61.68°F

Corresponding saturation humidity H_e = 82.31 gr/lb dry air.

$\therefore$ Average humidity difference $H_e - H_1$ = 30.18 gr/lb dry air

$\therefore$ Efficiency $E_{MV} = H_2 - H_1/H_e - H_1 = 81.7$

Entrainment = 3.93/7.526 = 0.522 lb/1,000 lb air

(ii) Specimen Calculation of Outlet Psychrometer Test

Test Data (Test No.23 on 30 in. Kuhni Plate)

Orifice plate pressure drop (P.D.) .... 0.203 in. water

Water rate .... 245 Gall/hr

Barometric pressure (P) .... 30.25 in.mercury

Mean inlet air dry bulb temperature .... 77.02 °F

Mean inlet air wet bulb temperature .... 58.96 °F

Mean outlet air dry bulb temperature .... 61.22 °F

Meen outlet air wet bulb temperature .... 59.23 °F

Mean inlet water temperature .... 59.30 °F

Mean outlet water temperature .... 59.20 °F

(i) Air Rate

From orifice plate calibration (BS 1042;1943)

$$G_M = 53.03\sqrt{P}\sqrt{P.D.} = 53.03,\ 5.50,\ 0.451 = 131.5\ \text{lb/ft.}^2\text{hr}$$

$$G_V = 131.5/0.0755 = 17423\ \text{ft.}^3/\text{ft.}^2\text{hr}$$

(ii) Water Rate

245 gall/hr, $\therefore L_M = 500$ lb/ft.^{2}hr

(iii) Efficiency

$H = H_S - 1.72\ (Td - Tw)$ (Equation 2;3)

$H_1 = 75.42 - 1.72\ (18.06) = 44.36$ gr/lb dry air

$H_2 = 76.15 - 1.72\ (1.99) = 72.73$ gr/lb dry air

Mean water temperature = 59.25 °F

$\therefore H_e = 76.20$ gr/lb dry air

Saturation Humidity data from IHVE Guide 1955[112]

$$E_{MV} = \frac{H_2 - H_1}{H - H_1} = 89.10\%$$

$N_G = -\log_e (1 - E_{MV}) = 2.22$

$K_Ga = NTU_G \times G_v = 3,868$ ft. /hr

Heat Balance on the 30 inch Plate.

Test No.23 (Outlet psychrometer test)

Data as on previous page.

Air rate = 131.5 lb./ft.^{2}hr = 644.4 lb./hr

Water rate = 245 gall/hr = 2,540 lb./hr

(i) Air Enthalpies

Air Enthalpy = 0.241 (Td - 32) + H.U/7,000 BTU/lb dry air.

Where Td = dry bulb temperature °F

H = humidity gr/lb dry air

U = water vapour enthalpy BTU/lb.

Inlet air : $Td_1 = 77.02$ $H_1 = 44.36$ $U_1 = 1095.2$

Outlet air : $Td_2 = 61.22$ $H_2 = 72.73$ $U_2 = 1088.2$

∴ Inlet air enthalpy = 17.79 BTU/lb dry air

Outlet air enthalpy = 18.35 BTU/lb dry air

(ii) Water Enthalpies

Inlet water temperature = 59.30 ∴ Enthalpy = 27.3 BTU/lb

Outlet water temperature = 59.10 Enthalpy = 27.2 BTU/lb

Water evaporated = $(H_1 - H_2)$ 644.4./7,000 = 2.612 lb/hr

∴ Inlet water = 2,540 lb. Outlet water = (2,540 - 2.61) lb

(iii) Heat balance on 1 hour basis

Heat input = Inlet air enthalpy + Inlet water enthalpy

= 644.4 x 17.79 + 2540 27.3 = 80806 BTU.

Heat output = Outlet air enthalpy + Outlet water enthalpy

= 644.4 x 18.35 + (2540 - 2.61) .27.2 = 80842 BTU

∴ Heat absorbed by the system = 36 BTU /hr. (1.5% of the heat transfer)

(iii) Specimen Calculation of Oxygen Desorption Test

Test Data, (Test No.19 on 30 in. Kuhni Plate)

Orifice plate pressure drop (PD) ....0.478 in water

Main rotameter reading ....247 gall/hr

Sample rotameter reading .... 2 gall/hr

Mean inlet water temperature ....13.65 °C

Mean outlet water temperature............13.55 °C

Inlet sample titration (v 250 cc sample)...38.56 cc

Outlet sample titration (v 250 cc sample) ..13.97 cc

Normality of thiosulphate solution 1.028 N/40

Barometric pressure (P) ....29.35 in. Hg or 745.2mm Hg

(i) Air Rate

From orifice plate calibration (BS 1042;1943)

$$G = 53.03 \sqrt{P} \sqrt{P.D.} = 53.03, 0.690, 5.41 = 198 \text{ lb/ft.}^2\text{hr}$$

(ii) Water rate

$$(247 - 2) \text{ gall/hr} = 245 \times 10/4.90 = 500 \text{ lb/ft}^2\text{hr}$$

$$L_V = 500/624 = 8.01 \text{ ft.}^3/\text{ft.}^2\text{hr}$$

(iii) Efficiency

$$\begin{array}{lccc} & \text{Inlet} & & \text{Outlet} \\ \text{Normality of 250 cc samples} = & \dfrac{1.028 \times 38.56}{250 \times 40} & \text{and} & \dfrac{1.028 \times 13.97}{250 \times 40} \\ = & 0.003964 \text{ N} & \text{and} & 0.001436 \text{ N} \end{array}$$

Dilution due to addition of 13 cc of reagents to 547 cc flasks =

$$1 + \frac{13}{547} = 1.0238$$

$$\therefore \text{ Corrected normalities} = 0.003964 \times 1.0238 \text{ and } 0.001436 \times 1.0238$$

$$= 0.004058 \text{ N and } 0.001470 \text{ N}$$

A normal solution of oxygen has an oxygen content of 8 g/litre or 8000p.p.m.

∴ Oxygen contents of sample = 0.004058 x 8000 and 0.001470 x 8000

= 32.47 p.p.m. and 11.76 p.p.m.

Thus X_1 = 32.47 p.p.m. and X_2 = 11.76 p.p.m.

Mean water temperature = 13.60 °C

∴ Henry's Law Constant $H_{O_2} = (2.486 + 0.0554\ (13.60 - 10)) \times 10^7 =$

2.686×10^7 mm Hg

Water vapour pressure at 13.6 °C = 11.7 mm Hg

∴ Partial pressure of the oxygen = 0.21 (745.2 - 11.7) = 154.0 mm Hg

∴ Equilibrium mol fraction = $154.0/2.686 \times 10^7 = 5.733 \times 10^{-6}$

∴ Equilibrium weight fraction = $\frac{32}{18} \times 5.733 \times 10^{-6}$ = 10.19 P.P.M.(X_e)

$$\text{Now } E_{ML} = \frac{X_1 - X_2}{X_1 - X_e} = 92.95\% \doteqdot 93.0\%$$

Conversion to N_L and K_La

The Peclet number for these operating conditions is 19.03

(see Specimen Calculation in Appendix A, iv)

The quantity $(1 - E_{ML})/E_{ML}$ = 0.0758

Substitution in Figure 52 gives N_L = 3.01

L_V = 8.02 ft.^{3}/ft.^{2}hr

∴ $K_La = N_L \times L_V$ = 24.1 ft./hr.

(iv) Specimen Calculation of Residence Time and Mixing Tests

Test Data (Test No.F15)

Air rate .... 200 lb./ft.^{2}hr

Water rate .... 245 gall/hr or 500 lb/ft.^{2}hr

Balance resistance .... 5,000 ohm

Chart speed .... 2.5 cm/sec.

Chart length (cm) (t)	0	3	6	9	12	15	18	21	24
Chart reading (mm)	7.2	7.2	90	230	270	289	290	288	279
Conductivity micromhos	254	254	277	559	803	1045	1060	1027	900
Conductivity increase (C)	0	0	23	305	549	791	806	773	646

Chart length (cm) (t)	27	30	33	36	39	42	45	48	51	54	57	60
Chart reading (mm)	270	255	244	213	175	151	130	120	93	84	75	72
Conductivity micromhos	803	687	620	494	406	360	330	316	281	269	258	254
Conductivity increase (C)	549	433	366	240	152	106	76	62	27	15	4	0

For conversion chart of chart reading to conductivity see Appendix F. Chart length is proportional to time "t" and conductivity increase to tracer concentration "C".

From the above data.

$$\sum C = C_1 + C_2 + C_3 \ldots\ldots \underline{\sum C} = 5{,}923$$

$$\sum Ct = C_1t_1 + C_2\,t_2 + \ldots\ldots\ldots \underline{\sum C}\ t = 135{,}303$$

$$\sum Ct^2 = C_1t_1{}^2 + C_2t_2{}^2 \ldots\ldots\ldots \underline{\sum C}\ t^2 = 3{,}598{,}119$$

$$\therefore \frac{\sum Ct}{\sum C} = \frac{135303}{5923} = 22.84 \text{ cm time units} = \frac{22.84}{2.5} = 9.14 \text{ sec}$$

$\therefore$ Mean residence time = 9.14 sec. = tm

$\therefore$ Liquid hold-up = 9.14 x 245/3600 = 0.622 gall water

$$\sigma^2 = \frac{\Sigma Ct^2}{\Sigma C} - \frac{(\Sigma Ct)^2}{(\Sigma C\ )} \Big/ tm^2 = 0.164 \quad \text{(dimensionless)}$$

Peclet Number Pe from Figure 86 $= 19.03 = \dfrac{(q - p)^2}{D_E\ tm}$

Eddy Diffusivity $D_E = (p - a)^2/Pe\ tm = 0.7225/19.03 \times 9.14$

0.00415 (ft.^{2}/sec)

(v) Specimen Calculation of Froth Volume and Air Residence Time

Test at air rate of 200 lb/ft.^{2}hr and water rate of 500 lb/ft.^{2} hr.

Water hold-up = 6.22 lb.

$$= \frac{6.22}{62.4} = 0.0997 \text{ ft.}^3$$

Froth height = 1.80 inches

"Volume" of plate up to the weir height of 1 inch = 0.1825 ft.^{3}

Bubbling area of plate = 4.41 ft.^{2}

$\therefore$ Each inch of froth above the weir = 0.3675 ft.^{3}

$\therefore$ Volume of froth = 0.1825 + 0.3675 (Froth height$''$ -1)

= 0.1825 + 0.2940

= 0.4765 ft.^{3}

$\therefore$ Volume of air hold-up = 0.4765 - 0.0996 = 0.3769 ft.^{3}

Air rate = 200 lb/ft.^{2}hr

= 200 x 13.3 x 4.90/3600 = 3.621 ft.^{3}/sec.

$\therefore$ Air residence time in the froth = 0.3769/3.621 = 0.104 sec.

APPENDIX B

Derivation of liquid residence time and mixing equations.

Under a given set of conditions let the volume of liquid on a bubbling plate be V_L ft^3. Let the liquid flow rate be v ft^3/sec. Let a quantity of tracer Q lb. be injected at the inlet at time t = 0. The subsequent changes in concentration at the outlet can be expressed as the function c(t) lb/ft^3, which will have the form as shown in diagram (i). Let the cumulative function F(t) be defined as the fraction of the tracer which has left the plate at time t seconds. Its form is given in diagram (ii).

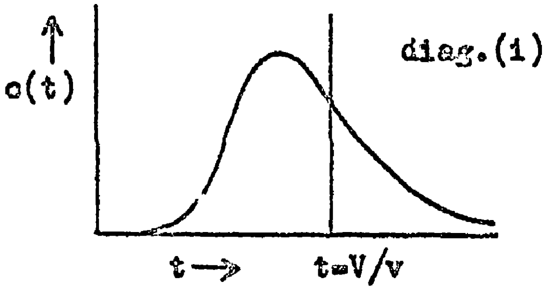

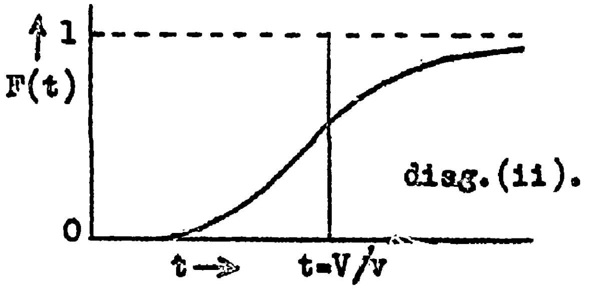

By the Law of Conservation of Mass,

$$\frac{v}{Q}\int_0^\infty c(t).dt. = 1 \qquad \text{and} \qquad F(t) = \frac{v}{Q}\int_0^t c(t).dt. \qquad (6:1)\ \&\ (6:2)$$

Itcan be shown that the mean residence time of the tracer in the system is

$$\frac{V}{v} = \int_0^\infty \left[1 - F(t)\right] dt. \qquad (6:3)$$

Restating this integral in terms of dF(t) instead of dt,

$$\frac{V}{v} = \int_0^1 t.dF(t). \qquad (6:4)$$

Substituting the differentiated form of equation (6:2) in equation (6:4)

$$\frac{V}{v} = \frac{v}{Q}\int_0^\infty (t).c(t).dt. \qquad (6:5)$$

If equations (6:1) and (6:5) are combined to eliminate v/Q,

then the mean residence time, $$t_m = \frac{V}{v} = \frac{\int_0^\infty t.c(t).dt.}{\int_0^\infty c(t).dt.} \qquad (6:5)$$

The mean residence time can thus be deduced numerically by finding a number of values of c(t) at equal increments of t and deducing the ratio

$$\frac{\sum c(t).t}{\sum c(t).}$$

The minimum number of values of c(t) and t taken was 20.

The variance of the time-concentration curve in diagram (1), normalized w.r.t. the mean residence time to give the dimensionless variance can be deduced from equation (6:6) below.

$$\sigma^2 = \left[\frac{\sum c(t).t^2}{\sum c(t).} - \left(\frac{\sum c(t).t}{\sum c(t).}\right)^2\right] \Big/ \left(\frac{\sum c(t).t.}{\sum c(t).}\right)^2$$

$$\sigma^2 = \frac{\sum c(t).t^2 \sum c(t).}{\left(\sum c(t).t.\right)^2} - 1$$

Relationship between Variance, Peclet Number, and Eddy Diffusivity.

Consider the flow of liquid radially inwards from the periphery of the Kuhni Distillation Plate. Let there be an injection of tracer at the periphery at time $t = 0 = t_o$ and at an angle $\theta = \theta_o$. Let the mass density of the tracer be measured at the outlet well .

Let r = any radius on the plate,(ft.),
q = the plate peripheral radius (ft.),
p = the outlet well radius (ft.),
V_1 = the inlet froth velocity (ft./sec.)
D_E = the eddy diffusivity (ft.^{2}/sec.),
ρ = the mass density of the tracer (lb./ft^3.).
δ = the Dirac delta function.
$A, B, E, F, I, K, \alpha, \phi, \psi, \gamma, \nu$ & S = functions defined as they appear in the derivation.

From a mass balance on an element of froth,

$$\frac{\partial \rho}{\partial t} - \frac{qV_1}{r}\frac{\partial \rho}{\partial r} = D_E\left(\frac{\partial^2 \rho}{\partial r^2} + \frac{1}{r}\frac{\partial \rho}{\partial r} + \frac{1}{r^2}\frac{\partial^2 \rho}{\partial \theta^2}\right) + \frac{V_1\delta(r-q)\delta(\theta-\theta_0)\delta(t-t_0)}{r}$$

Let $\phi = \int_0^\infty \rho e^{-st}.dt$

On application of a Laplace transform in time to the above equation,

$$s\phi - \frac{qV_1}{r}\frac{\partial \phi}{\partial r} = D_E\left(\frac{\partial^2 \phi}{\partial r^2} + \frac{1}{r}\frac{\partial \phi}{\partial r} + \frac{1}{r^2}\frac{\partial^2 \phi}{\partial \theta^2}\right) + \frac{V_1\delta(r-q)\delta(\theta-\theta_0)e^{-st_0}}{r}$$

Let $\psi = \int_0^{2\pi} \phi e^{in\theta} d\theta.$

$$\therefore s\psi - \frac{qV_1}{r}\frac{\partial \psi}{\partial r} = D_E\left(\frac{\partial^2 \psi}{\partial r^2} - \frac{1}{r}\frac{\partial \psi}{\partial r} - \frac{n^2}{r^2}\psi\right) + \frac{V_1\delta(r-q)e^{in\theta_0-st_0}}{r}$$

$$\therefore \frac{d^2\psi}{dr^2} - \frac{1}{r}\left(1 + \frac{qV_1}{D_E}\right)\frac{d\psi}{dr} - \left(\frac{n^2}{r^2} + \frac{s}{D_E}\right)\psi = -\frac{V_1 e^{-in\theta_0 - st_0}}{D_E r}.\delta(r-q)$$

equation (6:1)

$$\psi = A r^{-\alpha} I_\nu(\gamma r) + B r^{-\alpha} K_\nu(\gamma r) \quad , r > r_0$$

$$= E r^{-\alpha} I_\nu(\gamma r) + F r^{-\alpha} K_\nu(\gamma r) \quad , r < r_0$$

where $\alpha = \frac{qV_1}{2D_E}$ & $\nu = \sqrt{\alpha^2 + n^2}$ & $\gamma = \sqrt{\frac{s}{D_E}}$.

Now ρ is finite at $r = 0, \infty$

$$\therefore \psi = B r^{-\alpha} K_\nu(\gamma r) \quad r > q$$

$$\psi = E r^{-\alpha} I_\nu(\gamma r) \quad r < q$$

At $r = q$ ρ is continuous, $\therefore B K_\nu(\gamma q) = E I_\nu(\gamma q)$

Integration of equation (6:1) w.r.t. r from q_- to q_+ gives:-

$$\left[\frac{d\psi}{dr}\right]_{q-}^{q+} = -\frac{V_1}{qD_E}e^{in\theta-st_0}$$

$$\therefore -\alpha Bq^{-\alpha-1}.K_\nu(\gamma_q)+\gamma Bq^{-\alpha}K'_\nu(\gamma_q)+\alpha Eq^{-\alpha-1}I_\nu(\gamma_q)$$

$$-\gamma Eq^{-\alpha}.I'_\nu(\gamma_q) = \frac{V_1}{qD_E}e^{in\theta_0-st_0}$$

$$\therefore E\left[-\alpha q^{-\alpha-1}K_\nu(\gamma_q)I_\nu(\gamma_q)+\gamma q^{-\alpha}K'_\nu(\gamma_q)I_\nu(\gamma_q)+\alpha q^{-\alpha-1}I_\nu(\gamma_q)K_\nu(\gamma_q)\right.$$

$$\left.-\gamma q^{-\alpha}I'_\nu(\gamma_q)K_\nu(\gamma_q)\right] = \frac{V_1}{qD_E}e^{in\theta_0-st_0}K_\nu(\gamma_q)$$

$$\therefore E\gamma q^{-\alpha}\left[K'_\nu(\gamma_q)I_\nu(\gamma_q)-I'_\nu(\gamma_q)K_\nu(\gamma_q)\right] = -\frac{V_1}{qD_E}e^{in\theta_0-st_0}.K_\nu(\gamma_q)$$

$$\therefore E\gamma q^{-\alpha}\left[\frac{-1}{\gamma q}\right] = \frac{-V_1}{qD_E}e^{in\theta_0-st_0}K_\nu(\gamma_q)$$

$$\therefore E = \frac{V_1}{D_E}q^{\alpha}e^{in\theta_0-st_0}K_\nu(\gamma_q)$$

$$\therefore \psi = \left(\frac{q}{r}\right)^{\alpha}.\frac{V_1}{D_E}e^{in\theta_0-st_0}K_\nu(\gamma_q)I_\nu(\gamma_r)$$

$$\therefore \phi = \frac{1}{2\pi}\sum_{n=-\infty}^{\infty}\frac{q}{r}\frac{V_1}{D_E}e^{in\theta_0-st_0-in\theta}.K_\nu(\gamma_q)I_\nu(\gamma_r)$$

$$\therefore \phi = \frac{1}{2\pi}\left(\frac{q}{r}\right)^{\alpha}\frac{V_1}{D_E}e^{-st_0}K_\alpha(\gamma_q)I_\alpha(\gamma_r)+\frac{1}{2\pi}\sum_{n=-\infty}^{\infty}\left(\frac{q}{r}\right)^{\alpha}\frac{V_0}{D_E}e^{-st_0}.K_\nu(\gamma_q).I_\nu(\gamma_r)$$
$$\times\left[e^{in(\theta-\theta_0)}+e^{-in(\theta-\theta_0)}\right]$$

$$\therefore \phi = \frac{1}{2\pi}\left(\frac{q}{r}\right)^{\alpha}\frac{V_1}{D_E}e^{-st_0}K_\alpha(\gamma_q)I_\alpha(\gamma_r)+\frac{1}{\pi}\sum_{n=1}^{\infty}\left(\frac{q}{r}\right)^{\alpha}\frac{V_1}{D_E}e^{-st_0}.K_\nu(\gamma_q).I_\nu(\gamma_r).\cos n(\theta-\theta_0)$$

Let the average value of ϕ at a radius r from the plate centre be $\bar{\phi}$

$$\therefore \bar{\phi} = \frac{1}{2\pi}\int_0^{2\pi} \phi . d\theta.$$

$$= \frac{1}{2\pi}\left(\frac{q}{r}\right)^{\alpha} \frac{V_1}{D_E} e^{-st_0} K_\alpha(\gamma_q) I_\alpha(\gamma_r)$$

$$= \frac{1}{2\pi}\left(\frac{q}{r}\right)^{\alpha} \frac{V_1}{D_E} K_\alpha(\gamma_q) I_\alpha(\gamma_r) \quad \text{as } t_0 = 0.$$

$$= \frac{1}{2\pi}\left(\frac{q}{r}\right)^{\alpha} \frac{V_1}{D_E}\left[\frac{\left(\frac{r}{q}\right)^{\alpha}}{2\alpha} - \frac{s}{2D_E}\left\{\frac{r^{2+\alpha}}{4\alpha(1+\alpha)q^{\alpha}} - \frac{r^{\alpha}}{4q^{\alpha-2}\alpha(1-\alpha)}\right\} + \right.$$

$$\left. \frac{s^2}{2D_E^2}\left\{\frac{r^{4+\alpha}}{2^5 q^{\alpha}(2+\alpha)(1+\alpha)\alpha} + \frac{r^{2+\alpha}}{2^4 q^{\alpha-2}(1-\alpha)(\alpha)(1+\alpha)} + \frac{r^{\alpha}}{2^5 q^{\alpha-4}(2-\alpha)(1-\alpha)\alpha}\right\}\right] + 0.s^3$$

$$\therefore \bar{\phi}_{s=0} = \frac{1}{2\pi}\left(\frac{q}{r}\right)^{\alpha} \frac{V_1}{D_E} \frac{\frac{r}{a}}{2\alpha} = \int_0^{\infty} \bar{c}\, dt \quad \text{provided that } \alpha > 2$$

$$\phi_{s=0} = \frac{1}{2\pi q} \qquad \text{equation 6:2}$$

Let the radius at the point of measurement (the outlet well) be "b"

$$\therefore \left(\frac{d\bar{\phi}}{ds}\right)_{s=0} = \frac{1}{2\pi}\frac{V_1}{8D_E^2}\left[\frac{p^2}{\alpha(1+\alpha)} + \frac{q^2}{\alpha(1-\alpha)}\right] = \frac{1}{2\pi a}\frac{1}{4D_E}\left[\frac{p^2}{(1+\alpha)} + \frac{q^2}{(1-\alpha)}\right]$$

equation 6:3

$$\& \left(\frac{d^2\bar{\phi}}{ds^2}\right)_{s=0} = \frac{1}{2\pi a} \cdot \frac{1}{16D_E^2}\left[\frac{p^4}{(2+\alpha)(1+\alpha)} + \frac{2q^2p^2}{(1-\alpha)(1+\alpha)} + \frac{q^4}{(2-\alpha)(1-\alpha)}\right] \quad \text{equation 6:4.}$$

Now if σ^2 is the dimensionless variance of the time-concentration curve at the outlet well, normalized w.r.t. the mean residence time.

Then $$\sigma^2 = \left[\frac{\left(\frac{d^2\bar{\phi}}{ds^2}\right)_{s=0}}{\bar{\phi}_{s=0}} - \frac{\left(\frac{d\bar{\phi}}{ds}\right)^2_{s=0}}{\left(\bar{\phi}_{s=0}\right)^2}\right]\frac{\left(\bar{\phi}_{s=0}\right)^2}{\left(\frac{d\bar{\phi}}{ds}\right)^2_{s=0}} = \frac{\left(\frac{d^2\bar{\phi}}{ds^2}\right)_{s=0} . \bar{\phi}_{s=0}}{\left(\frac{d\phi}{ds}\right)^2_{s=0}} - 1$$

Substitution of equations 6:2, 6:3, 6:4. in the above equation gives on rearrangement:-

$$\sigma^2 = \frac{\left(\frac{q}{p}\right)^2\frac{(1+\alpha)^2}{(\alpha-2)} - \frac{(1-\alpha)^2}{(2+\alpha)}}{\left\{\left(\frac{q}{p}\right)^2(1+\alpha) + (1-\alpha)\right\}^2} \quad \text{where} \quad \alpha = \frac{qV_1}{2D_E}$$

equation 6:5

Now it can be shown that where t_m is the mean residence time

$$t_m = \frac{q^2 - p^2}{2V_1 q}$$

But the Peclet Number $$Pe = \frac{(q-p)^2}{D_E t_m} = \frac{(q-p)^2}{(q^2-p^2)}\frac{qV_1}{2D_E}.4 = 4\alpha\frac{(q-p)}{(q+p)}$$

equations 6:6 and 6:7

Calculated Values of the Variance and Peclet Number from Equations 6:5, 6:6, & 6:7, for the 30 inch Kuhni Plate.

Variance	α	Peclet No	Variance	α	Peclet No
1.1116	3	66183	0.1965	8	16.488
0.5676	4	8.244	0.1690	9	18.549
0.3831	5	10.305	0.1484	10	20.610
0.3306	5.5	11.335	0.1326	11	22.671
0.2908	6	12.366	0.1193	12	24.732
0.2593	6.5	13.396	0.1088	13	26.793
0.2341	7	14.427	0.0999	14	28.854
0.2135	7.5	15.457	0.0923	15	30.915

The above data are given graphically in Figure 86.

APPENDIX C

Oxygen Determination by the Winkler Method

The dissolved oxygen content of water was determined by the Winkler method as described in B.S. 1427;1949[115]. The method and quantities described in B.S. 1427 are suitable for oxygen contents up to 10 parts per million (p.p.m.) in water. It was found that the method required modification to deal with "Cellofas B" solutions and with oxygen concentrations up to 40 p.p.m.

(i) Theory of the Winkler Method

The water sample is collected in a special bottle and kept from direct contact with air. A sufficient quantity of manganous sulphate solution is added to the sample followed by solutions of potassium iodide and potassium hydroxide. The manganous hydroxide formed, reacts quantitatively with the dissolved oxygen precipitating brown manganic hydroxide. Excess sulphuric acid is then added where-upon the manganic valency state reverts to the stable manganous, oxidising iodide on to iodine. The iodine is titrated against standard sodium thiosulphate solution.

(ii) B.S. 1427 Method

A 250 cc. sample of the water is tested for interfering substances by acid penmanganate solution. No interfering substances were found in the water used in these tests.

A 550 cc sample of the water is collected in a sample flask (see Figure 8). 1 cc of manganous sulphate solution (480 g per litre) is added to the funnel and carefully run into the flask. The funnel is rinsed and the flask shaken. 3 cc of alkaline potassium iodide solution (700 g potassium hydroxide and 150 g potassium iodide per litre) is then added and the flask shaken and left for 2 minutes. 3 cc of sulphuric acid solution (500 cc concentrated sulphuric acid per litre) are added and the flask shaken till the precipitate dissolves.

The solution can now be exposed to air and duplicate 200 cc samples titrated against standard N/40 sodium thiosulphate solution using starch as indicator. The sodium thiosulphate solution was standardised against standard potassium iodate solution.

(iii) Modifications for concentrations up to 40 p.p.m.

The high concentrations of dissolved oxygen obtained in the oxygen desorption tests necessitated the use of larger quantities of reagents. The reagents added were those given below.

2 cc manganous sulphate solution, (480 g per litre),

1 cc potassium iodide solution, (500 g per litre),

5 cc alkaline potassium iodide solution (700 g potassium hydroxide and 150 g potassium iodide per litre),

5 cc sulphuric acid solution (500 cc conc sulphuric acid per litre).

The final titrations were done as in (ii)

(iv) Modifications in the presence of "Cellofas B"

In the Winkler method the final titration is done in acid solution. In acid solutions "Cellofas B" appears to catalyse the reaction,

$$O_2 + 2I^- + H_2O \rightarrow I_2 + 2OH^-$$

Thus oxygen dissolving in the solution during titration oxidises iodide to iodine. This reaction does not take place in alkaline solution but in such solutions the iodine tends to complex with potassium iodide and the titration is inaccurate. Various methods of overcoming this difficulty were tried including precipitation of the "Cellofas B" and shielding the solution from the atmosphere. It was decided that the best method is to do the titration at a pH of 8, in a bufferred solution of sodium bicarbonate having previously partially neutralised the solution with potassium hydroxide and sodium carbonate.

The modified reagents were added in the order given below.

2 cc of manganous sulphate solution (480 g per litre)

1 cc of potassium iodide solution (500 g per litre)

5 cc of alkaline potassium iodide solution (400 g potassium hydroxide and 400 g potassium iodide per litre)

5 cc of sulphuric acid solution (300 cc conc. sulphuric acid per litre)

1 cc of saturated potassium hydroxide solution (810 g per litre)

5 cc of saturated sodium carbonate solution (200 g per litre)

5 cc of saturated sodium bicarbonate solution (100 g per litre)

The final titrations were done as in Section (ii).

APPENDIX D

The Properties of Solutions of "Cellofas B" (Medium Grade) in Water

Cellofas B the sodium salt of carboxy methyl cellulose is an I.C.I. product used mainly in the paper industry and which is available in four viscosity grades, "Low", "Medium", "High" and "Extra High" Viscosity. To obtain a 100 cP solution in water the concentrations required are, 3%, 1.5%, 0.6% and 0.2% respectively. The "Medium" viscosity grade was used in this work, and since little reliable data were available on the physical properties of "Cellofas B" solutions the following properties were studied.

(i) Density of Cellofas B solutions in Water.

The density of Cellofas B solutions varies linearly with concentration up to a 1% solution. A 1% solution at 15°C has a density of 1.00356, (water is 0.99862), an increase of 0.5%. The data are shown graphically in Figure 87.

(ii) Lowering of Vapour Pressure

This effect, of importance, in humidification tests, was examined by measuring the freezing point depression of 0.1% and 1.0% solutions. The respective depressions were 0.093 °C and 0.135 °C which correspond to a lowering in water vapour pressure of 0.09% and 0.13%. This effect is thus so small as to be negligible.

(iii) Viscosity

A graph of viscosity against concentration is given in Figure 87. Viscosities were determined by standard Ostwald viscometers at 15°C in a thermostatic tank using the procedure described in B.S. 188(1957)[120].

(iv) Oxygen Solubility

The solubility data of oxygen in water were obtained from International Critical Tables[114] but no data were available on the solubility of oxygen in solutions of "Cellofas B." A knowledge of the solubility of oxygen in these solutions was necessary for both the oxygen desorption efficiency determinations and the oxygen diffusivity measurements. Some tests were done, bubbling humidified air through "Cellofas B" solutions under thermostatic conditions and these tests revealed no difference in oxygen solubility between water and "Cellofas B" solutions of 0.6% concentration, (18 cP)

It was decided that more accurate determinations could be made using pure oxygen instead of air, the dissolved oxygen concentrations being higher than for air. Humidified oxygen was passed through de-aerated water and 0.6% solutions of "Cellofas" B for 24 hours at 20°C. The solutions were analysed for dissolved oxygen by the Winkler method and no significant difference in dissolved oxygen concentration was found. This procedure of treating samples of water and "Cellofas B" solutions under identical conditions is advisable since the effect of changing atmospheric pressure on the system can be neglected.

It can be concluded, therefore, that the solubility of oxygen in "Cellofas B" solutions is not detectably different from the solubility in water.

(v) Oxygen Diffusivity

As discussed in Section 2;6, it was decided to determine the diffusivity of oxygen in Cellofas B solutions using the method of Davidson and Cullen[62].

(a) Theory

From a consideration of the fluid mechanics of flow over a sphere of radius R it can be shown that it is equivalent, in gas absorption, to a cylindrical wetted wall of height 1.68 R. The solutions by Pigford[124] and Vyazovov[125] of the absorption equations for a cylindrical wetted wall are used. Two solutions are possible, the simpler being applicable when the outlet liquid concentration is less than 40% of the saturation value, the other being applicable at greater approaches to saturation. The equations are given below.

(i) For outlet concentrations less than 40% saturation

$$G_d = (12 \times 1.68)^{1/2} (2\pi g/3\nu)^{1/6} (\bar{D}_G)^{1/2} L_d^{1/3} R^{7/6} (\bar{C}_e - \bar{C}_l) \qquad (6;8)$$

(ii) For outlet concentrations greater than 40% saturation

$$G_d = L_d(\bar{C}_e - \bar{C}_l) (1 - 0.786 \exp(-3.414\beta) - 0.100 \exp(-26.21\beta) - .035 \exp(-70.43\beta) - 0.018 \exp(-136.5\beta)) \qquad (6;9)$$

$$\text{where } \beta = 2 \times 1.68 \frac{(2\pi g)}{(3\nu)}^{1/3} \frac{\bar{D}_G R^{7/3}}{L_d^{4/3}} \qquad (6;10)$$

G_d = corrected gas absorption rate (g./sec.)

g = acceleration due to gravity (cm/sec.^{2})

ν = kinematic viscosity of the liquid (cm^2/sec.)

$\bar{D}_G$ = diffusivity of gas (cm^2/sec.)

L_d = liquid flow rate (cm^3/sec.)

R = radius of sphere (cm)

$\bar{C}_e$ = saturation concentration of the gas (gm/cm^3)

$\bar{C}_1$ = inlet concentration of the gas (gm/cm^3)

(b) Apparatus

Drawings of the apparatus are given in Figure 88.

A controlled flow of oxygen-free water was passed over the surface of a 1.498 inch diameter sphere (table-tennis ball) mounted vertically on a 1/8 inch diameter stainless steel rod in a Perspex absorption chamber. Oxygen was fed to the chamber at a rate exactly sufficient to maintain the pressure in the chamber constant, oxygen input being balanced by absorption.

The absorption chamber was thermostaticallycontrolled at 20°C. Water flowed into the top of the chamber past a thermometer(±0.1°C) and through the distributor block which also served to align the rod. The sphere was mounted 3 cm from the base of the distributor block and 1.5 cm. above the level of the water in the take-off tube. This level was maintained by a constant level device. Oxygen-free water was obtained by repeatedly spraying hot water into a vacuum. It was stored in an overhead tank, a plastic sheet floating on the surface preventing absorption of oxygen from the atmosphere. The water was metered by a "Rotameter" reading to 30 litres per hour and passed through copper coils immersed in a thermostatic bath before entering the absorption chamber.

Oxygen from a cylinder passed through regulating valves, a soap film meter and a copper tube packed with copper gauze, to bring the temperature to 20°C, before entering the absorption chamber. An inclined

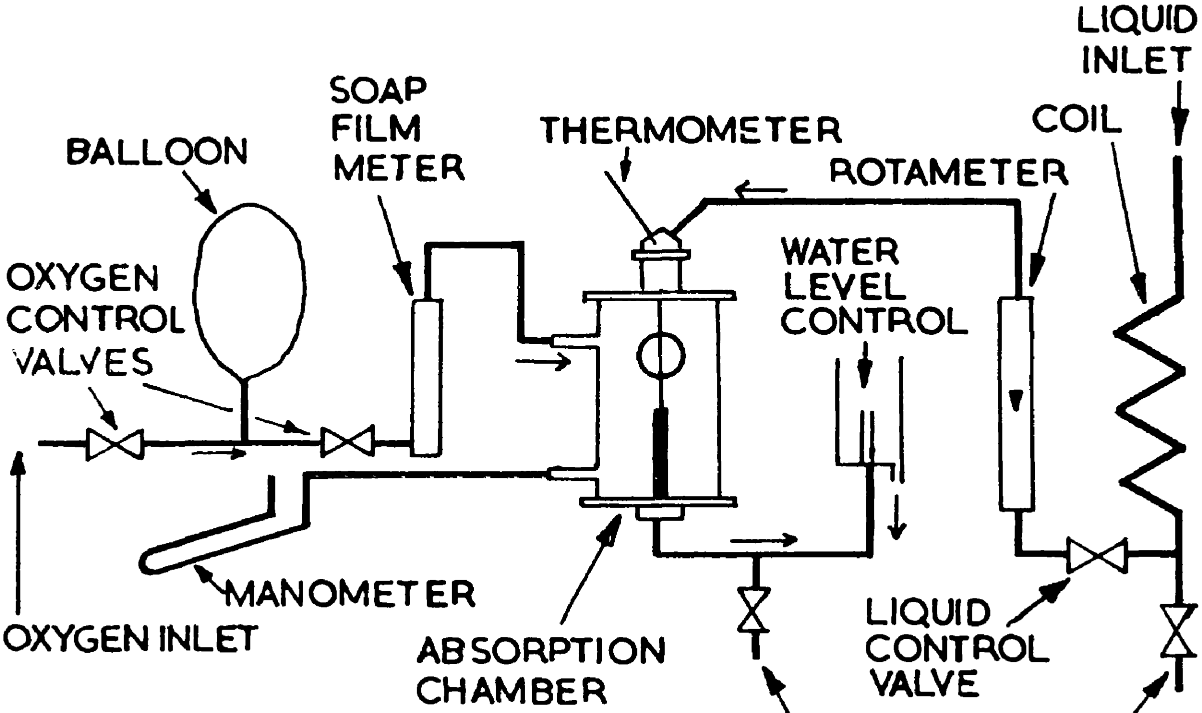
LIQUID INLET
SOAP FILM METER
BALLOON
THERMOMETER
COIL
ROTAMETER
WATER LEVEL CONTROL
OXYGEN CONTROL VALVES
MANOMETER
OXYGEN INLET
ABSORPTION CHAMBER
LIQUID CONTROL VALVE
SAMPLE POINTS

FLOW SHEET

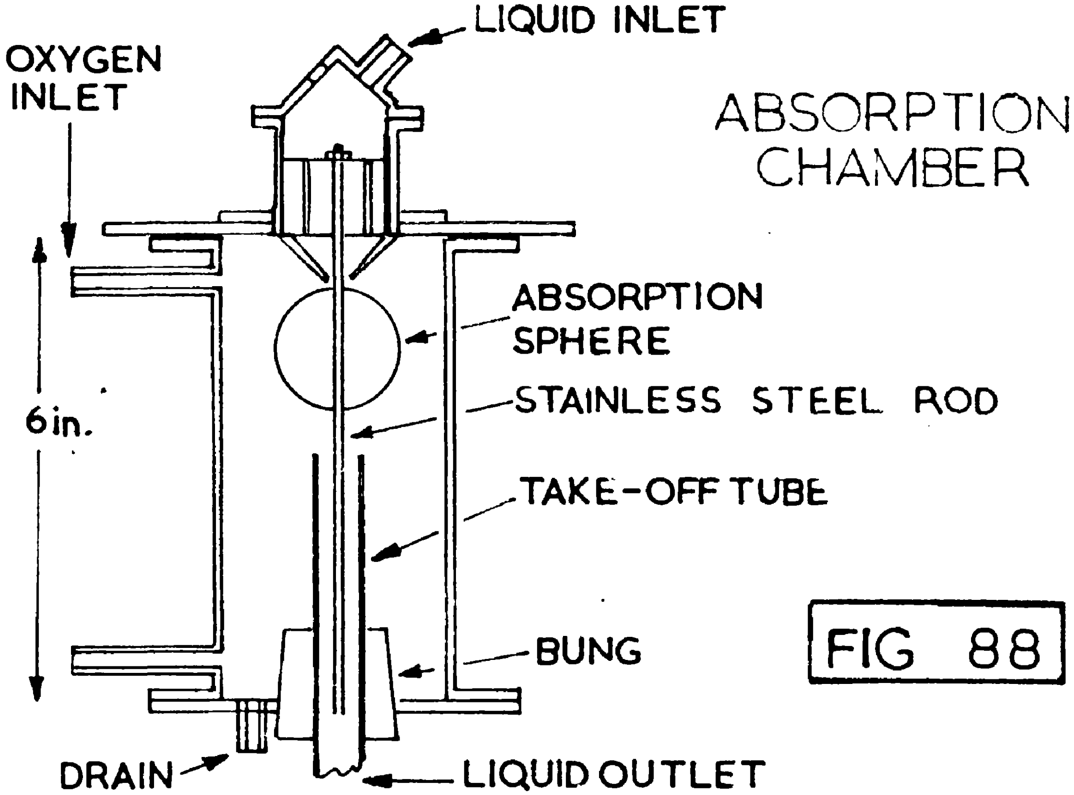
ABSORPTION CHAMBER

LIQUID INLET
OXYGEN INLET
ABSORPTION SPHERE
STAINLESS STEEL ROD
6 in.
TAKE-OFF TUBE
BUNG
DRAIN
LIQUID OUTLET

FIG 88

OXYGEN DIFFUSIVITY APPARATUS

manometer indicated the pressure inside the chamber and an outlet tap was provided for purging the chamber of nitrogen.

(c) Experimental Procedure

The thermostatic box, containing the absorption chamber, and the tank containing the water-temperature controlling coils were adjusted to 20°C and maintained at that temperature. By passing a current of oxygen through the absorption chamber any traces of nitrogen were removed.

Water flow over the sphere was started and adjusted to the required rate, care being taken to ascertain that the whole sphere was wetted. The water level in the take-off tube was adjusted to the required height.

Oxygen was passed into the chamber and its rate adjusted by trial and error till the pressure inside the chamber, as indicated on the inclined manometer, remained constant. When steady conditions had been achieved the oxygen flowrate was measured by the soap film meter. The barometric pressure was noted.

Winkler oxygen analyses were done on the inlet water before and after the test run.

A specimen calculation is given in Part (e) of this Appendix.

(d) Results and Conclusions

Fifty two determinations of the absorption rate of oxygen in "Cellofas B" solutions, of viscosities ranging from 1 to 16 cP, were done using the apparatus and procedure described earlier.

To compare the absorption rate and determine the effect of "Cellofas B" concentration on the oxygen diffusivity two corrections were made to the observed absorption rate.

(i) The absorption rate was corrected to an oxygen partial pressure of 760 mm Hg, thus eliminating any variation due to atmospheric pressure.

(ii) The absorption rate is inversely proportional to the sixth root of the liquid kinematic viscosity because of the effect of viscosity on the flow over the sphere. Each absorption rate was thus multiplied by the sixth root of the viscosity to correct all absorption rates to that at 1 cS.

The tests in part (iv) of this Appendix showed that the solubility of oxygen in Cellofas B solution of the concentrations under discussion is constant and equal to the solubility in water. Sources of variation in absorption rate due to pressure, fluid dynamics and solubility have therefore been removed and any remaining variation in absorption rate must be attributable to a change in diffusivity.

The resultant data are shown in Figure 89, each viscosity being denoted by a different symbol. The line drawn through the data is the best line for water. Deviations in absorption rate were measured for each point and summed for each viscosity level and for the whole series. The deviations were summed both by taking the sign of the deviation into account and by neglecting the sign. The mean deviations were deduced and are presented in the table below.

FIG 89

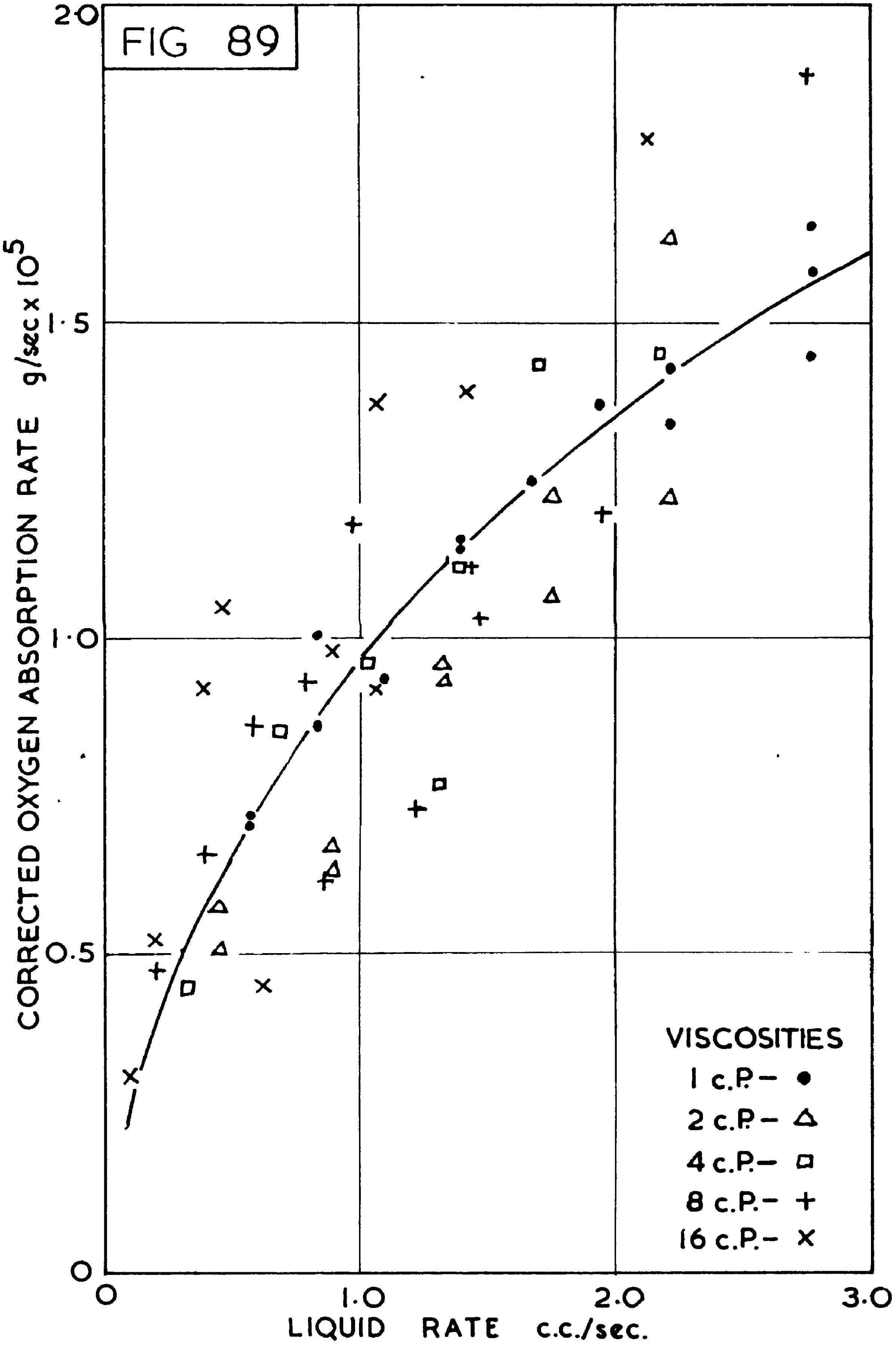

OXYGEN DIFFUSIVITY TESTS

Viscosity level	Number of tests	Mean deviation "including sign"	Mean deviation "excluding sign"
1 c.S	14	+ 0.001x10^{-5} g/sec.	0.043x10^{-5} g/sec.
2 c.S	10	- 0.126 "	0.172 "
4 c.S	7	- 0.065 "	0.148 "
8 c.S	11	- 0.008 "	0.174 "
16 c.S	10	+ 0.171 "	0.249 "
Total	52	+ 0.002 "	0.149 "

Consideration of Figure 89 and of the above table shows that the experimental accuracy is poor, the mean error being about 12%. Davidson and Cullen claim an accuracy of ± 5% for the method, but their apparatus and procedure were more refined. The probable reasons for the difference in accuracy are listed below.

(a) The de-aerated water in this work had an air content of 4 p.p.m. which was found to be constant since all the de-aerated water was prepared under identical conditions. Davidson and Cullen used water with an air content of about 0.5 p.p.m. The effect of using the water with 4 p.p.m. of air is that the dissolved nitrogen desorbs into the pure oxygen atmosphere and tends to reduce the partial pressure of the oxygen especially in the vicinity of the interface. This was partly obviated by purging between tests.

(b) Great difficulty was experienced in controlling the oxygen flow at such low flow rates, i.e. 0.01 cc/sec.

(c) Occasionally a dry spot formed on the sphere and this was difficult to detect.

Although the data are fairly scattered they are sufficiently accurate to permit the conclusion to be drawn that the addition of "Cellofas B" to water has a negligible effect on oxygen diffusivity within the range of concentrations used. Certainly it is very unlikely that the diffusivity changes by more than 10%. To have obtained data of accuracy equivalent to that of Davidson and Cullen it would have been necessary to spend a considerable length of time on the tests and it was felt that this was not justified.

It may be at first surprising that a sixteen fold change in viscosity produces no detectable change in diffusivity, since these two properties are normally closely related. The diffusion characteristics of dissolved material in liquids of high viscosity due to a "gelling" agent are, however, quite different from the characteristics in a liquid of naturally high viscosity such as a heavy oil. Stiles and Adair[126] observed that the diffusivity of electrolyte in a 2% gel of gelatin in water is only 4% less than the diffusivity in water. Since "Cellofas B" is a viscosity-increasing agent of the same type as gelatin, the independence of the diffusivity from viscosity is not really surprising.

Summarising the conclusions from this work, it has been shown that the diffusivity of oxygen in solutions of "Cellofas B" up to a viscosity of 16 c.S may be taken as constant and equal to the diffusivity in water. This is in accord with other observations of diffusion in "gelled" liquids.

(e) Specimen Calculation

Run No.16

Run Data -

Viscosity of solution	2.09 c.S
Barometric Pressure	759.0 mm Hg
Soap film meter reading	33.0 sec
Liquid rate	1.762 cc/sec.
Temperature	20 °C
Water vapour pressure	17.5 mm

Partial pressure of oxygen in absorption chamber = 759.0 - 17.5

= 741.5 mm Hg

Volume of soap film meter = 0.2682 cc

$$\therefore \text{ Flow rate } = \frac{0.2682}{33.0} = 8.127 \times 10^{-3} \text{ cc/sec}$$

Density of oxygen at 759 mm Hg and 20°C = 0.001297 g./cc

$\therefore$ Mass flow rate of oxygen = 1.055×10^{-5} g./sec

$$\therefore \text{ Absorption rate connected to 760 mm } = 1.055 \times 10^{-5} \times \frac{760}{741.5}$$

$$= 1.081 \times 10^{-5} \text{ g./sec.}$$

Viscosity ν = 2.09 c.S $\therefore \nu^{\frac{1}{6}} = 1.131$

$\therefore$ Absorption rate corrected to 1 c.S $= 1.131 \times 1.081 \times 10^{-5}$

$= 1.222 \times 10^{-5}$ g./sec.

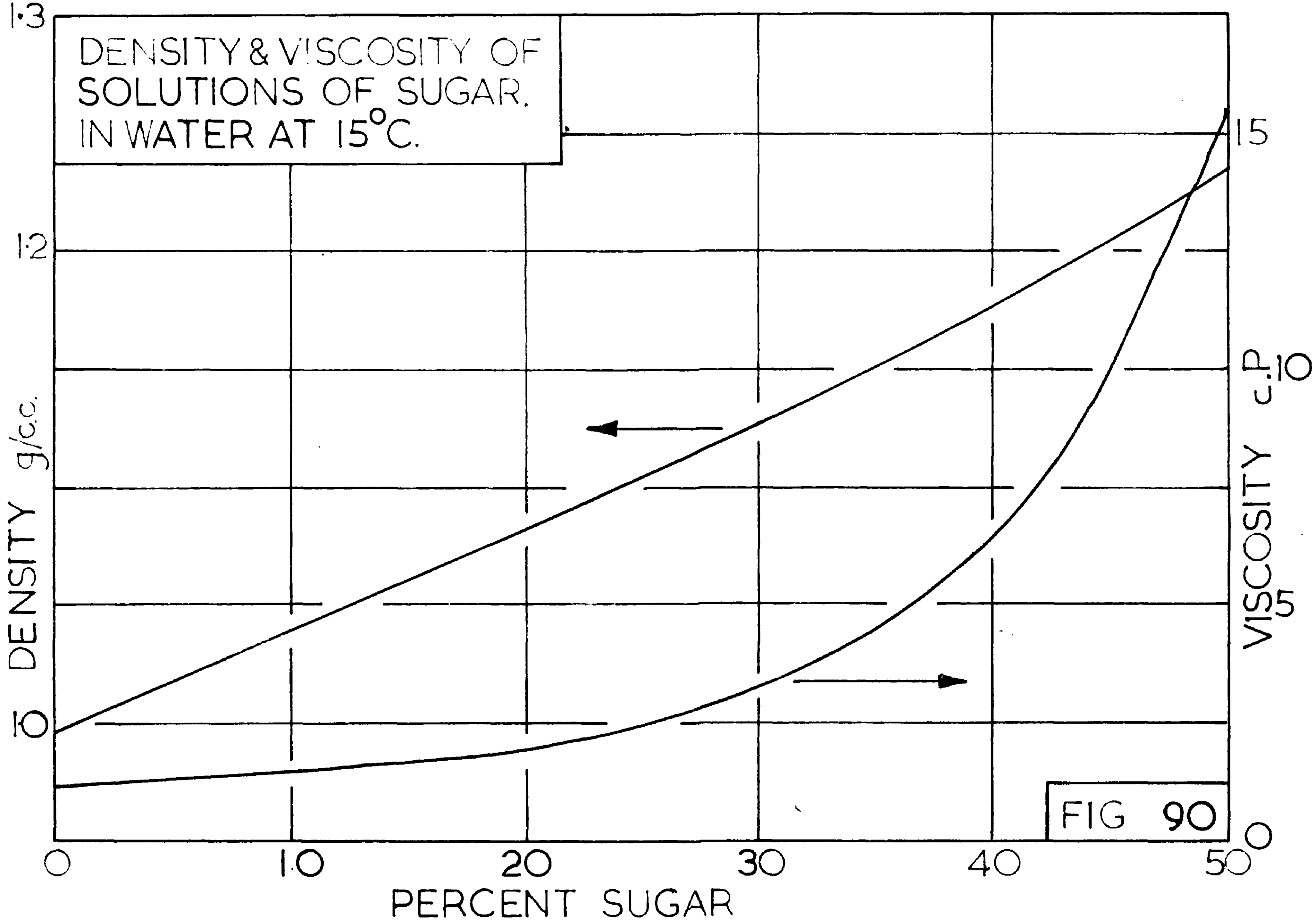

DENSITY & VISCOSITY OF SOLUTIONS OF SUGAR. IN WATER AT 15°C.

FIG 90

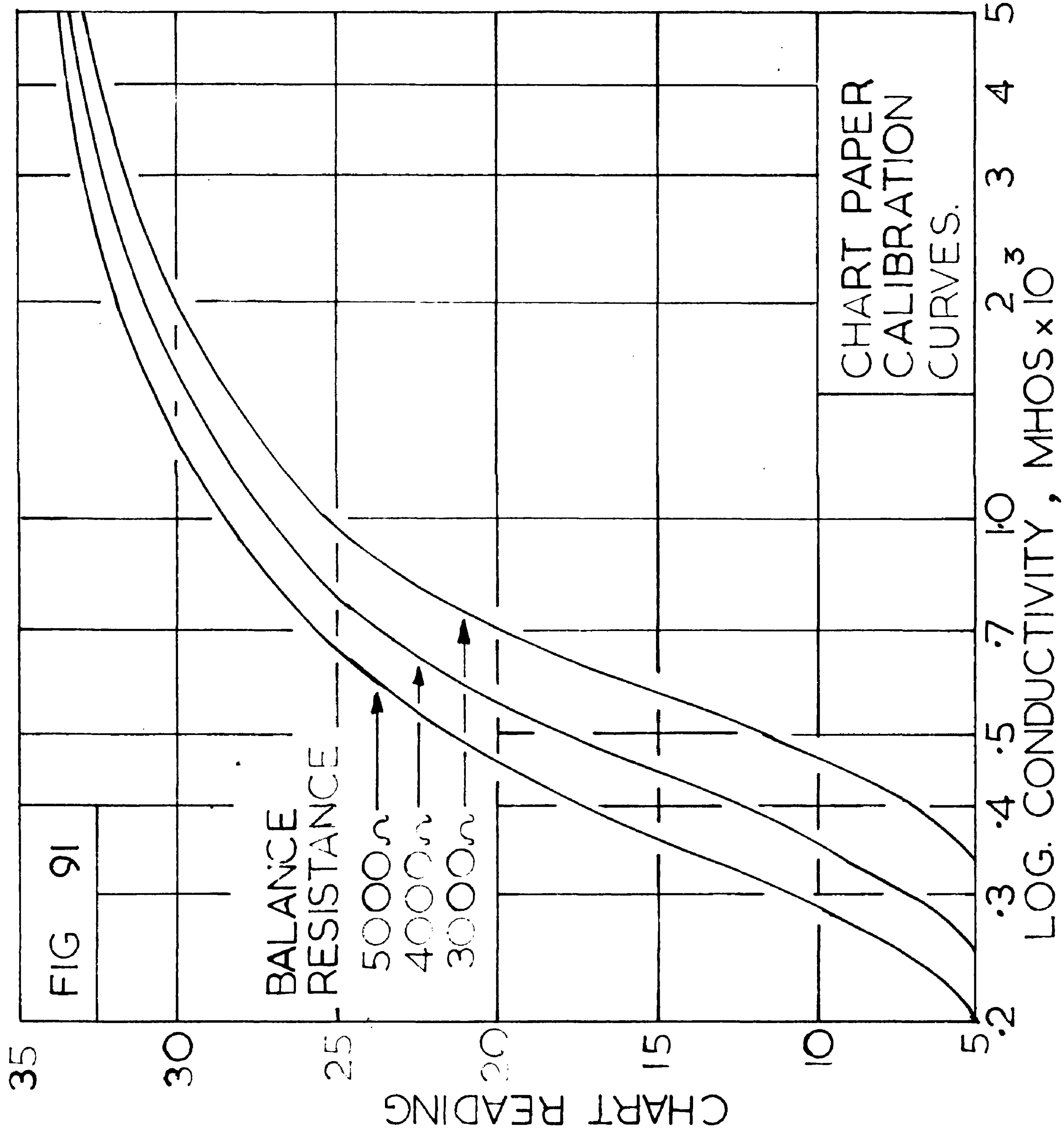

FIG 91

CHART PAPER CALIBRATION CURVES.

APPENDIX G

Maximum Probable Errors

(1) Humidification Efficiency by Outlet Hygrometer Method

The efficiency is deduced entirely from temperature measurements. All the thermometers used were checked and found to be accurate to within 0.1 °F. The sum of errors in calibration and errors in reading should never exceed 0.15 °F. Conversion of temperatures to saturation humidities should introduce no additional error as the graph could be read easily to 0.05 °F. An error of 0.15 °F is equivalent to an average humidity error of 0.33 grains per lb on the saturation humidity graph. Humidities were deduced from the equation.

$$H = H_s - 1.72\,(Tw - Td) \qquad (2;3)$$

Error in H_s = 0.33 gr/lb

Tw and Td = 0.15 °F each = 0.30 °F total

$\therefore$ Maximum error $= 0.33 + 1.72 \times 0.03 = 0.84$ gr/lb

The efficiency E_{MV} was found from the equation $H_2 - H_1/H_e - H_1$

Thus the maximum error in $H_e - H_1$ is $0.84 + 0.33 = 1.17$ gr/lb

or 5%

Since H_1 appears in the numerator and denominator, and the error in it acts in the same direction in both, the errors can not be added in the usual manner since this would indicate an oversensitivity of E_{MV} on H_1. The error in a group of the form $A + \Delta/B + \Delta$ where the error "Δ" is added or subtracted in both numerator and denominator can be shown to be

$$\Delta(B - A)/B^2$$

The error in A is the error in H_2 i.e. 0.84 gr/lb while the error in B is the error in H_e i.e. 0.33 gr/lb. The total error in the ratio A/B is thus

$$0.84/A \quad + \quad 0.33/B \quad + \quad 0.84\ (B - A)B^2\ \text{gr/lb}$$

Taking typical values of A and B as 27 and 30 respectively the total maximum probable error is

$$.031 \quad + \quad .011 \quad + \quad 0.003 \quad = \quad .045 \quad \text{or} \quad \underline{4.5\%}$$

Since the number of sources of error is 6 the probable error will be approximately $4.5/\sqrt{6} = \underline{1.9}\%$.

(ii) Humidification Efficiency by Solution Evaporation

The measured quantities which contribute an error to the efficiency are listed below with the maximum probable error in measurement.

Weight of Solution	(about 50 lb.)	± .05 lb.	0.1%
Titrations	(about 30 cc)	± .1 cc	0.3%
Gas rate		± 3%	
Temperatures		± 0.15°F	

The error in the gas rate is a 2% tolerance in the orifice plate (B.S.1042) and a 1% error in the square root of the pressure differential.

$$\text{Entrainment} = W_1 C_1 - W_2 C_2 \Big/ \frac{C_1 + C_2}{2}$$

$$= 1500 \pm 6.0 - 1400 \pm 5.6 \big/ 30 \pm 0.1$$

$$= 100 \pm 11.6/30 \pm 0.3\%$$

$$= 3 \pm 11.9\%$$

Thus owing to the nature of the subtraction $W_1 C_1 - W_2 C_2$ the maximum probable in the entrainment is approximately 12%.

$$\text{Evaporation} = 20 \text{ lb.} \pm 0.10 \text{ lb.} - 3 \text{ lb} \pm 0.36 \text{ lb.}$$

$$= 17 \text{ lb} \pm 0.46 \text{ lb. or } 2.7\%$$

Assuming that time is measured exactly and that the gas rate is accurate to 3% then the increase in humidity calculated by dividing the evaporation by the gas rate has a maximum probable error of 5.7%

$H_e - H_1$ has been shown (Section (i)) to be accurate to 5%

The total maximum probable error is thus 10.7%.

Since there are 9 sources of error, the probable error is approximately

$$10.7/\sqrt{9} = 3.6\%$$

(iii) Oxygen Desorption Efficiency

The equation used to calculate E_{ML} given below contains two terms (X_1 and X_2) deduced from titrations and one (X_e) deduced from temperature and pressure measurements.

$$E_{ML} = (X_1 - X_2)/(X_1 - X_e)$$

The errors in X_1 and X_2 are derived from :-

Titration error, .03 cc in 10 cc to 0.1 cc in 40 cc, i.e. 0.3%,

standard solution normality error - not more than 0.1%,

errors in measuring solution volumes and introducing dissolved oxygen in reagents, - less than 0.5%.

Thus the total error in X_1 or X_2 will be 0.3 + 0.1 + 0.5 = 0.9%

This is equivalent to .36 p.p.m. in an X_1 of 40 p.p.m.

The accuracy of temperature measurement is greater than 0.1 °C which corresponds to a change in Henry's Law Constant of 0.22% The barometric pressure and water vapour pressure were known to 0.1 mm Hg in 760 mm Hg i.e. 0.013%. Thus the maximum error in X_e is 0.24% or .024 p.p.m. in 10 p.p.m.

Again the occurrence of X_1 in both numerator and denominator gives rise to the use of the relationship used in Section (i).

The total error in E_{ML} is thus 0.90% + 0.24% + $.36(B - A)/B^2$ taking typical values of A and B as 27 and 30 p.p.m. the total error is 0.90 + 0.24 + 0.0012 = 1.15%.

There are 5 main sources of error thus the probable error will be approximately $1.15/\sqrt{5}$ = 0.52%.

It should be noted that no allowance has been made for unrepresentative sampling, since this error is almost impossible to estimate.

TABULATED RESULTS.

(i) Humidification Tests using the Solution Evaporation Method, (30 inch plate)

Test No	Water rate L_M	Air rate G_M	Humidities inlet H_1	outlet H_2	equil^m H_e	Efficy. $E_{MV}\%$	Entrainment lb/1000 lb air.
A1	1000	307	52.1	76.8	82.3	81.7	0.522
A2	1000	217	56.7	82.0	85.8	87.0	0.285
A3	1000	124	55.8	80.3	81.2	96.2	0.025
A4	500	312	51.5	75.6	80.6	83.0	0.466
A5	500	217	58.0	79.8	84.3	82.9	0.353
A6	500	122	57.5	81.1	84.1	88.5	0.060
A7	200	314	50.2	79.9	89.4	75.6	0.417
A8	200	215	53.7	82.1	88.1	82.6	0.209
A9	200	126	49.5	83.9	90.3	84.4	0.184
A10	100	315	47.9	79.7	90.7	74.3	0.603
A11	100	214	51.4	79.2	87.4	77.4	0.300
A12	100	126	53.2	81.5	86.1	85.9	0.148

(ii) Humidification Tests using the Outlet Psychrometer Method, (30 inch plate)

Test No	Water rate L_M	Air rate G_M	Humidities inlet H_1	outlet H_2	equil^m H_e	Effcy $E_{MV}\%$	NTU$_G$ N_G	K_Ga
B1	1000	313	57.2	76.0	80.5	80.8	1.65	6870
B2	1000	302	61.1	78.3	82.3	80.9	1.66	6670
B3	1000	277	56.4	74.8	78.7	82.7	1.75	6450
B4	1000	244	58.4	78.1	81.8	84.1	1.84	5970
B5	1000	212	57.9	77.1	80.3	86.2	1.98	5580
B6	1000	183	53.7	83.4	87.1	88.9	2.20	5350
B7	1000	154	47.4	78.0	81.4	89.7	2.27	4650
B8	1000	132	44.0	72.3	75.2	90.5	2.35	4130
B9	1000	108	51.6	83.0	85.9	91.7	2.49	3580
B10	1000	104	42.0	73.5	76.0	92.7	2.62	3620
B11	1000	92	41.8	74.0	76.4	93.1	2.67	3270
B12	1000	85	42.4	74.6	77.1	92.7	2.62	2960
B13	1000	75	42.7	75.3	77.6	93.3	2.70	2690
B14	1000	61	42.6	76.0	78.3	93.5	2.73	2210
B15	1000	58	41.9	75.9	78.5	92.9	2.64	2040
B16	500	315	52.4	72.7	78.3	78.3	1.53	6410
B17	500	300	51.1	72.1	77.8	78.5	1.54	6140
B18	500	269	54.2	76.1	80.1	80.5	1.63	5830
B19	500	246	58.5	77.6	81.9	81.5	1.69	5530
B20	500	213	57.2	77.4	81.3	83.7	1.81	5130
B21	500	185	53.1	82.0	86.6	86.5	2.00	4920
B22	500	156	48.1	77.4	81.5	87.9	2.12	4400
B23	500	132	44.4	72.7	76.2	89.1	2.22	3870
B24	500	108	51.4	82.9	86.5	89.7	2.27	3260
B25	500	105	48.4	69.1	71.6	89.3	2.23	3110
B26	500	94	49.4	70.4	72.9	89.4	2.24	2800
B27	500	85	51.6	71.8	74.3	89.1	2.22	2510
B28	500	73	52.8	73.1	75.9	88.1	2.13	2070
B29	500	63	53.3	75.0	77.8	88.7	2.18	1830

(ii) continued.

Test No	L_M	G_M	H_1	H_2	H_e	E_{MV}	N_G	K_Ga
B30	200	319	61.5	77.2	82.1	76.2	1.44	6110
B31	200	302	61.1	76.5	81.1	76.9	1.46	5860
B32	200	285	59.1	74.1	78.6	76.7	1.46	5530
B33	200	263	59.2	73.5	77.4	78.5	1.54	5390
B34	200	247	58.5	77.4	82.0	80.5	1.63	5350
B35	200	215	55.3	75.5	80.3	81.0	1.66	4750
B36	200	187	52.9	80.5	85.9	83.5	1.80	4480
B37	200	158	47.9	76.3	81.5	84.7	1.88	3950
B38	200	133	44.9	73.6	78.6	85.3	1.92	3400
B39	200	110	51.2	82.8	87.5	87.2	2.06	3010
B40	200	106	60.9	83.8	86.9	87.8	2.10	2960
B41	200	97	59.7	82.5	85.8	87.3	2.06	2660
B42	200	80	59.2	81.3	84.5	87.4	2.07	2200
B43	100	318	56.1	76.3	83.2	74.6	1.37	5790
B44	100	304	56.8	77.1	84.2	74.0	1.35	5460
B45	100	271	55.9	75.6	81.7	76.2	1.44	5190
B46	100	248	55.8	75.0	80.8	76.8	1.46	4820
B47	100	215	55.7	75.5	81.0	78.3	1.53	4380
B48	100	188	52.3	79.3	86.1	79.7	1.60	4000
B49	100	158	48.3	75.8	82.0	81.8	1.70	3570
B50	100	134	45.5	74.0	80.1	82.5	1.74	3100
B51	100	110	51.2	83.1	88.0	86.5	2.00	2930
B52	100	104	56.9	78.5	81.8	86.7	2.02	2790
B53	100	98	57.8	79.2	82.7	85.8	1.95	2540
B54	100	81	59.2	80.5	83.9	86.1	1.98	2130

(iii) Plate pressure drop, froth height and clear liquid height(30in.Plate)

L_M	G_M	P.D.(ins)	F.H.(ins)	C.L.H.(mean),(ins)
100	300	3.08	1.60	0.25
100	250	2.30	1.60	0.27
100	200	1.82	1.60	0.35
100	150	1.58	1.60	0.53
100	100	1.32	1.50	0.68
250	300	3.10	1.70	0.30
250	250	2.35	1.70	0.30
250	200	1.88	1.70	0.37
250	150	1.63	1.70	0.55
250	100	1.42	1.70	0.71
500	300	3.15	1.80	0.33
500	250	2.38	1.80	0.34
500	200	1.92	1.80	0.44
500	150	1.70	1.80	0.61
500	100	1.48	1.70	0.73
1000	300	3.22	2.00	0.43
1000	250	2.47	2.00	0.43
1000	200	2.00	2.00	0.53
1000	150	1.79	2.00	0.73
1000	100	1.62	1.90	0.93

(iv) Humidification tests using viscous solutions (30in plate)

Water rate L_M	Air rate G_M	Test No	Viscosity 2cP			Test No	Viscosity 4cP		
			E_{MV}	N_G	K_Ga		E_{MV}	N_G	K_Ga
1000	300	C1	83.3	1.79	7140	C21	88.8	2.19	8740
1000	250	C2	85.7	1.94	6450	C22	90.6	2.36	7850
1000	200	C3	89.2	2.23	5930	C23	91.3	2.44	6490
1000	150	C4	92.8	2.63	5250	C24	93.0	2.66	5310
1000	100	C5	94.0	2.81	3740	C25	96.1	3.24	4310
500	300	C6	79.0	1.56	6220	C26	85.1	1.90	7580
500	250	C7	82.5	1.74	5780	C27	85.9	1.96	6520
500	200	C8	87.9	2.11	5610	C28	90.5	2.35	6250
500	150	C9	90.3	2.33	4650	C29	92.7	2.62	5230
500	100	C10	91.6	2.48	3300	C30	94.1	2.83	3760
200	300	C11	77.6	1.50	6000	C31	83.0	1.77	7060
200	250	C12	80.1	1.62	5390	C32	82.5	1.74	5780
200	200	C13	85.6	1.94	5160	C33	88.5	2.16	5750
200	150	C14	88.9	2.20	4390	C34	90.2	2.32	4630
200	100	C15	89.3	2.23	2970	C35	92.7	2.62	3480
100	300	C16	75.1	1.39	5550	C36	80.2	1.62	6460
100	250	C17	78.7	1.55	5150	C37	82.3	1.73	5750
100	200	C18	82.2	1.73	4600	C38	84.2	1.84	4890
100	150	C19	85.5	1.93	3850	C39	87.8	2.10	4190
100	100	C20	85.7	1.94	2580	C40	90.9	2.40	3190

Water rate L_M	Air rate G_M	Test No	Viscosity 8cP			Test No	Viscosity 16cP		
			E_{MV}	N_G	K_Ga		E_{MV}	N_G	K_Ga
1000	300	C41	91.9	2.51	10010	C61	79.7	1.59	6340
1000	250	C42	93.0	2.66	8840	C62	82.9	1.77	5890
1000	200	C43	94.6	2.92	7770	C63	87.6	2.09	5560
1000	150	C44	95.9	3.20	6380	C64	89.1	2.22	4430
1000	100	C45	98.8	4.42	5880	C65	89.1	2.22	2950
500	300	C46	89.1	2.22	8860	C66	78.3	1.53	6100
500	250	C47	92.7	2.62	8710	C67	80.3	1.62	5390
500	200	C48	93.7	2.76	7340	C68	82.5	1.74	4630
500	150	C49	94.6	2.92	5830	C69	85.7	1.94	3870
500	100	C50	97.6	3.73	4960	C70	86.0	1.97	2620
200	300	C51	87.6	2.09	8340	C71	74.6	1.37	5470
200	250	C52	90.3	2.33	7750	C72	77.7	1.50	4990
200	200	C53	92.9	2.65	7050	C73	80.0	1.61	4280
200	150	C54	93.4	2.72	5430	C74	83.3	1.79	3570
200	100	C55	94.6	2.92	3880	C75	84.9	1.89	2510
100	300	C56	85.2	1.91	7620	C76	72.2	1.28	5110
100	250	C57	88.1	2.13	7080	C77	75.1	1.39	4620
100	200	C58	88.8	2.19	5820	C78	77.1	1.49	3930
100	150	C59	91.1	2.42	4830	C79	80.1	1.66	3310
100	100	C60	91.7	2.49	3310	C80	84.8	1.88	2500

(v) Oxygen desorption tests (30 inch plate).

Test No	Water rate	Air rate	Oxygen contents inlet	outlet	equib.	Efficy.	NTU	
	L_M	G_M	X_1	X_2	X_e	E_{ML}	N_L	$K_L a$
D1	100	310	47.9	10.9	9.7	96.8	4.35	6.97
D2	100	300	45.8	11.0	9.7	96.2	4.15	6.64
D3	100	250	45.4	11.2	9.6	95.4	3.80	6.08
D4	100	200	43.7	11.0	9.5	95.6	3.88	6.22
D5	100	150	42.2	10.8	9.4	95.7	3.91	6.26
D6	100	100	41.2	10.8	9.3	95.5	3.90	6.25
D7	100	76	39.1	10.6	9.2	95.4	3.87	6.20
D8	100	52	37.7	10.9	9.2	94.1	3.53	5.65
D9	200	310	45.8	11.5	10.0	96.1	4.04	12.9
D10	200	300	43.7	11.7	10.0	95.0	3.68	11.8
D11	200	250	42.9	11.5	10.0	95.4	3.72	11.9
D12	200	200	41.0	11.5	9.9	94.8	3.50	11.2
D13	200	150	39.0	11.2	9.8	95.3	3.65	11.7
D14	200	100	36.2	11.3	9.7	94.0	3.35	10.7
D15	200	75	34.8	12.0	9.6	90.7	2.79	8.94
D16	500	315	38.1	11.6	10.1	94.7	3.61	28.9
D17	500	300	41.1	11.4	10.2	96.1	4.01	32.1
D18	500	250	36.8	11.8	10.2	94.0	3.29	26.4
D19	500	200	32.5	11.8	10.2	93.0	3.01	24.1
D20	500	150	25.5	11.7	10.0	89.0	2.44	19.5
D21	500	100	23.8	12.3	9.9	82.5	1.93	15.5
D22	500	53	22.4	13.0	9.8	74.4	1.50	12.0
D23	750	314	44.8	12.3	10.2	93.9	3.38	40.6
D24	750	300	38.5	12.0	10.2	93.8	3.30	39.7
D25	750	250	41.4	12.4	10.1	92.6	2.94	35.3
D26	750	200	36.8	12.2	9.9	91.6	2.75	33.0
D27	750	150	33.3	12.3	9.9	89.4	2.46	29.6
D28	750	100	30.9	13.8	9.8	80.8	1.81	21.7
D29	750	82	26.0	13.5	9.6	76.7	1.59	19.1
D30	750	50	28.2	15.1	9.1	70.7	1.33	16.0
D31	1000	308	38.5	11.4	9.9	94.7	3.48	55.8
D32	1000	300	35.7	11.5	9.9	93.7	3.22	51.6
D33	1000	250	30.0	12.0	9.8	88.9	2.42	38.8
D34	1000	200	29.6	12.5	9.6	85.6	2.10	33.6
D35	1000	150	27.6	12.2	9.5	84.9	2.04	32.7
D36	1000	100	27.3	13.6	9.4	76.5	1.55	24.8
D37	1000	76	22.8	13.3	9.3	70.3	1.31	21.0
D38	1000	58	21.1	13.6	9.3	63.2	1.06	17.0

(vi) Oxygen desorption tests using viscous solutions (30 inch plate)

Water rate L_M	Air rate G_M	Test No	Viscosity 2cP			Test No	Viscosity 4cP		
			E_{ML}	N_L	K_La		E_{ML}	N_L	K_La
1000	300	E1	96.2	4.08	65.4	E17	95.7	3.90	62.5
1000	225	E2	95.1	3.63	56.6	E18	96.8	4.26	68.2
1000	150	E3	93.9	3.36	53.8	E19	94.6	3.52	56.4
1000	75	E4	83.0	2.03	32.5	E20	79.7	1.80	28.8
500	300	E5	97.6	4.86	38.9	E21	97.9	5.07	40.6
500	225	E6	97.9	4.97	39.8	E22	97.4	4.66	37.3
500	150	E7	92.2	3.03	24.3	E23	96.4	4.10	32.8
500	75	E8	89.8	2.73	21.9	E24	90.3	2.78	22.3
200	300	E9	99.1	5.55	17.8	E25	98.7	5.91	18.9
200	225	E10	99.1	5.60	17.9	E26	98.2	5.38	17.2
200	150	E11	99.2	5.71	18.3	E27	98.3	5.45	17.5
200	75	E12	95.3	3.90	12.5	E28	95.7	3.99	12.8
100	300	E13	99.1	6.70	10.7	E29	99.0	6.35	10.2
100	225	E14	99.2	6.83	10.9	E30	99.0	6.20	9.93
100	150	E15	98.8	6.02	9.64	E31	99.0	6.33	10.1
100	75	E16	98.5	5.82	9.32	E32	97.9	5.15	8.25

Water rate L_M	Air rate G_M	Test No	Viscosity 8cP			Test No	Viscosity 16cP		
			E_{ML}	N_L	K_La		E_{ML}	N_L	K_La
1000	300	E33	88.8	2.57	41.2	E49	83.9	2.09	33.5
1000	225	E34	83.4	2.51	40.2	E50	84.8	2.23	35.7
1000	150	E35	89.0	2.56	41.0	E51	83.5	2.02	32.4
1000	75	E36	71.8	2.07	33.2	E52	69.2	1.27	20.4
500	300	E37	93.4	3.34	26.7	E53	87.9	2.49	20.0
500	225	E38	92.4	3.13	25.1	E54	89.9	2.72	21.8
500	150	E39	90.3	2.83	22.7	E55	86.5	2.18	17.5
500	75	E40	75.1	1.56	12.5	E56	71.1	1.34	10.7
200	300	E41	97.7	5.00	16.0	E57	95.2	3.87	12.4
200	225	E42	98.1	5.25	16.8	E58	95.8	4.06	13.0
200	150	E43	97.9	5.04	16.2	E59	94.8	3.70	11.0
200	75	E44	95.0	3.74	12.0	E60	86.0	2.29	7.34
100	300	E45	98.5	5.90	9.45	E61	97.8	5.16	8.26
100	225	E46	98.9	6.10	9.87	E62	97.8	5.00	8.01
100	150	E47	98.2	5.35	8.57	E63	96.1	4.04	6.48
100	75	E48	97.6	4.90	7.85	E64	95.9	4.05	6.49

(vii) Residence time, hold-up and mixing tests (30 inch plate)

Test No	Water rate L_M	Air rate G_M	Resid. time tm	Liquid holdup gall.	Variance σ^2	Peclet No Pe	Eddy diffty. $D_E\ 10^5$	Air holdup ft^3	Air resid.time t_c(sec)
F1	100	300	34.1	0.464	0.320	11.60	183	0.329	0.061
F2	100	250	32.8	0.446	0.304	11.97	184	0.331	0.073
F3	100	200	33.8	0.461	0.300	12.08	177	0.329	0.091
F4	100	150	43.8	0.597	0.334	11.25	147	0.307	0.113
F5	100	100	40.0	0.544	0.362	10.72	169	0.279	0.154
F6	100	75	41.4	0.564	0.349	10.97	159	-	-
F7	250	300	17.4	0.594	0.285	12.54	331		
F8	250	250	16.8	0.574	0.275	12.87	335		
F9	250	200	16.0	0.546	0.298	12.13	372		
F10	250	150	16.9	0.579	0.200	16.25	263		
F11	250	100	18.5	0.632	0.265	13.21	296		
F12	250	75	26.4	0.901	0.321	11.55	237		
F13	500	300	10.2	0.694	0.283	12.62	561	0.366	0.067
F14	500	250	9.4	0.639	0.200	16.25	473	0.375	0.083
F15	500	200	9.1	0.622	0.164	19.03	415	0.377	0.104
F16	500	150	9.7	0.661	0.142	21.43	348	0.371	0.137
F17	500	100	13.3	0.905	0.198	16.36	332	0.295	0.163
F18	500	75	14.6	0.993	0.246	13.93	356	-	-
F19	750	300	7.8	0.795	0.254	13.62	680		
F20	750	250	6.6	0.672	0.153	20.13	544		
F21	750	200	7.4	0.752	0.185	17.31	564		
F22	750	150	8.0	0.816	0.125	23.75	381		
F23	750	100	11.5	1.180	0.223	14.98	419		
F24	750	75	13.2	1.350	0.222	15.05	364		
F25	1000	300	6.1	0.824	0.205	15.98	741	0.418	0.077
F26	1000	250	5.9	0.805	0.134	22.48	541	0.421	0.093
F27	1000	200	6.1	0.824	0.148	20.61	575	0.4.8	0.115
F28	1000	150	6.6	0.902	0.117	25.11	436	0.405	0.149
F29	1000	100	9.6	1.302	0.180	17.66	426	0.304	0.168
F30	1000	75	10.2	1.394	0.204	16.03	442	-	-

(viii) Residence time tests using viscous solutions (30 inch plate)

Test No	Water rate	Air rate	Resid. time	Liquid holdup	Variance σ^2	Pe	Eddy diffusivity(D_E-ft^2/sec)	
G1	100	300	32.6	0.444	0.377	10.43	0.00212	Viscosity 2cP
G2	100	200	34.8	0.374	0.303	12.01	0.00173	
G3	100	100	43.6	0.594	0.361	10.75	0.00154	
G4	250	300	19.1	0.650	0.337	11.20	0.00337	
G5	250	200	17.4	0.593	0.323	11.52	0.00360	
G6	250	100	31.2	1.063	0.319	11.61	0.00199	
G7	500	300	10.3	0.704	0.324	11.50	0.00610	
G8	500	200	11.6	0.791	0.309	11.86	0.00525	
G9	500	100	19.6	1.331	0.354	10.88	0.00339	
G10	1000	300	6.26	0.852	0.302	12.02	0.00960	
G11	1000	200	6.47	0.881	0.270	13.04	0.00856	
G12	1000	100	11.4	1.548	0.321	11.56	0.00549	
G13	100	300	38.1	0.518	0.335	11.26	0.00169	Viscosity 4cP
G14	100	200	38.7	0.527	0.303	12.00	0.00156	
G15	100	100	42.0	0.571	0.328	11.40	0.00151	
G16	250	300	19.4	0.661	0.354	10.88	0.00342	
G17	250	200	18.5	0.632	0.272	12.98	0.00301	
G18	250	100	34.4	1.171	0.300	12.07	0.00174	
G19	500	300	10.8	0.737	0.315	11.71	0.00571	
G20	500	200	12.5	0.854	0.289	12.42	0.00465	
G21	500	100	22.4	1.526	0.295	12.21	0.00264	
G22	1000	300	6.74	0.917	0.310	11.85	0.00905	
G23	1000	200	6.47	0.880	0.251	13.74	0.00812	
G24	1000	100	13.9	1.890	0.301	12.05	0.00432	
G25	100	300	40.6	0.552	0.429	9.62	0.00185	Viscosity 8cP
G26	100	200	43.6	0.593	0.286	12.52	0.00132	
G27	100	100	41.8	0.569	0.340	11.15	0.00155	
G28	250	300	25.5	0.871	0.325	11.47	0.00247	
G29	250	200	27.0	0.922	0.326	11.45	0.00234	
G30	250	100	36.3	1.239	0.324	11.50	0.00173	
G31	500	300	12.0	0.814	0.390	10.18	0.00591	
G32	500	200	13.0	0.881	0.294	12.27	0.00453	
G33	500	100	25.1	1.705	0.323	11.52	0.00250	
G34	1000	300	8.46	1.151	0.341	11.14	0.00767	
G35	1000	200	7.10	0.966	0.311	11.81	0.00861	
G36	1000	100	14.3	1.940	0.249	13.82	0.00366	
G37	100	300	43.9	0.598	0.423	9.75	0.00169	Viscosity 16cP
G38	100	200	45.8	0.623	0.314	11.80	0.00134	
G39	100	100	57.5	0.783	0.325	11.47	0.00110	
G40	250	300	26.8	0.915	0.365	10.47	0.00257	
G41	250	200	28.8	0.984	0.371	10.57	0.00237	
G42	250	100	32.9	1.124	0.313	11.76	0.00187	
G43	500	300	13.7	0.933	0.335	11.25	0.00469	
G44	500	200	13.5	0.919	0.287	12.49	0.00428	
G45	500	100	24.0	1.630	0.207	15.87	0.00190	
G46	1000	300	7.44	1.012	0.242	12.32	0.00788	
G47	1000	200	7.05	0.959	0.233	14.46	0.00709	
G48	1000	100	13.3	1.808	0.237	14.25	0.00381	

(ix) Humidification tests with varying weir height (slot area 4.25%),
(30 inch plate).

Water rate L_M	Air rate G_M	Humidn. effic^y E_{MV}	Press. drop (ins)	Froth ht. (ins)	Clear lq.ht. (ins)	Humidn. effic^y. E_{MV}	Press. drop (ins)	Froth ht. (ins)	Clear lq.ht. (ins)
100	300	75.0	3.17	1.9	0.39	76.4	3.35	2.4	0.50
100	250	79.1	2.50	1.9	0.41	80.3	2.65	2.4	0.55
100	200	80.4	2.09	2.0	0.49	81.5	2.08	2.5	0.68
100	150	83.0	1.89	2.2	0.83	84.0	2.06	2.7	0.97
100	100	84.2	1.85	2.2	1.18	82.5	2.20	2.8	1.50
250	300	78.4	3.15	2.0	0.43	80.8	3.32	2.7	0.61
250	250	82.4	2.56	2.0	0.46	82.0	2.60	2.7	0.66
250	200	82.0	2.14	2.2	0.55	84.5	2.27	2.7	0.80
250	150	85.1	2.02	2.3	0.95	87.7	2.18	2.8	1.15
250	100	88.8	1.99	2.4	1.28	91.7	2.26	2.9	1.63
500	300	85.4	3.20	2.3	0.53	85.5	3.40	2.8	0.71
500	250	86.0	2.65	2.3	0.54	87.0	2.75	2.8	0.72
500	200	87.3	2.15	2.3	0.61	90.0	2.38	2.8	0.90
500	150	88.7	2.10	2.5	1.00	91.0	2.33	3.0	1.29
500	100	92.1	2.02	2.5	1.33	92.7	2.30	3.1	1.69
1000	300	88.1	3.25	2.6	0.66	93.5	3.45	3.0	0.89
1000	250	90.5	2.70	2.6	0.70	92.4	2.86	3.0	0.95
1000	200	90.4	2.28	2.7	0.81	92.0	2.52	3.1	1.11
1000	150	92.0	2.15	2.7	1.13	94.0	2.47	3.2	1.45
1000	100	94.0	2.05	2.7	1.37	93.8	2.43	3.3	1.71

Weir Height 1.5 ins. Weir Height 2.0 ins.

Dry plate pressure drop with varying slot area

Air rate G_M	Slot area 4.25%	Slot area 7.32%	Slot area 9.76%
300	2.45	1.55	0.70
250	1.70	1.00	0.47
200	1.15	0.67	0.30
150	0.73	0.40	0.18
100	0.35	0.20	0.10
75	0.27	0.15	0.07

Pressure drops in inches of water.

(ix) Humidification tests with varying slot area and weir height (30 inch plate)

Water rate	air rate	Weir Height 1 in.		Weir Ht.1.5 in.		Weir Ht.2in.	
L_M	G_M	E_{MV}	ΔP(in)	E_{MV}	ΔP(in)	E_{MV}	ΔP(in)
100	300	62.0	1.90	73.5	2.10	72.0	2.30
100	250	64.2	1.52	77.1	1.80	74.9	2.00
100	200	65.7	1.40	79.1	1.65	79.8	1.85
100	150	71.2	1.20	80.4	1.65	84.6	1.95
100	100	72.4	1.10	84.7	1.60	90.3	2.00
250	300	64.5	1.98	76.8	2.15	79.4	2.40
250	250	67.9	1.65	80.0	1.85	82.9	2.10
250	200	72.8	1.50	81.6	1.80	83.0	2.00
250	150	76.6	1.30	84.2	1.75	89.5	2.05
250	100	81.0	1.18	88.0	1.65	94.1	2.10
500	300	69.1	2.05	81.2	2.20	82.3	2.45
500	250	73.4	1.70	85.5	2.00	85.5	2.20
500	200	77.8	1.50	86.2	1.85	85.5	2.10
500	150	82.8	1.40	87.0	1.80	91.1	2.20
500	100	88.4	1.30	90.6	1.75	94.6	2.20
1000	300	76.0	2.10	83.0	2.35	88.1	2.60
1000	250	82.0	1.80	89.9	2.05	91.5	2.40
1000	200	82.9	1.60	90.7	1.95	92.0	2.30
1000	150	85.1	1.50	90.5	1.90	96.0	2.30
1000	100	87.3	1.40	93.3	1.80	94.7	2.30

SLOT
AREA
7.32%

		Weir Ht. 1 in.		Weir Ht 1.5in.		Weir Ht 2in.	
L_M	G_M	E_{MV}	ΔP	E_{MV}	ΔP	E_{MV}	ΔP
100	300	67.9	1.15	66.1	1.20	68.9	1.30
100	250	68.4	1.02	67.2	1.10	71.0	1.10
100	200	68.0	0.95	69.3	1.00	72.2	0.95
100	150	69.0	1.10	72.0	1.40	75.7	0.90
100	100	69.7	1.02	77.6	1.40	75.1	0.90
250	300	72.0	1.22	73.9	1.50	77.9	1.70
250	250	74.5	1.10	75.6	1.35	82.3	1.70
250	200	73.5	1.05	79.0	1.32	80.4	1.75
250	150	78.4	1.20	78.2	1.45	85.9	1.75
250	100	77.8	1110	83.8	1.45	83.8	1.75
500	300	76.0	1.30	79.8	1.60	83.4	1.90
500	250	78.4	1.20	82.2	1.50	85.1	1.90
500	200	77.1	1.15	81.8	1.50	85.1	1.90
500	150	80.7	1.25	86.0	1.50	87.3	1.85
500	100	78.6	1.20	89.6	1.50	85.6	1.90
1000	300	80.5	1.40	85.7	1.70	87.0	2.10
1000	250	81.4	1.30	87.6	1.65	88.0	2.05
1000	200	83.5	1.30	88.2	1.60	89.0	2.00
1000	150	83.8	1.30	90.8	1.60	92.3	1.90
1000	100	86.5	1.25	92.4	1.55	90.0	1.92

SLOT
AREA
9.76%

(x) 12 inch Kuhni plate efficiencies pressure drop and mean clear liquid height.

Test No	Water rate L_M	Air rate G_M	Humid^n. efficy. E_{MV}	O_2Des^n efficy. E_{ML}	Pressure drop ΔP(in)	Clear liquid ht. (in)
1	200	500	72.8	96.3	1.02	0.22
2	200	400	73.5	97.2	0.84	0.24
3	200	300	75.0	96.2	0.74	0.35
4	200	200	75.7	89.2	0.63	0.53
5	200	100	80.6	87.4	0.61	0.64
6	400	500	75.7	91.4	1.11	0.26
7	400	400	77.2	93.4	0.91	0.28
8	400	300	76.1	92.6	0.80	0.37
9	400	200	77.7	81.3	0.68	0.60
10	400	100	81.2	75.7	0.70	0.71
11	600	500	77.6	90.2	1.18	0.30
12	600	400	78.5	90.5	0.96	0.32
13	600	300	80.0	89.6	0.82	0.39
14	600	200	82.1	75.5	0.71	0.57
15	600	100	85.1	69.5	0.77	0.79
16	800	500	78.3	85.7	1.25	0.37
17	800	400	79.8	87.8	1.02	0.40
18	800	300	81.5	87.9	0.88	0.43
19	800	200	83.9	68.9	0.80	0.67
20	800	100	84.6	63.2	0.82	0.82
21	1000	500	78.3	84.4	1.28	0.38
22	1000	400	79.6	84.7	1.08	0.39
23	1000	300	83.2	82.8	0.91	0.42
24	1000	200	84.2	63.4	0.83	0.68
25	1000	100	86.4	59.5	0.88	0.84

NOMENCLATURE

(i) Latin Symbols

A = An arbitrary constant

a = Interfacial area in the froth per ft^2 of column area (ft^2/ft^2)

$\bar{a}$ = Interfacial area (ft^2)

a' = Interfacial area per mol of vapour (ft^2/mol)

a_b = Surface area of a bubble (ft^2)

B = An arbitrary constant

b & b' = Arbitrary constants

c = Concentration of a diffusing component (lb.mol/ft^3)

c' = Concentration of solute in solution evaporation tests (any units)

$\bar{c}$ = Concentration of dissolved oxygen in diffusivity tests (g./cc.)

D_G = Molecular diffusivity in the gas phase (ft^2/hr)

D_L = Molecular diffusivity in the liquid phase (ft^2/hr)

D_E = Eddy diffusivity in the froth (ft^2/sec)

$\bar{D}_G$ = Molecular diffusivity of oxygen in water (cm^2/sec)

E^o = Overall column effciency

E^*_{MV} = Murphree vapour point efficiency

E_{MV} = Murphree vapour plate efficiency

E^*_{ML} = Murphree liquid point efficiency

E_{ML} = Murphree liquid plate efficiency

e = The base of natural logarithms

G_M = Mass gas rate in the column (lb/ft^{2}column area.hr)

G_V = Volumetric gas rate in the column (ft^3/ft^{2}column area.hr)

G_p = Gas rate (ft^3/hr)

G' = Gas rate in equation 1:3 (lb.mol/hr)

G_s = Gas rate per slot (cm^3/sec)

G_d = Gas absorption rate in the oxygen diffusivity tests (g./sec)

g = Acceleration due to gravity (cm./sec^2)

h = Bubble cap slot submergence (in)

h' = Height of the liquid crest above the slot centre (in)

h_l = Static liquid seal (cm)

h_s = Slot opening (cm)

H = Humidity of air ,(grains water / lb of dry air)
H' = Henry's Law constant (lb mol / ft^3.atm.)
H_{O_2} = Henry's Law constant for oxygen in water (mm.of mercury)
K_G = Overall mass transfer coefficient in gas terms (lb.mol/ft^2.hr.lb.mol/ft^3)
K_L = Overall mass transfer coefficient in liquid terms(lb.mol/ft^2.hr.lb.mol/ft^3)
K_g = Gas "film" mass transfer coefficient (lb.mol/ft^2.hr.lb.mol/ft^3)
K_l = Liquid "film" masstransfer coefficient (lb.mol/ft^2.hr.lb.mol/ft^3)
$\bar{K}$ = Conductivity (reciprocal ohms or mhos)
L_M = Mass liquid rate in the column (lb./ft^{2}column area.hr.)
L_V = Volumetric liquid rate in the column (ft^3/ft^{2}column area.hr.)
L_p = Liquid rate (ft^3/hr.)
L' = Liquid rate in equation 1:3 (lb.mol/hr.)
L_d = Liquid flow rate in the oxygen diffusivity tests (cc./sec.)
M = Molecular weight.
m = The dimensionless Henry's Law constant (mol fraction per mol fraction)
$\bar{H}$ = A dimensionless Henry's Law constant [(lb.mol/ft^3) per (lb.mol/ft^3)]
N_G = Overall number of transfer units in gas terms
N_L = Overall number of transfer units in liquid terms
N_g = Number of gas "film" transfer units
N_l = Number of liquid "film" transfer units.
N_A = Rate of mass transfer (lb.mol/hr.)
P = Pressure (atmospheres)
p = Radius of the outlet well of the Kuhni Plate (ft)
Pe = Peclet Number as defined in equation 1:13 $Pe = Z.V./D_E$
q = Peripheral radius of the Kuhni Plate (ft)
Q = Quantity of tracer (lb.)
R = Radius of the absorption sphere in the oxygen diffusivity tests (cm.)
r = Any radius on the Kuhni Plate (ft)
Sc = Schmidt Number $\mu_G/\rho_G.D_G$ or $\mu_L/\rho_L.D_L$
s = Rate of surface renewal (sec^{-1})
T = Temperature (^{o}F)
Td = Air dry bulb temperature (^{o}F)
Tw = Air wet bulb temperature (^{o}F)
T_K = Absolute temperature (^{o}K)
t = Time (sec.)

t_m = Mean residence time of the liquid on the plato (sec.)
t_b = Residence time of a bubble in the froth (sec.)
t_c = Contact time (sec.)
U_g = Column vapour velocity in equation 1:5 (cm./sec.)
U = Enthalpy of water vapour (BTU/lb.)
V = Froth velocity (ft/sec.)
V_b = Volume of a bubble (ft^3)
V_L = Volume of liquid hold-up (gall)
W = Weight of solution in solution evaporation tests (lb.)
W_V = Weight of water evaporated (lb.)
W_E = Weight of solution lost by entrainment (lb)
W_A = Weight of water added (lb.)
ω = Slot width (ins)
X = Dissolved oxygen content (parts per million)
x = Concentration in the liquid phase ($lb.mol/ft^3$)
y = Concentration in the gas phase ($lb.mol/ft^3$)
Z = Tray length (ft)

(ii) Subscripts and superscipts

1 = Inlet condition.
2 = Outlet condition
e = Equilibrium
G = Gas phase
g = Gas phase
i = Interfacial condition
L = Liquid phase
l = Liquid phase
m = Mean
s = Saturation
$'$ = Conditions at a point on a plate, also the derivative in Appendix B

(iii) Greek Symbols

α = Relative volatility in equation 1:5, also function defined in equation 6:5
β = Quantity defined in equation 6:10
ΔP = Plate pressure drop (ins of water)
θ = Angle
λ_w = Latent heat of evaporation of water (BTU/lb.)
λ = The function $\bar{E}.G_V/L_V$.
μ = Absolute viscosity (centi-Poise)

ν = Kinematic viscosity (centi-Stokes)

ρ = Density (lb./ft^3) also mass density of tracer (lb./ft^3)

σ^2 = Dimensionless variance

σ_L = Surface tension (dynes/cm.)

ϕ, γ, ν & ψ = Functions defined in Appendix B (liquid mixing)

REFERENCES

1 Murphree E.V. Ind. Eng. Chem. 1925 17 747.

2 Chilton T.H. & Colburn A.P. Ind.Eng.Chem.1934 26 1183.

3 Walter J.F.,& Sherwood T.K. Ind.Eng.Chem.1941 33 493

4 Carey J.S.,Griswold J.,Lewis W.K.,&McAdams W.H. Trans.Amer.Inst.Chem.
Eng. 1934 30 504

5 Robinson C.S. & Gilliland E.R. "Elements of Fractional Distillation"
McGraw-Hill Book Coy. New York 1950.

6 Drickamer H.G. & Bradford J.R. Trans.Amer.Inst.Chem.Eng.1943 39 319

7 O'Connell H.E. Trans.Amer.Inst.Chem.Eng.1946 42 741

8 Geddes R.L. Trans.Amer.Inst.Chem.Eng.1946 42 79

9 Sugden J. J. Chem.Soc.1922 121 858

10 O'Brien M.P. & Gosline J.E. Ind.Eng.Chem.1935 27 1436

11 Higbie R. Trans.Amer.Inst.Chem.Eng. 1935 31 365

12 Barrer R.M. "Diffusion in and Through Solids" Cambridge 1941

13 Chu J.C.,Donovan J.R.,Bosewell B.C. & Fuhrmeister L.C.
J. Appl.Chem 1951 1 524.

14 Bakowski S. Chem.Eng.Science 1952 1 266.

15 Spells K.E. & Bakowski S. Trans.Inst.Chem.Eng.1950 28 37

16 Spells K.E. & Bakowski S. Trans.Inst.Chem.Eng.1952 30 189

17 Chaiyavech P. & Van Winkle M. Ind.Eng.Chem.1961 53 187

18 "Final Report,Univ. of Michigan" Amer.Inst.Chem.Eng.Research Comm. 1960

19 "Final Report,Univ. of Delaware" Amer.Inst.Chem.Eng.Research Comm. 1959

20 "Final Report,North Carolina State College" Amer.Inst.Chem.Eng.Research
Committee 1959.

21 "Bubble Tray Design Manual" Amer.Inst.Chem.Eng.New York 1960.

22 Planovski reviewed Brit.Chem.Eng.October 1959

23 Quigley C.J. Johnson A.I.& Harris B.L. Chem.Eng.Prog.Vol 51 Symp Ser 16
page 31

24 Gilbert W.D. West F.B. & Shimzu T. Ind.Eng.Chem.1952 44 247.

25 Gerster J.A. Colburn A.P.,Bonnet W.E.,& Carmody T.W. Chem.Eng.Prog.
1951 47 523

26 Gerster J.A. Bonnet W.E.& Hess I. Chem.Eng.Prog. 1951 47 523

27 Gerster J.A. Bonnet W.E.& Hess I. Chem.Eng.Prog. 1951 47 621

28 Calderbank P.H. Trans.Inst.Chem.Eng. 1956 34 79.

29 Garner F.H. & Freshwater D.C. Trans.Inst.Chem.Eng. 1955 33 280

30 Ellis S.R.M.,Barker P.E.& Contractor R.N. Trans.Inst.Chem.Eng.1960 38 21

31 Marek J. & Novosad Z. Chem.Listy. 1956 50 337

32 Umholtz C.L. & Van Winkle M. Petr. Refr. 1955 34 114

33 Barker P.E. & Choudhury M.H. Brit. Chem.Eng 1954 4 348

34 Zuiderweg F.J. & Harmens A. Chem.Eng.Science. 1958 9 89.

35 Danckwerts P.V.,Sawistowski H. & Smith W. International Symposium on
Distillation 1960, Instn. of Chem. Engrs., London. page 7.

36 Garner F.H. & Hammerton D. Trans.Inst.Chem.Eng. 1954 32 S18.

37 Colburn A.P. Ind. Eng.Chem., 1936 28 526.

38 Souders M. & Brown G.C. Ind. Eng. Chem., 1934 26 98

39 Hunt C.,Hanson D.N. & Wilke C.R. Amer. Inst. Chem. Eng. J. 1955 1 441.

40 Eduljee H.E. Brit. Chem. Eng. 1958 3 474.

41 Freshwater D.C. "Chemical Engineering Practice" Vol 5, Butterworth
Publications Ltd 1958.

42 Kirschbaum E. "Distillation and Rectification" Chem.Pub.Coy.Inc.N.Y.1948.

43 Coulson J.M. & Richardson J.F. "Chemical Engineering" Pergamon Press 1959.

44 Mayfield F.D.,Church W.C.,Green A.C.,Lee D.C. & Rasmussen R.W.
Ind.Eng.Chem. 1952 44 2238.

45 British Patent 469117, 20 July 1937.

46 Jones J.B. & Pyle C. Chem. Eng. Prog. 1955 51 424

47 Garner F.H.,Ellis S.R.M. & Freshwater D.C. Trans.Inst.Chem.Eng.1957 35 61

48 Garner F.H.,Ellis S.R.M. & Hughill A.J. Trans.Inst.Chem.Eng. 1953 31 13

49 Garner F.H.,Ellis S.R.M. & Bershadsky Z. Trans.Inst.Chem.Eng. 1954 32 S161

50 Pollard B. Trans.Inst.Chem.Eng. 1957 35 69.

51 Robin B.J. Brit.Chem.Eng. 1959 4 351.

52 Whitman W.G. Chem.Met.Eng. 1923 29 146.

53 Fick A. Pogg.Ann. 1855 94 59.

54 Treybal R.E. "Mass Transfer Operations", McGraw-Hill Book Coy N.Y. 1955

55 Sherwood T.K. & Goodgame T.H. Chem.Eng.Science, 1954 3 37.

56 Toor H.L. & Marchello J.M. Amer.Inst.Chem.Eng.J. 1958 4 97.

57 Gilliland E.R. Ind.Eng. Chem. 1934 26 681.

58 Hirschfelder J.O.,Bird R.B. & Spotz E.L. Trans.Amer.Soc.Mech.Eng.
1949 71 921.

59 Fair J.R. & Lerner B.J. Amer.Inst.Chem.Eng.J. 1956 2 13.
60 Wilke J.R. & Lee C.Y. Ind.Eng.Chem, 1955 47 1253.
61 Johnson P.A. & Babb A.L. Chem.Rev. 1956 56 387.
62 Davidson J.F. & Cullen E.J. Trans.Inst.Chem.Eng. 1957 35 51.
63 Wilke C.R. & Chang P. Amer.Inst.Chem.Eng.J. 1955 47 1253.
64 Ibrahim S.H. & Kuloor N.R. Brit.Chem.Eng. 1960 5 795.
65 Danckwerts P.V. Ind.Eng.Chem. 1951 43 1460.
66 Gatreaux M.F. & O'Connell H.E. Chem.Eng.Prog. 1955 51 232.
67 Oliver E.D. & Watson C.C. Amer.Inst.Chem.Eng.J. 1956 2 18.
68 Johnson A.I. & Marangozis J. Can.J.Chem.Eng. 1958 36 161.
69 Ruckinchtein E. J.Appl.Chem.(U.S.S.R.) 1957 30 1012.
70 Danckwerts P.V. Chem.Eng.Science, 1953 2 1.
71 Levenspeil O. & Smith W.K. Chem.Eng.Science, 1957 6 227.
72 Van der Laan E.T. Chem.Eng.Science, 1958 7 187.
73 Werner J.F. & Wilhelm R.H. Chem.Eng.Science, 1956 6 89.
74 Garner F.H. & Hammerton D. Chem.Eng.Science, 1954 3 1.
75 Maier W. U.S. Bureau of Mines Bulletin 1927 260 62.
76 Swindin J. Proc.Chem.Eng.Grp. 1928 10 116.
77 Datta R.L. & Newitt D.M. Trans.Inst.Chem.Eng. 1950 28 14
78 Hughes R.R.,Handlos A.M.,Evans H.D. & Maycock R.L., Publication of the
Heat Transfer and Fluid Mechanics Inst.,Los Angeles 1953
79 Davidson J.F. & Schuler B.O.G. Trans.Inst.Chem.Eng. 1960 38 144.
80 Davidson J.F. & Schuler B.O.G. Trans.Inst.Chem.Eng. 1960 38 335.
81 Leibson I. & Holcomb E.G. Amer.Inst.Chem.Eng.J. 1956 2 296.
82 Davidson L. & Amick E.H. Amer.Inst.Chem.Eng.J. 1956 2 337.
83 Siemes W. & Gunther K. Chem.Ing.Tech. 1956 28 389.
84 Coppock P.D. & Meiklejohn G.T. Trans.Inst.Chem.Eng. 1951 29 75.
85 Van Krevelen D.W. & Hoftijzer P.J. Chem.Eng.Prog. 1950 46 29.
86 Calderbank P.H. Brit.Chem.Eng. 1956 1 267.
87 Siemes W. & Kaufman J.F. Chem.Eng.Science, 1956 5 127.
88 Bond W.N. & Newton D.A. Phil.Mag. 1928 5 794.
89 Garner F.H. & Hammerton D. Trans.Inst.Chem.Eng. 1954 32 S18.
90 Calderbank P.H. & Korschinski Chem.Eng.Science. 1956 6 65.
91 Calderbank P.H. Trans.Inst.Chem.Eng. 1958 36 443
92 Calderbank P.H. Trans.Inst.Chem.Eng. 1959 37 173.

93 Chu J.C., Forgrieve J., Grosso R., Shah S.M. & Othmer D.F. Amer.Inst.Chem.Eng.J. 1957 3 16.

94 Calderbank P.H., Evans F. & Rennie J. International Symposium on Distillation 1960 Inst.of Chem.Eng. London . page 51.

95 Calderbank P.H. & Moo Young M.B. *ibid.* p. 59

96 Van Wijk W.R. & Thijssen H.A.C. Chem.Eng.Science, 1954 3 153.

97 Haselden G.G. & Sutherland J.P. International Symposium on Distillation, Inst.of Chem.Eng. London 1960 page 27.

98 Forgrieve J. *ibid.* p. 185.

99 Garner F.H. & Porter K.E. *ibid.* p.43.

100 Stanislaus D.H. & Smith A.J. *ibid.* p.208.

101 Zuiderweg F.J., Verburg H. & Gilissen F.A.H. *ibid.* p.201.

102 "International Symposium on Distillation 1960" Brighton

103 Kishinevskii M.K. & Mochalova L.A. Zh.Prikl.Khim. 1958 31 1013.

104 Dummet G.A. Brit.Chem.Eng. 1958 3 563

105 Majewski J. Brit.Chem.Eng. 1959 4 336.

106 Foss A.S., Gerster J.A. & Pigford R.L. Amer.Inst.Chem.Eng.J.1958 4 231

107 Gilbert T.J. Chem.Eng.Science, 1959 10 243.

108 Gilliland E.R. & Sherwood T.K. Ind.Eng.Chem. 1934 26 516

109 Stephens E.J. & Morris G.A. Chem.Eng.Prog. 1951 47 232

110 Vivian J.E. & Peaceman D.W. Amer.Inst.Chem.Eng.J. 1956 2 437.

111 Taylor R.F. & Roberts F. Chem.Eng.Science. 1956 5 108.

112 Institute of Heating and Ventilating Engineers "Guide" 1955.

113 Lewis W.K. Trans.Amer.Soc.Mech.Eng. 1922 44 325.

114 "International Critical Tables" McGraw-Hill Book Coy Inc 1926.

115 British Standard 1427 (1949) Tests for Water used in Steam Generation.

116 Perry J.H. "Chemical Engineers'Handbook" 3rd Edn. 1950

117 Browne C.A. & Zerban F.W. "Sugar Analysis" John Wiley & Sons Ltd 1941.

118 Carrier W.H. & Mackey C.O. Trans .Amer.Soc.Mech.Eng. 1937 59 33.

119 British Standard 1042 (1957) Flow Measurement.

120 British Standard 188 (1957) Determination of the Viscosity of Liquids.

121 Gordon A.R. Ann. N.Y. Acad. Science, 1945 46 285.
122 Carlson T. J.Amer.Chem.Soc. 1911 33 1027.
123 Ringbom A. Z.Anorg.allgem.Chem. 1938 238 94.
124 Pigford R.L. Thesis in Chemical Engineering Univ. of Illinois 1941.
125 Vyazovov V.V. J.Tech.Phys.(U.S.S.R.) 1940 10 1519.
126 Stiles W. & Adair G.S. Biochem.J. 1921 15 620.
127 Jordan J.,Ackerman E.& Berger R.L. J.Amer.Chem.Soc. 1956 78 2979.
128 Dunn M.J. Thesis in Chemical Technology R.C.S.T. Glasgow 1961.
129 Payne B. Thesis in Chemical Technology R.C.S.T. Glasgow 1961.
130 Maroudas N.G. & Sawistowski H. Nature 1960 188 1186.
131 Poplavsky V.V. Khim.Mach.(U.S.S.R.) 1960 5 4, reviewed in
Brit.Chem.Eng. 1961 6 87.